

Die approbierte Originalversion dieser Dissertation ist an der Hauptbibliothek der Technischen Universität Wien aufgestellt (<http://www.ub.tuwien.ac.at>).

The approved original version of this thesis is available at the main library of the Vienna University of Technology (<http://www.ub.tuwien.ac.at/englweb/>).



DISSERTATION

TRANSITION METAL-CATALYZED C–H BOND FUNCTIONALIZATION OF SP³-CARBON CENTERS

Conducted at the

**Institute of Applied Synthetic Chemistry
Vienna University of Technology**

under the supervision of

**A.o. Univ.Prof. DI Dr. techn.
Marko D. Mihovilovic**

&

**DI Dr. techn.
Michael Schnürch**

Performed by

Dipl. Chem. Navid Dastbaravardeh

Reg.No. 0828770

Lerchenfelderstr. 9-11/21, 1070, Vienna

MEINEN ELTERN IN DANKBARKEIT GEWIDMET

*“Learn from yesterday, live for today, hope for tomorrow.
The important thing is not to stop questioning.”*

Albert Einstein

First of all I want to thank my parents Akbar and Zohreh to whom I dedicate this thesis. They supported me throughout the years of my studies and gave me the love and strength to achieve all my aims in my life. The same is true for my brother Omid, who is fortunately also one of my best friends. A very big kiss goes to my girlfriend Auri who believed in me all these years and is the love of my life.

My special thanks belong to Prof. Marko D. Mihovilovic for the opportunity to conduct my research in his research group. I want to thank him not only for his valuable suggestions and encouragement but also his full trust in me.

I am also very grateful to Dr. Michael Schnürch, who was not only my supervisor and mentor, but also my friend. I want to thank him for his great support, ideas and incalculable help during the last four years. I really appreciate all the good advice he gave me and I will never forget the wonderful and inspiring discussions we had about chemistry. In any event, I am certain that, without him, this thesis would never have been written.

I would also like to express a very special gratitude to all my friends of our institute, Max Haider (England wird nie wieder Weltmeister), Laurin Wimmer, Maria Vasiloiu, Michael Fink, Anna Ressmann, Gerit Pototschnig, Lukas Rycek, Nikolin Oberleitner and Toan Dao Huy. I will really miss our "Kochgruppe", the conversations we had during lunch, the legendary Christmas parties and the whole time we have spent together.

My thanks also go to all the current and former members of our, the Prof. Fröhlich and the Prof. Gärtner research group for providing a nice atmosphere and making the work enjoyable. A special thank goes to my friend and former group member Moumita Koley who helped me a lot in the beginning of this work.

In addition I would like to thank Prof. Erwin Rosenberg for measuring HR-MS, Dr. Christian Hametner for recording NMR-spectra on the 400 MHz machine and Prof. Karl Kirchner for the DFT calculations.

Another very special acknowledgement goes to Florian Untersteiner who helped me a lot to overcome all the computer related problems. In this context, I want to thank the whole institute staff for their support within the last years.

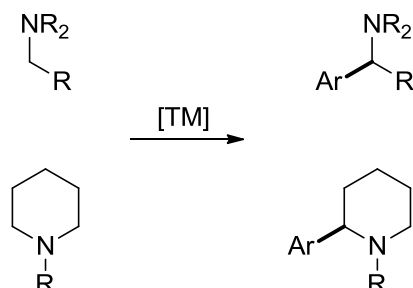
Finally, I want to say thank to my best friends, Sebastian & Janine Seidl, Mert Miser, Steffie Arndt, Martin Stapel, Jörg Bartel and Artur Nenov for helping me with all the issues outside the lab.

KEY

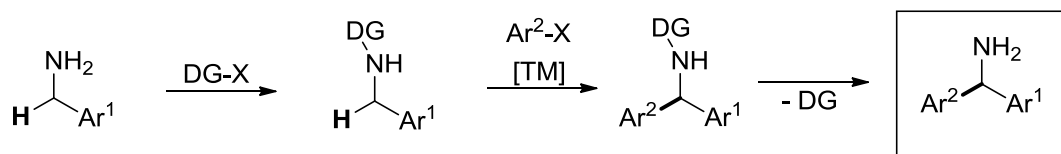
All compounds prepared or used as starting materials in this thesis are numbered in bold Arabic numbers. Compounds unknown to the literature are additionally underlined. Literature citations are indicated by superscript Arabic numbers.

ABSTRACT

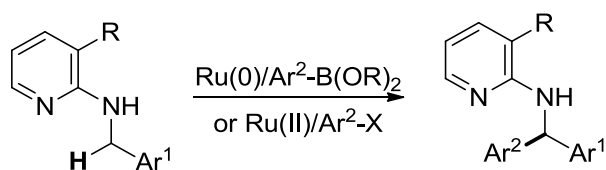
The task of the presented PhD thesis was the development of new transition-metal catalyzed arylation methods for sp^3 C–H bonds of cyclic and acyclic amines.



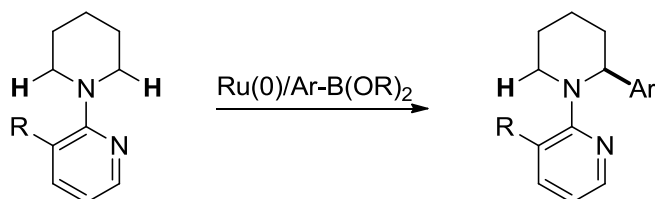
The regioselective C–H activation of the unactivated bond can be achieved by cyclometalation. One of the key steps for this transformation was the introduction of a suitable directing group which can be cleaved after the transformation. Different directing groups as well as different catalytic methods for the direct arylation of benzylic amines were investigated.



After intensive screenings, 3-substituted pyridines were found to be the best directing groups. Three different protocols could be established for the direct transformation of benzylic amines. The C–H bond functionalization could be performed with arylboronic acid esters, aryl bromides, and aryl chlorides. Furthermore, mechanistic studies were conducted to obtain a better understanding of the transformation.

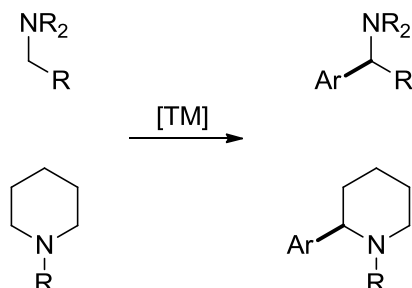


Finally, the general applicability of this directing group was also demonstrated for the selective mono arylation of piperidines.

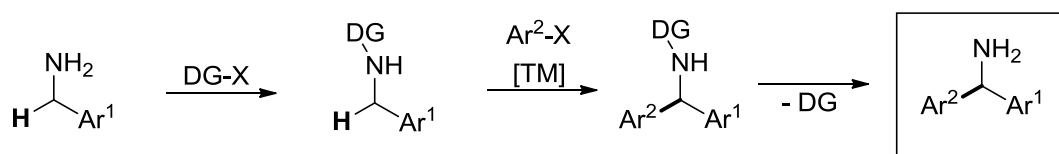


DEUTSCHE KURZFASSUNG

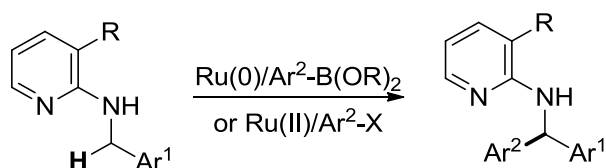
Hauptaufgabe der hier vorgelegten Arbeit war die Entwicklung neuer Übergangsmetall katalysierten Arylierungen an sp^3 C–H Bindungen cyclischer und acyclischer Verbindungen.



Die regioselective Funktionalisierung nicht aktivierter C–H Bindungen kann durch Cyclometallierung erreicht werden. Eine entscheidende Herausforderung ist die Einführung einer geeigneten dirigierenden Gruppe, die anschließend spaltbar ist. Im Rahmen dieser Arbeit wurden verschiedene dirigierende Gruppen sowie unterschiedliche katalytische Methoden für die direkte Arylierung benzyliischer Verbindungen untersucht.



Pyridin, welches in Position 3 substituiert ist, stellte sich dabei als beste DG heraus. Es wurden drei unterschiedliche Methoden für die direkte Funktionalisierung entdeckt. Die C–H Aktivierung konnte sowohl mit Arylboronsäureestern als auch mit Arylbromiden und Arylchloriden erfolgreich durchgeführt werden. Zum besseren Verständnis wurde eine Reihe an mechanistischen Experimenten durchgeführt.



Die generelle Anwendbarkeit dieser DG konnte außerdem anhand der spezifisch einseitigen Arylierung von Piperidinen dargelegt werden.

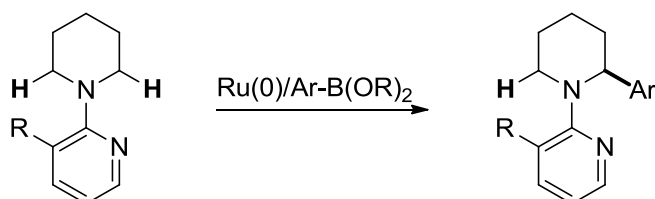


TABLE OF CONTENTS

1. INTRODUCTION.....	1
2. OBJECTIVES.....	3
3. THEORETICAL BACKGROUND.....	4
3.1 Homogeneous Catalysis.....	4
3.2 Metal-Ligand Complexes	7
3.2.1 <i>Carbon Monoxide Ligand</i>	7
3.2.2 <i>Organic Carbonyl Ligands</i>	8
3.2.3 <i>Phosphine Ligands</i>	9
3.2.4 <i>Amino Ligands</i>	12
3.3 Cross Coupling Reactions	13
3.3.1 <i>Catalytic Cycle</i>	13
3.3.2 <i>Catalyst Activation</i>	15
3.3.3 <i>Oxidative Addition</i>	16
3.3.4 <i>Transmetalation</i>	20
3.3.5 <i>Reductive Elimination</i>	20
3.4 Asymmetric Catalysis.....	22
3.5 C–H Activation.....	23
3.5.1 <i>Catalytic C–H Functionalization</i>	24
3.5.2 <i>Regioselectivity</i>	27
3.5.3 <i>Cyclometalation</i>	29
3.5.4 <i>Concerted Metalation Deprotonation - CMD</i>	31
4. RESULTS & DISCUSSION	33
4.1 Direct Arylation of Acyclic Amines	33
4.1.1 <i>State of the Art</i>	33
4.1.2 <i>Objective</i>	36
4.1.3 <i>Ru(0) System - Screening I</i>	37
4.1.4 <i>Directing group</i>	39
4.1.5 <i>Ru(0) System - Screening II</i>	44
4.1.6 <i>Ru(0) System – One Pot Synthesis</i>	46
4.1.7 <i>Ru(0) System - Scope</i>	47
4.1.8 <i>Ru(0) System – Mechanistic Studies</i>	53
4.1.9 <i>Ru(II) System – Screening</i>	64
4.1.10 <i>Ru(II) System – Scope</i>	72
4.1.11 <i>Ru(II) System – Mechanistic Studies</i>	77
4.1.12 <i>Rh System</i>	84

4.1.13 Asymmetric Catalysis.....	85
4.2 Direct Arylation of Cyclic Amines	89
4.2.1 Objective.....	89
4.2.2 Screening	91
4.2.3 Directing group	94
4.2.4 Scope.....	96
5. FINAL CONCLUSION	97
6. EXPERIMENTAL SECTION	99
6.1. General Notes	99
6.2 Synthesis of Arylboronate Esters	102
6.2.1 2-Phenyl-1,3,2-dioxaborinane (91a)	102
6.2.2 2-(2-Methylphenyl)-1,3,2-dioxaborinane (91b).....	103
6.2.3 2-(Naphthalen-1-yl)-1,3,2-dioxaborinane (91c).....	103
6.2.4 2-(3-Methylphenyl)-1,3,2-dioxaborinane (91d).....	104
6.2.5 2-(3-Chlorophenyl)-1,3,2-dioxaborinane (91e).....	104
6.2.6 2-(4-Methylphenyl)-1,3,2-dioxaborinane (91f).....	105
6.2.7 2-(4-(1,1-Dimethylethyl)phenyl)-1,3,2-dioxaborinane (91g).....	106
6.2.8 2-(4-Methoxyphenyl)-1,3,2-dioxaborinane (91h)	106
6.2.9 2-(4-Fluorophenyl)-1,3,2-dioxaborinane (91i).....	107
6.2.10 2-(4-Chlorophenyl)-1,3,2-dioxaborinane (91j).....	108
6.2.11 2-(4-(Trifluoromethyl)phenyl)-1,3,2-dioxaborinane (91k)	108
6.2.12 1-(4-(1,3,2-Dioxaborinan-2-yl)phenyl)ethanone (91l)	109
6.2.13 2-(4-Nitrophenyl)-1,3,2-dioxaborinane (91m).....	110
6.2.14 4-(1,3,2-Dioxaborinan-2-yl)benzotrile (91n).....	110
6.3 Synthesis of Precursors	111
6.3.1 N-Benzyl-3-methylpyridin-2-amine (92a)	112
6.3.2 3-Methyl-N-(4-methylbenzyl)pyridin-2-amine (92b)	113
6.3.3 N-(4-Isopropoxybenzyl)-3-methylpyridin-2-amine (92c).....	113
6.3.4 N-(4-Methoxybenzyl)-3-methylpyridin-2-amine (92d).....	114
6.3.5 N-(4-Fluorobenzyl)-3-methylpyridin-2-amine (92e).....	115
6.3.6 3-Methyl-N-[4-(trifluoromethyl)benzyl]pyridin-2-amine (92f).....	116
6.3.7 Methyl 4-[[3-methylpyridin-2-yl]amino]methyl]benzoate (92g)	116
6.3.8 N-Benzyl-3-(trifluoromethyl)pyridin-2-amine (92h).....	117
6.3.9 N-(4-Methylbenzyl)-3-(trifluoromethyl)pyridin-2-amine (92i)	118
6.3.10 N-(Naphthalen-2-ylmethyl)-3-(trifluoromethyl)pyridin-2-amine (92j)	119
6.3.11 N-Benzyl-3-chloropyridin-2-amine (92k)	119
6.3.12 3-Chloro-N-(4-methylbenzyl)pyridin-2-amine (92l)	120
6.3.13 N-Benzyl-3-phenylpyridin-2-amine (92m)	121
6.3.14 N-(4-Methylbenzyl)-3-phenylpyridin-2-amine (92n)	122
6.3.15 3-Methyl-2-(phenylethynyl)pyridine (93).....	123
6.3.16 3-Methyl-2-phenethylpyridine (94).....	123
6.3.17 2-(Benzoyloxy)-3-methylpyridine (95).....	124

TABLE OF CONTENTS

6.3.18 3-Methyl-N-phenethylpyridin-2-amine (96).....	125
6.3.19 N-Benzyl-N-methylpyridin-2-amine (97a)	126
6.3.20 N-Benzyl-N,3-dimethylpyridin-2-amine (97b)	126
6.3.21 2-(Pyridin-2-yl)-1,2,3,4-tetrahydroisoquinoline (98a)	127
6.3.22 2-(3-Methylpyridin-2-yl)-1,2,3,4-tetrahydroisoquinoline (98b)	128
6.3.23 N-Benzyl-N-(pyridin-2-yl)acetamide (99a).....	129
6.3.24 N-Benzyl-N-(3-methylpyridin-2-yl)acetamide (99b).....	129
6.3.25 N-Benzyl-N-(pyridin-2-yl)benzamide (99c)	130
6.3.26 N-Benzyl-N-(3-methylpyridin-2-yl)benzamide (99d)	131
6.3.27 N-Benzyl-N-(pyridin-2-yl)pivalamide (99e).....	132
6.3.28 N-Benzyl-N-(3-methylpyridin-2-yl)pivalamide (99f)	132
6.3.29 N-Benzylpyrimidin-2-amine (100)	133
6.3.30 N-Benzylpyrazin-2-amine (101).....	134
6.3.31 N-Benzylthiazol-2-amine (102).....	135
6.3.32 N-Benzyl-3,4-dihydro-2H-pyrrol-5-amine (103)	135
6.3.33 N-Benzyl-4-methylbenzenesulfonamide (104).....	136
6.3.34 N-Benzylpivalamide (105)	137
6.3.35 N,N,2-Trimethylaniline (106a).....	138
6.3.36 2-Ethyl-N,N-dimethylaniline (106b)	138
6.3.37 2-Benzyl-N,N-dimethylaniline (106c)	139
6.3.38 N-(2-Methylphenyl)acetamide (107a).....	140
6.3.39 N-(2-Benzylphenyl)acetamide (107b)	141
6.3.40 1-Methyl-2-(methylthio)-1H-benzo[d]imidazole (108).....	141
6.3.41 N-Benzyl-1-methyl-1H-benzo[d]imidazol-2-amine (109)	142
6.3.42 N-Benzylidene-3-methylpyridin-2-amine (111)	143
6.3.43 N-[Deuterio(phenyl)methyl]-3-methylpyridin-2-amine (112).....	144
6.3.44 N-[Dideuterio(phenyl)methyl]-3-methylpyridin-2-amine (113)	145
6.3.45 2-(Piperidin-1-yl)-3-(trifluoromethyl)pyridine (114a).....	146
6.3.46 3-Chloro-2-(piperidin-1-yl)pyridine (114b)	147
6.3.47 3-Phenyl-2-(piperidin-1-yl)pyridine (114c).....	147
6.3.48 3-Iodo-2-(piperidin-1-yl)pyridine (114d)	148
6.3.49 Ethyl 2-chloronicotinate (187).....	149
6.3.50 Ethyl 2-chloro-6-methylnicotinate (189)	149
6.3.51 Ethyl 2-(piperidin-1-yl)nicotinate (114e).....	150
6.3.52 Ethyl 6-methyl-2-(piperidin-1-yl)nicotinate (114f).....	151
6.3.53 2-(Pyrrolidin-1-yl)-3-(trifluoromethyl)pyridine (115a)	151
6.3.54 3-Chloro-2-(pyrrolidin-1-yl)pyridine (115b).....	152
6.3.55 3-Phenyl-2-(pyrrolidin-1-yl)pyridine (115c)	153
6.4 C-H Bond Functionalization	154
6.4.1 General Methods	154
6.4.2 N-Benzhydryl-3-methylpyridin-2-amine (116a).....	156
6.4.3 3-Methyl-N-[3-methylphenyl(phenyl)methyl]pyridin-2-amine (116b).....	157
6.4.4 N-[(3-Methoxyphenyl)(phenyl)methyl]-3-methylpyridin-2-amine (116c).....	158
6.4.5 N-[(3-Chlorophenyl)(phenyl)methyl]-3-methylpyridin-2-amine (116d).....	159
6.4.6 3-Methyl-N-[phenyl(4-methylphenyl)methyl]pyridin-2-amine (116e)	160
6.4.7 N-[(4-(1,1-Dimethylethyl)phenyl)(phenyl)methyl]-3-methylpyridin-2-amine (116f).....	162
6.4.8 N-[(4-Butylphenyl)(phenyl)methyl]-3-methylpyridin-2-amine (116g).....	163
6.4.9 N-[(4-Methoxyphenyl)(phenyl)methyl]-3-methylpyridin-2-amine (116h)	164

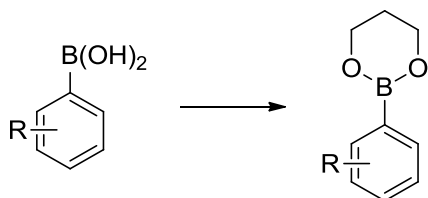
TABLE OF CONTENTS

6.4.10 <i>N</i> -[4-(Dimethylamino)phenyl](phenyl)methyl]-3-methylpyridin-2-amine (116i)	166
6.4.11 <i>N</i> -[4-Fluorophenyl](phenyl)methyl]-3-methylpyridin-2-amine (116j)	167
6.4.12 <i>N</i> -[4-Chlorophenyl](phenyl)methyl]-3-methylpyridin-2-amine (116k)	169
6.4.13 3-Methyl- <i>N</i> -[phenyl(4-(trifluoromethyl)phenyl)methyl]pyridin-2-amine (116l).....	170
6.4.14 Ethyl 4-[(3-methylpyridin-2-yl)amino](phenyl)methyl] benzoate (116m)	171
6.4.15 <i>N</i> -[4-Isopropoxyphenyl](phenyl)methyl]-3-methylpyridin-2-amine (116n)	172
6.4.16 Methyl 4-[(3-methylpyridin-2-yl)amino](phenyl)methyl]benzoate (116o)	173
6.4.17 <i>N</i> -[4-Chlorophenyl](4-methylphenyl)methyl]-3-methylpyridin-2-amine (116p)	174
6.4.18 3-Methyl- <i>N</i> -[4-methylphenyl(4-(trifluoromethyl)phenyl)methyl]pyridin-2-amine (116q).....	175
6.4.19 <i>N</i> -Benzhydryl-3-(trifluoromethyl)pyridin-2-amine (116r)	176
6.4.20 <i>N</i> -[4-Methylphenyl(phenyl)methyl]-3-(trifluoromethyl)pyridin-2-amine (116s)	176
6.4.21 <i>N</i> -[4-(1,1-Dimethylethyl)phenyl](phenyl)methyl]-3-(trifluoromethyl)pyridin-2-amine (116t).....	178
6.4.22 <i>N</i> -[4-Methoxyphenyl](phenyl)methyl]-3-(trifluoromethyl)pyridin-2-amine (116u)	179
6.4.23 <i>N</i> -[4-Fluorophenyl](phenyl)methyl]-3-(trifluoromethyl)pyridin-2-amine (116v)	180
6.4.24 <i>N</i> -Benzhydryl-3-phenylpyridin-2-amine (116w)	181
6.4.25 <i>N</i> -[3-Methylphenyl(phenyl)methyl]-3-phenylpyridin-2-amine (116x)	182
6.4.26 <i>N</i> -[3-Methoxyphenyl(phenyl)methyl]-3-phenylpyridin-2-amine (116y).....	183
6.4.27 <i>N</i> -[4-Methylphenyl(phenyl)methyl]-3-phenylpyridin-2-amine (116z)	184
6.4.28 <i>N</i> -[4-(1,1-Dimethylethyl)phenyl](phenyl)methyl]-3-phenylpyridin-2-amine (116aa)	186
6.4.29 <i>N</i> -[4-Butylphenyl](phenyl)methyl]-3-phenylpyridin-2-amine (116ab).....	187
6.4.30 <i>N</i> -[4-Fluorophenyl](phenyl)methyl]-3-phenylpyridin-2-amine (116ac)	188
6.4.31 <i>N</i> -[4-Chlorophenyl](phenyl)methyl]-3-phenylpyridin-2-amine (116ad)	189
6.4.32 Ethyl 4-[phenyl(3-phenylpyridin-2-yl)amino)methyl]benzoate (116ae).....	190
6.4.33 1-[4-(Phenyl(3-phenylpyridin-2-yl)amino)methyl]phenyl]ethanone (116af)	191
6.4.34 <i>N</i> -(Di-4-methylphenylmethyl)-3-phenylpyridin-2-amine (116ag).....	192
6.4.35 <i>N</i> -[4-(1,1-Dimethylethyl)phenyl](4-methylphenyl)methyl]-3-phenylpyridin-2-amine (116ah)	193
6.4.36 <i>N</i> -[4-Fluorophenyl](4-methylphenyl)methyl]-3-phenylpyridin-2-amine (116ai)	194
6.4.37 3-Phenyl- <i>N</i> -[4-methylphenyl(4-(trifluoromethyl)phenyl)methyl]pyridin-2-amine (116aj).....	195
6.4.38 3-Methyl- <i>N</i> -(1-phenyloctyl)pyridin-2-amine (116ak)	196
6.4.39 <i>N</i> -[Naphthalen-1-yl(phenyl)methyl]-3-(trifluoromethyl)pyridin-2-amine (116al)	197
6.4.40 <i>N</i> -Benzhydryl-1-methyl-1 <i>H</i> -benzo[<i>d</i>]imidazol-2-amine (110).....	198
6.4.41 2-(2,2-Diphenylethyl)-3-methylpyridine (127).....	198
6.4.42 <i>N</i> -(1,2-Diphenylethyl)-3-methylpyridin-2-amine (129)	199
6.4.43 <i>N</i> -(Diphenylmethylene)-3-methylpyridin-2-amine (117)	200
6.4.44 2-(2-Phenylpiperidin-1-yl)-3-(trifluoromethyl)pyridine (120a).....	201
6.4.45 2-[2-(4-methylphenyl)piperidin-1-yl]-3-(trifluoromethyl)pyridine (120b)	202
6.4.46 2-[2-(4-(1,1-Dimethylethyl)phenyl)piperidin-1-yl]-3-(trifluoromethyl)pyridine (120c).....	203
6.4.47 2-[2-(4-Fluorophenyl)piperidin-1-yl]-3-(trifluoromethyl)pyridine (120d).....	204
6.4.48 3-(Trifluoromethyl)-2-[2-(4-(trifluoromethyl)phenyl)piperidin-1-yl]pyridine (120e)	205
6.4.49 2-[2-(4-Chlorophenyl)piperidin-1-yl]-3-(trifluoromethyl)pyridine (120f)	206
6.5 KIE Experiments.....	207
6.5.1 Ru(0) Intermolecular Competition Experiment	207
6.5.2 Ru(0) Intramolecular Competition Experiment	207
6.5.3 Ru(II) Intermolecular Competition Experiment.....	208
6.5.4 Ru(II) Intramolecular Competition Experiment.....	209
6.6 Directing Group Cleavage.....	210
6.6.1 <i>tert</i> -Butyl benzhydryl(3-methylpyridin-2-yl)carbamate (118)	210

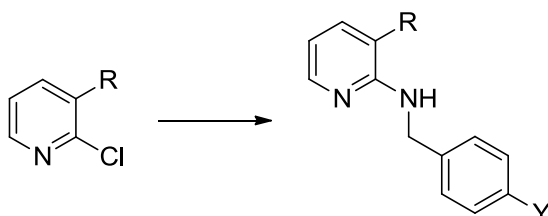
TABLE OF CONTENTS

6.6.2 <i>tert</i> -Butyl benzhydrylcarbamate (119).....	211
6.7 DFT Calculation.....	212
7. LITERATURE.....	213
CURRICULUM VITAE.....	220

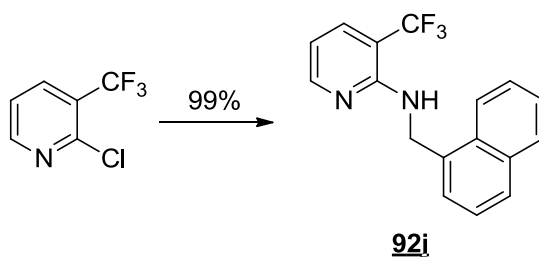
GENERAL SCHEMES



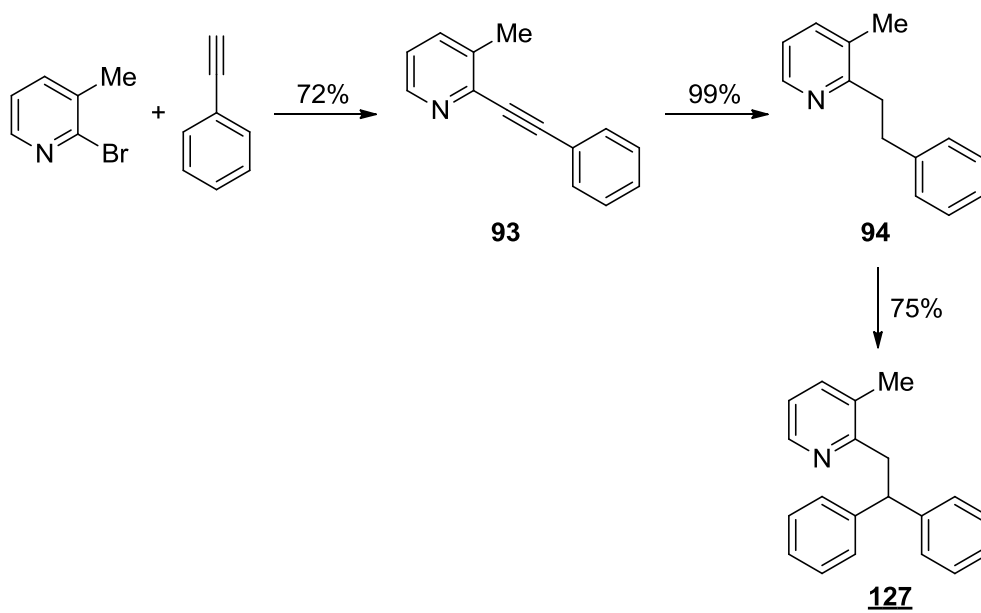
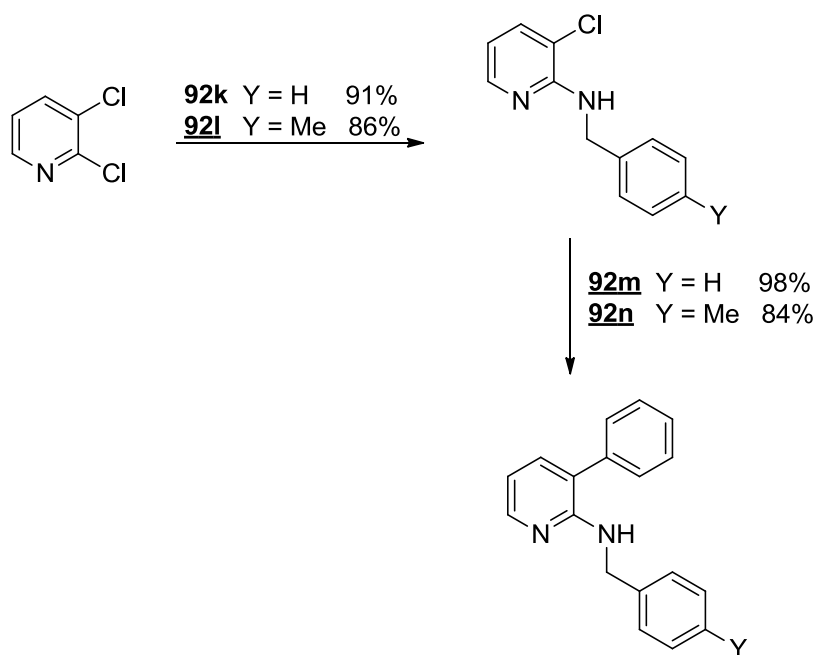
	R	yield [%]
91a	H	99
91b	2-Me	97
91c	naphtyl	94
91d	3-Me	97
91e	3-Cl	95
91f	4-Me	96
91g	4- <i>t</i> -Bu	94
91h	4-OMe	97
91i	4-F	99
91j	4-Cl	97
91k	4-CF ₃	98
91l	4-Ac	97
91m	4-NO ₂	97
91n	4-CN	99

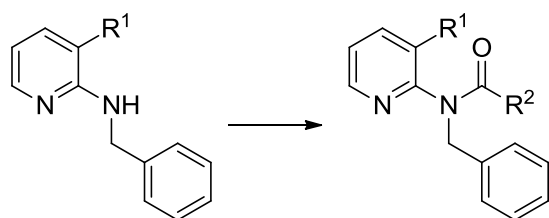
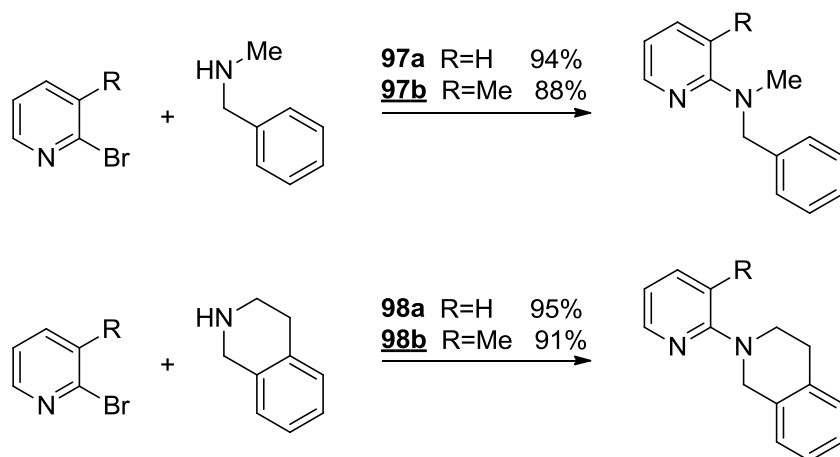
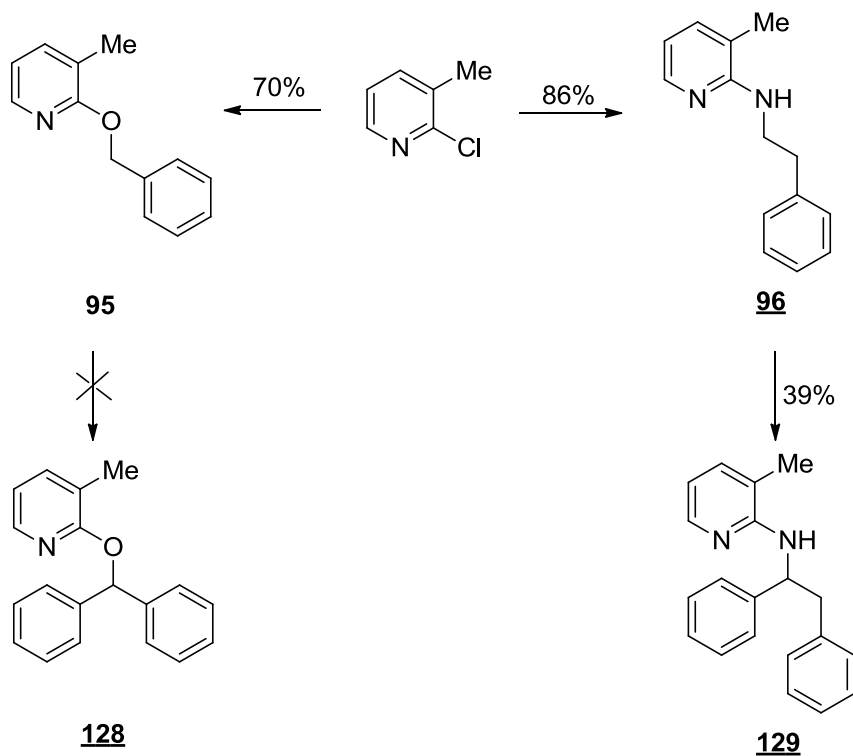


	R	Y	yield [%]
92a	Me	H	92
92b	Me	4-Me	88
92c	Me	4-OiPr	72
92d	Me	4-OMe	80
92e	Me	4-F	73
92f	Me	4-CF ₃	73
92g	Me	4-CO ₂ Me	87
92h	CF ₃	H	95
92i	CF ₃	4-Me	98



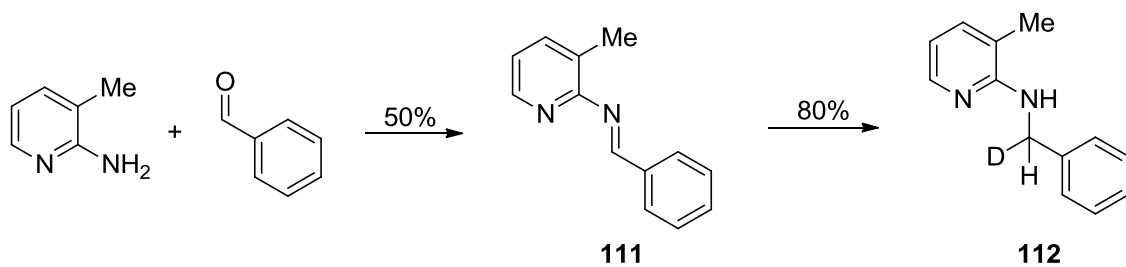
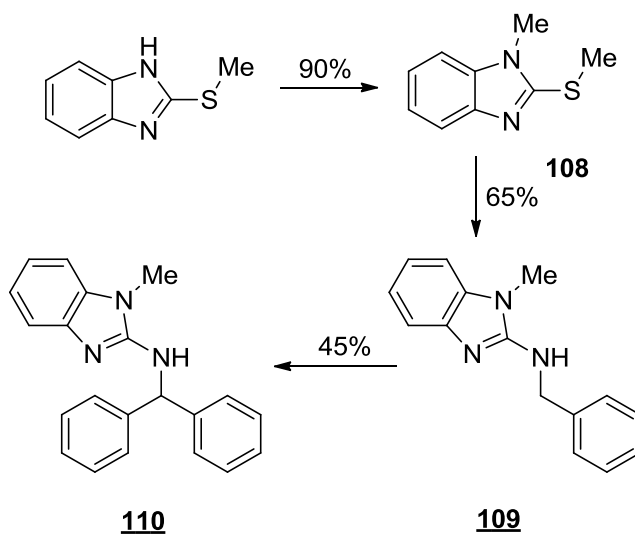
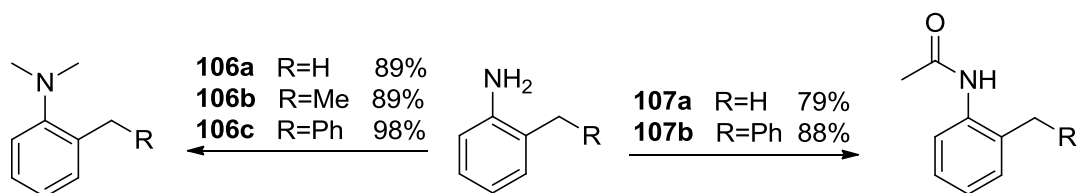
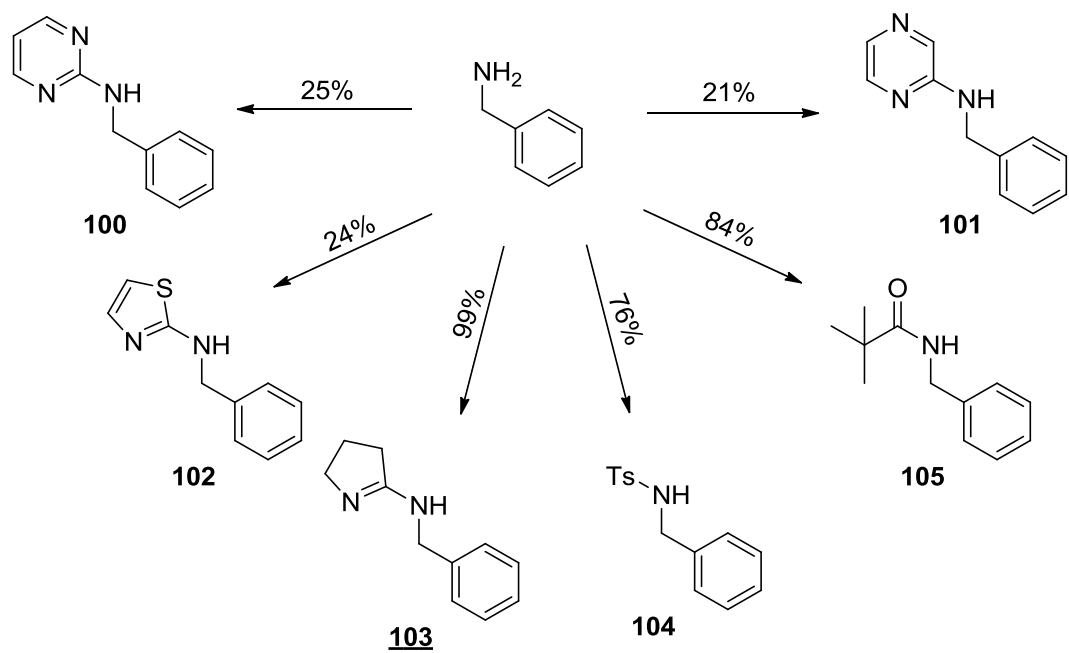
GENERAL SCHEMES



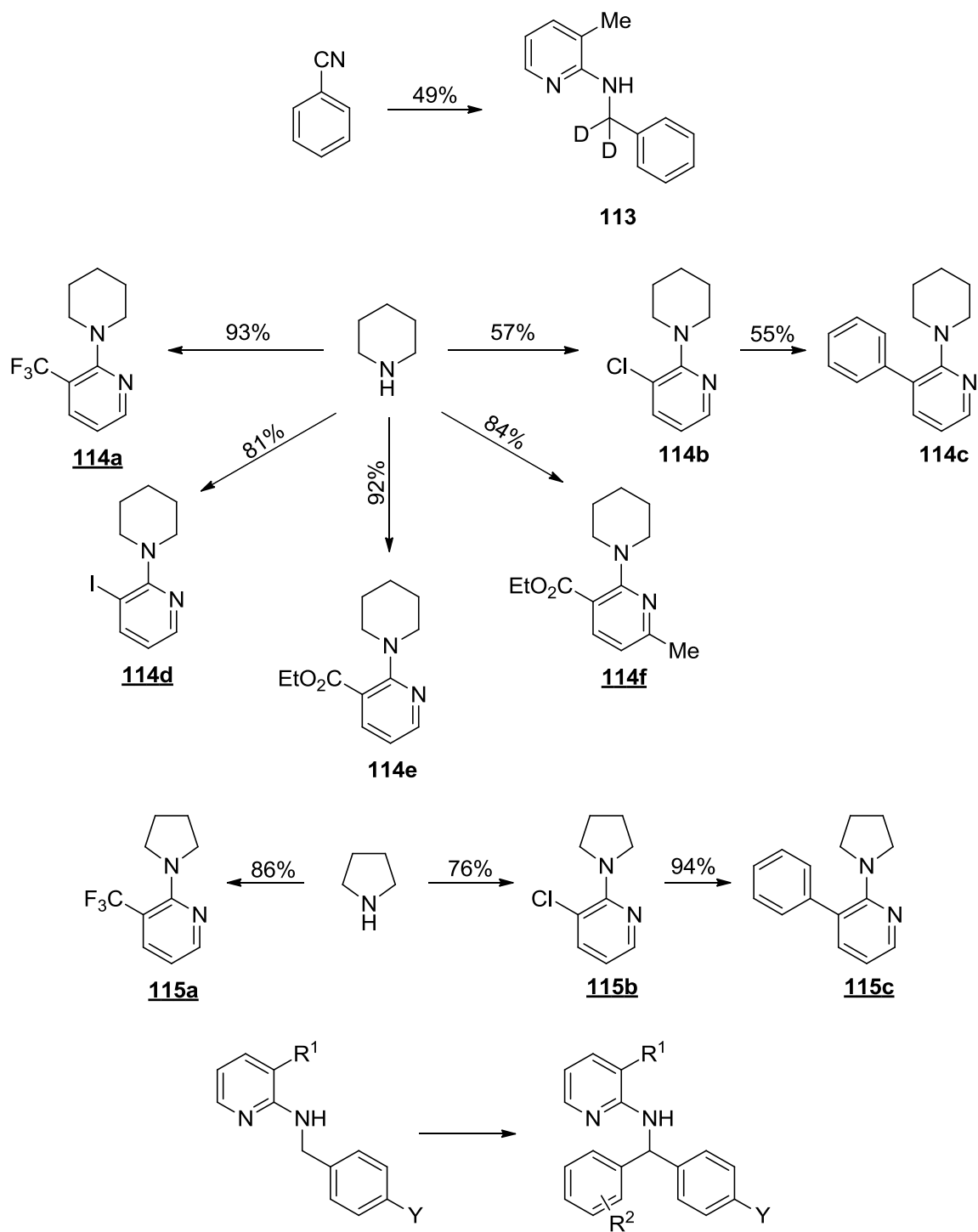


	R ¹	R ²	yield
99a	H	Me	94
99b	Me	Me	95
99c	H	Ph	78
99d	Me	Ph	83
99e	H	<i>t</i> -Bu	79
99f	Me	<i>t</i> -Bu	78

GENERAL SCHEMES



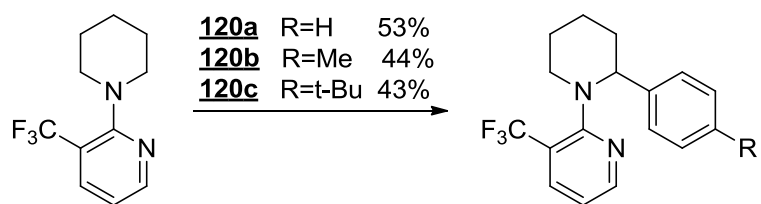
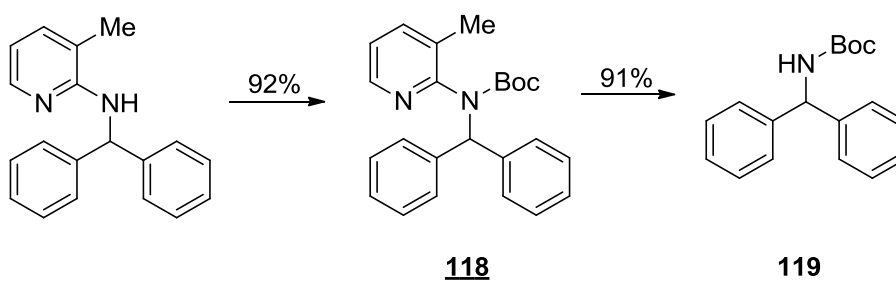
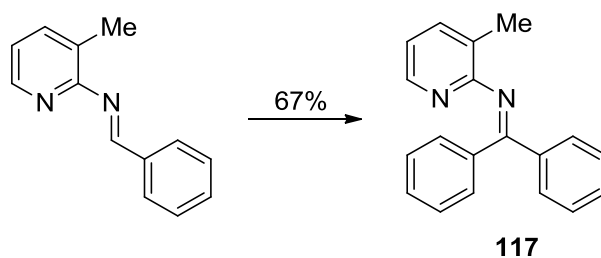
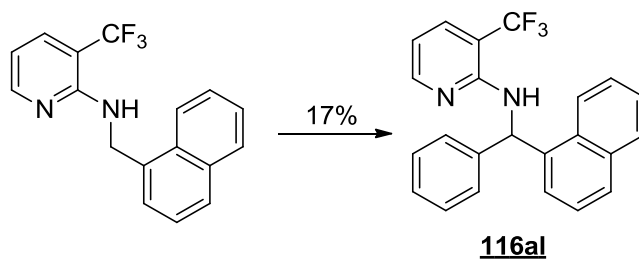
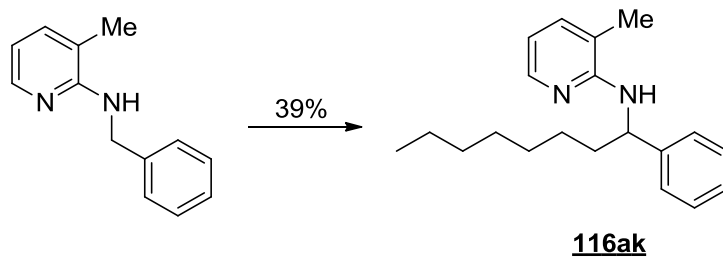
GENERAL SCHEMES



	R ¹	R ²	Y	yield [%]		
				method A	method B	method C
116a	Me	H	H	64	69	70
116b	Me	3-Me	H	61	55	72
116c	Me	3-OMe	H	--	60	--
116d	Me	3-Cl	H	38	37	--
116e	Me	4-Me	H	62	65	79

GENERAL SCHEMES

	Me	H	Me	76	48	--
<u>116f</u>	Me	4- <i>t</i> -Bu	H	64	64	--
<u>116g</u>	Me	4- <i>n</i> -Bu	H	--	67	--
<u>116h</u>	Me	4-OMe	H	39	63	64
	Me	H	OMe	32	28	--
<u>116i</u>	Me	4-NMe ₂	H	--	50	--
<u>116j</u>	Me	4-F	H	66	61	56
	Me	H	4-F	44	59	--
<u>116k</u>	Me	4-Cl	H	33	51	--
<u>116l</u>	Me	4-CF ₃	H	41	--	30
	Me	H	CF ₃	15	57	--
<u>116m</u>	Me	4-CO ₂ Et	H	--	33	--
<u>116n</u>	Me	H	O <i>i</i> Pr	25	43	--
<u>116o</u>	Me	H	CO ₂ Me	26	57	--
<u>116p</u>	Me	4-Cl	Me	50	--	--
<u>116q</u>	Me	4-CF ₃	Me	33	--	--
<u>116r</u>	CF ₃	H	H	78	--	--
<u>116s</u>	CF ₃	4-Me	H	77	--	--
	CF ₃	H	Me	80	--	--
<u>116t</u>	CF ₃	4- <i>t</i> -Bu	H	70	--	--
<u>116u</u>	CF ₃	4-OMe	H	61	--	--
<u>116v</u>	CF ₃	4-F	H	51	--	--
<u>116w</u>	Ph	H	H	90	70	48
<u>116x</u>	Ph	3-Me	H	--	68	58
<u>116y</u>	Ph	3-OMe	H	--	64	61
<u>116z</u>	Ph	4-Me	H	85	67	39
	Ph	H	Me	90	--	--
<u>116aa</u>	Ph	4- <i>t</i> -Bu	H	96	72	55
<u>116ab</u>	Ph	4- <i>n</i> -Bu	H	--	69	47
<u>116ac</u>	Ph	4-F	H	72	--	--
<u>116ad</u>	Ph	4-Cl	H	--	59	--
<u>116ae</u>	Ph	4-CO ₂ Et	H	--	42	--
<u>116af</u>	Ph	4-Ac	H	--	41	--
<u>116ag</u>	Ph	4-Me	Me	73	--	--
<u>116ah</u>	Ph	4- <i>t</i> -Bu	Me	67	--	--
<u>116ai</u>	Ph	4-F	Me	60	--	--
<u>116aj</u>	Ph	4-CF ₃	Me	33	--	--



1. Introduction

Organic chemists have always tried to obtain a better understanding for life. The synthesis of natural molecules and the creation of new compounds has consequently been a prior goal for them. Thus, the development of new synthetic methods is an essential part of this field. Organic chemistry has become the science of carbon-based compounds and is amongst other things focused on the formation of new C–C bonds. Carbon-carbon bond formation is a central part of many chemical syntheses, and innovations in these types of reactions will profoundly improve overall synthetic efficiency. Nowadays, there is a vast number of methods for the formation of this kind of bonds. Over 140 years ago, Glaser reported the first homocoupling of metallic acetylides.¹ He described the oxidative dimerization of copper phenylacetylide to give diphenylacetylene in an open flask. Following this development, the method was extended to C(sp²)-C(sp²) bond formation by Ullmann and further investigations of scientists such as Turner, Meerwein, Castro, and Stephens enriched this field with synthetic useful methods.¹ Hundred years after the discovery of Glaser, Heck published the first palladium catalyzed coupling of arenes with alkenes.² This was the initial trigger for palladium catalyzed carbon-carbon bond formation and opened a new field for organic chemists recently recognized by awarding the 2010 Noble Prize to Heck, Negishi,³ and Suzuki.⁴ Their observations revolutionized the way of constructing molecules and inspired plenty of chemists all over the world to develop a wide-range of additional cross coupling reactions.⁵ These days, cross coupling is an integral part of organic chemistry and it is used for many transformations in synthetic and industrial processes. Cross coupling methods are key steps in the synthesis of many pharmaceutical compounds, such as Losartan (angiotensin receptor blockers)⁶, Singulair (leukotriene inhibitor)⁷, and Gleevec (tyrosine kinase inhibitor)⁸ (Figure 1).

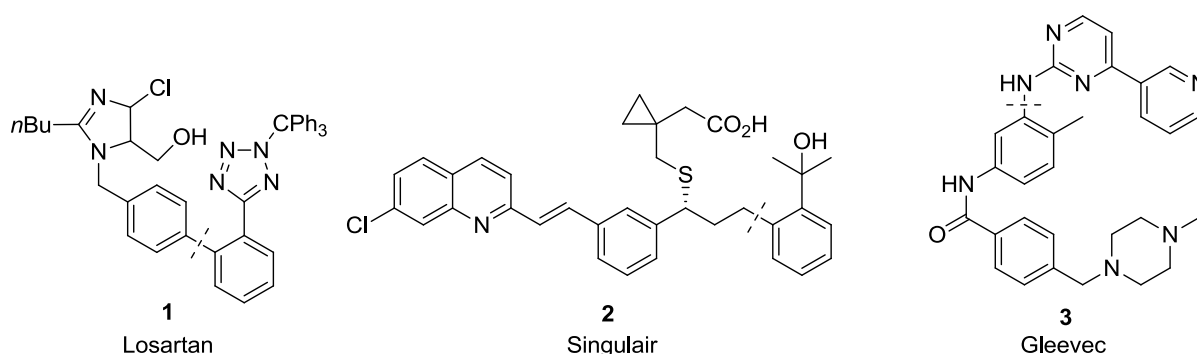


Figure 1 Cross coupling in the synthesis of pharmaceutical active compounds.

Although this field is well established, there are still a lot of challenges to overcome. The community is searching for new synthetic pathways, but also tries to find “greener” and milder conditions for commercial applications. By performing a reaction at lower temperature, for example, a catalyst can save energy in industrial processes and be more efficient. One other main task remains the reduction of waste arising during the production steps.

Commercial processes tend to give side products that have to be discarded, such as inorganic salts. Along this line, the idea of atom economy was designed which describes the efficiency of a process concerning the in- and outcome of reagents.⁹ The higher the value for the reaction, the “greener” the reaction is. For example, the Monsanto process is considered to be a “green” process because it converts MeOH and CO to MeCOOH with no atoms left over. The atom economy can be quantified by using the theoretical masses from the balanced equation.

$$\text{Atom economy (\%)} = \frac{\text{mass of desired products}}{\text{mass of total products}} \times 100$$

For a classical cross-coupling reaction (e.g. the Suzuki,¹⁰ Negishi,¹¹ or Stille¹² reaction) two functional groups are required, one organo metal and one organo halide species, to form a new C–C bond. In the Suzuki coupling, for example, a carbon-boronate and a carbon-halide derivative will be typically used. Thus, need several synthetic steps are eventually required for the introduction of these groups, which obviously requires time, energy, and produces waste. Besides, the atom economy of these reactions is usually not high due to the formed side products.

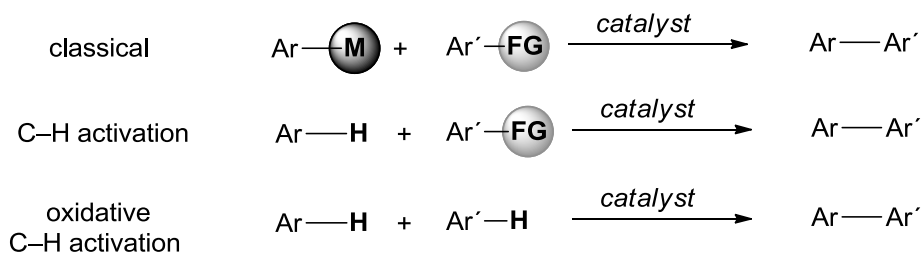


Figure 2 Classical cross coupling vs. C–H activation.

Therefore, one of the most important quests for synthetic chemists is the development of new, more efficient and direct transformations which allow eliminating synthetic detours. In this regard, the direct catalytic cleavage of C–H bonds is highly attractive and one of the most investigated but also most challenging topics in modern organic synthesis.¹³ The general aim of the so called “C–H activation” reactions is the introduction of groups with a higher complexity to hydrocarbon structures (Figure 2). The possibility of direct formation of a new C–C bond *via* a direct C–H bond transformation is a highly attractive strategy in covalent synthesis, owing to the ubiquitous nature of C–H bonds in organic substances and the high atom economy. These methods provide an alternative to the separate steps of prefunctionalization and defunctionalization that have traditionally been part of synthetic design. Furthermore, the range of substrates is immense, including hydrocarbons (lower alkanes, arenes and polyarenes), complex organic compounds of small molecular weight, and synthetic polymers.¹⁴

2. Objectives

Although many direct functionalizations for sp^2 -carbon centers have been reported in recent years,¹⁵ there are only few examples of performing such a transformation on an unactivated sp^3 -carbon center.¹⁶ The direct functionalization of sp^3 C–H bonds is a highly attractive process since regioselective functionalization of such sp^3 C–H bonds still requires multi-step sequences in many cases in order to address a specific C–H bond without compromising others. One outstanding quest is the development of new strategies for the direct arylation of such sp^3 -centers, which allows new environmentally and economically attractive pathways to C–C bond formation. These methods would allow an easy access to a multiplicity of biological interesting motifs. For example, molecules with a diarylmethylamine subunit represent a promising class of pharmaceutical active compounds.¹⁷ They are of great interest and many of them display antihistaminic (e.g. Cetirizine),¹⁸ antimalarial¹⁹ or antidepressant (e.g. Tianeptine)²⁰ activity (Figure 3). There are different strategies for synthesizing these structural motifs in the literature, ranging from nucleophilic substitution to asymmetric imine arylation.²¹ However, the direct arylation of benzylic amines would be a powerful tool for the synthesis of such compounds.

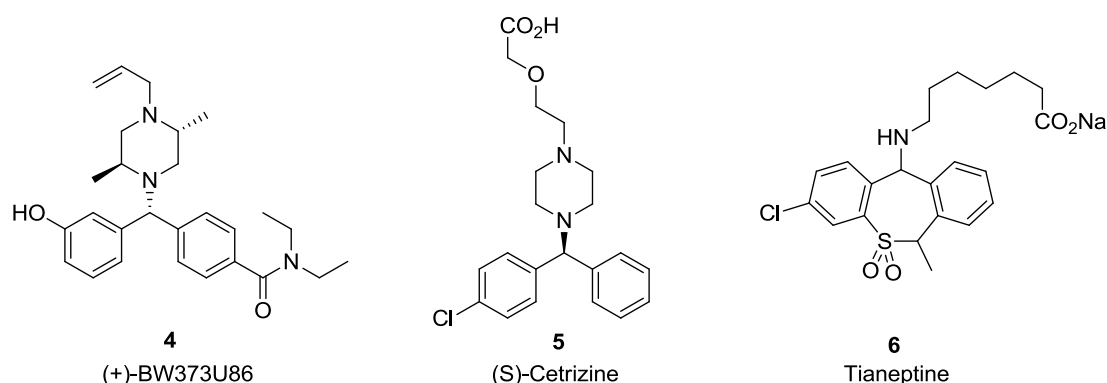
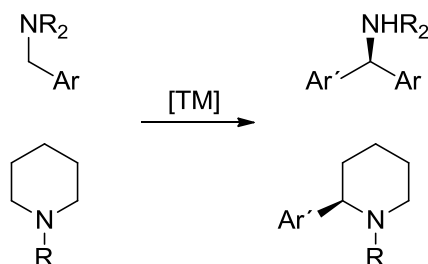


Figure 3 Pharmaceutical active compounds with diarylmethylamine subunit.

The goal of this thesis was to develop synthetically useful and simple methods for the direct arylation of cyclic (e.g., piperidine) and acyclic (e.g., benzylamine) amines. Furthermore, starting from a prochiral carbon-center, the transition-metal catalyzed reaction should be performed in an asymmetric way. The relevant theoretical information and results are discussed in the next chapters.



3. THEORETICAL BACKGROUND

This chapter covers some specific information, which is essential for a better understanding of the topic, starting from basic organometallic knowledge via cross-coupling methods to C–H bond functionalization, finally. However, this field is too vast to be covered in this thesis in a comprehensive fashion. There are excellent textbooks and reviews available, discussing the topic in more detail.²²

3.1 Homogeneous Catalysis

Catalysis of organic reactions has always been one of the most important applications for organometallic chemistry and continuously encouraged chemists to further developing the field. During the last decades, these catalysts were optimized constantly, and new ways for resolving economic and environmental problems were found. Organometallic catalysts are now being routinely applied in pharmaceutical, fine chemical, and commodity chemical industries. As the name already implies, homogeneous catalysts are soluble complexes in the same phase as the substrate, in contrast to the heterogeneous catalysts, where catalysis takes place on the surface. This solubility facilitates mechanistic investigations, since powerful methods such as NMR and IR can be used for assigning the structure and monitoring reaction conditions. On the other hand, a major disadvantage is difficult separation from the product, requiring additional time and special separation techniques.

A catalyst (and this applies to all kind of catalysts) usually binds the reactant and, subsequently, undergoes a series of transformations to generate the product. At the end of the catalytic cycle the reaction product is liberated and the catalyst is regenerated. As a consequence, the catalyst can be used for several catalytic cycles and is therefore administered in substoichiometric amounts for the desired reaction. Depending on the efficiency, the catalyst may participate in the catalytic cycle up to 10^6 times or more. The optimization of the catalyst for a specific reaction allows for reduction of catalyst amount to ppm regions. However, before setting out to find a catalyst for a given reaction, first consideration had to address thermodynamics: whether the reaction is favorable. One example is the conversion of H_2O to H_2 and O_2 , where the reaction is thermodynamically extremely disfavored, and no catalyst, however efficient, could bring about the reaction on its own. For such an unfavorable reaction, one needs to provide the necessary driving force in some way, such as coupling a strongly favorable process to the unfavorable one. This can be realized in different ways, for instance, by selective distillation of the product, or, as Nature commonly does, with the hydrolysis of the energy rich molecule ATP (adenosine triphosphate). But what does the catalyst actually do during the reaction? It reduces the free energy of the highest energy transition state and thereby increases the reaction rate (Figure 4).²³

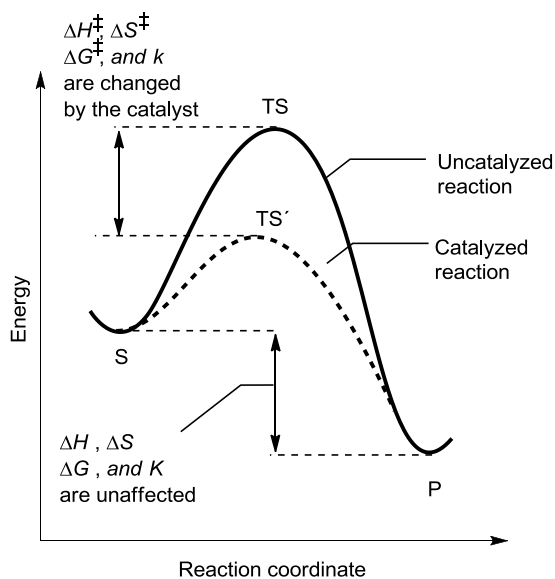


Figure 4 Reaction coordinate diagram for a catalyzed and uncatalyzed reaction.

Hence, the catalyst only increases the rate of the process and has no influence on the equilibrium, which is determined by the relative thermodynamic stabilities of substrate and product. However, it can influence the concentration of product for other reasons. According to Le Châtelier's principle, the equilibrium is shifted by changing the conditions, which can be the temperature, for instance. Subsequently, an exothermic reaction will form higher concentrations of product at lower temperatures. As already mentioned, a catalyst may not change the stability of the product, but possesses the ability to decrease the reaction temperature and therefore shift the reaction to the right side, resulting in a higher product concentration.

Because the transition state is an unstable species and is fleeting, the catalyst binds normally to the substrate and remains bound through the transition state of the catalytic process. The starting catalyst, or a species that will be converted to the starting catalyst, is then regenerated by dissociation of the product. The reaction coordinate shown in Figure 4 is the simplest way for a catalyst to act, but there are other possibilities for the catalyst to work, which complicate the case. Comparing the transition-state energies with ground-state energies of reactants and intermediates helps to get a better understanding for different kind of reactions.

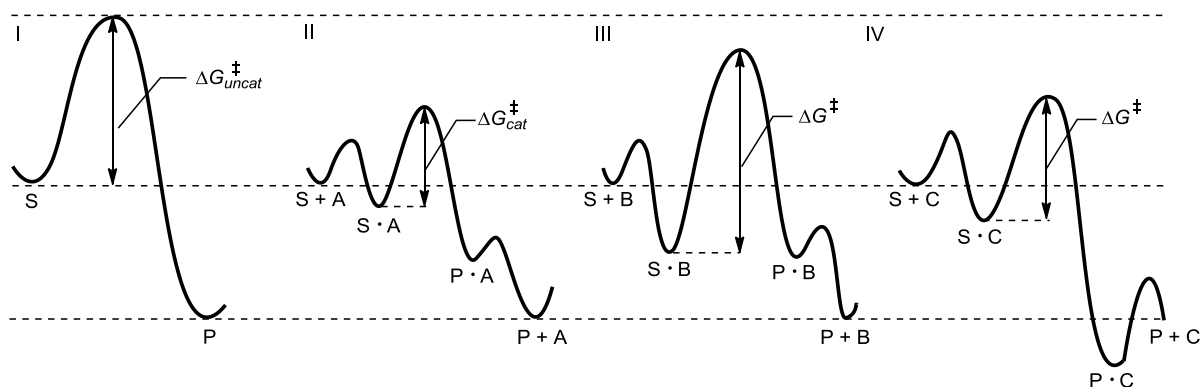


Figure 5 Reaction coordinate diagram for: I uncatalyzed; II catalyzed by A; III catalyzed by B; IV catalyzed by C.

Figure 5²⁴ illustrates three different options for an additive to react with the reactant. In the first case, the reaction is uncatalyzed. Reaction coordinate II corresponds to a catalyzed reaction, where catalyst A binds to substrate S before it undergoes rearrangement. This substrate-catalyst complex S·A has weak binding, but not too weak, otherwise substrate S would be excluded from the metal and fail to be activated by the metal at all. Thus, catalyst A stabilizes the transition state more than it stabilizes the ground state S (by forming S·A). Similarly, product P will be formed as the complex P·A. Species A releases the product and reforms A, which can now reenter the catalytic cycle and bind to the next substrate. This scenario constitutes a catalytic process and A can be considered as a catalyst. In the third case, additive B binds too strong to the substrate. Hence, additive B stabilizes S (by forming S·B) more than it stabilizes the transition state. The activation energy is higher than the uncatalyzed way, and S would be converted to P by the lower uncatalyzed pathway in the presence of substoichiometric amounts of B. In the last scenario, additive C binds too strong to the product, and the reaction ends with P·C. The catalyst C is “poisoned” and the complex P·C has to be dissociated by another reagent (such as water or acid). Thus, C is a reagent and not a catalyst, which can be used in substoichiometric amounts.

It is clear from this information, that identifying the right catalyst for the right reaction requires significant optimization. The catalyst is not allowed to bind too strongly to the reactant or product, but strong enough to stabilize the transition state. Fortunately, there are different possibilities to tune the metal center, for instance by choosing the right ligand. The nature and number of ligands are a key element in altering the electronic and steric environment of the metal and thus the reactivity of the complex. Endless ligands have been synthesized during the last decades and there is still a lot of work to do in this field. Figuring out a suitable ligand for the right reaction is a kind of art and needs a lot of experience. Small changes in ligand can entirely change the chemistry. The right choice of ligand relies often on empirical studies. However, there are different rules and principles one has to consider for determining the best ligand. Different ligands are discussed in the following chapters which allow a better understanding of the metal ligand interactions in this work.

3.2 Metal-Ligand Complexes

As already mentioned, the role of the ligand is crucial for transition-metal catalyzed reactions. Electron density, coordination number, and steric properties of the metal can be tuned by the ligand and there are many ways of interactions between the main group elements and the transition metals. This variety is a blessing and curse at the same time and choosing the right ligand is still something of an art because subtle stereoelectronic effects, still not fully understood, can play an important role. The interesting interactions for this work are discussed in the following chapters.

3.2.1 Carbon Monoxide Ligand

CO binds to transition metals as a neutral ligand and is most commonly bound to the metal through the lone pair of electrons on carbon. In contrast to the dative ligands, such as NH_3 , which are good σ donors but no significant π acceptors, CO is an exceptional good π acceptor. This π accepting interaction is extremely important for the stabilization of complexes in low formal oxidation states. CO is a very high field ligand and forms strong M–L bonds. The right symmetry of the π^* orbital allows a strong overlap with the filled d_π orbital of the metal and to generate a lower energy filled bonding orbital and a higher energy unoccupied antibonding orbital (Figure 6).²⁵

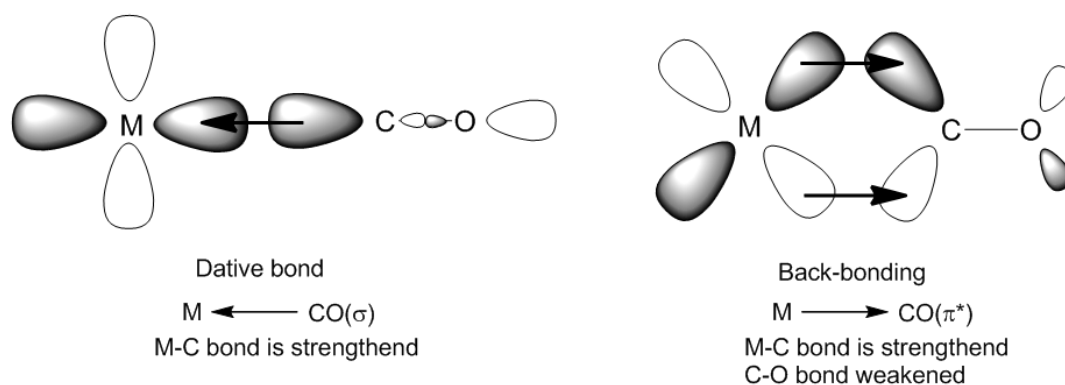


Figure 6 π -Back bonding for a CO ligand.

This backbonding is a key feature of M–L bonds, where L is unsaturated (i.e., has multiple bonds). The frontier orbitals of each fragment dominate the bonding. The HOMO (= highest occupied molecular orbital) of each fragment, M and L, is usually closest in energy to the LUMO (= lowest unoccupied molecular orbital) of the partner fragment than to any other vacant orbital of the partner. While the LUMO of L accepts electrons of the HOMO of the metal, the HOMO of the ligand is a donor to the LUMO of the metal. This backbonding leads to strong metal-carbonyl complexes, which makes the complexes (e.g., $\text{Ru}_3(\text{CO})_{12}$) often air and water stable. It is expected, that the smaller the HOMO-LUMO gap of the partners, the stronger the bonding is (Figure 7).²⁶

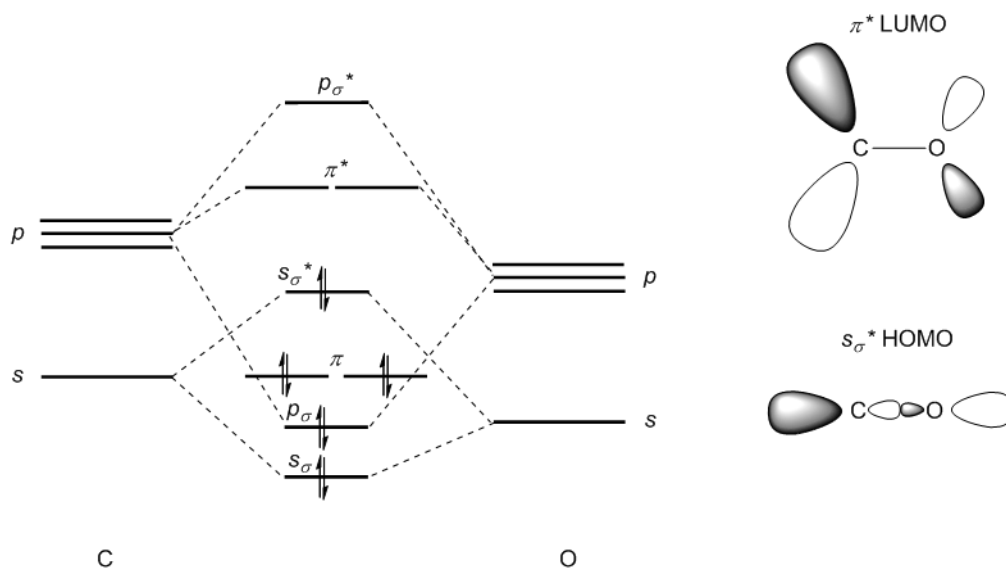


Figure 7 HOMO and LUMO of CO.

Two important consequences occur from this information:

1. CO binds strongly to electron-rich, low valent metals. Hard Lewis acids, such as a proton, or d^0 transition metal complexes are a poor match for the soft carbon on CO. The metal has to be of d^1 or higher configurations, which explains why metals such as Ti^{4+} seldom form stable complexes with CO.
2. The donation from low-valent, electron-rich metals into the LUMO of CO, which is the π^* orbital, provides an additional bonding interaction but also weakens the C–O bonding strength which can be detected by IR.²⁵

3.2.2 Organic Carbonyl Ligands

Organic carbonyls such as ketones, aldehydes, esters, and amides have two binding options: an η^1 -mode through the carbonyl oxygen or in an η^2 -mode that is analogous to the binding of an alkene. The way of binding depends on the electron density of the metal:

1. Electron poor, hard transition metal centers, such as Lewis-acid early transition metals, tend to bind to oxygen, because they are less capable of participating in backbonding into the carbonyl π -system.
2. Electron rich, soft transition metal centers, such as low-valent late transition metals, tend to bind in an η^2 -fashion and create stable complexes by back-donation into the C=O π^* orbital.

However, some metal species, such as the low-valent, cationic, middle transition metals, can bind with nearly equal energies in both modes (Figure 8).²⁷

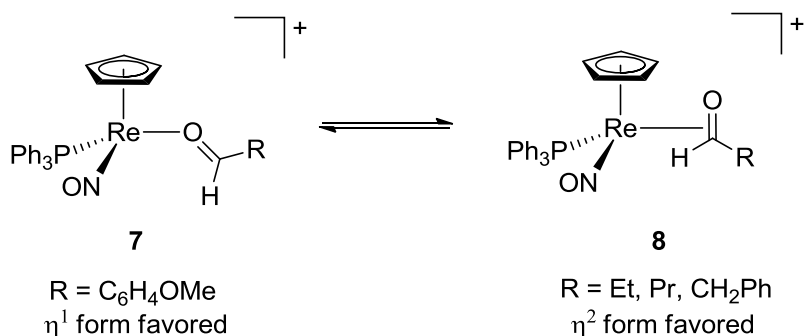


Figure 8 η^1 -Mode vs. η^2 -mode for the binding of a carbonyl group.

If the metal-oxygen binding is weak enough not to create a stable complex, one can use this kind of binding for directing the metal center to a specific position (the so called cyclometalation) which is discussed in the chapter 3.5.3.

3.2.3 Phosphine Ligands

The disadvantage of CO is that there is no way to manipulate the properties of the ligand. In contrast, tertiary phosphine ligands, PR_3 , can be tuned electronically as well as sterically in different ways and be altered in a systematic and predictable way over a very wide range by varying the substituents on phosphorus (Figure 9).²⁸

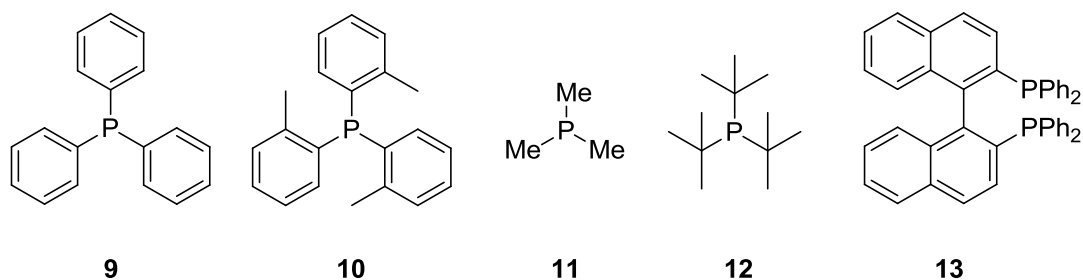


Figure 9 Different phosphine ligands.

The soft phosphorus donor matches well with soft low-valent metals. Their ability to promote catalytic reactions is remarkable. During a catalytic reaction, the metal species is constantly changing the oxidation state. Phosphines are ligands of intermediate hardness and π -acceptor power and therefore able to stabilize a broad range of oxidation states. Though, the π -acidity depends strongly on the nature of the R group. Since the phosphine has no double bonds and therefore no π^* -orbital, the σ^* -orbital plays the role of acceptor. Originally, the π -acceptor orbitals were considered to be the phosphorus 3d orbitals, but more recent studies on the potential of phosphines and phosphites to act as π -acceptors have indicated that the acceptor orbital is a hybrid of the P–R σ^* -orbitals and the phosphorus d-orbital with the dominant component the P–R σ^* -orbitals. In contrast, the N–H σ^* antibonding orbitals are of high energy and do not serve as good acceptor ligands (Figure 10).²⁸

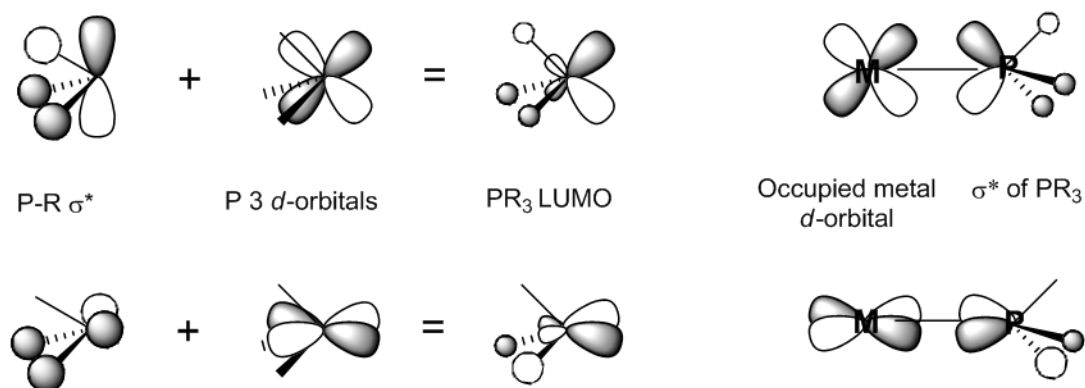


Figure 10 Orbital interaction of the phosphine to the metal.

These investigations lead to the following conclusions:

1. Whenever the R group becomes more electronegative, the orbital that the R fragment uses to bond to phosphorus becomes more stable and subsequently the σ^* -orbital of P–R becomes also more stable.
2. The contribution of the phosphorus to the σ^* -orbital increases simultaneously which leads to a better overlapping of the metal and phosphine orbitals (Figure 11).²⁸

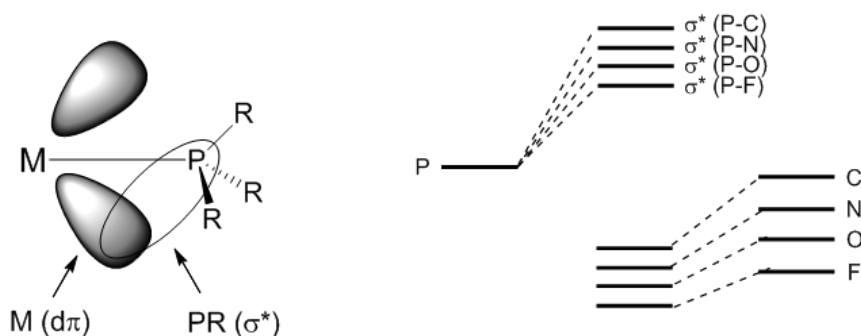
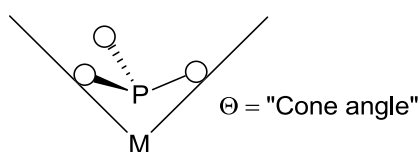


Figure 11 Electronic influence of the phosphine substituent on the M–P bonding.

Both of the factors make the empty σ^* -orbital more accessible for back donation which results in an increase of the π -acidity. π -Acidity is weak for alkyl phosphines; aryl, dialkylamino, and alkoxy groups are on the other hand more effective in promoting π -acidity. In the extreme case of PF_3 , the π -acidity exceeds that of CO : $\text{PMe}_3 \approx \text{P}(\text{NR}_2)_3 < \text{PPh}_3 < \text{P}(\text{OMe})_3 < \text{P}(\text{OPh})_3 < \text{PCl}_3 < \text{CO} \approx \text{PF}_3$. On the other hand, trialkylphosphines are the most electron donating of dative phosphorus ligands, and arylphosphines are less electron donating. This trend is observed, in part, because the greater s -character of the sp^2 hybridized orbital of the aryl group makes it a weaker electron donor than an alkyl group.

Besides the electronic properties, phosphines have the advantage to influence the reactivity of a catalyst by steric properties. Much effort has been spent to describe the steric effects of the ligand. The “cone-angle”, a well-established parameter described by Tolman, provides a rough measure of trends in steric properties. The value of the angle is defined by the outer

edge of the substituents at phosphorus and the metal center of a space-filling model (Figure 12).



phosphorus ligand	cone angle (°)
PH ₃	87
PF ₃	104
PMe ₃	118
PPh ₃	145
PCy ₃	170
P(o-Tol) ₃	194

Figure 12 Cone-angle of different phosphine ligands.

The cone angle depends on the conformation of the ligand, which in turn depends on the conformation of the complex. As a consequence, it can vary significantly from one structure to another, because it is based on the conformation that is the least hindered. The determination for unsymmetrical ligands is more complicated and difficult to predict. But how do the electronic and steric properties influence the catalysis? The answer results from the following facts:

1. The equilibrium for the dissociation of the ligand from the metal is correlated to the cone angle. Tolman described the increase of ligand dissociation in NiL₄ complexes and in related palladium complexes in the following order: PMe₃ < PMe₂Ph < PMePh₂ < PPh₃ < PiPr₃ < PCy₃ < PPh/Bu₂. There are different ligand dissociations and associations to the metal center, which take place during a catalytic reaction. Thus, the coordination number of the metal varies in different steps, which allows in turn different catalytic pathways. With increasing cone angle, the ligand can easier dissociate and opens a vacant side of the metal for the subsequent reaction (e.g., oxidative addition). Grubbs, for instance, has studied different nickel complexes in the presence and absence of excess phosphine and has found that there are three decomposition pathways, one for each of the different intermediates, 14e⁻, 16e⁻ and 18e⁻ that can be formed (Figure 13).²⁹

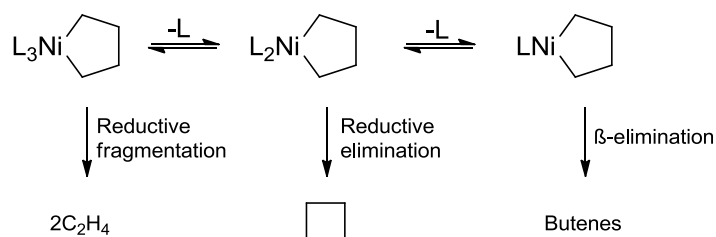


Figure 13 Different pathways for the nickel complex depending on the ligand dissociation.

2. In contrast to CO, where as many can bind as are needed to achieve 18e⁻, only a certain number of phosphines can fit around the metal. By using bulky PR₃ ligands, low-coordinated metals can be favored, which have still room for small but weakly binding ligands. That would be excluded by a direct competition with a smaller ligand such as PMe₃ or CO. This

small ligand is the substrate (e.g. an alkene or carbonyl group) and can be converted to the product.³⁰

3. A key feature of PR_3 ligands is that the electronic effects can easily be changed without changing steric effects (e.g. PBU_3 vs. P(OiPr)_3) or the steric effects without changing electronic effects (e.g. PMe_3 vs. P(o-toly)_3). Increasing the electron donor strength, for example, can favor a higher oxidation state and thus shift an oxidative addition/reductive elimination equilibrium in favor of the oxidative addition product.

3.2.4 Amino Ligands

Amines are less commonly used as ancillary ligands in organo-transition metal compounds. Besides the reactivity of the N–H proton, tertiary amines bind weakly. This is the result of the shorter C–N bond in comparison to the C–P bond, which leads to a larger C–N–C bond angle relative to the C–P–C bond. Thus, complexes of tertiary amines tend to be more sterically congested. This fact, together with the hard-soft mismatch with most metals, causes amines to bind weaker to the metal than phosphines. However, unsaturated imines, pyridines, and oxazolines are better suitable, since these compounds can act as π -acceptors and have no N–H bonds (Figure 14).³¹

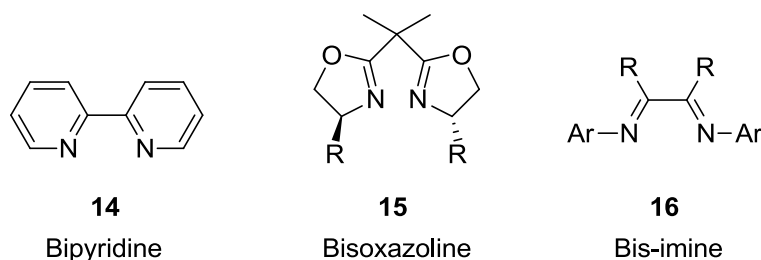


Figure 14 Different unsaturated amine ligands.

In the case of monoimines, the intrinsic reactivity of the functional group has to be considered rather than complexing effects as ligands. These motifs bind more often to transition metals through the lone pair on nitrogen than through the C=N π -system. For this reason, imine complexes of transition metals often react with external nucleophiles at the imine carbon rather than undergoing intramolecular processes that parallels the reaction of η^2 -olefin complexes. This fact can be exploited to create chiral amines for instance by the rhodium-catalyzed arylation of *N*-tosylarylimines with arylboronic acids, which is an alternative pathway to diarylmethylamines (Figure 15).³²

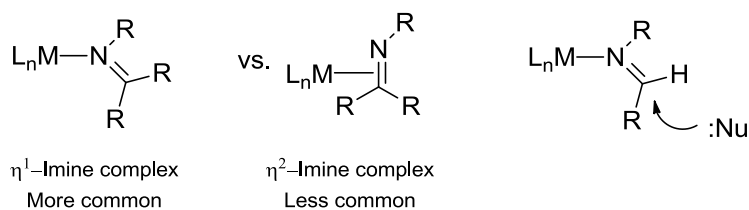


Figure 15 Reactivity of η^1 -imine complexes towards nucleophiles.

3.3 Cross Coupling Reactions

As already mentioned, cross-coupling reactions represent a class of synthetic transformations, where an organometallic reagent (that contains a main group metal in most cases) is reacting with an organic electrophile in the presence of a transition-metal catalyst to achieve a new C–X, (X = C, H, N, O, S, P, or M) bond. Many organometallic reagents (such as organoboron, organotin, organosilicon, or organozinc) as well as electrophiles and metal complexes have been successfully employed in these reactions. Since C–H activation can occur by a similar mechanistic pathway, relevant mechanistic aspects of cross-coupling are discussed in the following chapters.

3.3.1 Catalytic Cycle

By definition, a catalyst is lowering the energy of the highest transition state, as shown in Figure 16, by interacting with the substrate and stabilizing a structure that is similar to that of the uncatalyzed reaction. Diels Alder reactions, for example, can be catalyzed often by Lewis acids, which change the electronic properties of the substrate and subsequently reduce the barrier for the [4+2] cycloaddition (Figure 16).³³

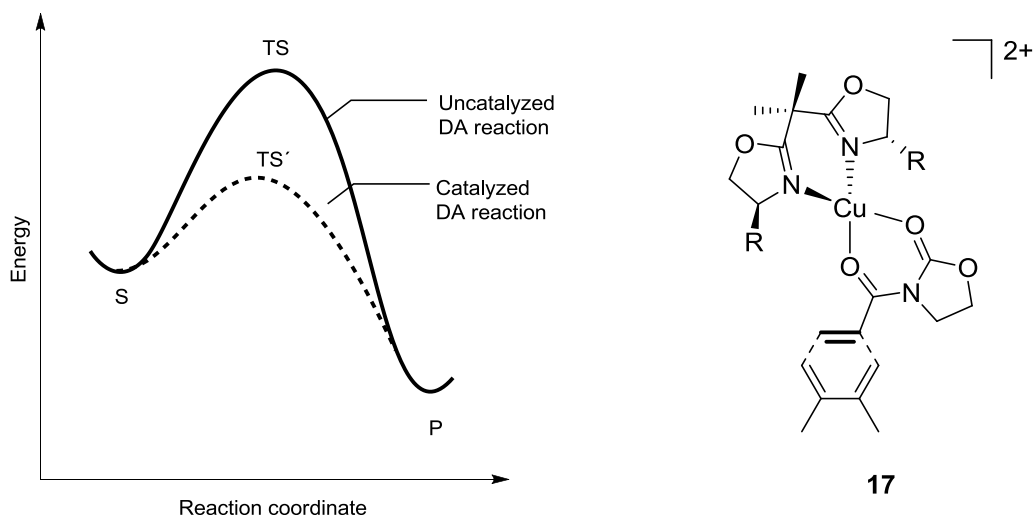


Figure 16 Functionality of a catalyst in a Diels Alder reaction.

However, in most of the organometallic reactions, the catalytic reaction occurs by a completely different mechanism in comparison to the uncatalyzed reaction. Normally, the catalytic reaction occurs by more steps where the activation energy of each individual step is lower than the activation energy of the uncatalyzed reaction and therefore has a lower overall barrier. Thus, the transition metal stabilizes the intermediates that are stable only when bound to the metal. Since the catalyst has to be regenerated after each turn, and the starting point of the process is also the end point of the process, the combination of steps can be illustrated as a catalytic cycle (Figure 17). Each catalytic cycle corresponds to one catalytic turnover. The efficiency of the catalyst can be conveniently given in terms of the turnover frequency (TOF)

measured in turnovers per unit time; the lifetime of the catalyst before deactivation is measured in terms of total turnovers (or total turnover number TTN).³⁴

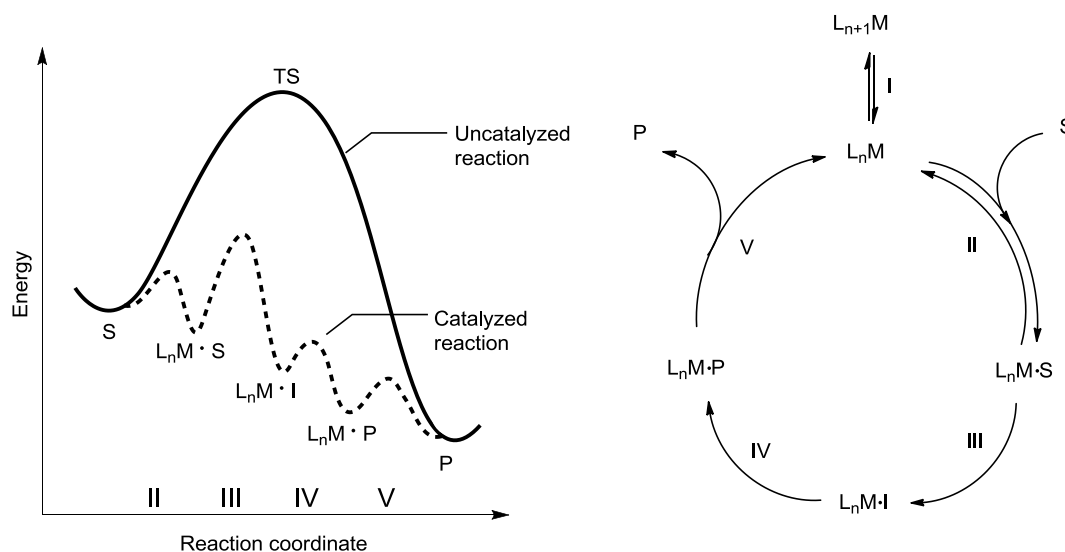


Figure 17 Reaction coordinate for a catalytic cycle.

The catalytic process consists of the following steps:

1. The catalyst precursor, $L_{n+1}M$, is converted to the active catalyst L_nM .
2. The active catalyst binds to the substrate and forms a catalyst-substrate adduct, $L_nM \cdot S$.
3. This adduct undergoes some kind of transformation on the metal to form intermediate $L_nM \cdot I$.
4. The intermediate is converted to $L_nM \cdot P$.
5. Dissociation of the product P regenerates the catalyst, which can reversibly exit the catalytic cycle by coordination of the ligand L to form $L_{n+1}M$ or bind another substrate molecule to restart the cycle.

This reaction pattern is also valid for cross coupling reactions (Figure 18). The mechanism of the various cross-coupling reactions, with the exception of the Heck reaction, includes three main stages: oxidative addition, transmetalation, and reductive elimination. In general, a low valent metal complex of $Pd(0)$ or $Ni(0)$ enters the catalytic cycle and undergoes oxidative addition with an aryl halide to form an aryl palladium or aryl nickel halide complex. This complex, in turn, reacts with the organo metal reagent, generating a species bearing two metal-carbon bonds. This order of steps can vary for C–H activation reactions:

1. First, oxidative addition into the C–H bond and subsequent transmetalation with the aryl halide can take place;

or

2. First, oxidative addition into the aryl halide bond occurs followed by subsequent transmetalation with the C–H substrate.

Subsequent *cis*-isomerization and reductive elimination deliver the final product and regenerate the active catalyst which can bind to the next substrate. The specific steps of this cycle are discussed in more detail in the following chapters.

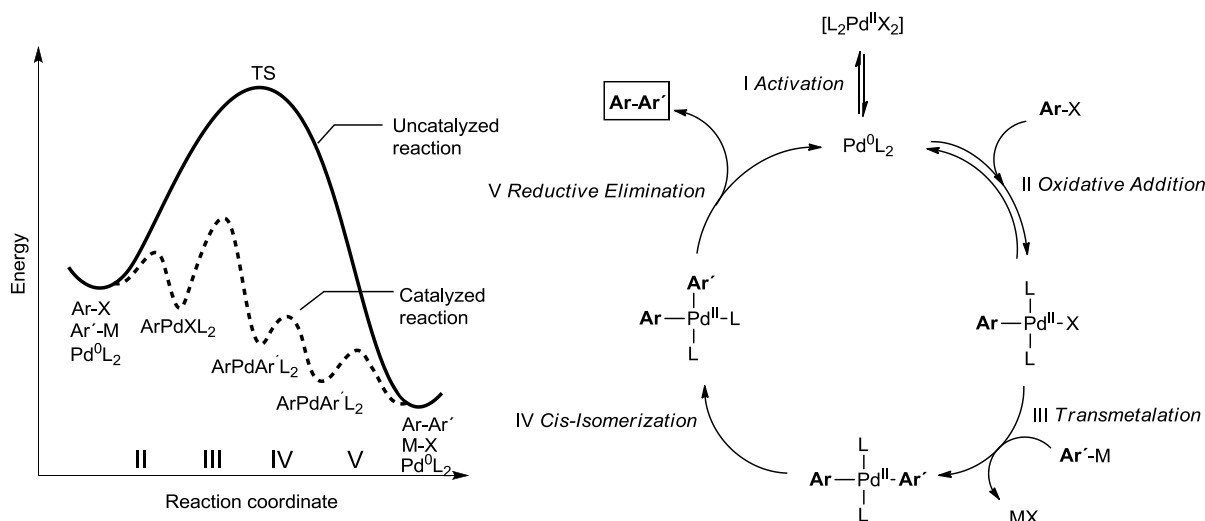
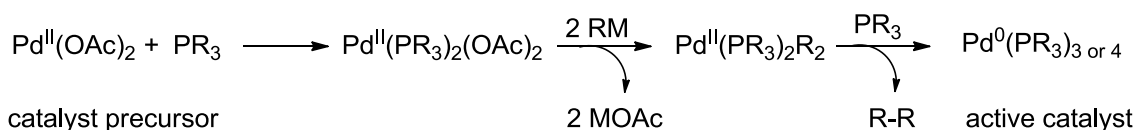


Figure 18 Reaction coordinate for a cross coupling reaction.

3.3.2 Catalyst Activation

The efficiency of the catalytic cycle depends on the concentration of the active catalyst. Maximum efficiency is achieved when all of the catalyst is active and participates in the catalytic cycle. The active catalytic species can be generated in different ways, for instance, by a combination of different precursors. Likewise, the active catalyst in many palladium catalyzed cross-coupling reactions is generated by addition of a phosphine (e.g., PPh₃) to Pd(OAc)₂ which generates an active Pd(0) complex (Scheme 1). The efficiency of the catalyst is often limited by the rate and yield for formation of the active catalyst by the precursors.³⁵



Scheme 1 Activation of Pd(OAc)₂ catalyst with PPh₃.

As shown in Scheme 1, the active Pd(0) species is commonly generated by dissociation of a dative ligand which depends on the equilibrium between [L₂Pd(II)X₂] and [L₂Pd(0)]. This equilibrium lies external to the catalytic cycle and determines the concentration of the active Pd(0) species that can undergo oxidative addition with the Ar-X compound. This equilibrium can be influenced by the amount of phosphine or by addition of other types of co-catalysts (e.g., protic acids or Lewis acids) which can promote the reaction.

3.3.3 Oxidative Addition

In the oxidative addition step a bond is broken and the oxidation state, the coordination number, and the electron count of the metal all raise by two units (Figure 19). This requires the metal fragment to be stable at +2 higher oxidation state, to tolerate an increase of the coordination number by two, and to accept two more electrons. This last condition requires that the metal fragment has a vacant $2e^-$ site and be an $16e^-$ or less complex. An $18e^-$ complex has to lose first at least one $2e^-$ ligand such as PPh_3 or Cl^- to undergo oxidative addition. As a consequence, oxidative additions are particularly favored for electron rich (i.e., low-valent) late transition metals such as Rh(I) , Ir(I) or Pt(0) . It should also be mentioned, that only the formal oxidation state of the metal is increased by two. The real charge on the metal changes much less than that because A and B do not end up with pure -1 charges in LnM(A)(B) .³⁶

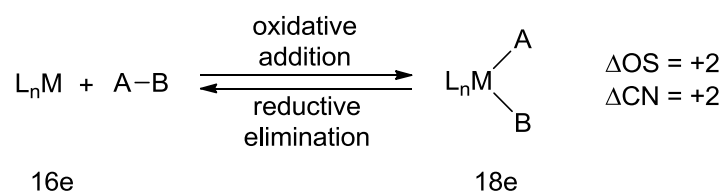


Figure 19 Oxidative addition vs. reductive elimination.

There is a transfer of two electrons from the metal to the σ^* -orbital of the A–B bond leading to concomitant breaking of this bond, and of the A–B electrons to the metal, resulting in a new M–A and M–B bond. However, the oxidative addition is always in equilibrium with the reductive elimination process, which is just the reversed reaction. This equilibrium depends on two factors: (i) preference of the metal based on oxidation state; (ii) preference of the A–B bond based on bond strength. Metals in reduced state prefer oxidative addition, while metals in higher oxidation state undergo reductive elimination. Although oxidative additions and reductive eliminations are in principle reversible reactions, the position of the equilibrium, which is governed by the overall thermodynamics of the species involved, is often completely shifted to one of the sides. For instance, the oxidative addition is enthalpically favored when the strengths of the two new M–A and M–B bonds exceed the strength of the initial A–B bond. This is the reason why weak carbon-iodine bonds tend to give the oxidative addition product, since the resulting metal-iodide bond is similar in strength to the metal-methyl bond. Strong C–H bonds, in contrast, are often formed from C–M–H complexes by reductive elimination.³⁷ The relative rates for oxidative addition of aryl halides follow the trend $\text{ArI} > \text{ArBr} > \text{ArCl}$, and the relative rates for reactions of aryl sulfonates follow the trend $\text{ArOTf} > \text{ArOTs}$. Another point that has to be considered is the entropy: Although the oxidative addition of the C–H bond of methane and the C–C bond of ethane would be slightly favored enthalpically, the free energy is positive because of the large positive $T\Delta S$ term for the process that generates one product from two reactants.

For cross coupling reactions, the oxidative addition normally occurs to a low-valent Pd(0) species, such as $14e^-$ bisphosphine compound or a $12e^-$ monophosphine compound. Furthermore, as already discussed in chapter 3.2.3, ancillary ligands can significantly change

the thermodynamics for an oxidative addition reaction. The electronic and steric properties of phosphines are crucial for the oxidative addition. For example, electron rich ligands promote the oxidative addition reaction by stabilizing the higher oxidation state of the metal. Complexes bearing hindered monodentate ligands undergo faster oxidative addition than ligands with less hindered substituents (Figure 20).³⁶ This phenomenon is observed because steric hindrance of the ligand enables better dissociation from the metal and, subsequently, higher concentration of the unsaturated, activated intermediate. The less reactive aryl chlorides react in general with complexes containing strongly electron-donating and sterically hindered ligands, such as trialkyl or biaryl alkylphosphines.

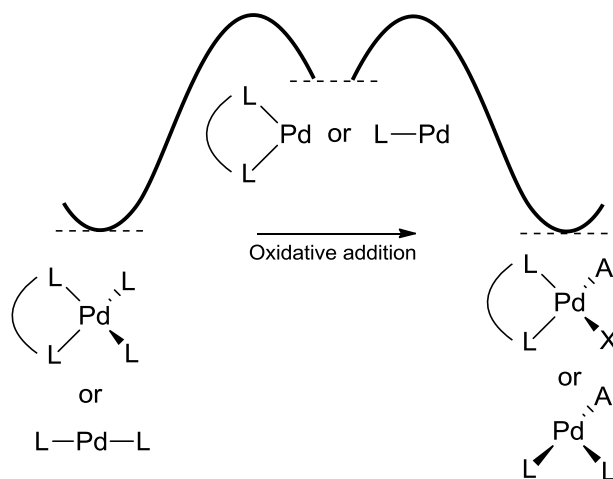


Figure 20 Energetic process for an oxidative addition.

There are different mechanisms for oxidative addition. Nonpolar reagents, such as H_2 or $C-H$, and aryl halides tend to react via a concerted, three-center oxidative addition. In this case, the metal-complex binds as a σ -complex to the $A-B$ bond and then undergoes $A-B$ bond breaking as a result of a strong back donation from the metal into the σ^* -orbital of $A-B$ (Figure 21).³⁸ The addition progresses with retention of stereochemistry at carbon, as expected from the mechanism. It can happen sometimes that the formed σ -complex is too stable and the reaction stops at this stage.

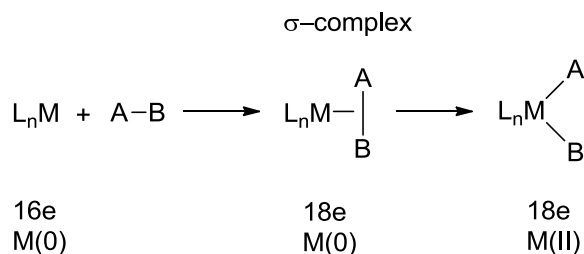


Figure 21 Mechanistic pathway of an oxidative addition.

One of the best studied cases is the addition of H_2 to the $\text{IrCl}(\text{CO})(\text{PPh}_3)_2$, Vaska's complex **18** (Figure 22). The addition occurs to the $16e^-$ square planar d^8 species **18** and forms over an $18e^-$ trigonal bipyramidal species **19** an $18e^-$ d^6 octahedral dihydride complex **20**.³⁶

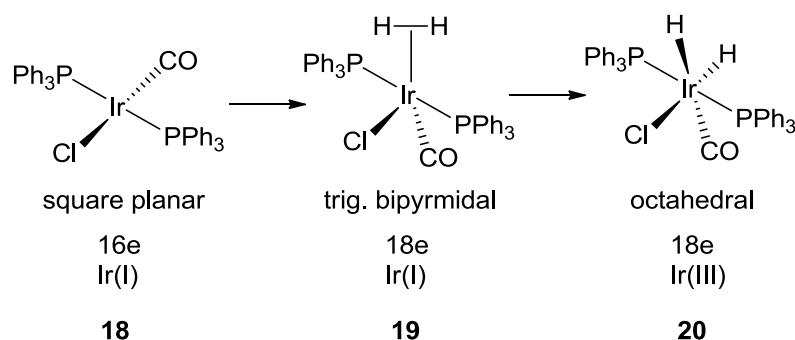


Figure 22 Oxidative addition of H₂ to the Vaska's complex.

Table 1 compares the bond energies for the iridium-methyl, -hydride, and -iodide bonds of different Vaska-type complexes and the corresponding Ir(III) complexes Cp*Ir(PMe₃)X₂. The values for the metal-ligand bond strength in Cp*Ir(PMe₃)X₂ are much higher than those for the same metal-ligand bonds in Vaska-type complexes, supporting again the strong influence of the ligands.³⁹

Table 1 Comparison of different bond energies for two different iridium complexes.

X	Cp*Ir(PMe ₃)X ₂	L ₂ Cl(CO)IrX ₂
H	74.2	60
Cl	90.3	71
Br	76.0	53
I	63.8	35
CH ₃		35.4
C ₆ H ₅	80.6	

^aAverage uncertainties in absolute bond strength values are on the order of ±5 kcal/mol.

The value for the addition of the C–C bond of ethane is thermodynamically more favorable than the addition of the C–H bond. However, the addition of the C–H bond is kinetically favored. There is no example in the literature where the intermolecular oxidative addition of the C–C bond of an alkane is faster than intermolecular addition of the C–H bond of the alkane. Chatt and Davidson reported the first example of the oxidative addition of a C–H bond to a zero-valent ruthenium center to give the Ru(H)(2-naphthyl)(dmpe)₂ [dmpe = 1,2-bis(dimethylphosphino) ethane] complex **22**, which is in equilibrium with a coordinated naphthalene ruthenium complex, [Ru(naphthalene)(dmpe)₂] **21** (Figure 23).⁴⁰

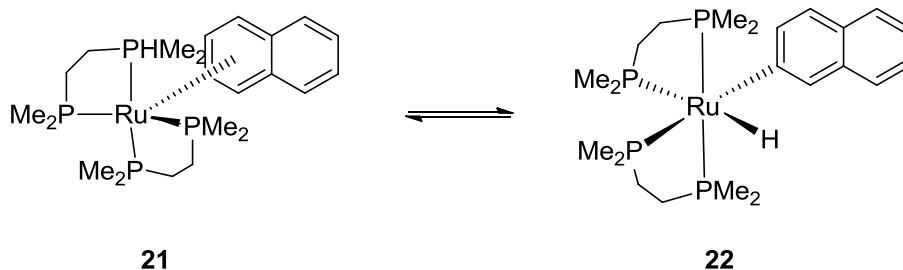
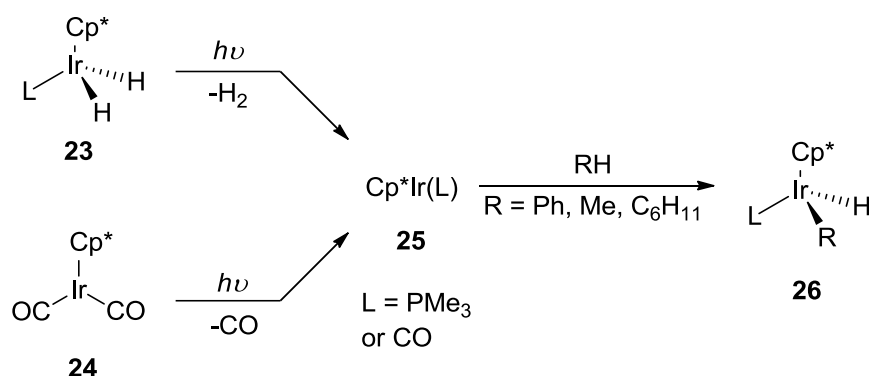


Figure 23 Oxidative addition of the C–H bond of naphthalene.

They also reported, that the sp^3 C–H bond of the methyl group in the dmpe ligand can be cleaved by the ruthenium(0) complex.⁴¹ However, the addition of arene C–H bonds is both, kinetically and thermodynamically favored over the addition of alkane C–H bonds, even though the arene C–H bonds are stronger than the alkane C–H bonds. This is the result of the following factors:

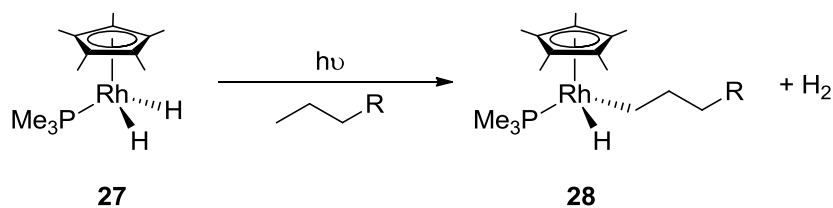
1. The arene is coordinating to the metal center as an η^2 -arene complex.
2. The arene C–H bond is sterically better accessible.
3. The sp^2 -hybridized orbital has a lower directionality than the sp^3 -hybridized orbital, which allows a better overlapping with the metal orbitals.
4. The greater thermodynamic driving force for addition of arene C–H bonds results from a difference between metal-aryl and metal-alkyl bond strengths that is greater than the difference between aryl C–H and alkyl C–H bond strengths.

These facts show the challenge of an sp^3 C–H bond activation compared to an sp^2 C–H bond. In 1982, Janowicz and Bergman reported the first oxidative addition of the C–H bond of a saturated hydrocarbon to a transition metal (Scheme 2).⁴²



Scheme 2 First oxidative addition of a saturated C–H bond.

At the same time, Jones observed a similar oxidative addition to the analogous rhodium complex **27** (Scheme 3).⁴³ Nowadays, there are different examples for transition-metal alkyl – hydride complexes for group 7–10 metals in the literature.⁴⁴



Scheme 3 Oxidative addition of a saturated C–H bond to a rhodium complex.

3.3.4 Transmetalation

During the transmetalation step, the halide or pseudo halide in the transition metal is replaced by the organic group of a metal organyl, in most cases a magnesium, zinc, tin, silicon, or boron reagent. This generates a transition metal species with two covalently bound, organic ligands which can undergo reductive elimination. The transmetalation step of a cross coupling reaction has not been studied in any depth since the formed intermediates are often not stable toward reductive elimination and therefore difficult to catch. One proposed mechanism for this transformation is shown in Figure 24, where the main group element coordinates to the halogen and simultaneously assists dissociation of the halogen while delivering the carbon nucleophile to the palladium metal center.⁴⁵ This mechanism may be true for the polar organo metal species, such as organomagnesium, but considerably less likely for the less polar and less electrophilic organosilanes, stannanes, and boronates.

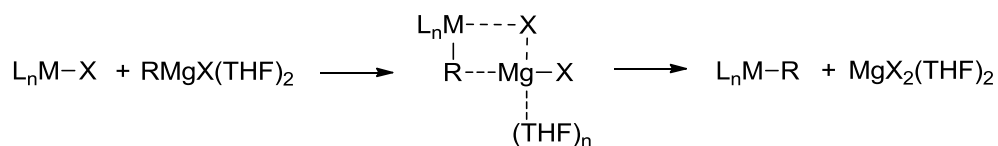
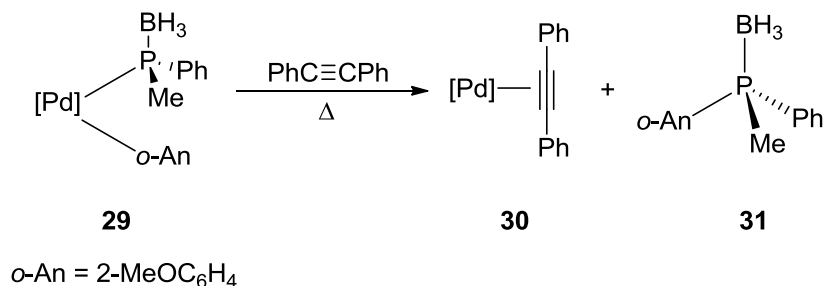


Figure 24 Mechanism of the transmetalation.

3.3.5 Reductive Elimination

Reductive elimination is the reversed pathway to oxidative addition and proceeds therefore also through a three-center transition state. This again implies that the reaction will occur with retention of configuration of a stereocenter directly attached to the metal which allows asymmetric catalysis (Scheme 4).⁴⁶

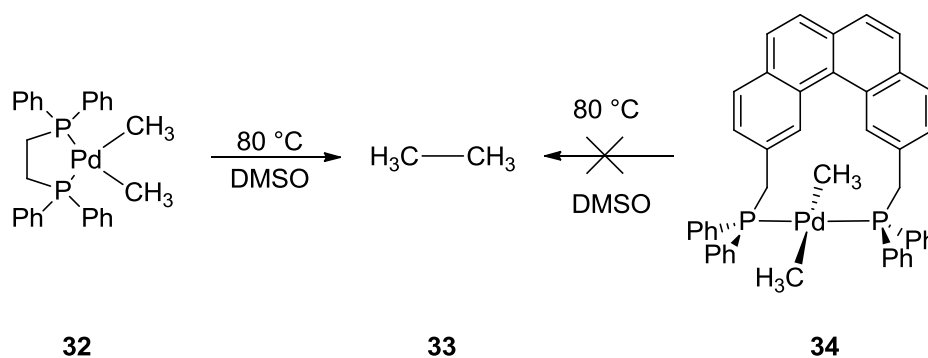


Scheme 4 Reductive Elimination of a palladium complex.

Many factors influence the reductive elimination reaction:

1. Reductive elimination occurs faster for electron-poor complexes than for more electron-rich complexes, because the formal oxidation state of the metal is reduced by two units and the electron density on the metal is increased. The reaction is most often seen with metals in higher oxidation state, such as the d^8 metals Pd(II) and Ni(II), or the d^6 metals Pt(IV), Pd(IV), Ir(III) and Rh(III).
2. The rate of the reaction is also enhanced by the presence of a positive charge, which may be initiated by chemical or electrochemical oxidation, or by generation of a coordinatively, more electrophilic metal center by the thermally or photolytically induced dissociation of a ligand prior to reductive elimination.
3. The reaction equilibrium depends on thermodynamics and, thus, on the metal-ligand bond strength. Hence, first row complexes react faster than second row complexes, which react faster than third row complexes. The reason for this is that the metal-ligand bonds in the second row reactant are weaker than that from the third row reactant.
4. The reaction is favored in the presence of bulky ligands (because the steric congestion is relieved when the product is released from the metal) and/or good π -acceptor ligands (e.g. CO, which stabilize the reduced metal species).
5. The reaction rate depends also on kinetics and, thus, on the nature of the groups. Reactions that involve H are particularly fast, because the s-orbital of a hydride ligand is less directional than the sp^n -hybridized orbital of a hydrocarbyl group. Thus, the overlap in transition state is greater for reductive eliminations forming bonds to hydride ligands than for those forming bonds to ligands bound through heavier atoms. The same fact is (besides the coordination of the π -system to the metal) responsible for the lower transition energy for reductive elimination involving sp^2 -hybridized carbon atoms compared to sp^3 -hybridized carbon atoms. The two dimensionality of the aryl or vinyl group reduces steric hindrance that occurs upon canting of the ligands to form the carbon-carbon bond. Furthermore, the sp^2 -hybridized orbital is less directional than the sp^3 -hybridized orbital because of the increase in s-character, which leads to a greater overlap and multi-center bonding in the three-centered transition state.

The last factor points out, why reductive elimination of C–C is more difficult than for C–H bonds. The reason is not thermodynamics, it is mostly kinetics. Reductive elimination to form the C–C bond between two saturated carbon centers requires canting of the alkyl groups, and this distortion creates steric hindrance between the substituents on the alkyl groups and the ancillary ligands at the metal. This is also the reason for the cis-isomerization step in the catalytic cycle of cross-coupling reactions. The reductive elimination is a concerted process and necessitates therefore cis-coordination geometry, as shown in Scheme 5. The geometry of the right complex **34** prevents the cis-isomerization and subsequently also the reductive elimination.⁴⁷



Scheme 5 Essential cis-isomerization for the reductive elimination step.

3.4 Asymmetric Catalysis

A catalyst cannot just save energy by lowering the temperature, it often also gives higher selectivity which minimizes formation of side products. With growing regulatory pressure to synthesize drugs in enantiopure form, asymmetric catalysis received considerable attention during recent years together along with enzyme catalysis, as the prime practical ways to make such products on a large scale. Chiral transition-metal catalysts can discriminate between the two faces of a prochiral substrate, and the reaction occurs preferentially at one prochiral face, at one of two enantiotopic groups, or with one of two enantiomers in a racemic mixture. The chiral catalyst interacts with the prochiral substrate, resulting in two different diastereomeric transition states with unequal energies. The larger the differences in energies of the diastereomeric transition states, the larger the differences in rates for production of the two enantiomeric products.

Phosphines are again suitable chiral ligands for providing the essential chiral information to the complex, because the barrier to inversion at phosphorus is quite high. It is much higher than the barrier to inversion at nitrogen and typically ranges from 29-35 kcal/mol (Figure 25).⁴⁸ Thus, an amine bearing three different substituents will consist of a racemic mixture of conformers in solution, but most phosphines containing three different substituents can be prepared in optically active form. Nowadays, there are plenty chiral phosphines (e.g., (R)-BINAP) and phosphites (e.g., (R)-Ship) commercially available.

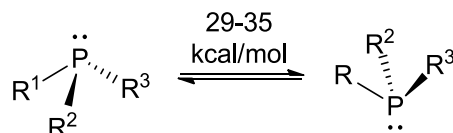


Figure 25 Energy barrier for inversion of the substituents on phosphorus.

The mechanism of the asymmetric catalysis has to contain a step that controls enantioselectivity, often called the enantioselectivity-determining step. This step has to be irreversible to avoid racemization. Later steps in the reaction have no impact on the enantioselectivity of the process. For example, Figure 26 shows the ruthenium-catalyzed asymmetric hydrogenation of β -keto esters. The BINAP-ligand provides the chiral information in the metal-complex. The ketone carbonyl is thought to coordinate in a π -fashion

to the ruthenium while the ester binds through the oxygen lone pair, resulting in two different possible diastereomers:⁴⁹

Left diastereomer: the η^2 -binding of the ketone group leads to an interaction of the carbonyl group with the protruding equatorial phenyl group, which in turn destabilizes this diastereomer.

Right diastereomer: the placement of the ketone carbonyl in the quadrant with the axial P-bound phenyl group, which is directed away from the substrate, stabilizes this diastereomer.

This basic concept can be transferred to other asymmetric transformations, for instance, for a direct prochiral sp^3 C-H bond arylation.

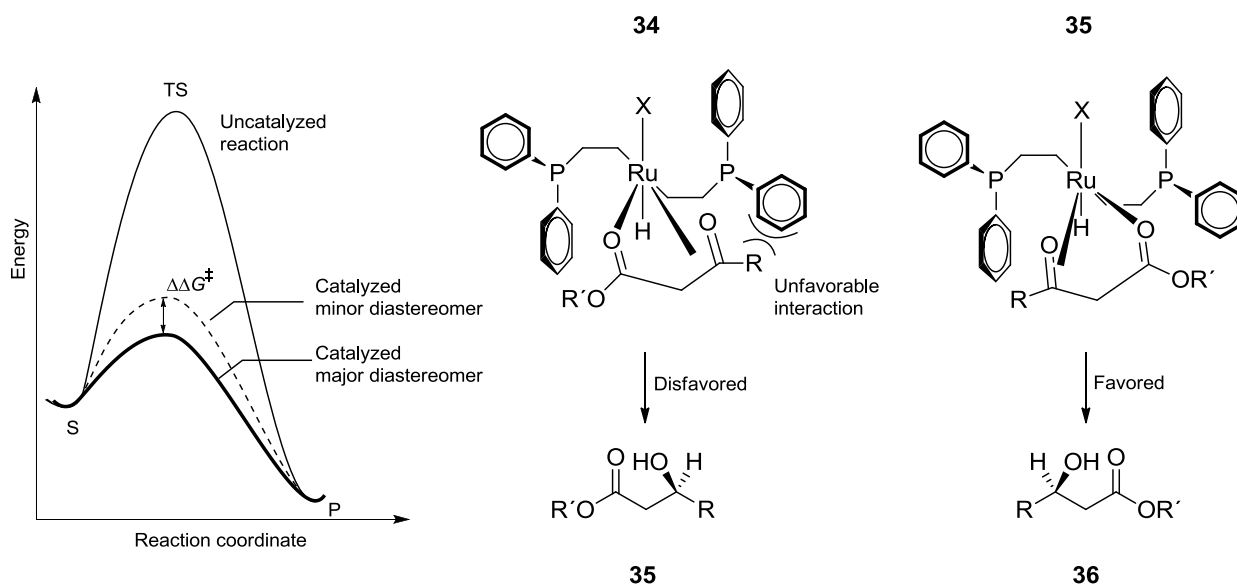
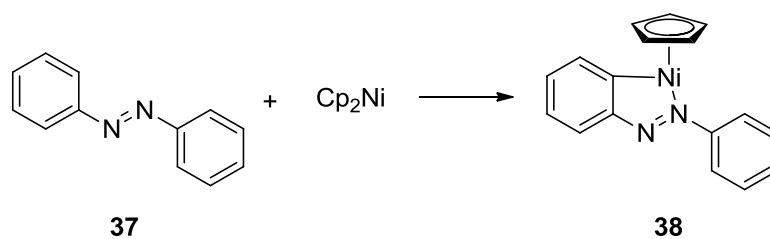


Figure 26 Reaction coordinate and transition state for an asymmetric catalyzed reaction.

3.5 C–H Activation

The cleavage of C–H bonds was generally believed to be difficult because of the high C–H bond energies. One of the first examples of C–H bond activation was the H–D exchange in methane catalyzed by a heterogeneous Ni^0 catalyst in 1936.⁵⁰ In the 1960s, Hodges and Garnett demonstrated that a homogeneous aqueous solution of platinum(II) salts catalyzed deuteration of arenes and alkanes.⁵¹ In 1963, Kleiman and Dubeck reported the possibility of C–H bond cleavage in azobenzene by the Cp_2Ni complex (Scheme 6).⁵² The reaction mechanism for this metalation reaction has not been elucidated, but the ortho-C–H bond was apparently cleaved.



Scheme 6 C–H bond cleavage of azobenzene by Cp_2Ni .

After these pioneering studies, many research groups have reported on the cleavage of C–H bonds via the use of transition metal complexes. To date, a large number of review articles are available and the fundamental features of the C–H bond cleavage reactions have been elucidated.¹³ These discoveries provided the basis for a new area in synthetic applications, the transition-metal catalyzed C–H bond transformation.

3.5.1 Catalytic C–H Functionalization

The challenge of C–H activation is not to cleave C–H bonds by using stoichiometric amounts of transition metal complexes, but to cleave one C–H bond in a selective fashion and to incorporate this C–H bond cleavage step into a catalytic process that leads to functionalization. Transition-metal catalyzed cross-coupling reactions are one of the most applied methods for creating new C–C bonds. However, the required organometallic nucleophilic reagents, particularly when being functionalized, are often not commercially available or are relatively expensive. As already mentioned in Chapter 1, their preparation from the corresponding arenes usually involves a number of synthetic operations, during which undesired byproducts are formed. One way to overcome this problem is the introduction of new functional groups directly through transformation of C–H bonds which unlocks opportunities for markedly different synthetic strategies. For example, as shown in Figure 27, the same target molecule may be accessed in a single step by displacement of a hydrogen atom.⁵³

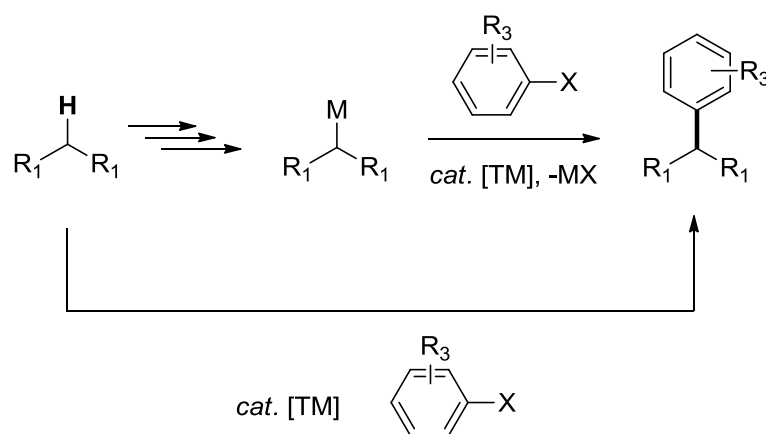
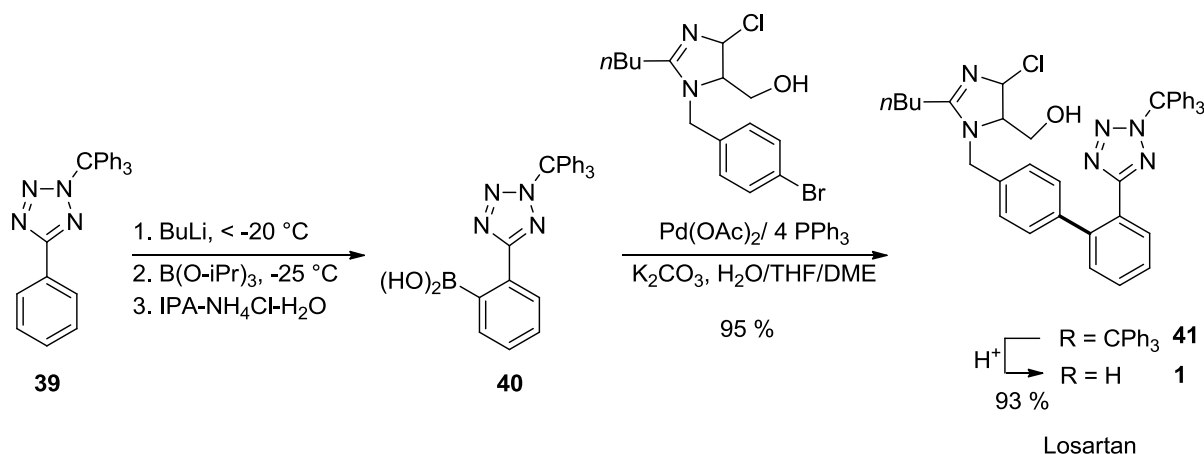


Figure 27 Advantage of the C–H activation towards cross coupling.

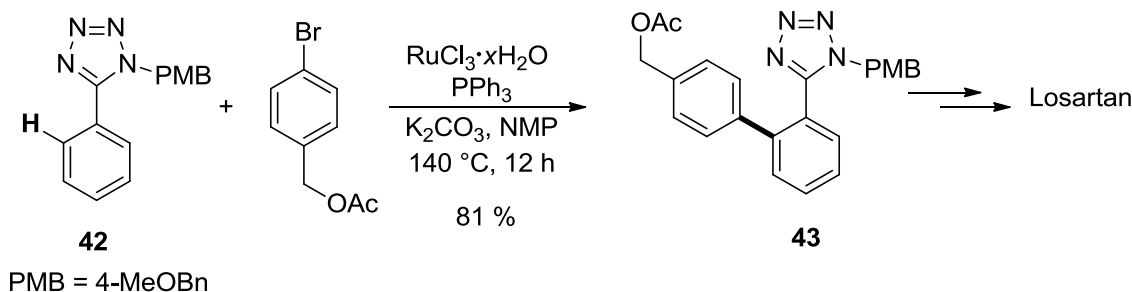
This concept can be applied on different synthetically useful reactions. The transition-metal catalyzed cross coupling reaction step in the large scale synthesis of the pharmaceutical compound Losartan was already described in Chapter 1. The key step in this synthesis is the

arylation of the protected tetrazole via the Suzuki cross-coupling method.⁶ The corresponding arylboronic acid species **40** is generated in the first step by the reaction of protected tetrazole **39** with butyllithium and quenching the organolithium reagent with trialkylborate, followed by hydrolysis. Coupling this species with aryl bromide, followed by deprotection of the tetrazole generates Losartan **1** (Scheme 7).



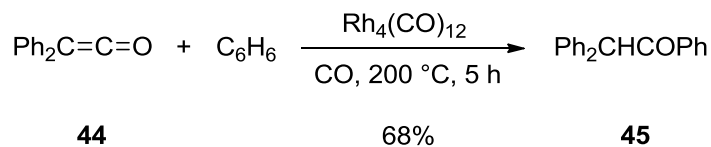
Scheme 7 The Suzuki cross coupling in the synthesis of Losartan.

It would certainly facilitate the reaction and save several steps if the desired C–C bond could be generated directly from the protected tetrazole. Thus, Seki et al. reported a ruthenium-catalyzed direct arylation method for the synthesis of a Losartan precursor (Scheme 8).⁵⁴



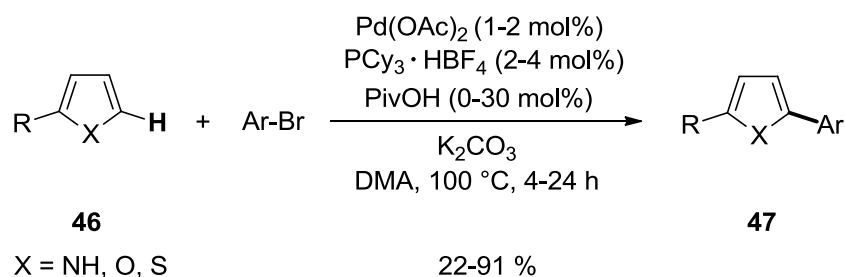
Scheme 8 The direct C–H arylation of compound **42** in the synthesis of Losartan.

This example shows the importance of new catalytic reactions. One of the first pioneering studies of the catalytic functionalization of C–H bonds was reported by Yamazaki et al in 1978.⁵⁵ They described the reaction of benzene, used as a solvent, with diphenylketene in the presence of CO and catalytic amounts of Rh₄(CO)₁₂, forming diphenylmethyl phenyl ketone in good yield (Scheme 9).



Scheme 9 One of the first examples for a catalytic C–H activation reaction.

In 1985, Ohta and co-workers published the first intermolecular direct heterocycle arylation example.⁵⁶ Ohta showed that chloropyrazines regioselectively arylate *NH*-indoles at C-2 position if Pd(PPh₃)₄ catalyst is employed. This was also one of the first examples for palladium-catalyzed direct arylation. Nowadays, there is a variety of Pd-catalyzed C–H bond functionalizations known in the literature.⁵⁷ Pd-catalyzed arylation of heteroaromatics with aryl halides is the most developed type of C–H functionalization of heterocyclic compounds, which is shown in the next examples. Fagnou and co-workers reported 5-arylation of 2-substituted heterocycles **46** using 2 mol% of Pd(OAc)₂, 4 mol% of PCy₃ and 30 mol% of pivalic acid as catalytic system (Scheme 10).⁵⁸ The reaction could be performed with a wide range of substrates, including substituted thiophenes, furans, pyrroles, and other heterocycles in good yields.



Scheme 10 The direct arylation of heterocyclic compounds.

The mechanism of this palladium-catalyzed direct arylation is in the same fashion as for the cross coupling-reaction (Figure 28). The catalytic cycle starts with the catalyst activation, followed by oxidative addition of Pd(0) species into Ar–X forming Ar–Pd(II)–X species. The difference primarily results from the fact that there is no organo metal species which can undergo transmetalation. This step is now replaced by the C–H bond activation at the Ar–Pd(II)–X species. Final cis-isomerization and reductive elimination furnishes the product.

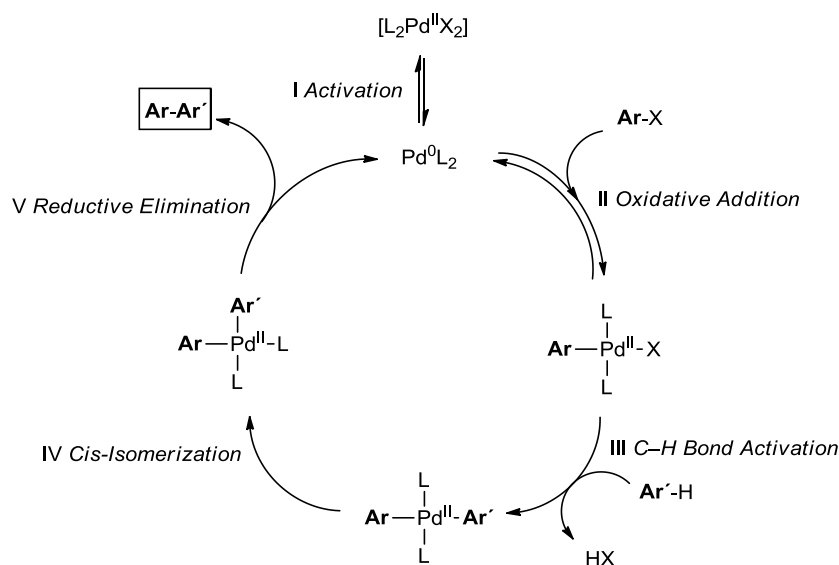


Figure 28 Mechanism of palladium-catalyzed direct arylation.

Several pathways for the reaction of the oxidative addition product with arene have been proposed and are outlined in Figure 29. These include an electrophilic aromatic substitution (S_{EAr} , a), a concerted metalation deprotonation process (CMD, b), a Heck-type carbometalation (c), and an oxidative addition (d).⁵⁹

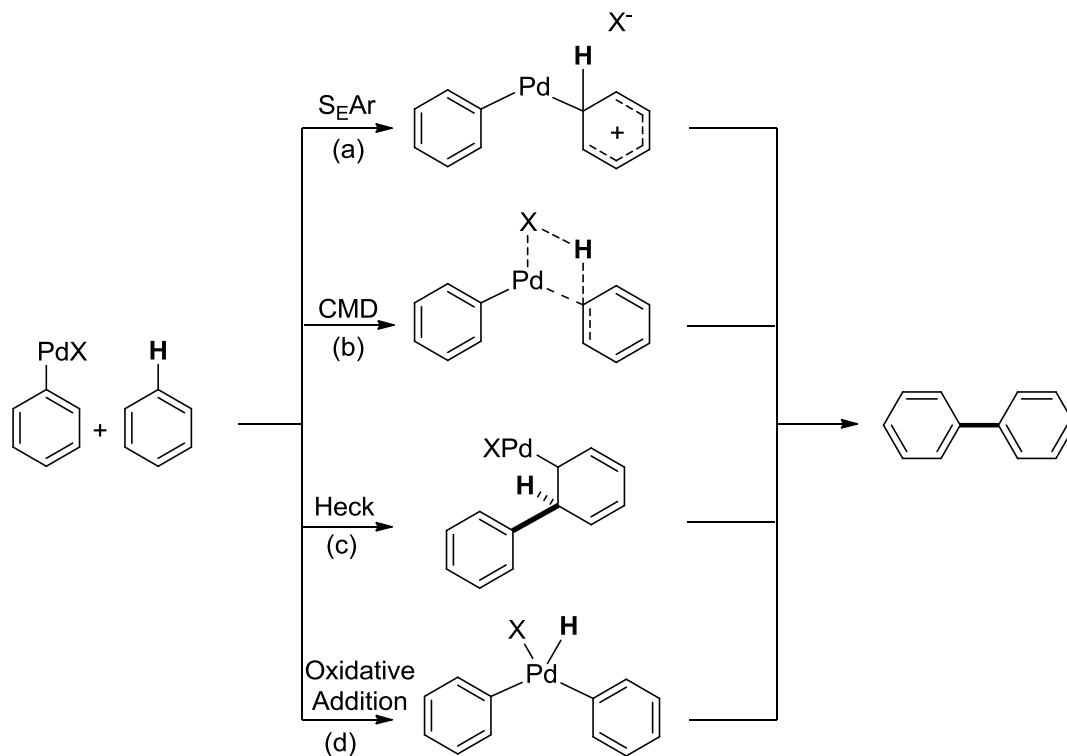
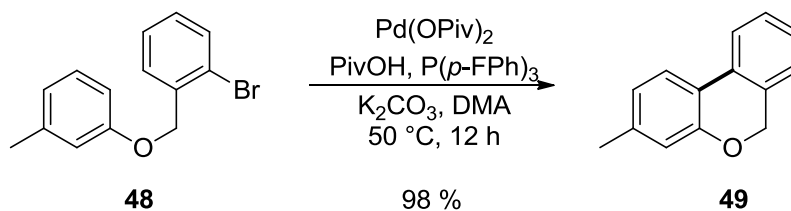


Figure 29 Different possible pathways for the direct functionalization of the C-H bond.

3.5.2 Regioselectivity

The example shown in Scheme 10 demonstrates also one major challenge in direct arylation: regioselectivity. The heterocycle is blocked in the 2-position to avoid bisarylation. Regioselective direct arylations are difficult to achieve because the arene reagents often contain several non-equivalent C-H bonds that can react with the metal center at similar rate. It is easy to imagine that this selectivity problem usually furnished undesired side products. However, there are several approaches to overcome this problem. For example, intramolecular reactions of two arene compounds linked by a tether can occur regioselectively because of the geometric constraints. Fagnou again reported such an intramolecular direct arylation under mild conditions (Scheme 11).⁶⁰ Intramolecular arylation reactions are typically used for the construction of five, six, and seven-membered rings and tend to occur at the less-hindered aryl C-H bond.



Scheme 11 An intramolecular direct functionalization.

Besides, the electronic properties of the arene can control the position of C–H bond cleavage. This electronic preference for the cleavage of one C–H bond over another is particularly pronounced in heteroaromatic systems (Figure 30).⁶¹

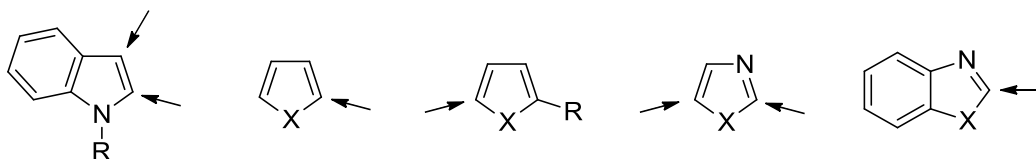
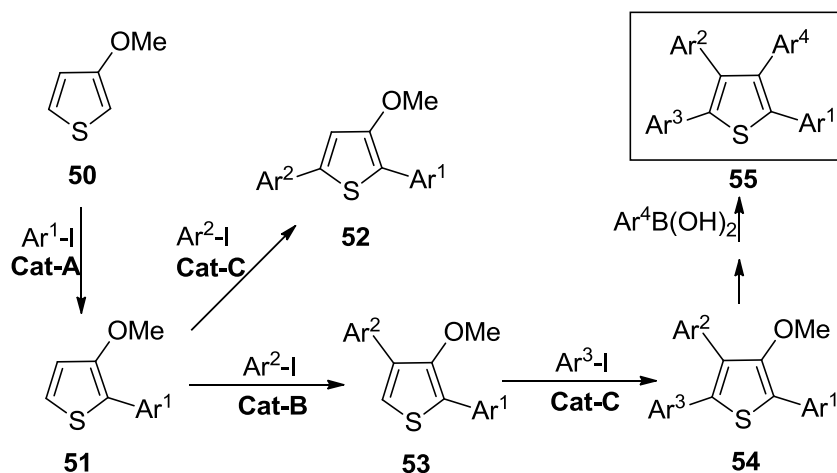


Figure 30 Electronic preferences for the direct transformation of heterocycles. The arrows are showing the preferred position for the C–H insertion.

These electronic properties can be difficult to override and limits the scope of reagents. The problem encouraged different groups to develop methods for complementary or improved regioselectivities. This goal can be obtained in certain cases by changing the reaction solvent, adding co-catalyst, or by conducting the reaction with more sterically encumbered substrates. The group of Itami reported an interesting synthetic route for the multiple arylation of thiophene (Scheme 12).⁶² They could achieve different regioselectivity of thiophene by changing the catalyst. The arylation in 2-position was achieved with $\text{RhCl}(\text{CO})_2/\text{P}[\text{OCH}(\text{CF}_3)_2]_3$ as catalyst. By switching the catalyst to $\text{PdCl}_2/\text{P}[\text{OCH}(\text{CF}_3)_2]_3$, a change in regioselectivity could be realized. Finally, the third C–H bond arylation was carried out by switching the ligand to 2,2'-bipyridyl. The electronic and steric effects of the ligand in combination with the metal have obviously a huge impact on the regioselectivity. By tuning these parameters, one can overcome the preferred electronic properties of the substrate for the C–H bond activation.



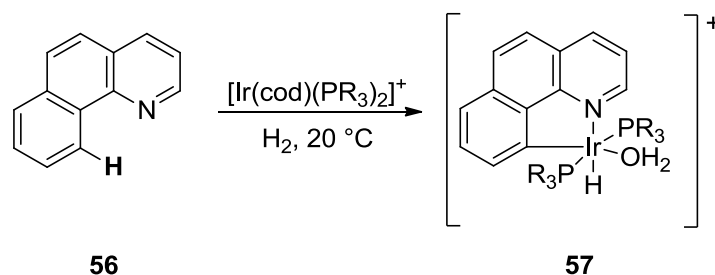
Cat-A: Rh^I/P[OCH(CF₃)₂]₃, **Cat-B:** Pd^{II}/P[OCH(CF₃)₂]₃, **Cat-C:** Pd^{II}/bipy

Scheme 12 The arylation of thiophene in different positions depending on the catalyst.

However, the most common strategy for conducting regioselective direct coupling of arenes involves the use of substrates containing directing groups. Ligating substituents installed on the arene can direct the metal to cleave the ortho C–H bond forming five- or six-membered metallacycle. This method is discussed in the next chapter in more detail.

3.5.3 Cyclometalation

A special case of oxidative addition is cyclometalation, in which a C–H bond in a ligand oxidatively adds to a metal to give a ring.⁶³ Because of this ring formation, the reaction can be highly selective, for example, only one of the nine distinct C–H bonds in benzoquinoline **56** is cleaved when cyclometalation occurs (Scheme 13).⁶⁴ Another example of stoichiometric cyclometalation was shown in Scheme 6.



Scheme 13 Stoichiometric cyclometalation of [Ir(cod)(PR₃)₂]⁺.

Synthetic chemists use this directing ability of certain functional groups to functionalize one specific C–H bond. This method is based on a well-known reaction, the directed ortho metalation. In the cyclometalation, Lewis basic functionalities coordinate to transition metal complexes, leading to cyclometalated intermediates. The functional group forces the metal to a desired geometry where it can only undergo oxidative addition to a specific C–H bond (Figure 31). The bond-strength of the Lewis-base and metal should be strong enough to direct

the metal, but weak enough to release the metal species after the transformation. Otherwise it would prohibit the catalytic reaction.

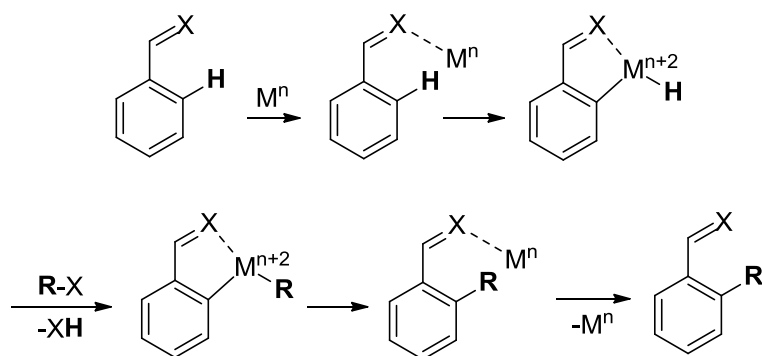
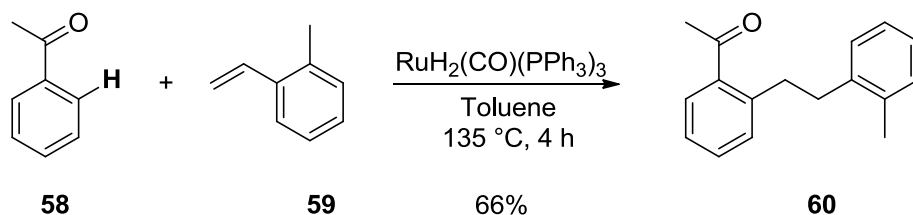


Figure 31 Mechanistic consideration of the cyclometalation.

The ring size of the cyclometalation product depends strongly on the metal species. Palladium prefers five-, six-, and seven-membered rings,⁶⁵ while ruthenium usually only forms five membered rings.⁶⁶ In 1993, Murai and coworkers developed an effective ruthenium-catalyzed method for the direct alkylation of acetophenone (Scheme 14). Thereby, regioselective ruthenium-catalyzed anti-Markovnikov alkylations were accomplished using alkenes as substrate.⁶⁷



Scheme 14 Ruthenium-catalyzed direct alkylation of acetophenone.

This pioneering work attracted much attention in the scientific community and provided the starting point for chelation-assisted C–H bond transformation. Many research groups focused on this kind of reaction and improved both scope and conditions for the direct transformation. The directing group could be extended to a variety of functional groups, such as alcohols,⁶⁸ ketones,⁶⁹ carboxylates,⁷⁰ ketimines,⁷¹ amides,⁷² oxazolines,⁷³ pyridines,⁷⁴ pyrazoles,⁷⁵ triazoles,⁷⁶ tetrazoles,⁵⁴ triazenes,⁷⁷ and thiazoles⁷⁸ (Figure 32).

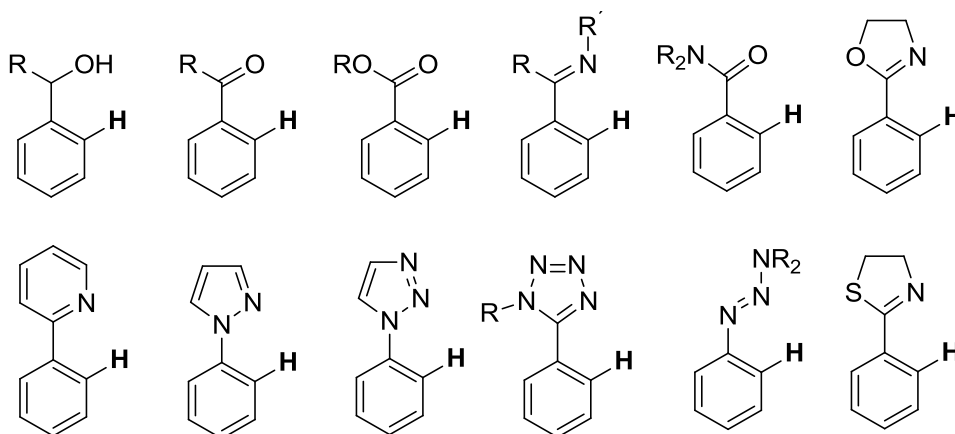


Figure 32 Commonly used directing groups in C–H bond functionalization reactions.

Amongst these directing groups, pyridine is usually used for testing new catalytic methods, because of its stability and good directing ability. New catalytic methods for various transformations, such as alkylation,⁷⁹ alkenylation,⁸⁰ arylation,⁸¹ carbonylation,⁸² silylation,⁸³ and sulfonation⁸⁴ have been developed in recent years (Figure 33).

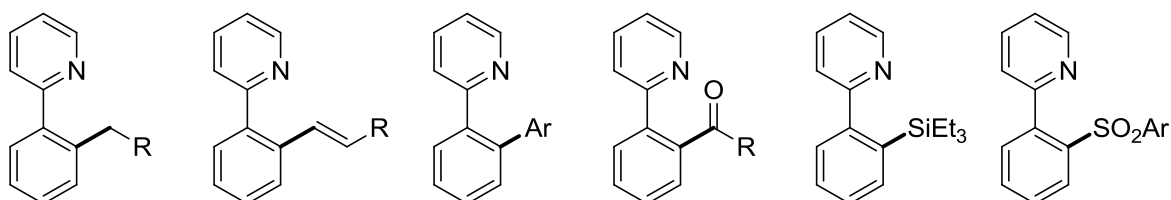
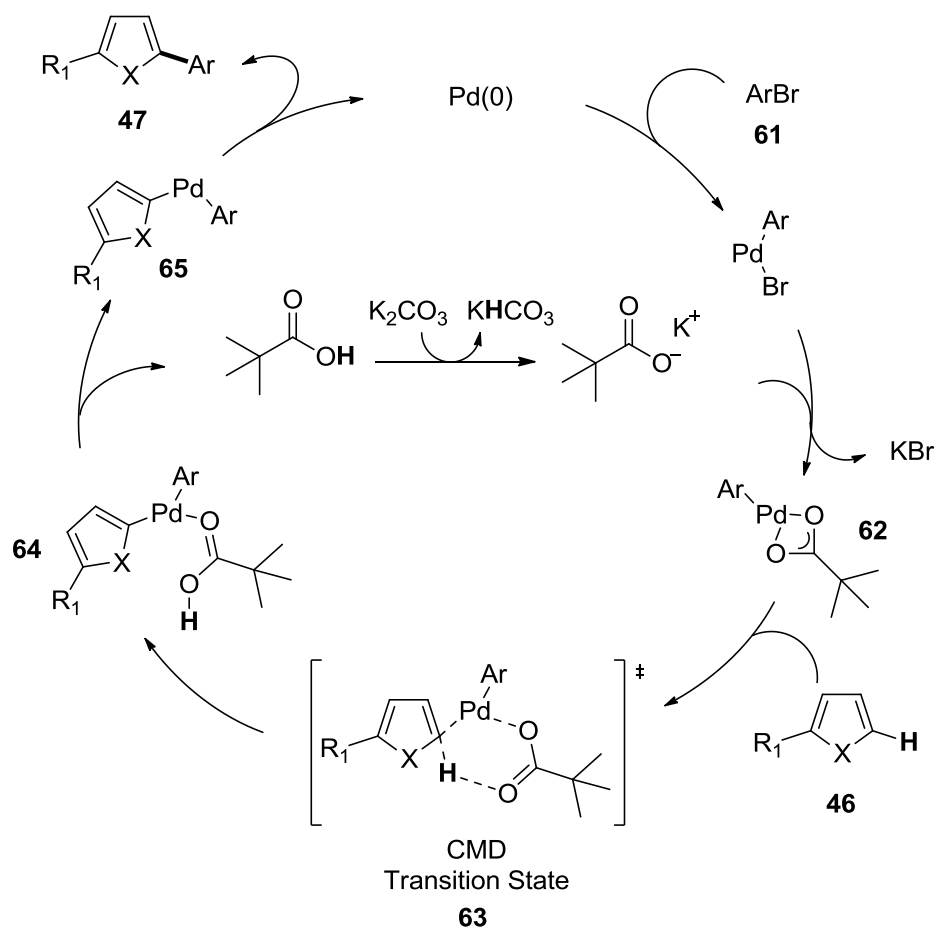


Figure 33 Different C–H bond functionalizations for the pyridine directing group.

3.5.4 Concerted Metalation Deprotonation - CMD

The concerted metalation deprotonation (CMD) is a widely used method for the direct transformation of unactivated C–H bonds. Most of the direct C–H bond functionalizations are improved by addition of a carboxylate source. The previously discussed method for the direct arylation of thiophene, for instance, requires the addition of pivalic acid. Fagnou proposed the following mechanism where the Pd(0) species undergoes oxidative addition into the aryl halide bond of **61**, followed by a bromide/pivalate ligand exchange, which generates **62** in situ from the catalytic pivalic acid and the insoluble stoichiometric carbonate base.⁵⁸ Reaction with the heteroaromatic partner **46** leads to a concerted metalation- transition state **63**, enabled by the pivalate ligand which gives rise to **64**. The carboxylate stabilizes this transition state and facilitates the hydrogen dissociation. Subsequent reductive elimination produces biaryl product **47** and regenerates the active catalytic species (Scheme 15). This plausible mechanism is supported by different computational calculations, and transferable to other direct C–H bond functionalizations.⁸⁵



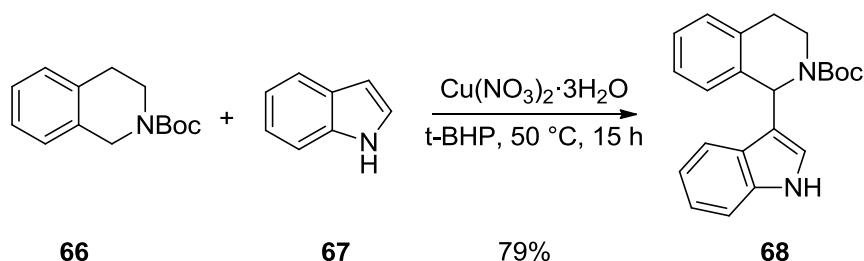
Scheme 15 Concerted Metalation Deprotonation mechanism.

4. RESULTS & DISCUSSION

4.1 Direct Arylation of Acyclic Amines

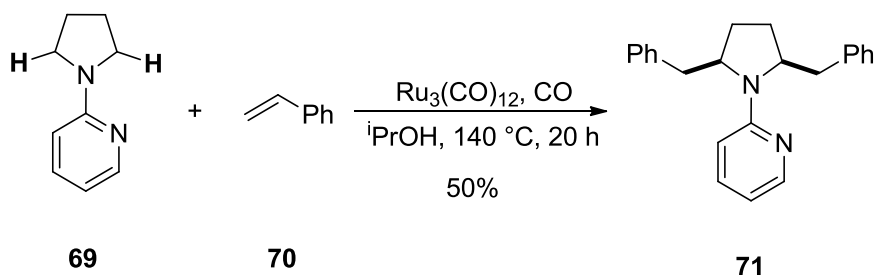
4.1.1 State of the Art

The direct functionalization of cyclic amines, such as pyrrolidine⁸⁶ and piperidine,⁸⁷ but also benzylic compounds, such as tetrahydroisoquinoline, has been reported in the literature. In particular, the transformation of tetrahydroisoquinoline has attracted a lot of attention in recent years and many groups have developed different methods for the direct functionalization of the benzylic C–H bond.⁸⁸ The group of Mihovilovic showed for instance a high yielding copper- and iron-catalyzed arylation of tetrahydroisoquinoline under mild conditions (Scheme 16).⁸⁹ This sp^3 C–H bond is activated, since it is adjacent to nitrogen, in benzylic position, and in a cyclic configuration. It is well-known in C–H activation chemistry that a sp^3 C–H bond adjacent to a heteroatom or in a benzylic position is more easily activated compared to one surrounded only by carbons.⁹⁰



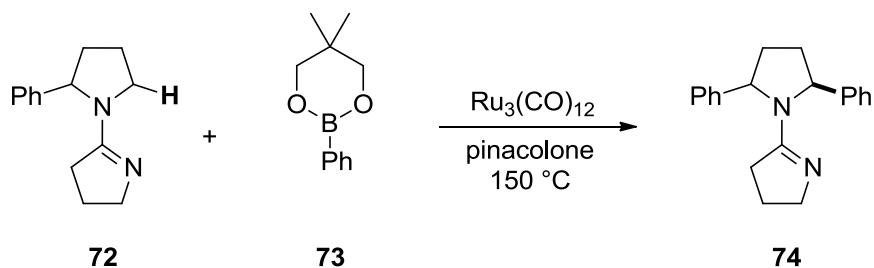
Scheme 16 Copper-catalyzed direct indolation of tetrahydroisoquinoline.

In 2000, Chatani et al. reported the rhodium-catalyzed direct carbonylation of pyrrolidines, using pyridine as directing group.⁸² They also claimed, that the C–H bond adjacent to nitrogen is more activated and therefore easier to functionalize than other sp^3 C–H bonds. This method could be extended to the direct alkylation of saturated amines (**69**, Scheme 17).⁹¹ The use of $\text{Ru}_3(\text{CO})_{12}$ as catalyst resulted in the addition of the sp^3 C–H bond across the alkene bond to give the coupling products. The authors demonstrated the importance of the coordination of pyridine nitrogen to ruthenium. The regiochemistry of the functionalization is dictated by five-membered ruthenium chelate formation. Jun and co-workers expanded the scope of this alkylation reaction to acyclic amines.⁹²



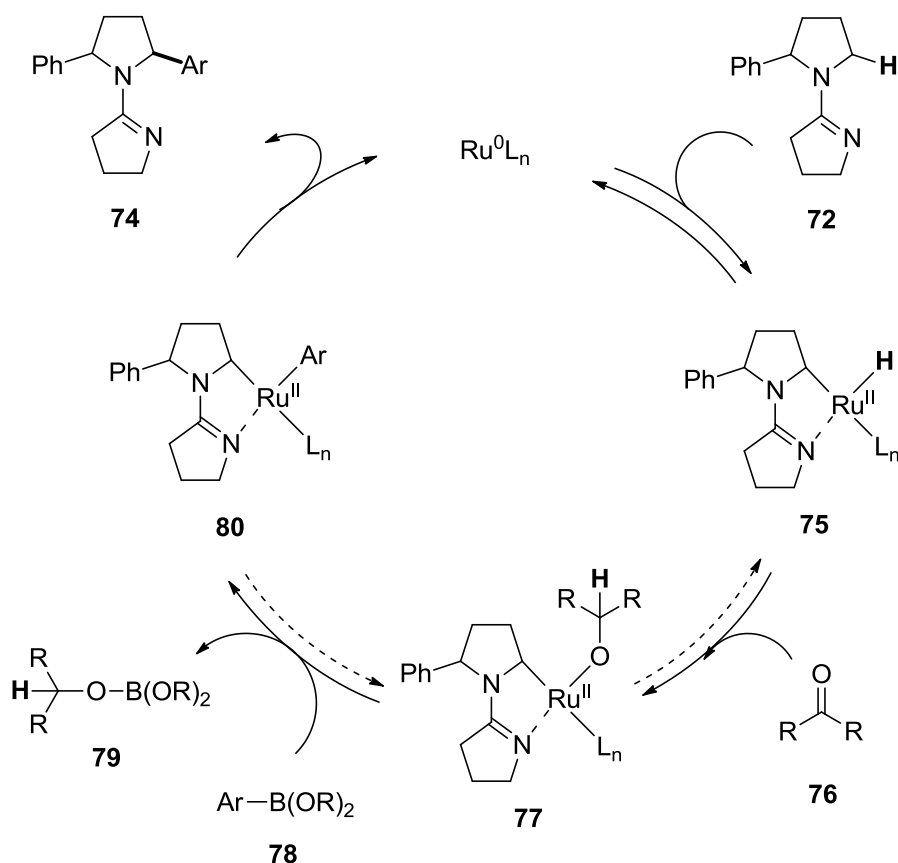
Scheme 17 Rhodium-catalyzed direct alkylation of pyrrolidines.

Based on these studies, Sames and coworkers reported the direct arylation of pyrrolidines using an amidine directing group (**72**, Scheme 18).⁹³ This operationally simple method requires aryl boronic acid esters, which are commercially available, and tolerates a variety of functional groups. The strong directing group has the advantage to be cleavable, resulting in 2-arylated cyclic amines. Furthermore the presence of a ketone was crucial and enhanced the yield significantly.



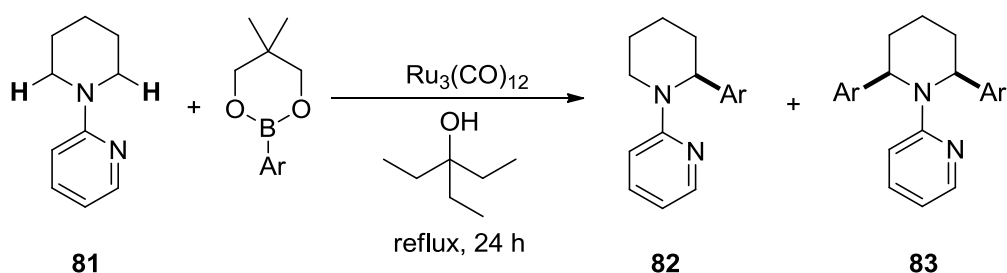
Scheme 18 Ruthenium-catalyzed direct arylation of pyrrolidines.

Sames supported the mechanism of Chatani and coworkers, initially proposed for the direct arylation of acetophenone under similar conditions. The mechanism starts with the oxidative addition of the $\text{Ru}(0)$ species into the C–H bond of **72**, directed by the amidine nitrogen. The ketone **76** works as hydrogen acceptor, and is reduced to the corresponding alcohol. Transmetalation with the aryl boronic acid ester **78** and subsequent reductive elimination delivers the final product **74** (Scheme 19).



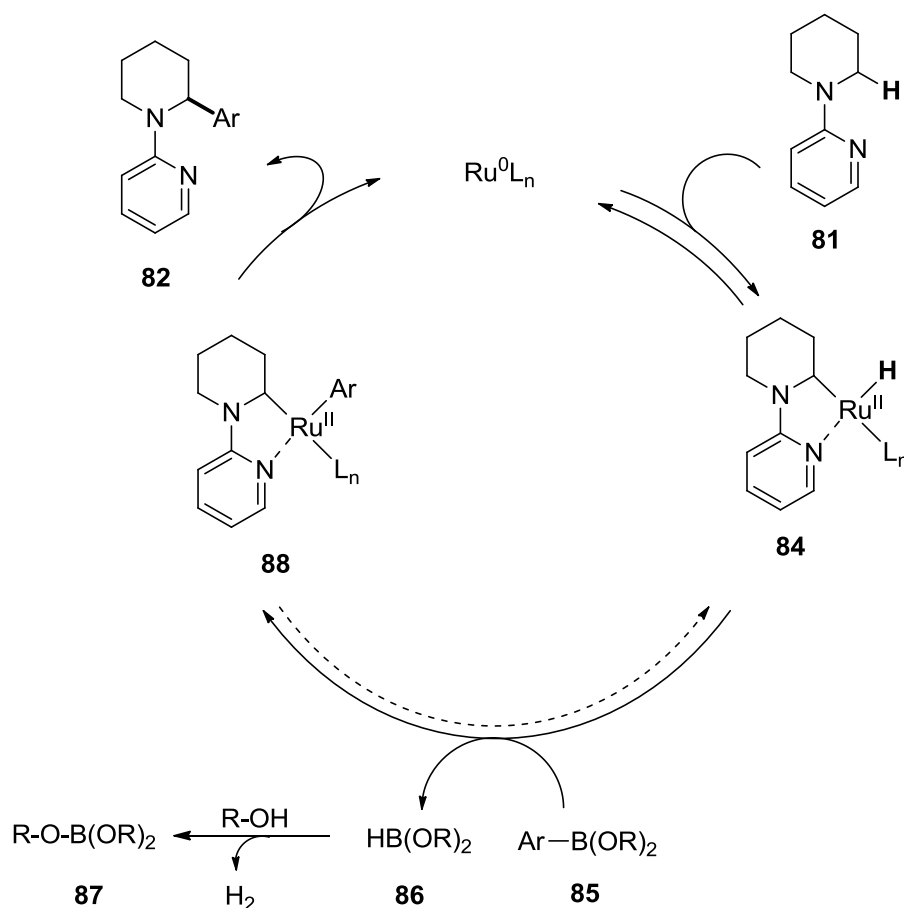
Scheme 19 Proposed mechanism of the direct arylation of pyrrolidines.

Maes and coworkers expanded this protocol for the direct arylation of piperidines (**81**, Scheme 20).⁹⁴ They used again pyridine as directing group and developed a reductive method for the cleavage of the pyridine group. Furthermore, the ketone was replaced by alcohol and the reaction was performed in an open vial. Under these conditions, H_2 was formed, proved by Raman spectroscopy, and could be released.



Scheme 20 Ruthenium-catalyzed direct arylation of piperidines.

The proposed mechanism is similar to the previous one, with the exception of the hydrogen transfer (Scheme 21). The initial complexation of the $\text{Ru}(0)$ species to pyridine is followed by the oxidative addition to the sp^3 C–H bond. The so formed $\text{Ru}(\text{II})$ species **84** is undergoing the transmetalation with the arylboronate ester forming the $\text{Ru}(\text{II})\text{-Ar}$ species **88**. Final reductive elimination delivers the product **82**. The authors hypothesize that the formed pinacolborane species **86** is scavenged by the alcohol and H_2 is formed during this step.



Scheme 21 Proposed mechanism of the direct arylation of piperidines.

4.1.2 Objective

Despite the growth, challenges remain including the establishment of direct functionalization of acyclic compounds. To the best of our knowledge, there are no examples for the direct arylation of acyclic benzylic amines in the literature. The limitation to saturated N-heterocycles lies probably in the preferred geometrical alignment of such systems where the directing group is excellently positioned to activate the CH_2 group adjacent to the heteroatom. In acyclic systems where such a conformational lock is not possible, the directing group and positions to be activated rather position themselves in a way of greatest distance to minimize energy. This challenging quest inspired us to develop a simple method for the direct arylation of such benzylic amines. The idea was to find a suitable directing group for the selective cyclometalation of the desired C–H bond. Furthermore, the directing group should be cleavable afterwards to deliver the free amine which can then be used as building unit in further synthesis. The final goal was to find an asymmetric catalytic pathway, generating high enantiomeric excess of the chiral amine (Figure 34).

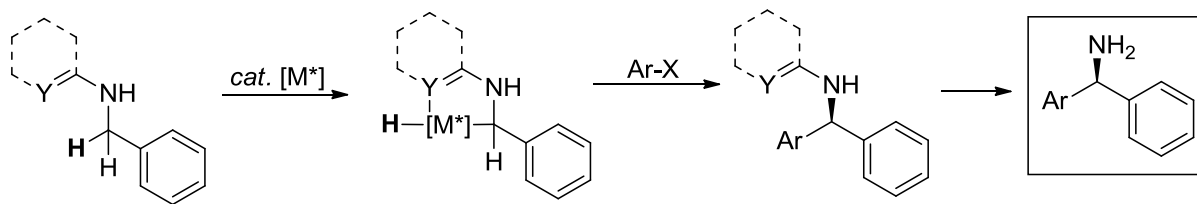
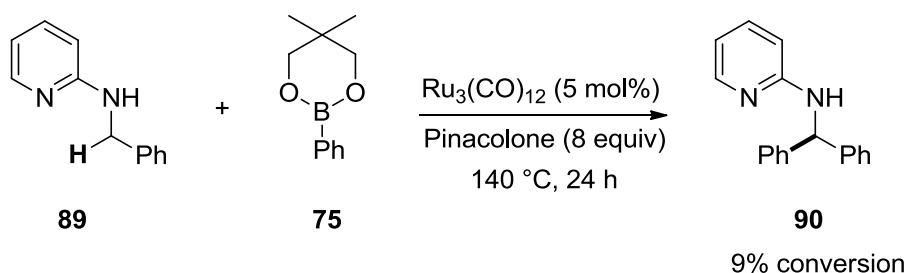


Figure 34 Concept for the cyclometalation assisted direct arylation of acyclic benzylic amines.

4.1.3 Ru(0) System - Screening I

The investigations started with the conditions described by Sames and coworkers.⁹³ It was rationalized that this process might be adapted to form C–C bonds for acyclic amines. Ruthenium prefers five membered cyclometalation intermediates. Thus, it was concluded to use pyridine as directing group. As already outlined, pyridine is a widely applied directing group in cyclometalation processes. The lone pair of nitrogen is especially suitable for coordinating low-valent metal centers and, consequently, positioning them in proximity to the desired C–H bond. In the initial experiment, simple *N*-benzylpyridine-2-amine **89** was used as starting material to react with phenyl boronic acid ester **75** in the presence of pinacolone. Gratifyingly, the expected product **90** was detected, but only a very low conversion of 9% was obtained (Scheme 22). However, this experiment provided a promising result for the direct functionalization of benzylic amines and served as starting point for subsequent optimization efforts of the reaction conditions.



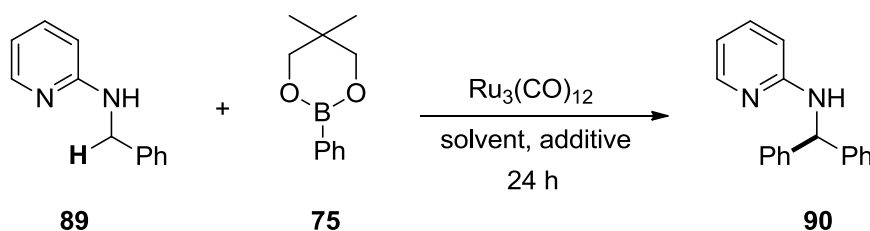
Scheme 22 Ru₃(CO)₁₂-catalyzed arylation of *N*-benzylpyridine-2-amine **89**.

Within a systematic study, temperature was increased (Table 2, entries 1-4), but the conversion did not increase. The conversion could be improved by increasing the catalyst loadings (Table 2, entries 5-7). However, the catalyst then performed with low turnover numbers (TON) in an almost stoichiometric way. As a consequence, further experiments were continued with 5 mol% in order to optimize TON. By decreasing the amount of ketone (Table 2, entry 8) or changing the solvent (Table 2, entries 10-16), the conversion dropped significantly. The addition of 1 equivalent base, which should catch the liberated boronate species similar to the Suzuki coupling, inhibited the reaction (Table 2, entries 17-19). It was reasoned that the present base is responsible for catching the dissociated hydrogen which then cannot reduce the ketone to the alcohol and prevents the transmetalation.

A reason for low turnover numbers is often that the metal species stays in a specific oxidation state, and therefore cannot reenter the catalytic cycle. This, for instance, happens in the case of oxidative C–H transformation. One way to overcome this problem is the addition of an oxidant, such as Cu(II) salts. Thus, 1 equivalent of different metal salts (Table 2, entries 20–28), Zn powder (Table 2, entry 29), and DDQ (Table 2, entry 30) were added to the reaction mixture. A slightly increase of the conversion was could only detected in the presence of Cu(I) salts (Table 2, entries 20 & 22). In all the other cases, the conversion dropped.

Finally, different ligands were tested. The advantages of these ligands in catalytic reactions were already discussed in previous chapters. Unfortunately, the addition of phosphine (Table 2, entries 31 & 32), amine (Table 2, entry 33), and carbene (Table 2, entry 34) ligands did not lead to significant conversion. The trimeric $\text{Ru}_3(\text{CO})_3$ catalyst is likely dissociated into unsaturated metal species while heating up and subsequently undergoes oxidative addition into the C–H bond. If, however, a ligand is added to the reaction, this ligand will coordinate to the vacant side of the metal and prevent the oxidative addition.

Table 2 Screening for the direct arylation of *N*-benzylpyridine-2-amine **89**.



entry	additive	solvent	catalyst [mol%]	t [°C]	conv
1		pinacolone (8 equiv)	5	140	9
2		pinacolone (8 equiv)	5	150	8
3		pinacolone (8 equiv)	5	160	8
4		pinacolone (8 equiv)	5	180	10
5		pinacolone (8 equiv)	10	140	16
6		pinacolone (8 equiv)	20	140	22
7		pinacolone (8 equiv)	30	140	31
8		pinacolone (4 equiv)	5	140	3
9		pinacolone (16 equiv)	5	140	8
10		toluene	5	140	2
11		o-xylene	5	140	3
12		DMF	5	140	0
13		DMA	5	140	0
14		1,2-dichlorobenzene	5	140	2
15		NMP	5	140	0
16	K_2CO_3	pinacolone (8 equiv)	5	140	0
17	Cs_2CO_3	pinacolone (8 equiv)	5	140	0
18	K_3PO_4	pinacolone (8 equiv)	5	140	0

19	CuBr	pinacolone (8 equiv)	5	140	12
20	CuSO ₄	pinacolone (8 equiv)	5	140	0
21	CuI	pinacolone (8 equiv)	5	140	13
22	CuCl ₂	pinacolone (8 equiv)	5	140	0
23	Cu(OAc) ₂	pinacolone (8 equiv)	5	140	2
24	Cu(NO ₃) ₂ ·3H ₂ O	pinacolone (8 equiv)	5	140	6
25	Cu ₂ O	pinacolone (8 equiv)	5	140	0
26	FeCl ₂ ·4H ₂ O	pinacolone (8 equiv)	5	140	0
27	LiCl	pinacolone (8 equiv)	5	140	9
28	Zn	pinacolone (8 equiv)	5	140	4
39	DDQ	pinacolone (8 equiv)	5	140	0
30	PPh ₃ ^b	pinacolone (8 equiv)	5	140	0
31	BINAP ^b	pinacolone (8 equiv)	5	140	0
32	o-phenanthroline ^b	pinacolone (8 equiv)	5	140	0
33	IMes·HCl ^b	pinacolone (8 equiv)	5	140	0

^aReaction conditions: **89** (0.5 mmol), **75** (0.75 mmol), Ru₃(CO)₁₂, additive (0.5 mmol), and solvent (0.5 mL).

^b10 mol%. ^cConversion determined by GC analysis with respect to **89**.

In summary, substrate **89** could be arylated in the benzylic position in low conversion. However, the success of arylation required further investigations of the directing group.

4.1.4 Directing group

The pyridine group was replaced by different directing groups which were likely able to coordinate the metal to the right position (Figure 35). Unfortunately, none of these groups have been suitable for this reaction. The directing group has to bind to the metal strong enough to bring the metal center in proximity to the C–H bond, but weak enough to release the metal after the transformation. This is obviously not the case with these compounds. It is assumed that pyrimidine **100** and pyrazine **101** are coordinating the metal between the two nitrogens of the ring and hinder the metal to insert into the C–H bond or, alternatively, the right conformation is not given. This could be also the case for the thiazole **102**, amidine **103**, amide **105**, and carbamate **121**.

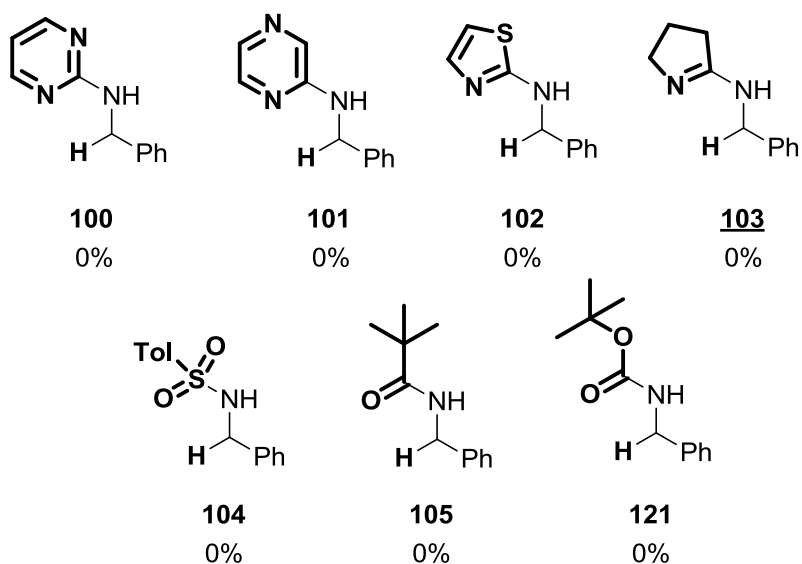


Figure 35 Unsuitable directing groups.

Besides benzylic amines, different substrates with different directing groups were prepared and tested under the same conditions. However, none of them showed any conversion (Figure 36).

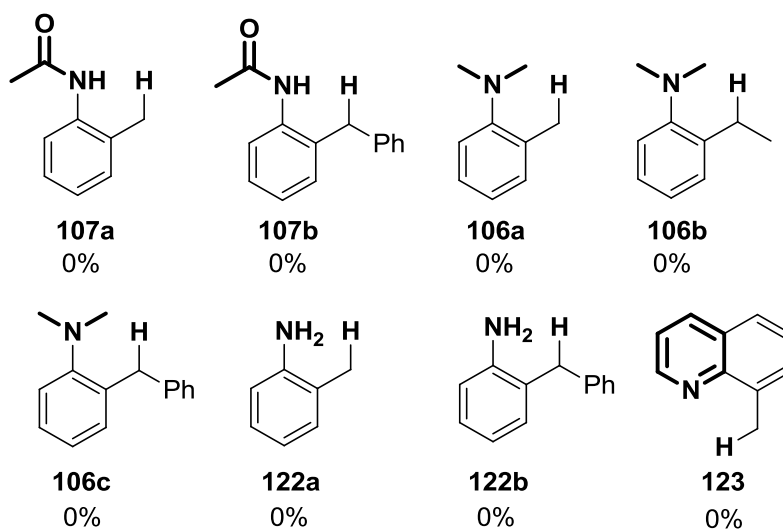


Figure 36 Not tolerated compounds for the direct C-H bond transformation.

With these results in hand, it was decided to change the properties of the pyridine ring. It was considered that the benzylic amine can rotate without hindrance around the bond. This rotation will make coordination of the metal difficult. If the metal is already coordinated to the nitrogen, the equilibrium will shift to the right side due to steric reasons (Figure 37).

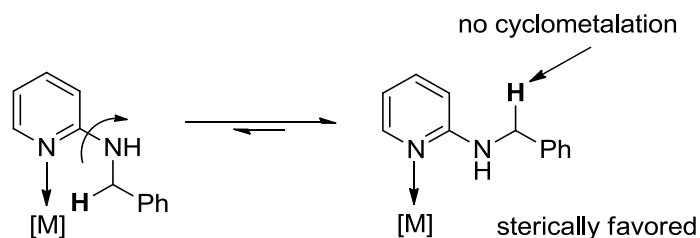


Figure 37 Two different rotamers for compound X.

Consequently, placing a bulky group in 3-position of pyridine was expected to shift the equilibrium to the left side and favor cyclometalation (Figure 38).

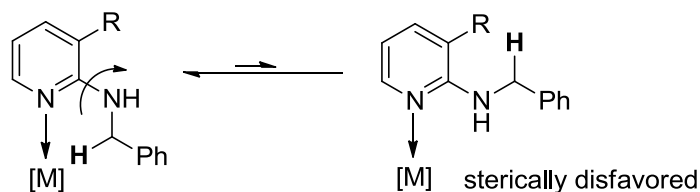


Figure 38 Influence of the substituent on the 3-position of pyridine on the equilibrium.

Indeed, the installation of a methyl group in 3-position resulted in high conversion (85%, Figure 39). Furthermore, the installation of a trifluoromethyl group (**92h**) gave a similar result (86%). Hence, electronic effects of the substituent in 3-position have no influence on the yield of the reaction. The phenyl group (**92m**) was also suitable (84%). Only the chloro substituent (**92k**) gave 18% conversion, which can be explained by the smaller size of this substituent, supporting this hypothesis.

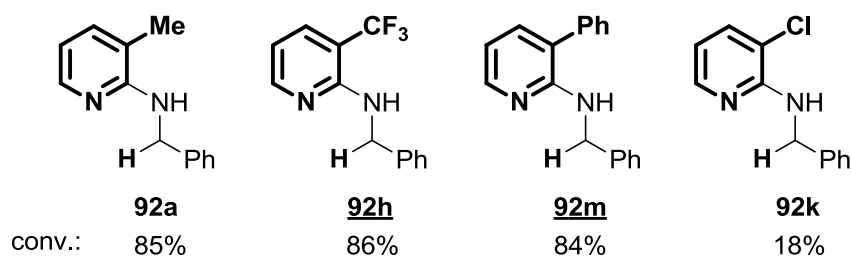
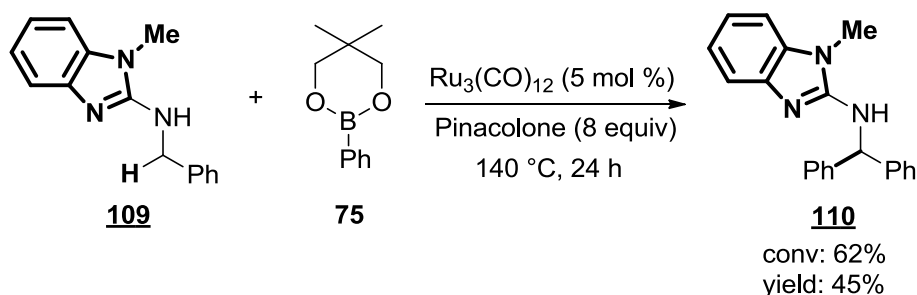


Figure 39 Conversion for different substituents on the 3-position of pyridine.

It was expected that *N*-substituted benzimidazole **109** would perform in a similar way due to the analogous geometry of the directing group. Indeed, this group showed activity, albeit with comparatively lower conversion and yield (Scheme 23).



Scheme 23 *N*-substituted benzimidazole **109** as directing group.

To further strengthen the hypothesis, the relative energy of two specific rotamers of *N*-benzyl-3-methylpyridine-2-amine **92a** and *N*-benzylpyridine-2-amine **89** and the corresponding transition states for their interconversion by means of DFT calculations (Gaussian 03/PBE1PBE, see experimental part) were calculated. The energy profiles, optimized structures, and transition states obtained are presented in Figure 40 (the results for the *N*-benzylpyridine-2-amine system are given in parenthesis). The methyl substituent in 3-position of the pyridine moiety stabilizes rotamer **A** over rotamer **B** by 4.4 kcal/mol, while in the case of parent amine the energies of both rotamers are essentially the same differing merely by 0.5 kcal/mol. The energy barriers for the interconversion of **A** to **B** via a rotation by 180° around the C–N bond is slightly higher in the case of *N*-benzyl-3-methylpyridine-2-amine **92a** by 1.6 kcal/mol. Accordingly, chelate assisted C–H bond activation at the benzylic C–H bonds by transition metals is facilitated in the case of the *N*-benzyl-3-methylpyridine-2-amine **92a** and most likely generally by derivatives with bulky substituents in the 3-position.

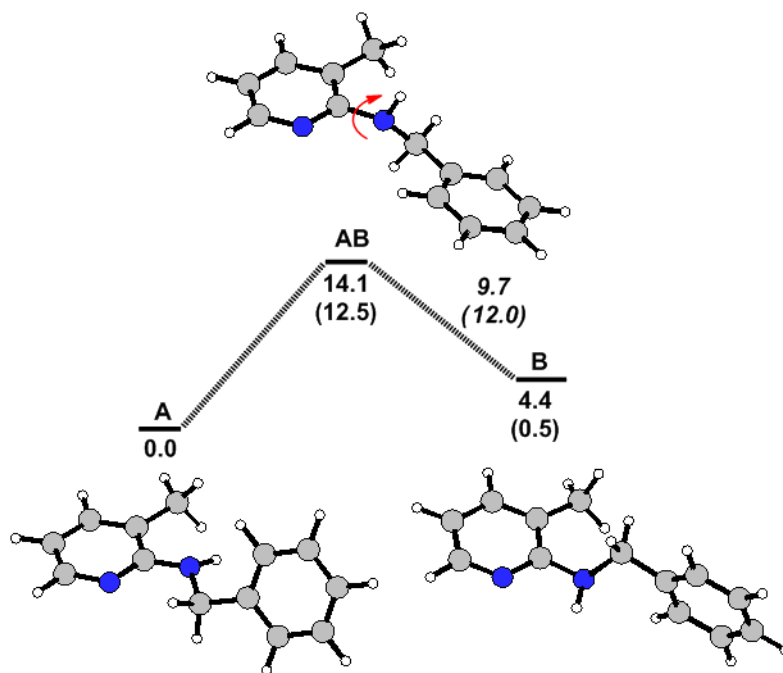
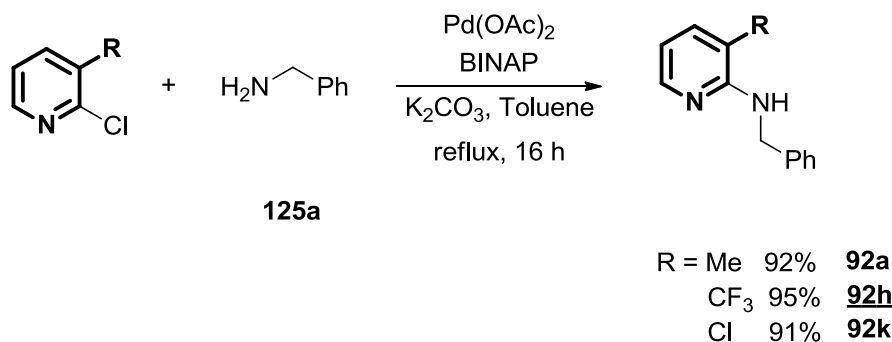


Figure 40 Energy profile (PBE1PBE) for the interconversion of the stable *N*-benzyl-3-methylpyridine-2-amine **92a** rotamers A and B via rotation around the C–N bond. The numbers in parenthesis refer to parent *N*-benzylpyridine-2-amine **89**. The energy values (in kcal mol⁻¹) are referred to the more stable rotamer A.

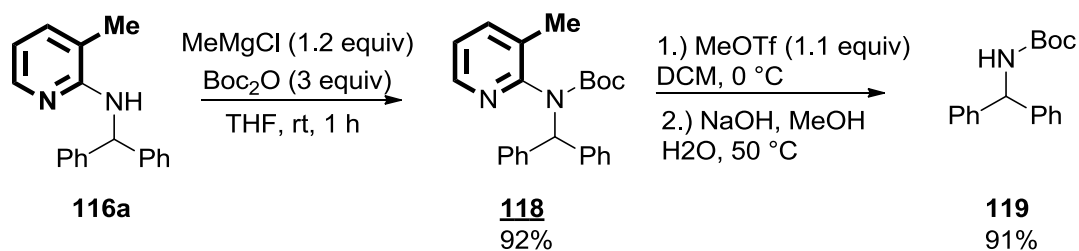
Directing groups can easily be introduced via Buchwald-Hartwig-Amination, starting from commercially available 2-chloro-3-substituted pyridine derivatives and benzylic amine **125a**. This operationally simple, high yielding reaction provides an applicable way to the starting materials (Scheme 24).



Scheme 24 Introduction of the 3-substituted pyridine directing group by Buchwald-Hartwig amination.

One additional requirement for the appropriate directing group was the cleaving of the group from the benzylic amine. Serendipitously, a strategy for this purpose could be found. The used method was recently reported by Studer and co-workers:⁹⁵ *N*-carbamoylation of the amino group of **116a** and subsequent *N*-methylation of the pyridyl group of **118**, followed by hydrolysis of the pyridiniumsalt, delivers Boc protected diphenylmethanamine **119** in high yield (Scheme 25, 84% overall). *N*-Boc deprotection can then be accomplished easily and

often quantitatively following well established protocols.⁹⁶ However, also the Boc-protected compounds can be useful in case further manipulations of the products require the protection of the amino functionality.

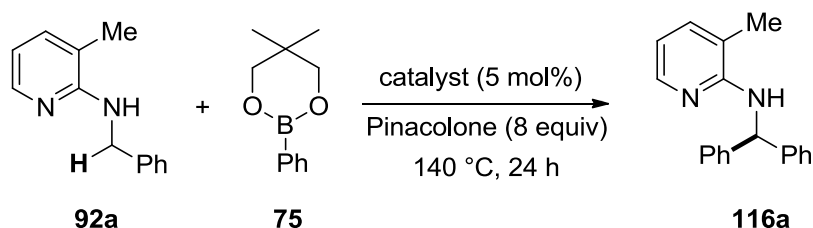


Scheme 25 Cleavage of the directing group.

4.1.5 Ru(0) System - Screening II

A wide range of metal catalysts, including Ru, Rh, and Pd, have been exploited with the previously identified suitable directing group. However, only Ru₃(CO)₁₂ showed good activity (85%, Table 3, entry 2). It was reasoned that the catalyst has to be a bi- or trimetallic ruthenium(0) species which can dissociate and form the active species of the catalyst during heating.

Table 3 Screening of different catalysts for the direct arylation of **92a** with aryl boronates.



entry	catalyst	conv	yield
1	Ru/C	0	0
2	Ru ₃ (CO) ₁₂	85	67
3	Ru(PPh ₃) ₃ H ₂ (CO)	2	0
4	[Ru(<i>p</i> -cymene)Cl ₂] ₂	0	0
5	Ru(PPh ₃) ₃ Cl ₂	0	0
6	Ru(PPh ₃) ₂ Cl ₂ (CO) ₂	0	0
7	[RuCl ₂ (cod)] _n	0	0
8	[RuCl ₂ (CO) ₃] ₂	0	0
9	RuCl ₃	0	0
10	Ru(acac) ₃	0	0
11	[Rh(cod)Cl] ₂	0	0
12	Rh ₄ (CO) ₁₂	0	0
13	Pd(OAc) ₂	0	0

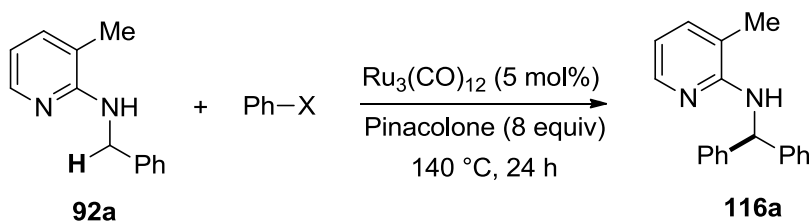
4. RESULTS & DISCUSSION

14	PdCl ₂	0	0
15	Pd(PPh ₃) ₄	0	0
16	Fe(CO) ₅	0	0
17	Fe ₃ (CO) ₁₂	0	0
18	Fe(CO) ₃ (PPh ₃) ₂	0	0

^aReaction conditions: **92a** (0.5 mmol), **75** (0.75 mmol), catalyst (5 mol%), and pinacolone (0.5 mL). ^bConversion determined by GC analysis with respect to **92a**. ^cIsolated yield.

In the next step, different aryl sources were tested. Aryl boronic acid performed worse than the ester (13%, Table 4, entry 1). This might be a solubility problem of the more polar acid. The addition of base could increase the conversion, however still insufficiently (30%, Table 4, entry 2). Potassium phenyltrifluoroborate performed in the same range (13%, Table 4, entry 3). Amongst the phenylboronic acid esters, the propanediol ester was selected due to the simple separation (86%, Table 4, entry 6) from the resulting products. Aryl halides were not suitable for this reaction (Table 4, entries 7 & 8).

Table 4 Screening of aryl donors.



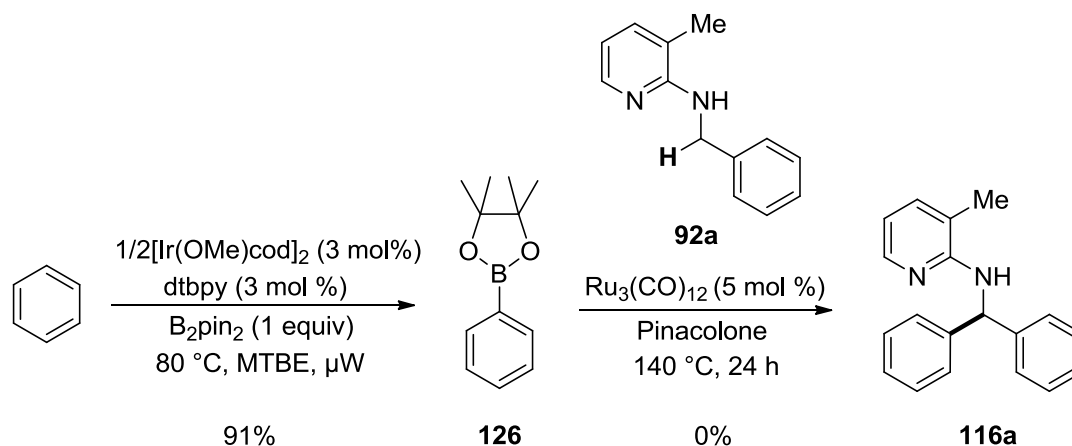
entry	X	conv [%] ^b	yield [%] ^c
1	B(OH) ₂	34	13
2	B(OH) ₂ ^d	38	30
3	BF ₃ K	20	13
4		85	67
5		81	63
6		86	69 (64)^e
7	Br	0	0
8	I	0	0

^aReaction conditions: **92a** (0.5 mmol), PhX (0.75 mmol), Ru₃(CO)₁₂ (5 mol%), and pinacolone (0.5 mL). ^bConversion determined by GC analysis with respect to **92a**. ^cYield determined by GC analysis with respect to **92a** (dodecane as internal standard). ^dAddition of K₂CO₃ (1 mmol). ^eNumber in parentheses is the isolated yield of **116a**.

Hence, it was decided that 1,3-propanediol derived boronic esters were to be used as aryl donors for all further reactions, investigating the scope and limitations of the presented methodology.

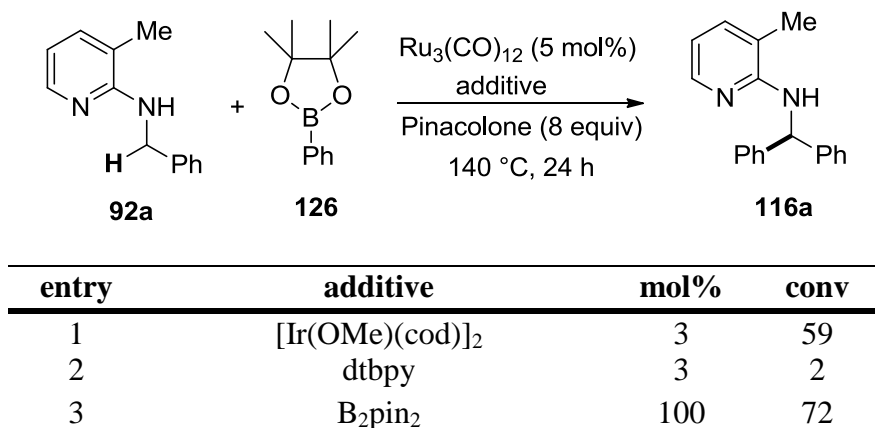
4.1.6 Ru(0) System – One Pot Synthesis

In 2002, Ishiyama, Miyaura, and Buchwald reported an iridium catalyzed method for the direct borylation of arenes.⁹⁷ This powerful and synthetically useful method is an excellent example for selective C–H bond activation. Hence, it was decided to use this method in combination with the arylation method and prepare the required boronate species in situ which would save additional steps and facilitate the synthesis of the products. In a first experiment, phenylboronic acid ester **126** was prepared according to the protocol of Hartwig, resulting in a high yield of the desired product (91%). Subsequently, *N*-substituted benzylic amine **92a**, Ru₃(CO)₁₂ (5 mol%), and pinacolone were reacted at 140 °C for 24 h. Unfortunately, no conversion to the arylated product **116a** (Scheme 26) could be observed.



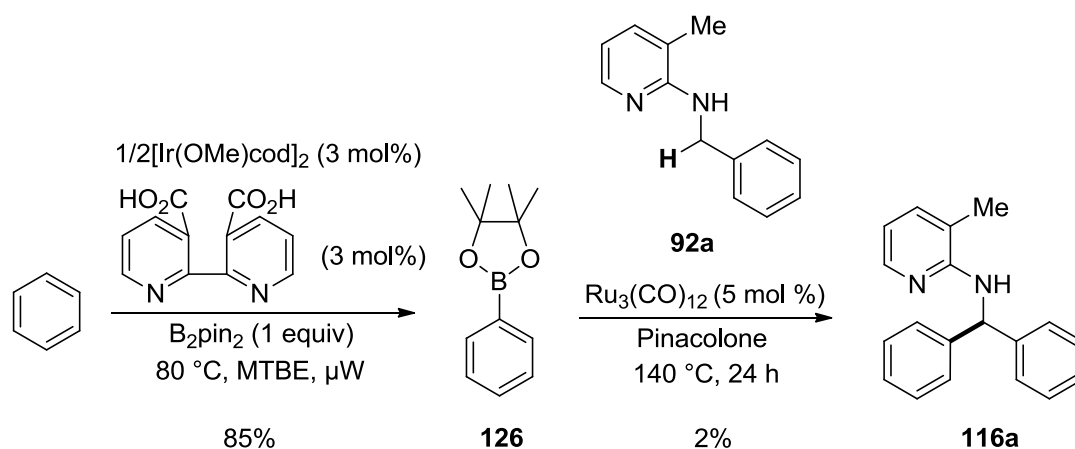
Scheme 26 One-pot synthesis of **116a** starting from benzene.

It was assumed that one of the components of the first experiment was inhibiting the reaction. Therefore, the second step was performed in the presence of each substance of the first step. The previous experiments demonstrated that bidentate ligands such as BINAP or *o*-phenanthroline (Table 5, entries 1-3) are inhibiting the reaction by forming stable and saturated complexes with ruthenium. Indeed, as shown in Table 5, the 4,4'-di-*tert*-butyl-2,2'-bipyridine (dtbpy) ligand, which is essential for the first step, is inhibiting the reaction.

Table 5 Investigation of the inhibiting additive for the ruthenium(0)-catalyzed arylation.

^aReaction conditions: **92a** (0.5 mmol), **126** (0.75 mmol), Ru₃(CO)₁₂ (5 mol%), additive, and pinacolone (0.5 mL). ^bConversion determined by GC analysis with respect to **92a**.

It was decided to change the ligand to 2,2'-bipyridine-3,3'-dicarboxylic acid, which should form a heterogeneous complex with [Ir(OMe)(cod)]₂ according to the literature.⁹⁸ It was expected to avoid interference of the catalyst by this route. Unfortunately, also this experiment failed (Scheme 27). The C–H borylation occurred in high yield, but no conversion was observed in the second step. Since the bipyridine ligand is essential for the first step, but inhibiting the second step, further experiments were cancelled at this point.

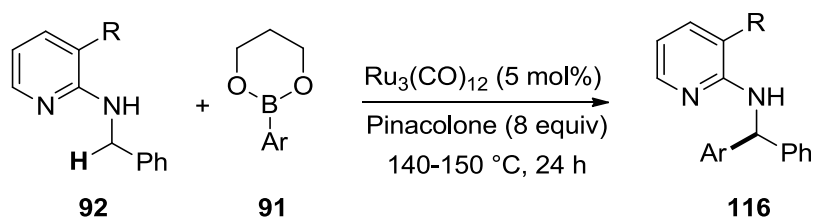
**Scheme 27** One-pot synthesis in the presence of 2,2'-bipyridine-3,3'-dicarboxylic acid as ligand for the iridium catalyzed borylation.

4.1.7 Ru(0) System - Scope

This catalytic method was found to be sensitive towards the electronic and steric properties of the aryl donor. Sterically demanding ortho-substituted aryls (2-Me and 1-Naph <10%, Table 6, entries 2 & 3) gave significantly lower conversions, but meta-substituted aryls (3-Me 61%, Table 6, entry 4) showed good conversion. The best results were obtained with weak electron withdrawing (4-F 66%) or donating aryls (4-Me 62% and 4-*t*-Bu 64%, Table 6, entries 6-9).

Strong electron donating (4-OMe 39%, Table 6, entry 8), withdrawing (4, Cl 33%, 4-CF₃ 41%, 4-Ac 11% and 4-NO₂ 0%, Table 6, entries 10-13) and/or coordinating substituents (4-CN 0%, 3-pyridyl 0%, Table 6, entries 14-15) were much less tolerated compared to their neutral and electron donating counterparts. Furthermore, heterocycles were also not suitable for this transformation (2-thienyl 0%, Table 6, entry 16). The trifluoromethyl and the more bulky phenyl substituent in 3-position of pyridine showed in general better conversions (Table 6, entries 17-25). This trend is supporting the hypothesis that increasing the bulk of the group in 3-position of pyridine favors the presence of a conformation which is readily arylated.

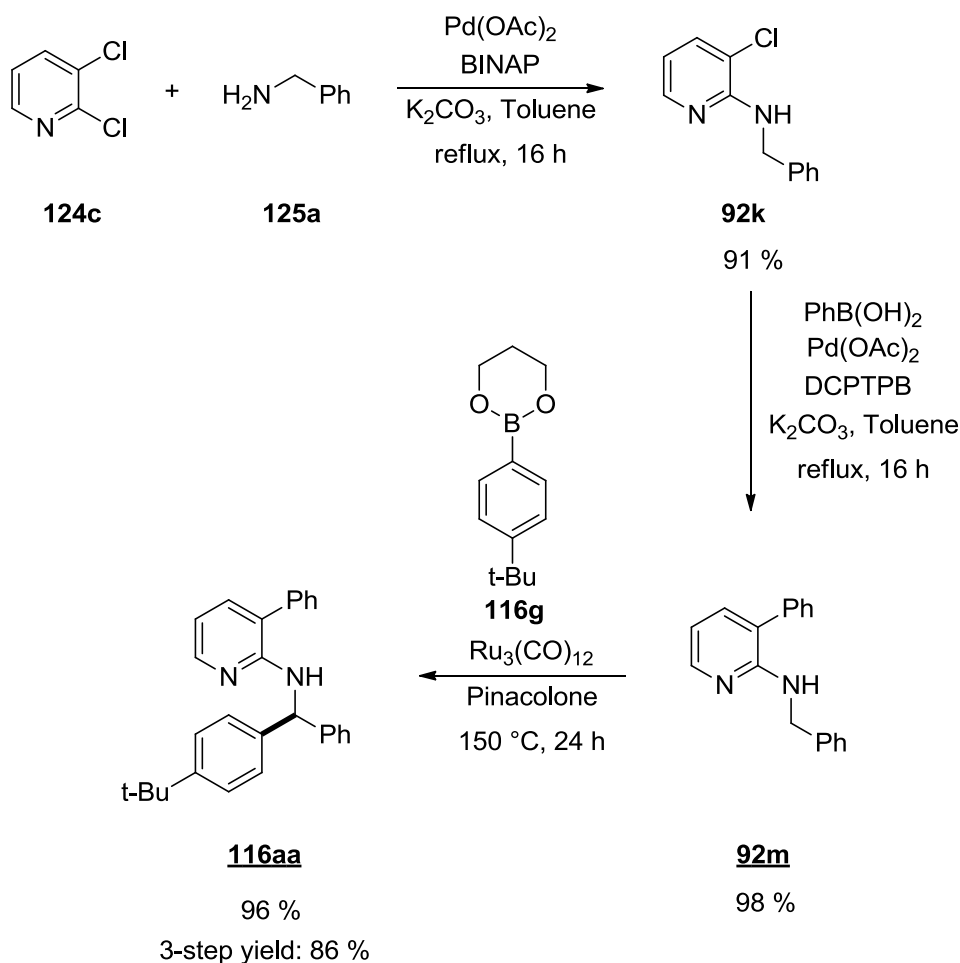
Table 6 Ruthenium(0)-catalyzed arylation of pyridine derivatives.



entry		R	Ar	conv	yield
1	116a	Me	Ph	86	64
2	116am	Me	2-Me-Ph	55	n.i. ^{d,e}
3	116an	Me	1-Naph	8	n.i. ^d
4	116b	Me	3-Me-Ph	87	61
5	116d	Me	3-Cl-Ph	59	38
6	116e	Me	4-Me-Ph	88	62
7	116f	Me	4- <i>t</i> -Bu-Ph	87	64
8	116h	Me	4-OMe-Ph	50	39
9	116j	Me	4-F-Ph	89	66
10	116k	Me	4-Cl-Ph	49	33
11	116l	Me	4-CF ₃ -Ph	61	41
12	116ao	Me	4-Ac-Ph	11	n.i. ^d
13	116ap	Me	4-NO ₂ -Ph	0	0
14	116aq	Me	4-CN-Ph	0	0
15	116ar	Me	3-pyridyl	0	0
16	116as	Me	2-thienyl	0	0
17	116r	CF ₃	Ph ^f	90	78
18	116s	CF ₃	4-Me-Ph ^f	92	77
19	116t	CF ₃	4- <i>t</i> -Bu-Ph ^f	84	70
20	116u	CF ₃	4-OMe-Ph ^f	76	61
21	116v	CF ₃	4-F-Ph ^f	65	51
22	116w	Ph	Ph ^f	100	90
23	116z	Ph	4-Me-Ph ^f	100	85
24	116aa	Ph	4- <i>t</i> -Bu-Ph ^f	100	96

25	116ac	Ph	4-F-Ph ^f	100	72
^a Reaction conditions: 92 (0.5 mmol), ArB(OR) ₂ (0.75 mmol), Ru ₃ (CO) ₁₂ (5 mol%), and pinacolone (0.5 mL). ^b Conversion determined by GC analysis with respect to 92 . ^c Isolated yield. ^d n.i. = not isolated. ^e Could not be isolated because of side products. ^f 150 °C.					

Table 6 shows good results for the direct arylation of benzylic amines. In particular, no protecting group for the NH was required for this transformation which facilitates the reaction. The overall process of benzylamine **125a** attachment, Suzuki-Miyaura coupling and finally direct arylation is very efficient with yields over 90% for each individual step and 86% overall yield over 3 steps (Scheme 28).

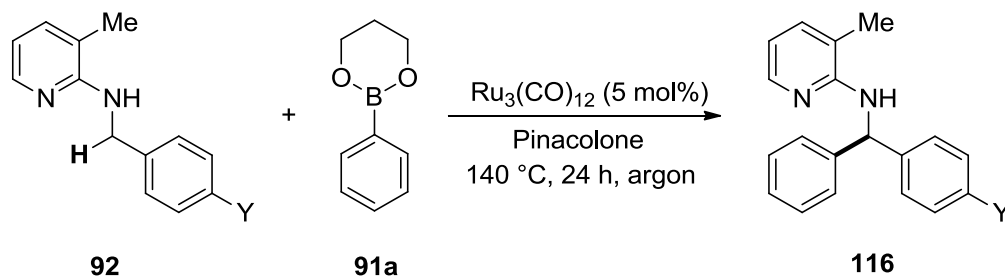


Scheme 28 Synthesis of **116aa** over 3 steps with an overall yield of 86%.

Next, the electronic influence of the benzylic position on the transformation was investigated. Hence, different starting materials were synthesized and reacted under the optimized conditions. In general, it appears that the reaction is very sensitive to the electronic properties of the benzylic amines. Strong electron donating (4-*OiPr* 25% & 4-*OMe* 32%, Table 7, entries 1 & 2) and withdrawing (4-*CF*₃ 15% & 4-*CO*₂*Me* 26%, Table 7, entries 6 & 7) substituents diminished the conversion. The best results could again be achieved with weak electron donating or withdrawing substituents (4-*Me* 76% & 4-*F* 44%, Table 7, entries 3-5). In the

case of methyl ester **116o**, decarboxylated product **116a** was detected as a major side product. This is not too surprising since the catalyst is known to undergo decarboxylation.⁹⁹

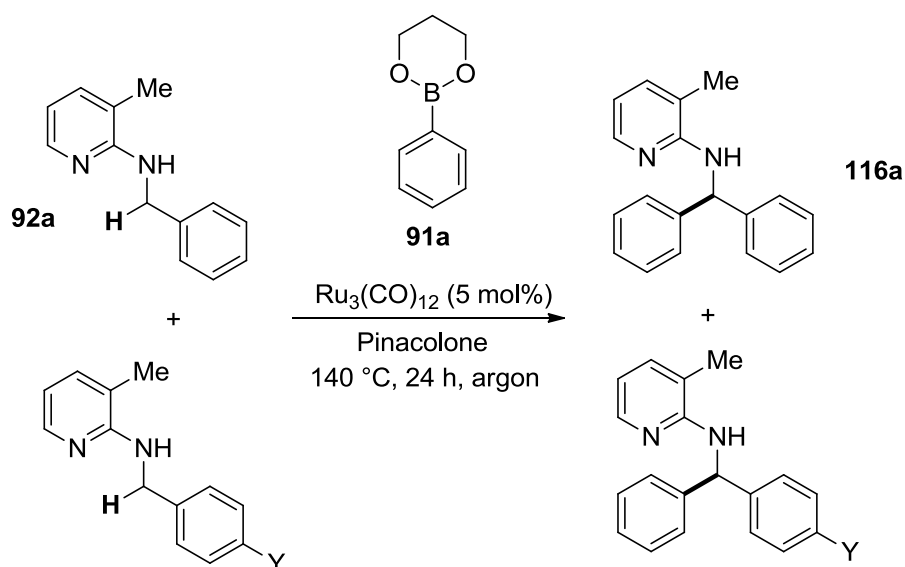
Table 7 Influence of the substituent on the benzylic group for the ruthenium(0)-catalyzed reaction.



entry		Y	conv	yield
1	116n	O <i>i</i> Pr	35	25
2	116h	OMe	58	32
3	116e	Me	99	76
4	116a	H	86	64
5	116j	F	73	44
6	116l	CF ₃	24	15
7	116o	CO ₂ Me	43 ^d	26 ^d

^aReaction conditions: **92** (0.5 mmol), **91a** (0.75 mmol), Ru₃(CO)₁₂ (5 mol%), and pinacolone (0.5 mL). ^bConversion determined by GC analysis with respect to **92**. ^cIsolated yield. ^dDecarboxylated product as side product detected but could not be quantified due to overlap with the substrate peak.

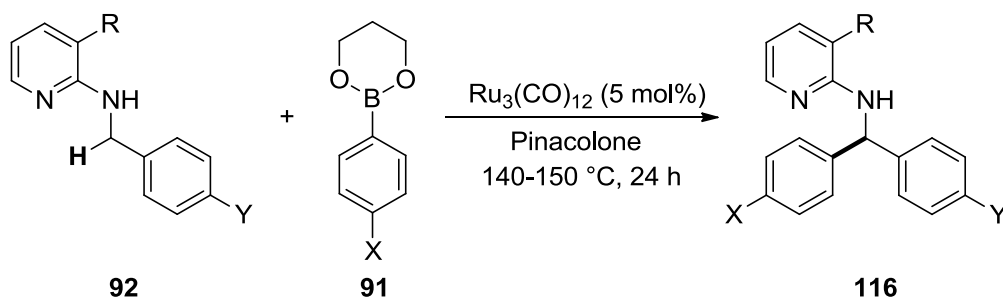
In this context, a series of competition experiments was performed. 1 Equivalent of two different starting materials was added to the reaction mixture and reacted with 1 equivalent of phenylboronic acid ester. The reaction was monitored via GC. This results support the previous results in general. The starting materials carrying electronically relatively neutral substituents (4-Me, Table 8, entry 3) react with a similar rate as the unsubstituted benzyl substrate does. The electron donating (4-O*i*Pr & 4-OMe, Table 8, entries 1 & 2) and withdrawing (4-CF₃ & 4-CO₂Me, Table 8, entries 5 & 6) substituents react comparatively slower. In the case of the methyl ester decarboxylation was observed, leading to the high H:Y product ratio (Table 8, entry 7).

Table 8 Competition experiments for the ruthenium(0)-catalyzed reaction.

entry	Y	H:Y ^b
1	OiPr	1.3
2	OMe	1.4
3	Me	1
5	F	1.6
6	CF ₃	2.2
7	CO ₂ Me	5.3

^aReaction conditions: **92a** (0.5 mmol), substituted SM (0.5 mmol), **91a** (0.5 mmol), $\text{Ru}_3(\text{CO})_{12}$ (5 mol%), and pinacolone (0.5 mL). ^bRatio determined by GC analysis.

Because the *N*-substituted *p*-tolylmethanamine starting material **92b** showed the best reactivity (99% conv., Table 7, entry 3), the reaction was performed with substrates carrying this tolyl residue and compared to the results for benzylamine. However, the *p*-tolylmethanamine did not show in general better results (e.g. for 3-CF₃: Y=H 77% and Y=Me 80%, for 3-Ph: Y=H 90% and Y=Me 90%, Table 9, entries 5-8). Different aryl donors were tested in combination with 3-phenylpyridine **92n** which showed again the best performance and higher yields compared to the 3-methylpyridine **92b** (Table 9, entries 9-12). The trend of decreased conversion from electron donating to withdrawing substituents is again similar to the previous observed results.

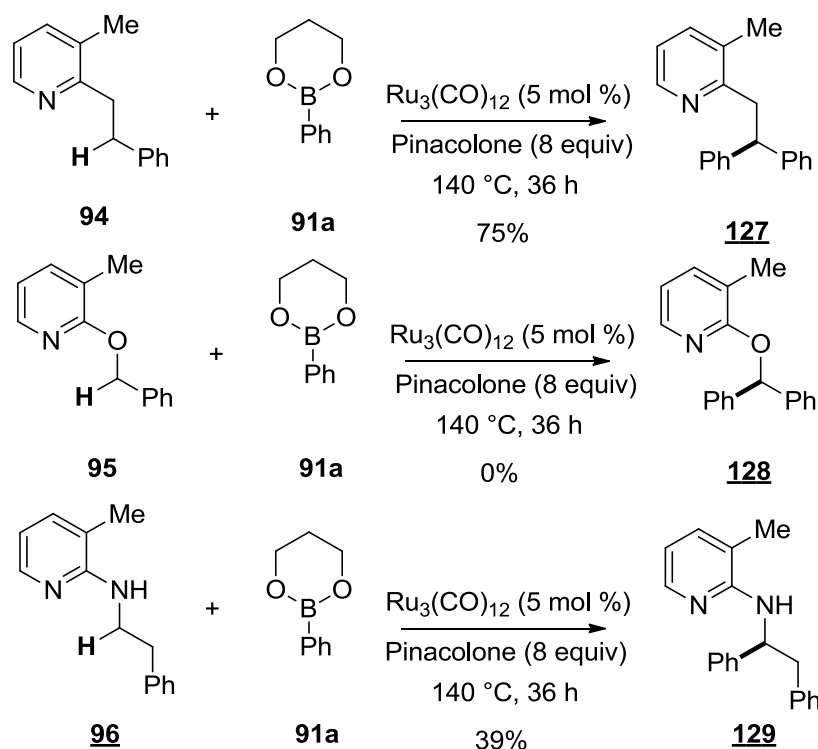
Table 9 Scope for *p*-tolylmethanamine.

entry		R	Y	X	conv	yield
1	116a	Me	H	H	86	64
2	116e	Me	Me	H	99	76
3	116p	Me	Me	Cl	69	50
4	116q	Me	Me	CF ₃	48	33
5	116r	CF ₃	H	H	90	77
6	116s	CF ₃	Me	H	95	80
7	116w	Ph ^d	H	H	100	90
8	116z	Ph ^d	Me	H	98	90
9	116ag	Ph ^d	Me	Me	88	73
10	116ah	Ph ^d	Me	<i>t</i> -Bu	76	67
11	116ai	Ph ^d	Me	F	71	60
12	116aj	Ph ^d	Me	CF ₃	47	33

^aReaction conditions: **92** (0.5 mmol), **91** (0.75 mmol), Ru₃(CO)₁₂ (5 mol%), and pinacolone (0.5 mL). ^bConversion determined by GC analysis with respect to **92**.

^cIsolated yield. ^d150 °C.

Finally, it was investigated if the reaction is limited to benzylamine substrates and to benzylic positions. It was found that the NH group is not essential and can be replaced by a CH₂ group with comparable yield (**94**, 75%, Scheme 29). Only a prolonged reaction time (36h instead of 24h) was required. However, the reaction did not work by replacing the NH with oxygen (**95**), which can be explained by coordination of the lone pair of the oxygen to the metal. Notably, the reaction also works with non-benzylic sp³ C–H bonds as shown with **96**. However, the reaction takes again longer (48h) and the yield was considerably lower (39%). This shows that the activation of a CH₂ group due to its benzylic nature is more important than activation via an adjacent NH group.

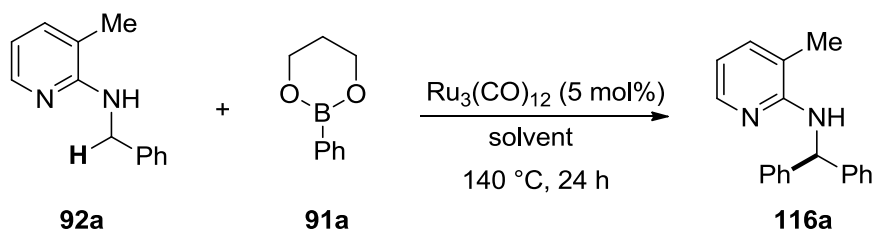


Scheme 29 Expanding the scope of the direct arylation to compound **94**, **95**, and **96**.

4.1.8 Ru(0) System – Mechanistic Studies

The further improvement of reaction condition for this transformation required a greater mechanistic understanding of these processes. Mechanistic investigations were started with the role of the ketone performing the reaction in the absence and presence of different ketones. Table 10 illustrates the crucial role of the ketone. The conversion rises significantly by addition of a ketone, supporting the observations of Chatani and Sames.⁹³ During a survey of the effect of various ketones, it was determined that the size and electronic properties of the ketone are less important. Interestingly, the product was also formed in good yields in the presence of high excess of acetophenone (61%, Table 10, entry 4) which can also be arylated under these conditions,⁶⁹ indicating pyridine being a stronger directing group than the ketone. Only traces of the arylated acetophenone could be detected via GC-MS. Furthermore, the reduced alcohol of pinacolone could be detected via GC-MS, supporting the mechanism proposed by Chatani and Sames.

Table 10 Screening of different ketones.

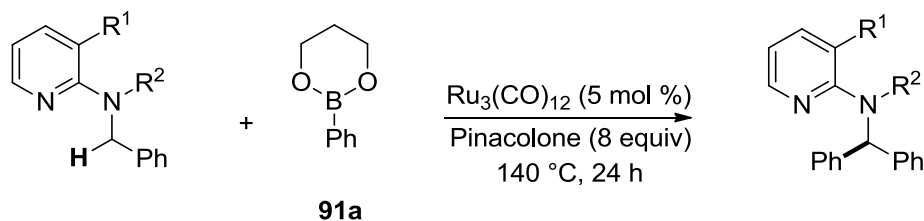


entry	solvent	conv	yield
1	toluene	20	6
2	pinacolone	86	69
3	acetone/dioxane (1:1)	82	62
4	acetophenone	80	61
5	cyclohexanon	83	61

^aReaction conditions: **92a** (0.5 mmol), **91a** (0.75 mmol), Ru₃(CO)₁₂ (5 mol%), and solvent (0.5 mL). ^bConversion determined by GC analysis with respect to **92a**. ^cYield determined by GC analysis with respect to **92a** (dodecane as internal standard).

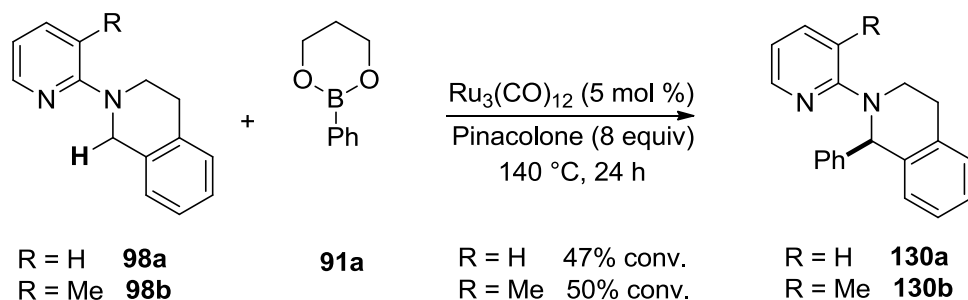
So far, all experiments had been conducted with the free NH group. Thus, it was decided to test the catalytic system on *N*-substituted amines. Different combinations of substituted amines with substituted pyridines were tried to exclude the steric influence. The results are summarized in Table 11. Best result could be accomplished with the free amine (86%, Table 11, entry 2). In the case of methyl substituted amine conversion decreased significantly (Table 11, entry 3 & 4). All amide compounds did not show any conversion (Table 11, entries 7-10). *N*-Substituted tetrahydroisoquinoline showed moderate conversion (Scheme 30).

Table 11 Ruthenium(0)-catalyzed direct Arylation of *N*-substituted compounds.



Entry	R ¹	R ²	conv
1	H	H	9
2	Me	H	86
3	H	Me	8
4	Me	Me	17
5	H	Ac	0
6	Me	Ac	0
7	H	Bz	0
8	Me	Bz	0
9	H	Piv	0
10	Me	Piv	0

^aReaction conditions: Amine (0.5 mmol), **91a** (0.75 mmol), Ru₃(CO)₁₂ (5 mol%), and pinacolone (0.5 mL). ^bConversion determined by GC analysis with respect to amine.



Scheme 30 Ruthenium(0)-catalyzed direct arylation of *N*-substituted THIQ.

Further DFT calculations showed that the *N*-Me substitution lead to a decreased stability of rotamer B, which has the preferred conformation for the C–H insertion of the metal, over rotamer A. As shown in Figure 40, rotamer B of *N*-benzyl-3-methylpyridine-2-amine **92a** is stabilized by 4.4 kcal/mol over rotamer A. After *N*-methylation, rotamer B of *N*-benzyl-*N*,3-dimethylpyridin-2-amine **97b** shows only 1.5 kcal/mol stability of over A (the stability of rotamer B of compound **97a** was even lower 0.5 kcal/mol). This decreased stability causes a lower energy barrier for the rotation of the benzylic amine around the N–C bond which hinders the metal to insert into the C–H bond. This information explains the lower conversion (17%, Table 11, entry 4) of **97b** compared to the unsubstituted compound **92a** (86%, Table 11, entry 2).

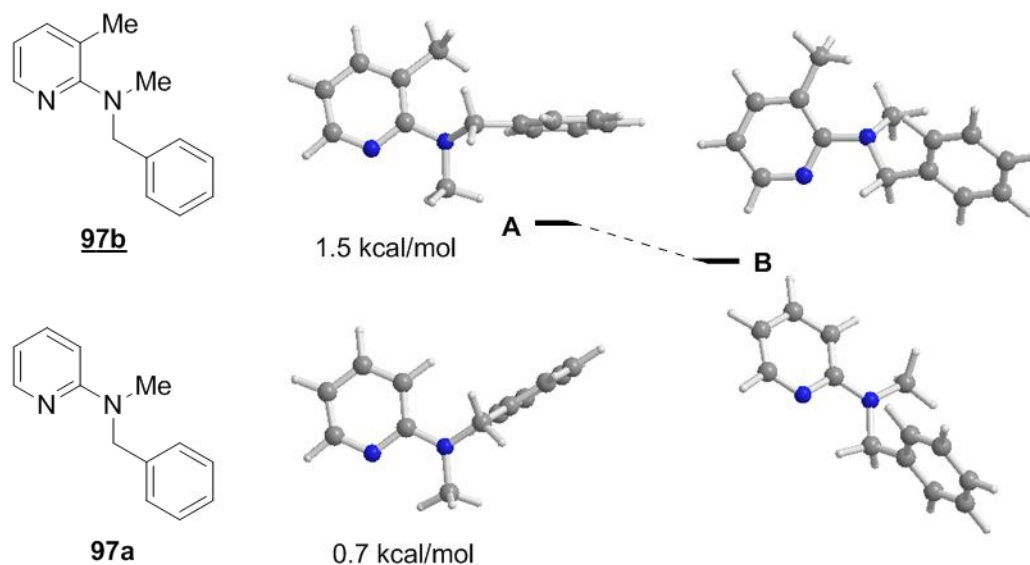
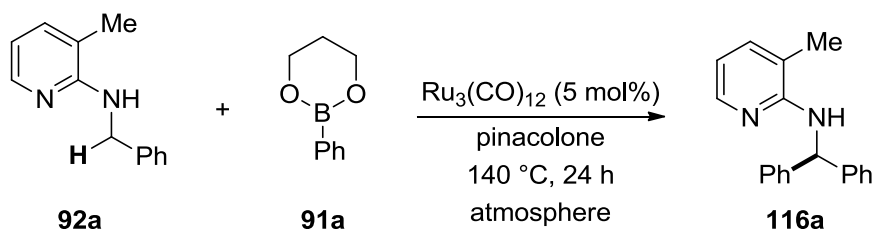


Figure 41 Energy profile (PBE1PBE) for the interconversion of the stable **97a** and **97b** rotamers A and B via rotation around the C–N bond. The energy values (in kcal mol⁻¹) are referred to the more stable rotamer A.

Next, the behavior of the catalyst under different atmospheres was examined. These experiments should provide information about the required oxidation state of the metal during

the reaction. All of the preceding reactions were performed under argon (e.g. 86% conversion, Table 12, entry 1). Surprisingly, the catalyst performed even slightly better under air (91% conversion Table 12, entry 2). The catalyst is known to be air stable. However, it was concluded to perform further reactions under argon due to better aryl donor stability under inert conditions. It was determined that carbon monoxide is decreasing the conversion (65%, Table 12, entry 3), which can be explained by the strong ligand properties of CO. The ligand is likely to bind to the active metal species forming an inactive catalyst. Interestingly, a hydrogen atmosphere pushed the reaction (97%, Table 12, entry 4), resulting in high yields. Hydrogen is obviously facilitating the reductive elimination step of the metal species or activating the catalyst before entering the catalytic cycle. The reaction was also working under microwave conditions at higher temperatures and shorter reaction times. The somewhat lower yield can be explained by the formation of unidentified side products (Table 12, entries 5 & 6).

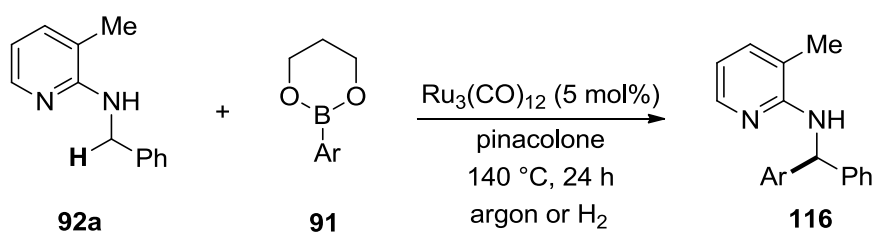
Table 12 Ruthenium(0)-catalyzed arylation under different atmospheres.



entry	atmosphere	conv	yield
1	argon	86	69 (64) ^d
2	air	91	73
3	CO	65	43
4	H ₂	97	93 (91)^d
5	argon (μW) ^e	99	59 (53) ^d
6	H ₂ (μW) ^e	98	84

^aReaction conditions: **92a** (0.5 mmol), **91a** (0.75 mmol), Ru₃(CO)₁₂ (5 mol%), and pinacolone (0.5 mL). ^bConversion determined by GC analysis with respect to **92a**. ^cYield determined by GC analysis with respect to **92a** (dodecane as internal standard). ^dNumber in parentheses is isolated yield of **116a**. ^eμW reaction: 170 °C for 2.5 h.

These results inspired a more detailed comparative study of the reaction by various aryl donors under argon and hydrogen. The yield could be increased significantly with electron neutral substituents on the boronic acid ester (Table 13, entries 2 & 4), but other substituents, such as methoxy or trifluoromethyl (Table 13, entries 6 & 8), performed worse.

Table 13 Ruthenium(0)-catalyzed arylation of **92a** under argon and hydrogen.

entry		Ar	atmosphere	conv	yield
1	116a	Ph	argon	86	64
2	116a	Ph	H ₂	97	91
3	116e	4-Me-Ph	argon	88	62
4	116e	4-Me-Ph	H ₂	98	83
5	116h	4-OMe-Ph	argon	50	39
6	116h	4-OMe-Ph	H ₂	23	n.i. ^d
7	116l	4-CF ₃ -Ph	argon	61	41
8	116l	4-CF ₃ -Ph	H ₂	65	35

^aReaction conditions: **92a** (0.5 mmol), **91** (0.75 mmol), Ru₃(CO)₁₂ (5 mol%), and pinacolone (0.5 mL). ^bConversion determined by GC analysis with respect to **92a**.

^cIsolated yield. ^dn.i. = not isolated.

Furthermore, the kinetics of the reaction was investigated carefully. Thus, conversion at different reaction times were measured. Figure 42 illustrates the gradient of the process indicating the reaction to be of second or higher-order.

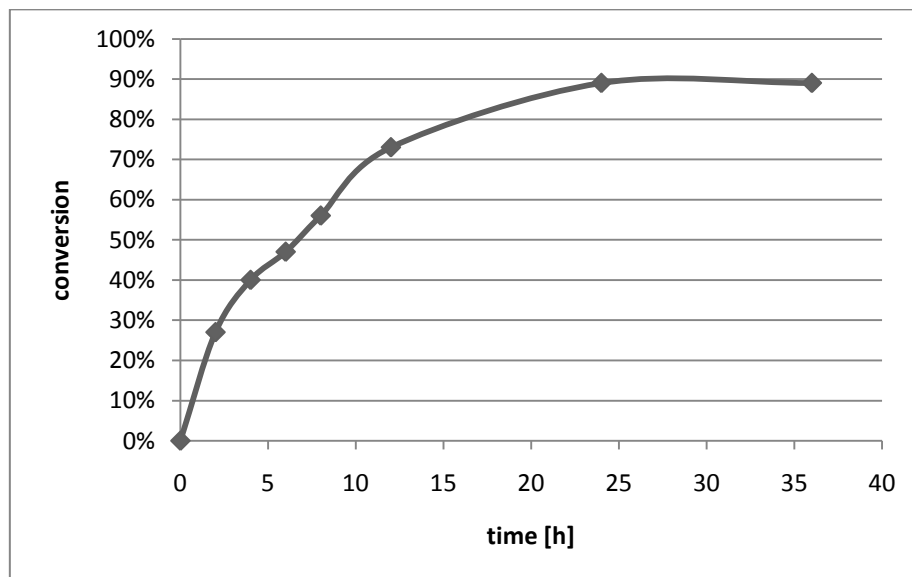
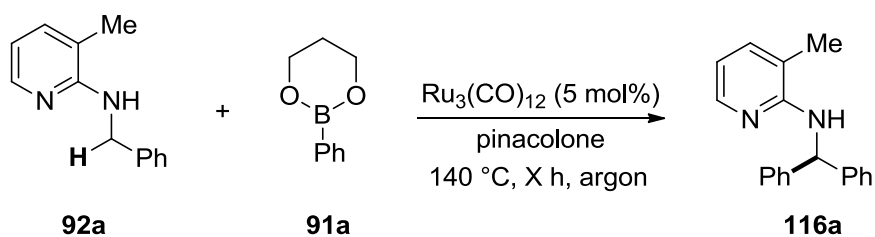


Figure 42 Kinetic studies of the ruthenium(0)-catalyzed direct arylation.

Kinetic Isotope Effect-KIE

To get more detailed information about the kinetics, kinetic isotope effect studies were conducted. Therefore, the benzylic proton(s) were replaced by deuterium. The origin of the isotope effect relies on the difference in zero point energies between unlabeled (C–H) and labeled (C–D) bonds.¹⁰⁰ The stretching vibration of the bond is related to the reduced mass (m_r).

$$v = \frac{1}{2\pi} \sqrt{\frac{k}{m_r}} \text{ where } m_r = \frac{m_1 m_2}{m_1 + m_2}$$

The reduced mass of a C–H bond is considerably affected by the replacement of the light H by a twice heavier D. This results in a lower stretching frequency of a C–D bond and higher activation energy for the C–D bond cleavage (Figure 43).

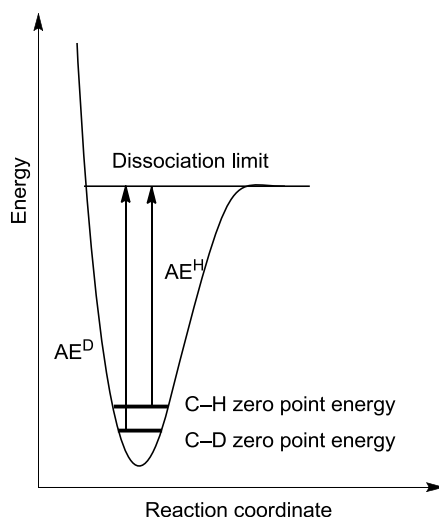


Figure 43 Reaction coordinate diagram for a C–H/C–D bond activation.

The magnitude of the KIE depends on the changes when passing from the reactants to the activated complex in the TS. If the $k_H/k_D = 1$, there is no isotope effect, and the conclusion of this experiment is that the C–H bond cleavage is not the rate determining step of the process. Values of $k_H/k_D > 1$ are called normal, values of $k_H/k_D < 1$ inverse KIEs. When the isotope replacement C–H/C–D has occurred in the bond that is broken in the rate determining step, values higher than $k_H/k_D > 1.5$ are expected (primary isotope effect). Figure 44 shows an example for a primary isotope effect. As the C–H/C–D bond is being broken in the activated complex, zero point energies of the C–H and C–D bond are much closer. Subsequently, the C–H activation energy (AE^H) is smaller than the C–D activation energy (AE^D), and the reaction is faster for C–H than for C–D ($k_H/k_D > 1$) (It has to be mentioned that a positive KIE value does not necessarily mean that the C–H bond breaking is the rate determining step.¹⁰¹ However, this topic is too comprehensive and out of scope of this work).

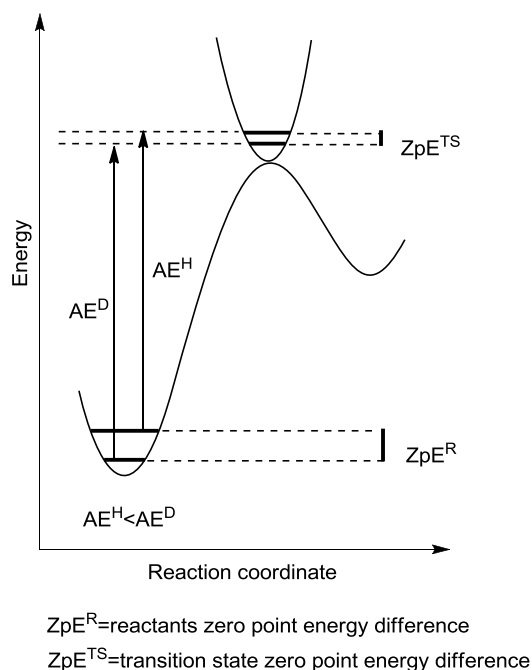
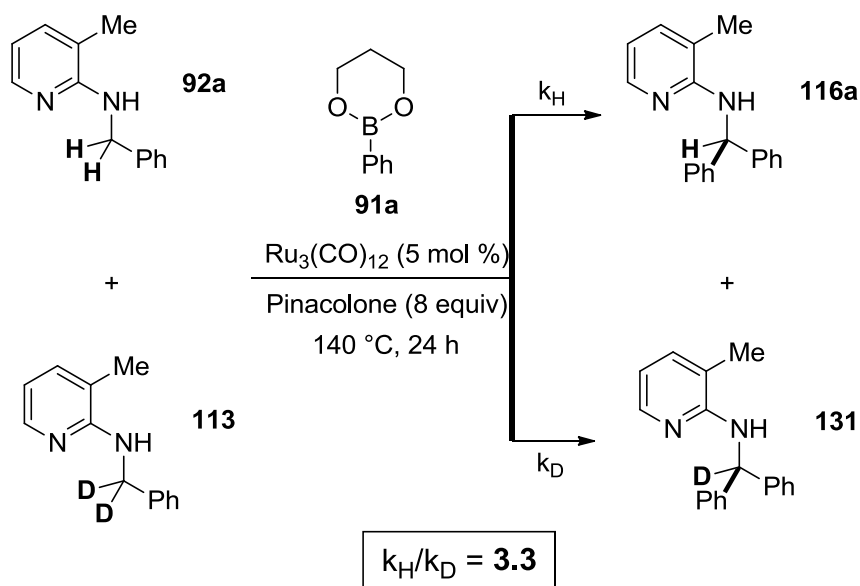


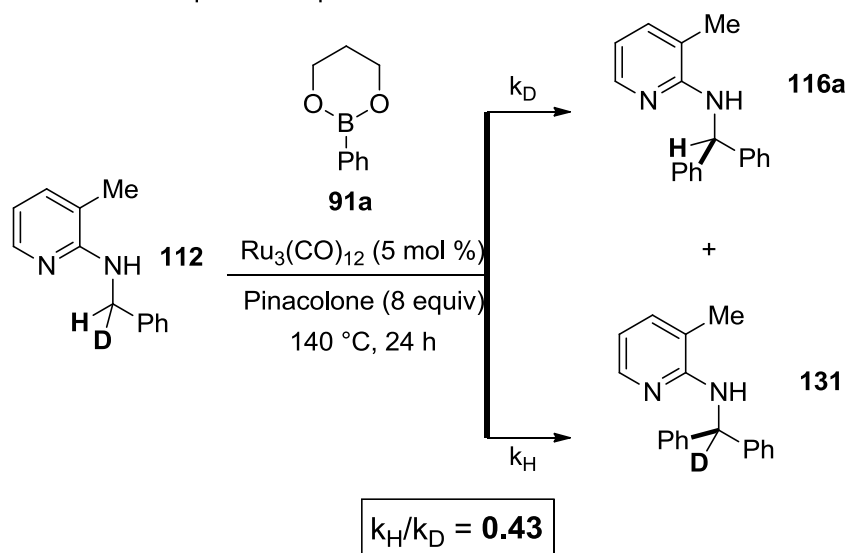
Figure 44 Reaction coordinate for a catalyzed C–H/C–D bond activation.

For this kind of experiment, an intermolecular competition experiment was set up for compounds **92a** and **113** (Scheme 31). The reaction was carried out with 1 equivalent of *N*-benzyl-3-methylpyridin-2-amine **92a**, 1 equivalent of the deuterated analog **113**, and 1 equivalent of phenylboronic acid 1,3-propanediol ester **91a** to achieve a maximum of 50% conversion. The mixture of both products was isolated and analyzed by ^1H NMR. The KIE was found to be $k_{\text{H}}/k_{\text{D}}=3.3$. This is a relatively high value for KIE experiment and indicates a primary isotope effect. However, such a single result is no proof of the C–H activation step being rate determining; this indicates only that the C–H bond is of course weaker compared to the C–D bond, and hence the rate of C–H insertion is higher than the rate of C–D insertion. Interestingly, when the intramolecular KIE was investigated starting from substrate **112** an inverse KIE of 0.43 was measured. Inverse KIEs have been previously reported in C–H bond activation reactions and were attributed to a reversible C–H activation step (hence also termed inverse equilibrium isotope effect) eventually involving a σ -complex preceding C–H insertion.¹⁰⁰ The so formed metal-hydride or metal-deuteride complexes are of different stability, the metal deuteride complex being obviously more stable (and hence a slower back reaction) in case of an inverse equilibrium isotope effect. Hence, the metal-deuteride complex is accumulated to some extent and undergoes the subsequent steps of the catalytic cycle more frequently.

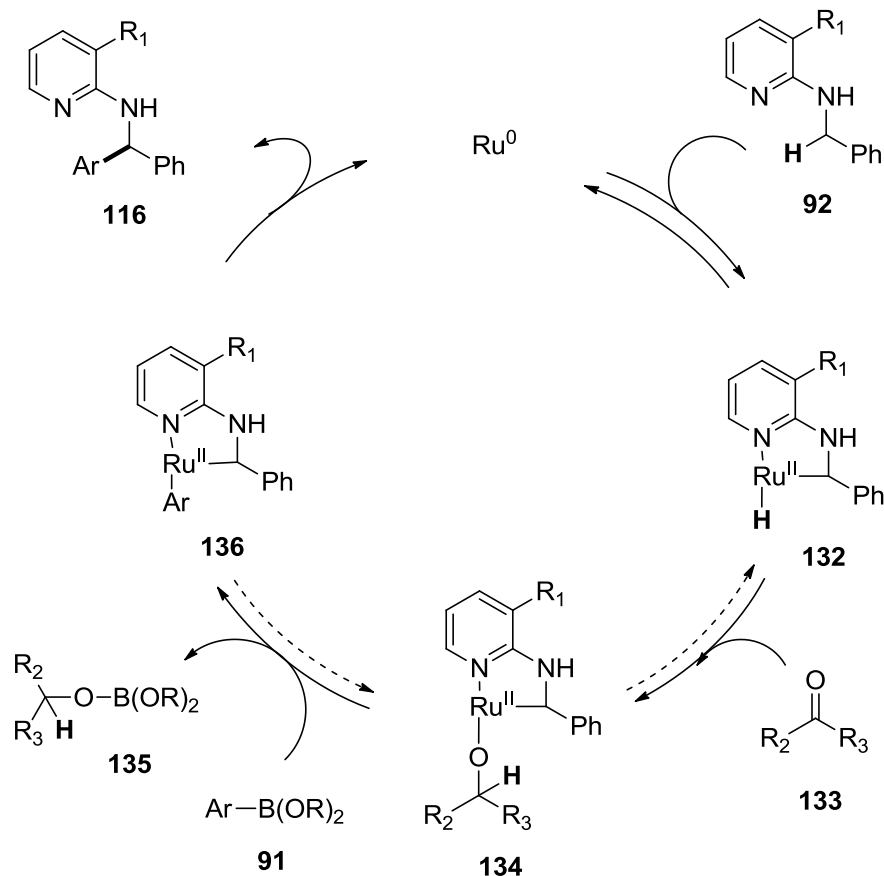
Intermolecular Competition Experiment:



Intramolecular Competition Experiment:

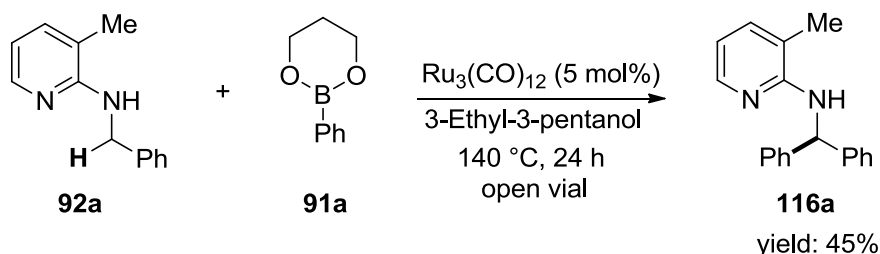
**Scheme 31** Competitive deuterium labeling experiments for the ruthenium(0)-catalyzed reaction.

According to these results and the plausible mechanism of Kakiuchi, Chatani, and Murai, the following mechanism is proposed: The catalytic process is initiated by coordination of ruthenium(0) to the pyridine nitrogen, followed by oxidative addition to **132**. This step is reversible. Subsequently, the ketone is reduced to the corresponding alcohol, followed by the formation of a metal-alkoxy (Ru-OR) species **134**. This intermediate facilitates the transmetalation with Ar-B(OR)₂ to **136**. The ketone acts as hydrogen and boron scavenger, simultaneously. The reductive elimination delivers finally product **116** and regenerates the catalyst. Sames supported this mechanism in his work (Scheme 32).



Scheme 32 Proposed mechanism for the ruthenium(0)-catalyzed reaction.

However, these conditions gave unsatisfactory results for the pyridine directing group and piperidine substrates: As already mentioned, Maes could achieve a higher conversion for the piperidine/pyridine system by using alcohol instead of ketone (Scheme 20).⁹⁴ His group proved the formation of H₂ under these conditions by Raman spectroscopy. Not surprisingly, the reaction performed much better in an open system. The reaction was performed under the same conditions as Maes. Interestingly, in this case, the closed vial/ketone conditions gave much higher yields (Scheme 33) which might be because of unidentified sideproducts formed under this specific condition.

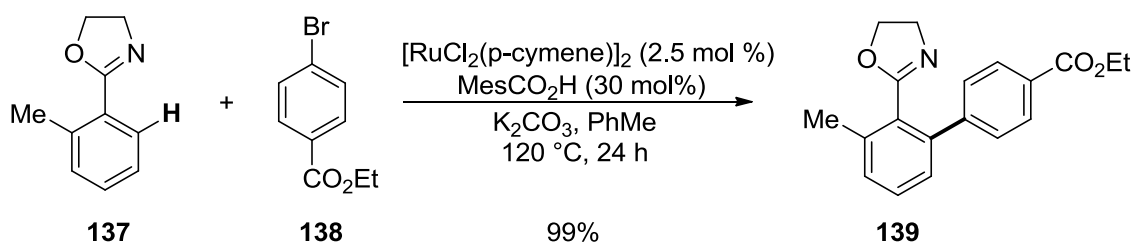


Scheme 33 Changed reaction conditions to open vial and alcohol.

For further supporting this statement, the reaction was also performed in the presence of 1 equivalent pinacolborane (HBpin) to investigate the influence of the produced borane species. Maes speculated that such a pinacolborane species could poison the catalyst eventually by oxidative addition. Since all other experiments so far point to the mechanism displayed in Scheme 32, a significant decrease of conversion was not expected. If HBpin is really poisoning the catalyst, the reaction should actually be shut down almost completely when such a great excess of HBpin is present. It was found that the conversion decreased to 75 % in comparison to the 95 % without the HBpin. However, even with a high excess of HBpin with respect to catalyst, the conversion is still high. This result suggests that HBpin eventually produced in the reaction is not poisoning the catalyst and the decrease of conversion in the control experiment could be explained by other reasons (e.g. dilution, change of the internal temperature, etc.).

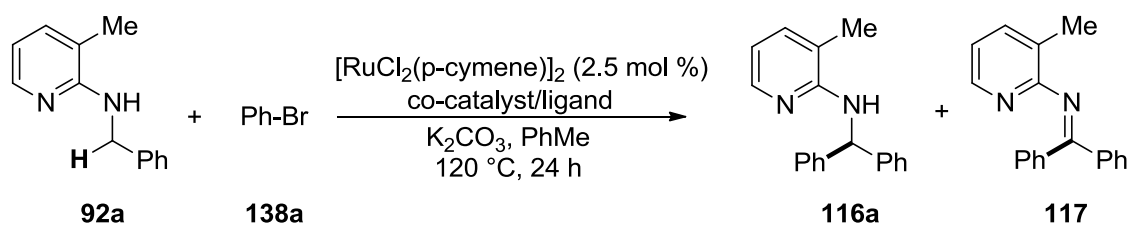
4.1.9 Ru(II) System – Screening

Although many boronic esters are already commercially available or can be easily prepared from the corresponding boronic acids, aryl halides are a more conveniently employable aryl source. A significantly larger number of structurally diverse halides is commercially available at present, usually at a substantially lower price and displaying superior storage stability. Hence, the goal was to develop an alternative method enabling the application of aryl halides as aryl donors. The starting point was a publication of Ackermann and coworkers (Scheme 34).⁷⁶ They reported a ruthenium-catalyzed cyclometalation method for the direct arylation of sp^2 carbon centers (**137**) with aryl halides.



Scheme 34 Ruthenium(II)-catalyzed direct arylation of a sp^2 C–H bond with aryl halides.

It was assumed that this method could also be applicable on the sp^3 system. The optimization process was initiated with 1 equivalent of *N*-benzyl-3-methylpyridin-2-amine **92a**, 1.5 equivalent of bromobenzene **138a**, 2.5 mol% of $[RuCl_2(p\text{-cymene})]_2$,¹⁰² and 3 equivalents of K_2CO_3 (a base is usually required in such coupling reactions to quench the formed halide) in 0.5 mL toluene. The reaction mixture was stirred 24 h at 120 °C. Gratifyingly, the desired product **116a** was formed during the reaction (Table 14, entry 1) but only in 21% yield. Interestingly, the corresponding dehydrogenated imine derivative **117** could be detected as a major side product although the reaction was performed under inert atmosphere and no oxidant was present (the amount of imine was determined by GC and was not isolated in the further optimization studies due to hydrolysis of the imine product). To optimize the yield and suppress imine formation, different ligands were tested in a first series of experiments. In particular, various carboxylates (see chapter 3.5.4, CMD mechanism) and phosphines (see chapter 3.2.3) were tested which are known to enhance catalyst performance.

Table 14 Co-catalyst/ligand screening for the ruthenium(II)-catalyzed direct arylation of **92a** with bromobenzene.

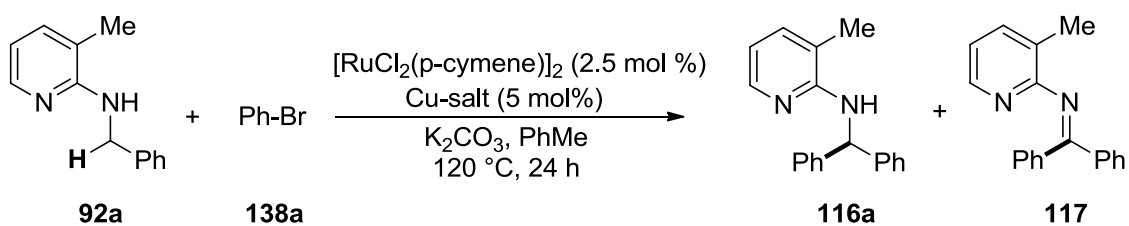
entry	co-catalyst/ligand	mol%	conv	116a:117 ^c	yield
1	--	--	35	5.8	21
2	AcOH	30	63	2.4	34
3	KOAc	30	63	1.6	32
4	PivOH	30	66	2.0	42
5	KOPiv	30	63	5.9	46
6	KOPiv	5	53	6.1	40
7	KOPiv	50	61	6.0	45
8	MesCO ₂ H	30	46	2.9	27
9	AdCO ₂ H	30	49	4.4	34
10	AdCO ₂ K	30	64	6.0	48
11	AdCO ₂ K	5	59	5.2	42
12	Mosher's acid	30	41	3.4	24
13	4-OMe-PhCO ₂ K	30	40	4.0	24
14	3,4,5-Trimethoxyphenylacetic acid	30	57	3.5	38
15	(+)-Camphor-10-sulfonic acid	30	37	4.2	21
16	Lacton	30	53	4.0	31
17	L-Proline	30	0	0	0
18	N-Acetyl-L-Proline	30	25	3.2	14
19	PPh ₃	30	17	5.3	11
20	PPh ₃	10	35	5.4	21
21	PPh ₃	5	43	5.4	28
22	PPh ₃	2.5	36	5.1	21
23	P(2-Me-Ph) ₃	5	11	3.8	7
24	P(4-Me-Ph) ₃	5	59	5.0	38
25	P(4-OMe-Ph) ₃	5	56	4.5	37
26	P(4-Cl-Ph) ₃	5	46	3.7	25
27	P(naph) ₃	5	13	1.4	5
28	P(<i>t</i> -Bu) ₃	5	54	4.4	31
29	P(Cy) ₃	5	52	4.3	30
30	dppf	5	0	--	0
31	JohnPhos	5	44	1.7	21
32	XPhos	5	56	2.5	29
33	<i>t</i> -BuXPhos	5	51	4.4	27

34	tBuMePhos	5	48	2.4	25
35	BINAP	5	12	0.2	1
36	KOPiv/PPh ₃ (1:1)	5	24	3.9	15

^aReaction conditions: **92a** (0.5 mmol), **138a** (0.75 mmol), [RuCl₂(*p*-cymene)]₂ (2.5 mol%), cocatalyst/ligand, K₂CO₃ (1.5 mmol), and PhMe (2 mL). ^bConversion determined by GC analysis with respect to **92a**. ^cRatio determined by GC. ^dYield determined by GC analysis with respect to **92a** (dodecane as internal standard).

The best results could be achieved with more sterically demanding carboxylates, such as KOPiv and AdCO₂K (Ad = Adamantyl; 46% & 48%, Table 14, entries 5 & 9). This increased reactivity was rationalized by invoking the CMD pathway. Carboxylates displayed a slightly better activity towards amine formation (Table 14, entries 5-9) compared to the acids. A decrease of co-catalyst amount from 30 mol% to 5 mol% led to a slight decrease in yield (40%, entry 6), but an increase did not show any effect (45%, Table 14, entries 6 & 7). Different chiral acids (e.g., Mosher's acid, (+)-camphor-10-sulfonic acid, L-proline) were tested which unfortunately diminished the conversion (Table 14, entries 12, 15 & 7). It was assumed that the nitrogen of L-proline is binding to the metal forming a stable complex which in turn cannot enter the catalytic cycle. The addition of phosphines resulted also in a higher conversion. The best result could be observed with a 1:1 ratio of phosphine and metal (Table 14, entries 19-22). Electron donating species amongst the phosphines showed substantially better activity than electron withdrawing substituted systems (Table 14, entries 23-29). Nonetheless, a mixture of phosphine and carboxylate led to a comparatively lower yield (29%, Table 14, entry 32). This can again be explained by a saturation of the complex which can bind no more to the starting material. This is also the case for bidentate ligands, such as dppe and BINAP (Table 14, entries 30 & 31), which were not accepted.

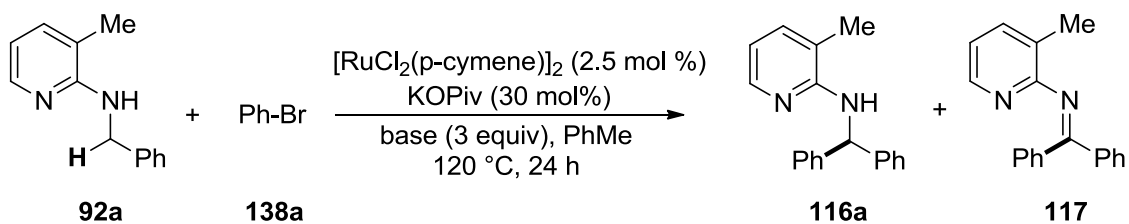
In the next step, it was investigated whether an additional metal species, such as copper, is supporting the catalyst by oxidation/reduction processes and influencing the amine to imine ratio. The reactions were performed in the absence of any ligand to examine only the influence of the copper salts on the reoxidation process. Screening various copper salts revealed no improvement of the conversion (Table 15, entries 1-8). Only the addition of Cu(OAc)₂ gave higher yield, presumably because of the function of the acetate, but also forming more imine **117** (38%, Table 15, entry 7).

Table 15 Cu-salt screening for the ruthenium(II)-catalyzed direct arylation of **92a** with bromobenzene.

entry	Cu salt	conv	116a:117 ^c	yield
1	--	35	5.8	21
2	CuBr	33	5.7	20
3	CuBr ₂	26	5.1	16
4	CuCl	35	6.1	21
5	CuCl ₂ ·2H ₂ O	27	4.9	16
6	CuSO ₄ ·5H ₂ O	27	4.4	15
7	Cu(OAc) ₂	71	2.6	38
8	Cu(NO ₃) ₂ ·3H ₂ O	26	4.3	14

^aReaction conditions: **92a** (0.5 mmol), **138a** (0.75 mmol), $[\text{RuCl}_2(\text{p-cymene})]_2$ (2.5 mol %), KOPiv (30 mol %), Cu-salt (5 mol %), K_2CO_3 (1.5 mmol), and PhMe (2 mL). ^bConversion determined by GC analysis with respect to **92a**. ^cRatio determined by GC. ^dYield determined by GC analysis with respect to **92a** (dodecane as internal standard).

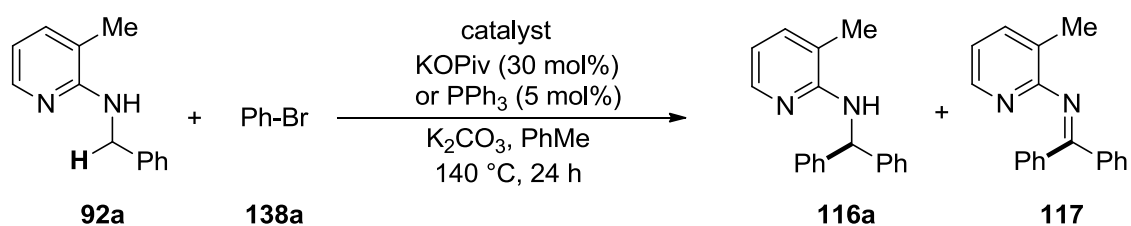
A series of experiments was also carried out to determine the role of base in combination with KOPiv (30 mol %). Remarkably, the nature of the base is crucial for the transformation. In the absence of base, no transformation occurred (Table 16, entry 1). The best result could be achieved with K_2CO_3 (46%, Table 16, entry 2). The corresponding sodium and cesium bases (Table 16, entries 4 & 5) performed worse. K_3PO_4 showed slightly worse activity compared to K_2CO_3 (36%, Table 16, entry 6). Interestingly, organic bases such as NEt_3 or the Hünig base were not suitable for this reaction (Table 16, entries 9 & 10).

Table 16 Base screening for the ruthenium(II)-catalyzed direct arylation of **92a** with bromobenzene.

entry	base	conv	116a:117 ^c	yield
1	--	2	--	1
2	K_2CO_3	63	5.9	46
3	KHCO_3	20	15.1	13
4	Na_2CO_3	15	16.8	9

In the last series of experiments, the catalytic activity of different complexes was tested. Thus, different active complexes from the literature were tested in combination with the reaction conditions. The reaction was performed with different combinations of catalyst (5 mol% with respect to the metal) and KO₂Piv (30 mol%) or PPh₃ (5 mol%). The results are summarized in Table 18. Besides [RuCl₂(*p*-cymene)]₂, the [RuCl₂(cod)]_n complex showed good activity (Table 18, entries 7-9). However, 5 mol% of [RuCl₂(cod)]_n polymer was used, which might contain a different amount of ruthenium metal centers than in 2.5 mol% [RuCl₂(*p*-cymene)]₂. The other catalysts performed worse or not at all. Interestingly, the combination of [RhCl(cod)]₂ and PPh₃ delivered almost exclusively the imine product in poor yield (Table 18, entry 18).

Table 18 Catalyst screening for the direct arylation of **92a** with bromobenzene.



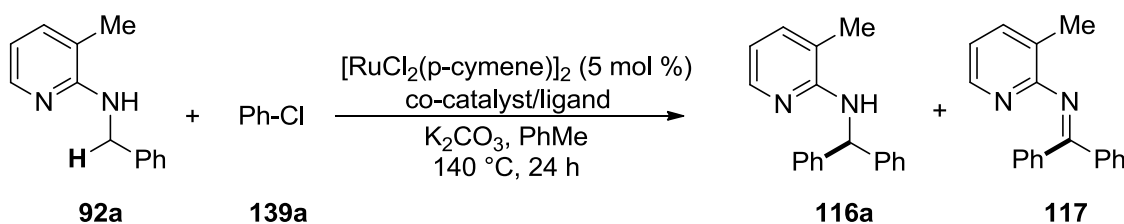
entry	catalyst	ligand	conv	116a:117 ^c	yield
1	[RuCl ₂ (<i>p</i> -cymene)] ₂	--	59	4.0	34
2	[RuCl ₂ (<i>p</i> -cymene)] ₂	KO₂Piv	96	6.0	75
3	[RuCl ₂ (<i>p</i> -cymene)] ₂	PPh ₃	85	4.6	51
4	RuCl ₃ ·(H ₂ O) _n	--	28	3.5	17
5	RuCl ₃ ·(H ₂ O) _n	KO ₂ Piv	0	--	0
6	RuCl ₃ ·(H ₂ O) _n	PPh ₃	4	0.8	1
7	[RuCl ₂ (cod)] _n	--	94	12.2	61
8	[RuCl ₂ (cod)] _n	KO₂Piv	94	5.9	75
9	[RuCl ₂ (cod)] _n	PPh ₃	82	4.5	50
10	RuCl ₂ (PPh ₃) ₃	--	47	2.4	27
11	RuCl ₂ (PPh ₃) ₃	KO ₂ Piv	0	--	0
12	RuCl ₂ (PPh ₃) ₃	PPh ₃	37	2.2	20
13	Rh ₄ (CO) ₁₂	--	0	--	0
14	Rh ₄ (CO) ₁₂	KO ₂ Piv	0	--	0
15	Rh ₄ (CO) ₁₂	PPh ₃	0	--	0
16	[RhCl(cod)] ₂	--	8	--	5
17	[RhCl(cod)] ₂	KO ₂ Piv	0	--	0
18	[RhCl(cod)] ₂	PPh ₃	41	0.2	4
19	[RhCl(C ₂ H ₄)] ₂	--	8	8.3	4
20	[RhCl(C ₂ H ₄)] ₂	KO ₂ Piv	6	0.4	1
21	[RhCl(C ₂ H ₄)] ₂	PPh ₃	16	1.1	5

^aReaction conditions: **92a** (0.5 mmol), **138a** (0.75 mmol), catalyst (2.5 mol%), ligand, K₂CO₃ (1.5 mmol), and PhMe (2 mL). ^bConversion determined by GC analysis with respect to **92a**. ^cRatio

determined by GC. ^dYield determined by GC analysis with respect to **92a** (dodecane as internal standard).

At this point, it was decided to continue with the $[\text{RuCl}_2(p\text{-cymene})]_2/\text{KOPiv}$ system. All of the preceding reactions were performed with bromobenzene. Under the standard conditions developed herein, aryl chlorides afforded no conversion. The reactions of aryl chlorides have been the target of catalyst development because they are less expensive than aryl bromides and more derivatives are commercially available. Thus, an alternative pathway for the conversion of aryl chlorides was desirable. The screening started with the initial conditions and the co-catalyst/ligand was changed in a first series of experiments. Interestingly, the reaction was inhibited in the presence of carboxylate (Table 19, entries 2-4). In the absence of carboxylate, a moderate conversion of 24% could be achieved (Table 19, entry 1). Because of the low conversion, the catalyst amount was increased to 5 mol% and the amount of aryl chloride to 3 equivalents. Amongst the carboxylates, only KOAc and CuTc showed activity (37% & 69%, Table 19, entry 5 & 6). However, the phosphines seemed to be the right choice for this transformation. The conversion could be enhanced rigorously by addition of PPh_3 (74%, Table 19, entry 8). Other phosphines showed a similar behavior, but were less effective (Table 19, entries 10-20).

Table 19 Co-catalyst/ligand screening for the ruthenium(II)-catalyzed direct arylation of **92a** with chlorobenzene.

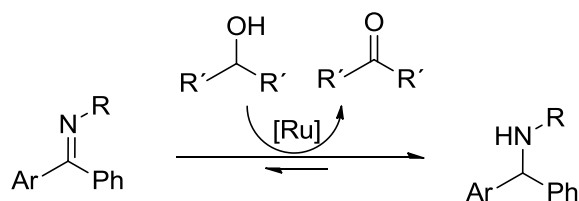


entry	co-catalyst/ligand	mol%	conv [%] ^b	116a:117 ^c
1	--	--	24	1.8
2	KOPiv	30	7	--
3	KOPiv	10	8	--
4	AdCO ₂ K	10	7	--
5	KOAc	10	37	2.0
6	CuTc	10	69	2.0
7	PPh_3	5	49	2.3
8	PPh_3	10	74	1.9
9	PPh_3	20	37	4.1
10	$\text{P}(o\text{-Tol})_3$	10	64	2.3
11	$\text{P}(4\text{-OMe-Ph})_3$	10	61	2.5
12	$\text{P}(4\text{-Cl-Ph})_3$	10	50	1.6
13	$\text{P}(\text{Cy})_3$	10	73	1.5
14	XPhos	10	62	2.1
15	JohnPhos	10	51	2.9

16	RuPhos	10	56	1.4
17	DavePhos	10	66	1.5
18	IMes·HCl	10	45	0.8
19	BINAP	5	34	1.9
20	BINAP	10	9	2.6

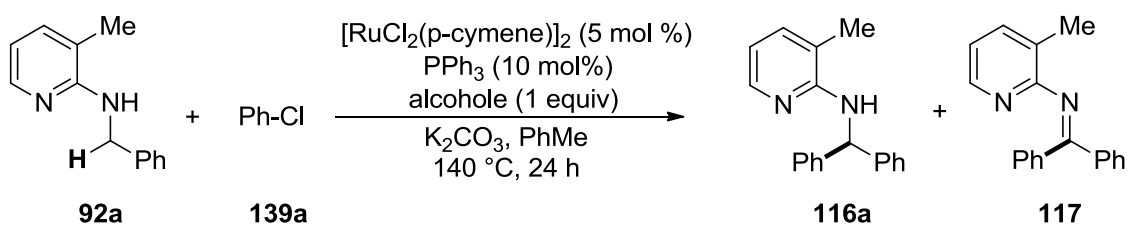
^aReaction conditions: **92a** (0.5 mmol), **139a** (1.5 mmol), [RuCl₂(*p*-cymene)]₂ (5 mol%), ligand, K₂CO₃ (1.5 mmol), and PhMe (2 mL). ^bConversion determined by GC analysis with respect to **92a**. ^cRatio determined by GC.

One main problem for the transformation of aryl chlorides has been the high concomitant imine formation. This imine formation can be explained by β-hydride elimination (see chapter 3.2.3). Unfortunately, a better ratio than 2.9 (Table 19, entry 15) could not be obtained which is far below the reaction with aryl bromides (6.0, Table 17, entry 9). Therefore, it was assumed that the presence of an additional compound might help to reduce the formed imine. In the ruthenium(0) reaction it was observed that the dissociated hydrogen can be scavenged by the ketone, which is reduced to the alcohol. Subsequently, the implication of an alcohol should deliver the required hydrogen which can be used for the reduction of the imine (Scheme 35).



Scheme 35 Influence of a secondary alcohol on the imine/amine equilibrium.

Fortunately, the addition of secondary alcohols led to a high amine to imine ratio (Table 20, entries 1-4). Compared with other alcohols, such as *i*PrOH and 3-pentanol (Table 20, entries 1 & 2), cyclohexanol was more effective (38%, Table 20, entry 4). Notably, the corresponding cyclohexanone was detected via GC-MS. Finally, conducting the reaction at 160 °C for 30 h and changing the solvent to *o*-xylene furnished 70% isolated yield of product **116a** (Table 20, entry 5).

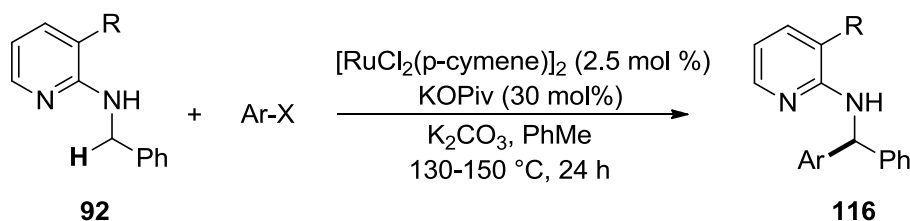
Table 20 Alcohol screening for the ruthenium(II)-catalyzed direct arylation of **92a** with chlorobenzene.

entry	alcohol	conv	116a:117 ^c	yield
1	iPrOH	17	n.d.	12
2	3-pentanol	26	n.d.	18
3	cyclopentanol	9	n.d.	6
4	cyclohexanol	49	n.d.	38
5	cyclohexanol ^e	93	12.0	79 (70)^f

^aReaction conditions: **92a** (0.5 mmol), **139a** (1.5 mmol), $[\text{RuCl}_2(\text{p-cymene})]_2$ (5 mol%), PPh_3 (10 mol%), alcohol (0.5 mmol), K_2CO_3 (1.5 mmol), and PhMe (2 mL). ^bConversion determined by GC analysis with respect to **92a**. ^cRatio determined by GC. ^dYield determined by GC analysis with respect to **92a** (dodecane as internal standard). ^e160 °C. ^fNumber in parentheses is isolated yield of **116a**.

4.1.10 Ru(II) System – Scope

Based on the optimized reaction conditions, transformations with different aryl halides were performed. This catalytic method displayed a similar behavior towards the steric and electronic properties of the aryl donor species. Sterically demanding ortho-substituted aryls (2-Me 18% & 1-Naph 14%, Table 21, entries 3 & 4) gave again significantly lower conversions, but meta-substituted aryls showed good conversion (3-Me 98%, 3-OMe 97%, 3-Cl 60%, Table 21, entries 5-7). Again, electron neutral or weak donating aryls (e.g. 4-Me 98%, Table 21, entries 8-10) could be implied with the best results, while strong electron withdrawing or coordinating substituents (e.g. 4-Ac 15%, Table 21, entries 17-22) were much less tolerated. The phenyl substituent in 3-position of pyridine (**92n**) showed slightly better conversions (Table 21, entries 23-28).

Table 21 Ruthenium(II)-catalyzed arylation of pyridine derivatives.

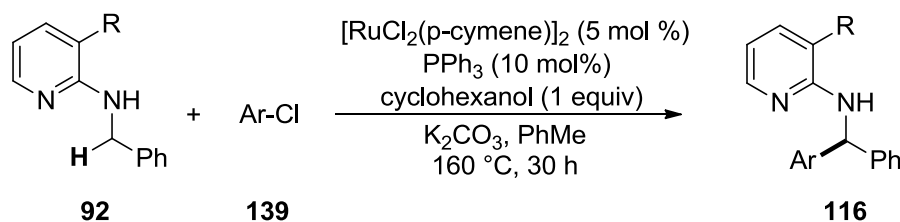
entry	R	X	Ar	conv [%] ^b	yield [%] ^c	
1	116a	Me	Br	Ph	96	69
2	116a	Me	I	Ph	100	48

3	<u>116ai</u>	Me	Br	2-Me-Ph	18	n.i. ^d
4	<u>116aj</u>	Me	Br	1-Naph	14	n.i. ^d
5	<u>116b</u>	Me	Br	3-Me-Ph	98	55
6	<u>116c</u>	Me	Br	3-OMe-Ph	97	60
7	<u>116d</u>	Me	Br	3-Cl-Ph	60	37
8	<u>116e</u>	Me	Br	4-Me-Ph	98	65
9	<u>116f</u>	Me	Br	4- <i>t</i> -Bu-Ph	96	64
10	<u>116g</u>	Me	Br	4- <i>n</i> -Bu-Ph	98	67
11	<u>116h</u>	Me	Br	4-OMe-Ph	95	63
12	<u>116h</u>	Me	I	4-OMe-Ph	98	61
13	<u>116i</u>	Me	Br	4-NMe ₂ -Ph ^e	94	50
14	<u>116j</u>	Me	Br	4-F-Ph	92	61
15	<u>116j</u>	Me	I	4-F-Ph	97	55
16	<u>116k</u>	Me	Br	4-Cl-Ph	98	51
17	<u>116m</u>	Me	Br	4-CO ₂ Et-Ph	72	33
18	<u>116ao</u>	Me	Br	4-Ac-Ph	15	n.i. ^d
19	<u>116ap</u>	Me	Br	4-NO ₂ -Ph	0	--
20	<u>116aq</u>	Me	Br	4-CN-Ph	0	--
21	<u>116ar</u>	Me	Br	3-pyridyl	0	--
22	<u>116as</u>	Me	Br	2-thienyl	0	--
23	<u>116w</u>	Ph	Br	Ph ^f	98	70
24	<u>116x</u>	Ph	Br	3-Me-Ph ^f	97	68
25	<u>116y</u>	Ph	Br	3-OMe-Ph ^f	95	64
26	<u>116z</u>	Ph	Br	4-Me-Ph ^f	97	67
27	<u>116aa</u>	Ph	Br	4- <i>t</i> -Bu-Ph ^f	98	72
28	<u>116ab</u>	Ph	Br	4- <i>n</i> -Bu-Ph ^f	97	69
29	<u>116ad</u>	Ph	Br	4-Cl-Ph ^f	81	59
30	<u>116ae</u>	Ph	Br	4-CO ₂ Et-Ph ^f	64	42
31	<u>116af</u>	Ph	Br	4-Ac-Ph ^f	65	41

^aReaction conditions: **92** (0.5 mmol), ArX (0.75 mmol), [RuCl₂(*p*-cymene)]₂ (2.5 mol%), KO₂Piv (30 mol%), K₂CO₃ (1.5 mmol), and PhMe (2 mL). ^bConversion determined by GC analysis with respect to **92**.

^cIsolated Yield. ^dn.i. = not isolated. ^e130 °C. ^f150 °C.

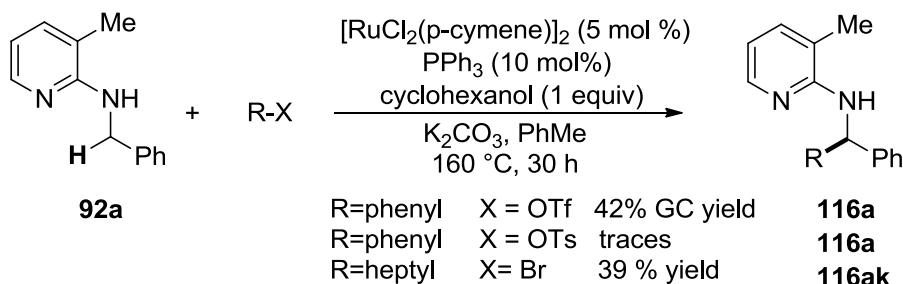
The corresponding aryl chlorides showed analogous results, albeit reaction conditions were harsher (Table 22, entries 1-5). In this case, the reaction is obviously again sensitive to electron withdrawing substituents (Table 22, entries 6 & 7).

Table 22 Ruthenium(II)-catalyzed arylation of **92a** with aryl chlorides.

entry	R	Ar	conv [%] ^b	yield [%] ^c
1	116a	Me	93	70
2	116b	Me	95	72
3	116e	Me	93	79
4	116h	Me	88	64
5	116j	Me	76	56
6	116l	Me	79	30
7	116n	Me	23	n.i. ^d
8	116w	Ph	60	48
9	116x	Ph	68	58
10	116y	Ph	72	61
11	116z	Ph	58	39
12	116aa	Ph	69	55
13	116ab	Ph	55	47

^aReaction conditions: **92** (0.5 mmol), **139** (1.5 mmol), [RuCl₂(*p*-cymene)]₂ (5 mol%), PPh₃ (10 mol%), cyclohexanol (0.5 mmol), K₂CO₃ (1.5 mmol), and PhMe (2 mL). ^bConversion determined by GC analysis with respect to **92**. ^c160 °C. ^dIsolated Yield. ^en.i. = not isolated.

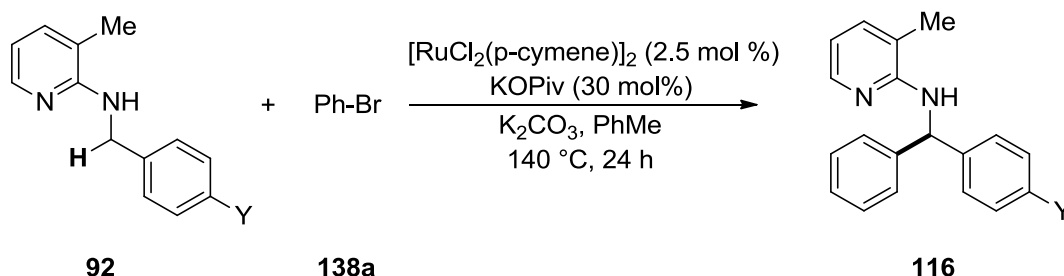
Notably, these conditions were also suitable for the alkylation of the C–H bond in moderate yield. Furthermore, this reaction is not only limited to halides, but also triflates were accepted; tosylates were not tolerated (Scheme 36).

**Scheme 36** Ruthenium(II)-catalyzed arylation of **92a** with triflates and alkylation with bromides.

Next, the electronic influences of the benzylic group were again investigated. Thus, the benzylic group of starting material **92** was varied and the reaction performed under the standard conditions. The results are in accordance with the ruthenium(0) series, indicating that electron neutral groups are performing best (Table 23, entry 4). However, this method

performs better with electron withdrawing substituents than electron donating substituents, which is complementary to the ruthenium(0) method. It is worth mentioning that no decarboxylation with starting material **92g** (Table 23, entry 7) was detected as it was the case with the Ru(0) method.

Table 23 Influence of the substituent on the benzylic group for the ruthenium(II)-catalyzed reaction.

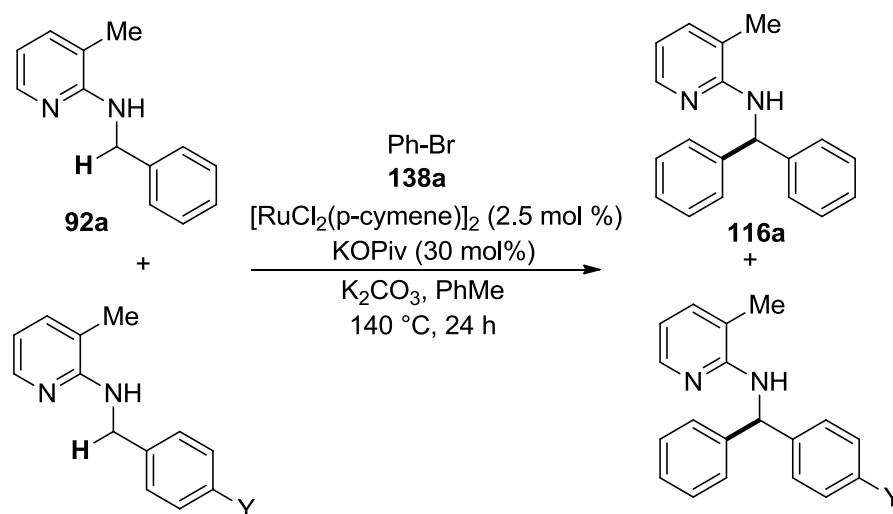


entry		Y	conv	yield
1	116h	OMe	49	28
2	116o	O <i>i</i> Pr	75	43
3	116e	Me	77	48
4	116a	H	96	69
5	116j	F	85	59
6	116l	CF ₃	97	57
7	116n	CO ₂ Me	88	57

^aReaction conditions: **92** (0.5 mmol), **138a** (0.75 mmol), [RuCl₂(*p*-cymene)]₂ (2.5 mol%), KOPiv (30 mol%), K₂CO₃ (1.5 mmol), and PhMe (2 mL).

^bConversion determined by GC analysis with respect to **92**. ^cIsolated Yield.

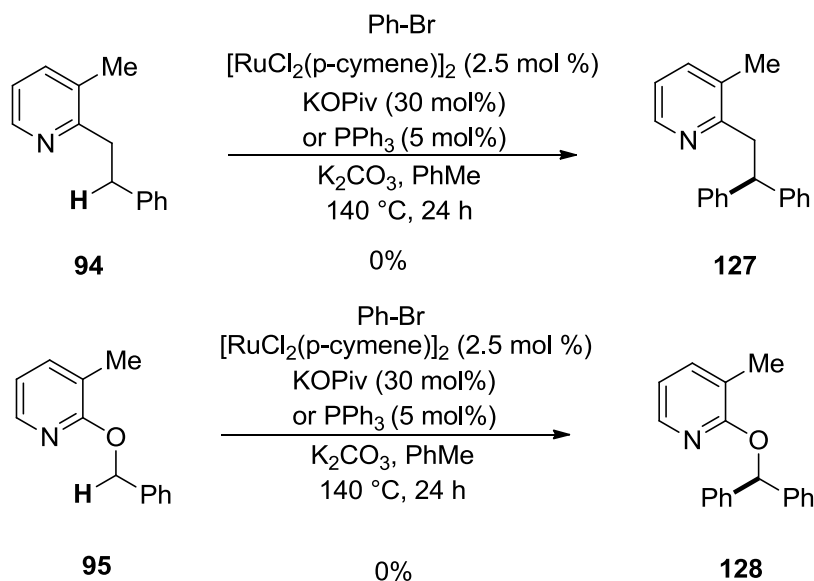
Competition experiments were carried out to support the results. A mixture of 1 equivalent of the unsubstituted and 1 equivalent substituted starting material was used with the optimized reaction conditions. The results are shown in Table 24. Weak electron donating substituents such as F or CF₃ (Table 24, entries 5 & 6) react faster than the electron donating substituents such as OMe or O*i*Pr (Table 23, entries 1 & 2).

Table 24 Competitive experiments for the ruthenium(0)-catalyzed reaction.

entry	Y	H:Y ^b
1	OMe	2
2	OiPr	1.3
3	Me	1.1
5	F	1.1
6	CF ₃	0.9
7	CO ₂ Me	1.8

^aReaction conditions: **92a** (0.5 mmol), substituted amine (0.5 mmol), **138a** (0.5 mmol), $[\text{RuCl}_2(p\text{-cymene})]_2$ (2.5 mol%), KOPiv (30 mol%), K_2CO_3 (1.5 mmol), and PhMe (2 mL). ^bRatio determined by GC analysis.

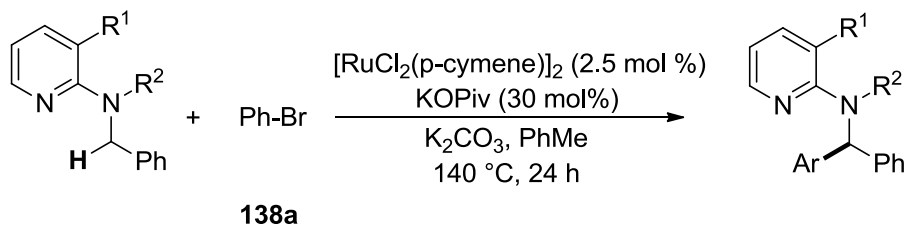
In the next step, the role of the nitrogen adjacent to the C-H bond was investigated. Therefore, the nitrogen was substituted with a CH₂ group (**94**) or oxygen (**95**). In the ruthenium(0) protocol, the oxygen was not working, but CH₂ gave a good yield. In the ruthenium(II) protocol, both substituents were not suitable for this transformation, indicating that the ruthenium(II) mechanism is completely different from the ruthenium(0) and requires a nitrogen in this position (Scheme 37).

Scheme 37 Ruthenium(II)-catalyzed direct arylation of **94** and **95**.

4.1.11 Ru(II) System – Mechanistic Studies

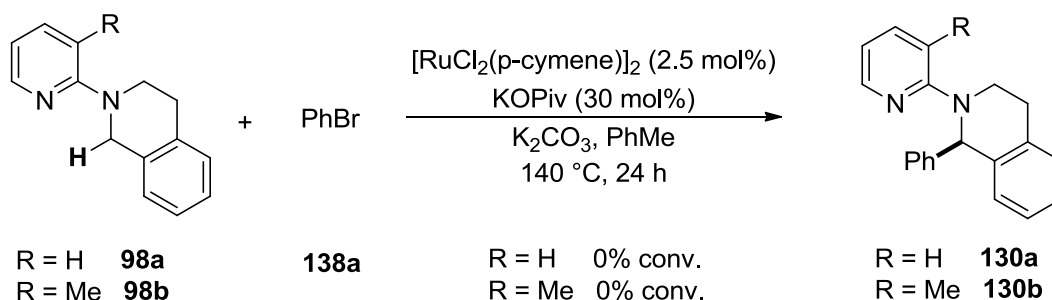
The last experiments raised the question whether a free NH group is essential for this transformation. The reaction was performed with different N-substituted benzylic amines in combination with substituted and unsubstituted pyridine. In contrast to the ruthenium(0) system, only free amines showed any conversion (Table 25, entry 1 & 2). All other substrates were not tolerated (Table 25, entries 3-10 & Scheme 38).

Table 25 Ruthenium(II)-catalyzed direct arylation of N-substituted compounds.



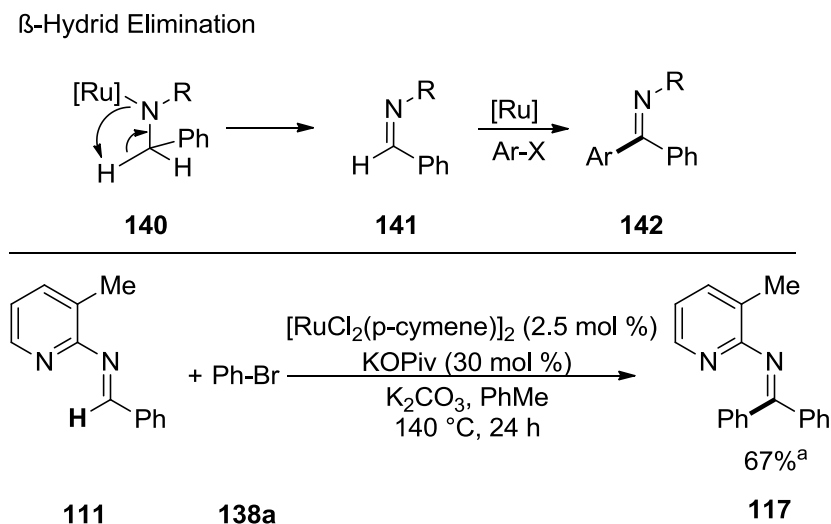
Entry	R ¹	R ²	conv
1	H	H	23
2	Me	H	96
3	H	Me	0
4	Me	Me	0
5	H	Ac	0
6	Me	Ac	0
7	H	Bz	0
8	Me	Bz	0
9	H	Piv	0
10	Me	Piv	0

^aReaction conditions: Amine (0.5 mmol), **138a** (0.75 mmol), $[\text{RuCl}_2(\text{p-cymene})]_2$ (2.5 mol%), KOiv (30 mol%), K_2CO_3 (1.5 mmol), and PhMe (2 mL). ^bConversion determined by GC analysis with respect to Amine.



Scheme 38 Ruthenium(II)-catalyzed direct arylation of THIQ.

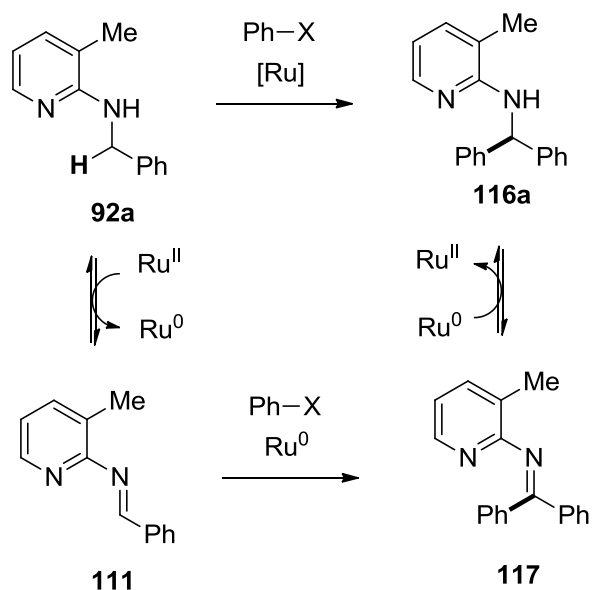
It is likely that the mechanism is not progressing via a direct sp^3 C–H insertion of the metal, but over a β -hydride elimination of the amine to the corresponding imine. These kind of β -hydride eliminations are known to the literature and normally lead to side products in Buchwald-Hartwig aminations.¹⁰³ The so formed imine can further react in the next step and be arylated to imine product **117**, which is most likely in equilibrium with the desired product. This equilibrium explains the detected imine **117** in the reaction and can be shifted to the right side by a secondary alcohol. An experiment with the already dehydrogenated benzylic imine **111** was conducted to support this hypothesis. As expected, the imine compound **117** could be isolated with 67% yield (Scheme 39). Furthermore, Jun and co-workers have shown that **111** can be arylated with $\text{Ru}_3(\text{CO})_{12}$ and phenyl boronic acid ester.¹⁰⁴



Scheme 39 Hypothesis for imine formation and ruthenium(II)-catalyzed direct arylation of **111**.

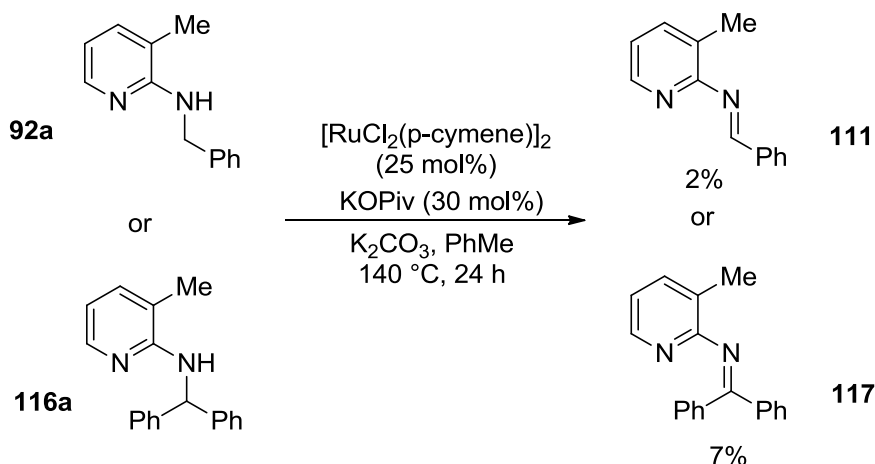
The expected overall reaction pathway is illustrated in Scheme 40. The initial ruthenium(II) complex is abstracting the two hydrogens via a β -hydride elimination, forming a ruthenium(0) species. This ruthenium(0) species undergoes the catalytic reaction with the sp^2 carbon center

of imine **111**, forming compound **117**. The regenerated ruthenium(0) complex can now either reenter the catalytic cycle for the arylation of **111** or reduce the imine **117** to amine **116a**, forming again ruthenium(II) which can in turn oxidize the amine **92a** to the imine **111**.



Scheme 40 Direct arylation of **92a** over sp^2 C-H bond arylation pathway.

If the reaction is progressing via this pathway, it should be able to detect the formed imine **111** during the reaction. However, only traces of imine **111** could be detected via GC. The reason for this could be that the equilibrium in the first step is strongly shifted to the left side and this step is the rate limiting step. The so formed imine **111** is reacting fast enough to the arylated product **117** and therefore difficult to detect. In order to investigate this equilibrium, the reaction was performed without any aryl halide source with the starting material **92a** and the product **116a** with stoichiometric amounts of catalyst. Indeed, in both cases the dehydrogenated product could be detected (Scheme 41). These results show that the catalyst is undergoing β -hydride elimination but the reaction is not going to completion. Imine and amine could be in equilibrium with each other with the amine being the preferred species. However, when the formed imine is arylated the reaction is driven towards the arylated imine which is then slowly hydrogenated to the final product (which could also be a reversible process).



Scheme 41 Detected imine formation under the reaction conditions.

Moreover, the rate of both reactions, the arylation of amine **92a** and of imine **111**, were compared. If the reaction of the imine would be much faster than the reaction of the amine, this dehydrogenation would be the rate determining step in the arylation process. However, the rate of arylation of imine **111** is equal to the arylation of amine **92a**, indicating that the rate limiting step is occurring at a later stage (Figure 44).

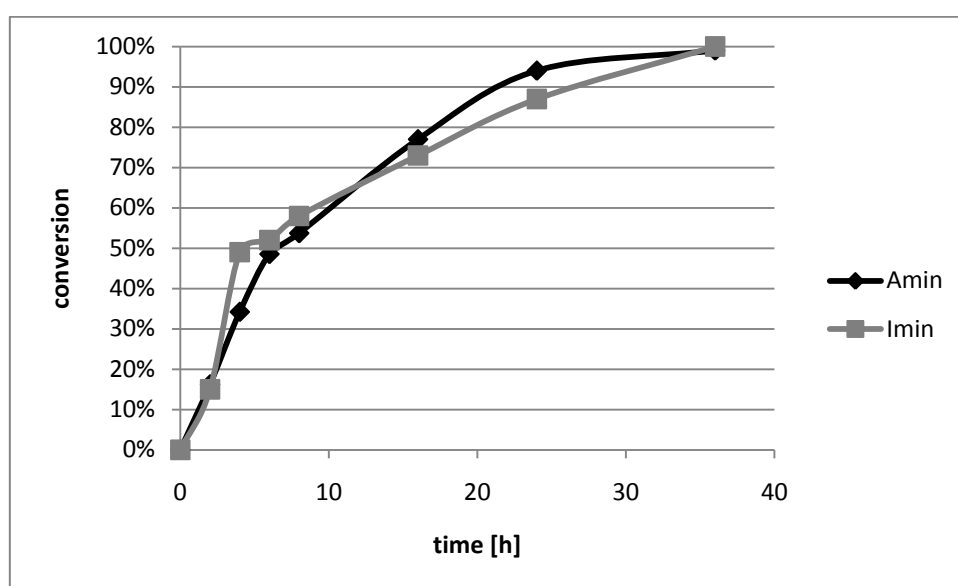
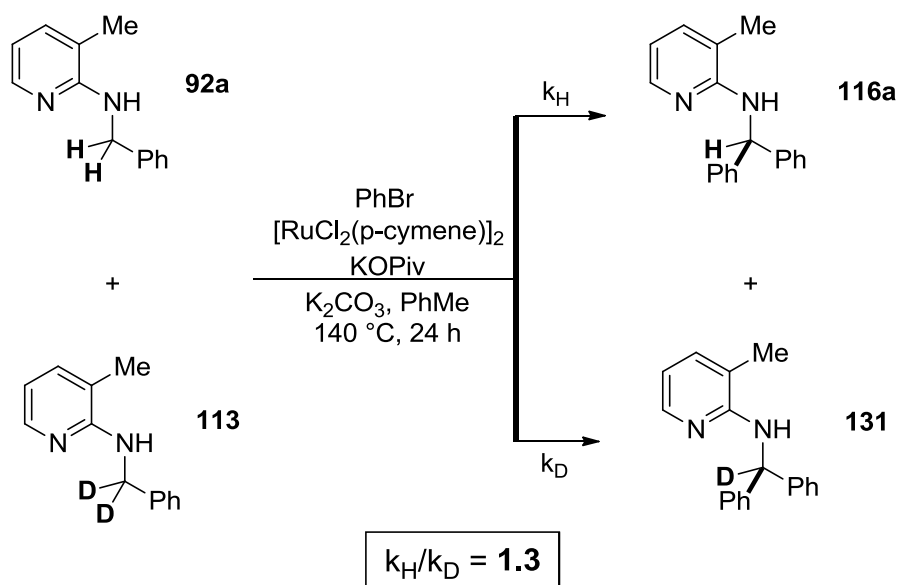


Figure 45 Kinetic measurements for the ruthenium(II)-catalyzed direct arylation of **92a** and **111**.

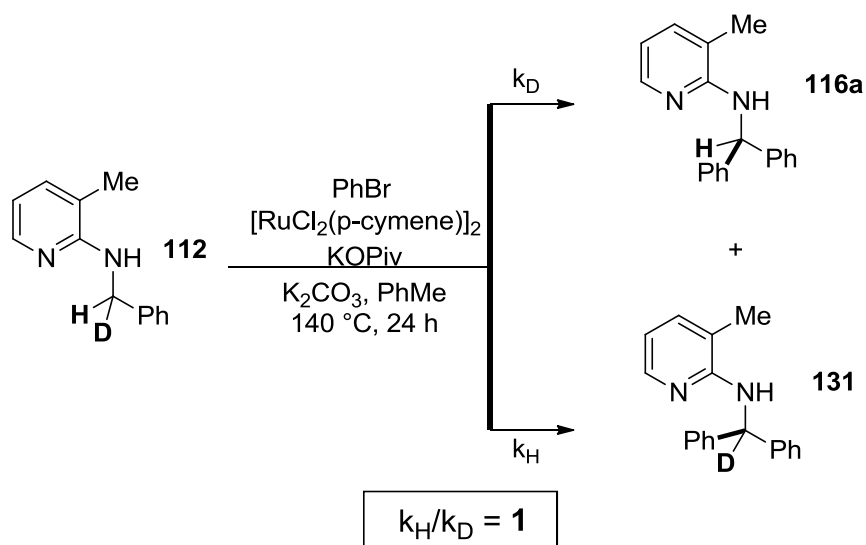
Next, kinetic isotope effect experiments were performed to determine whether the C–H activation step is the rate limiting step (Scheme 42). For the intermolecular competition experiment, 1 equivalent of starting material **92a** and 1 equivalent of the corresponding deuterated compound **113** were reacted under the optimized reaction conditions in the presence of only 1 equivalent of bromobenzene. Finally, the mixture of products was isolated and the ratio of **116a**:**131** was determined by $^1\text{H-NMR}$. A KIE of 1.3 was found, indicating that C–H insertion of the metal is not the rate determining step in this reaction since otherwise a much higher KIE could be expected. This result is in contrast to the previously observed

$\text{Ru}_3(\text{CO})_{12}$ /phenylboronic acid ester protocol displaying a KIE of 3.3. Consequently, an intramolecular competition experiment with compound **112** was carried out. Here, the KIE was found to be 1, again in contrast to the $\text{Ru}_3(\text{CO})_{12}$ protocol (KIE=0.43) indicating again that C–H insertion is not rate determining.

Intermolecular Competition Experiment:



Intramolecular Competition Experiment:

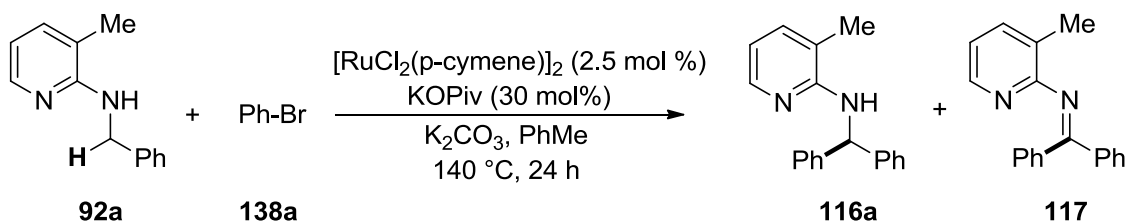


Scheme 42 Competitive deuterium labeling experiments for the ruthenium(II)-catalyzed reaction.

Finally, the reaction was performed under different atmospheres in order to get more information about the ongoing processes during the reaction. The ruthenium(0) protocol demonstrated that the catalyst is stable under air and even performing better under H_2 atmosphere. In the ruthenium(II) case, the catalyst is performing slightly worse under air and significantly worse under hydrogen (Table 26, entries 2 & 4). This can be explained by hydrogenation of the ruthenium(II) complex, forming a ruthenium(0) species which can in

turn no longer undergo the dehydrogenation of the starting material **92a** and thus enter the catalytic cycle. Furthermore, the reaction is not working under CO, which is obviously because of the strong binding character of the CO ligand (Table 26, entry 3). The so formed complex is no longer active.

Table 26 Ruthenium(II)-catalyzed arylation of **92a** under different atmospheres.

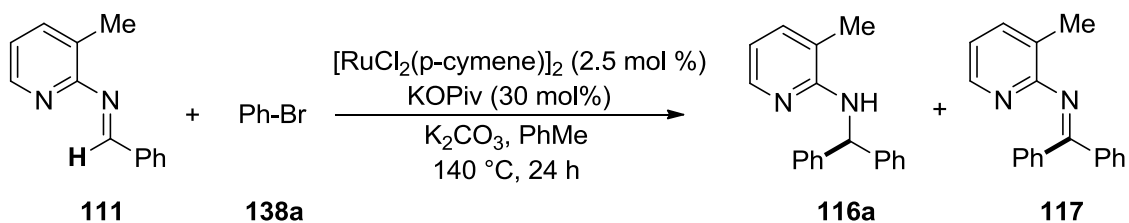


entry	atmosphere	conv	116a:117 ^c	yield
1	argon	96	6.0	75 (69) ^e
2	air	79	4.0	56
3	CO	0	--	0
4	H ₂	53	8.3	37
5	argon (μW) ^f	92	5.1	66

^aReaction conditions: **92a** (0.5 mmol), **138a** (0.75 mmol), [RuCl₂(*p*-cymene)]₂ (2.5 mol%), KOPIV (30 mol%), K₂CO₃ (1.5 mmol), and PhMe (2 mL). ^bConversion determined by GC analysis with respect to **92a**. ^cRatio determined by GC. ^dYield determined by GC analysis with respect to **92a** (dodecane as internal standard). ^eNumber in parentheses is isolated yield of **116a**. ^fμW conditions: 180 °C for 2.5 h.

The same series of experiments was conducted with the imine starting material. It appears logical that this reaction should be favored under an oxidative atmosphere such as air. Indeed, the conversion was slightly better under air. The catalyst was not active under CO atmosphere for the same reason as before (Table 27, entry 3). As expected, the formation of the reduced amine species could only be detected under hydrogen atmosphere (Table 27, entry 4).

Table 27 Ruthenium(II)-catalyzed arylation of **111** under different atmospheres.

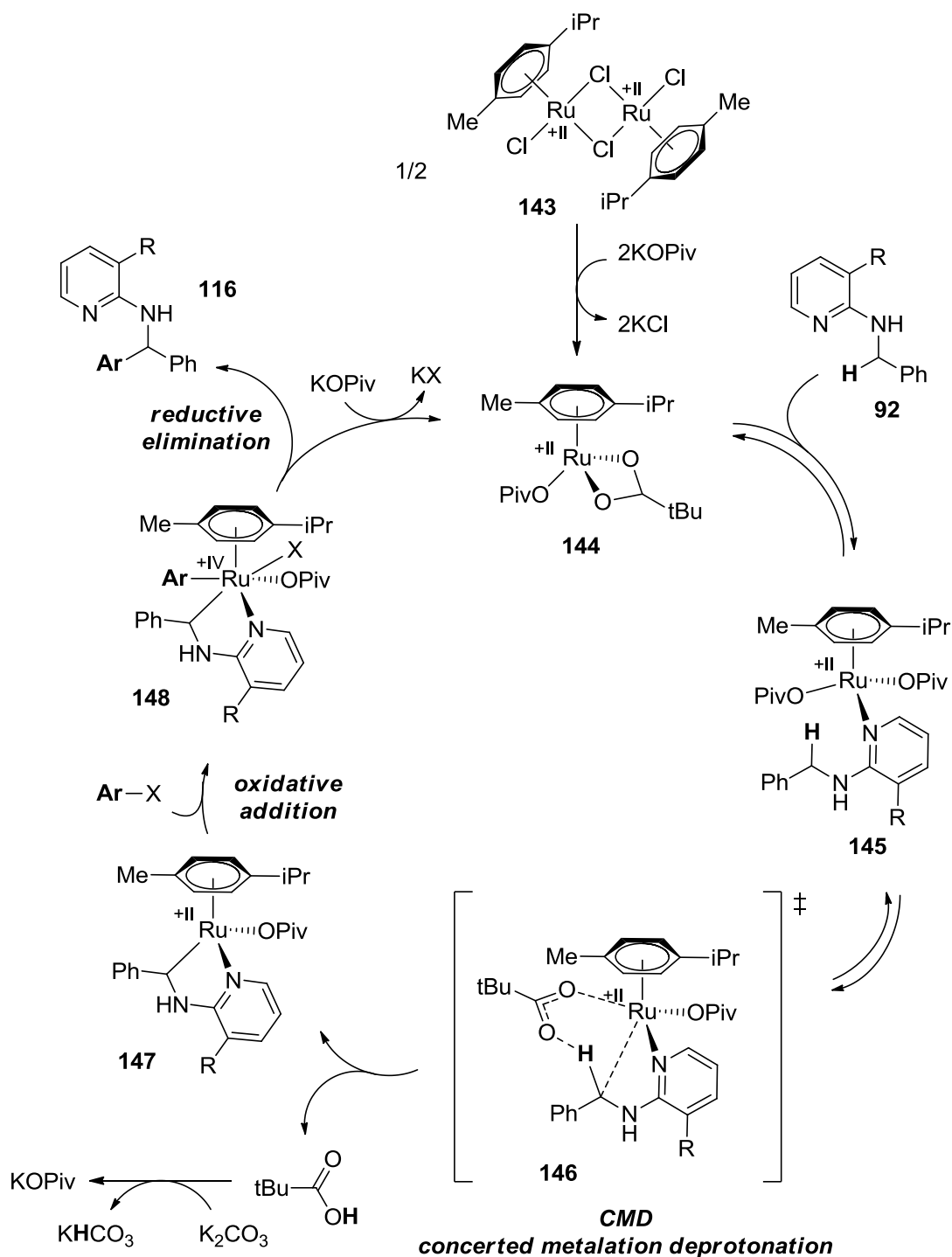


entry	atmosphere	conv	116a:117 ^c	yield
1	argon	89	--	69
2	air	92	--	73
3	CO	0	--	0
4	H ₂	87	0.05	64

^aReaction conditions: **111** (0.5 mmol), **138a** (0.75 mmol), [RuCl₂(*p*-cymene)]₂ (2.5 mol%),

KOPiv (30 mol%), K₂CO₃ (1.5 mmol), and PhMe (2 mL). ^bConversion determined by GC analysis with respect to **111**. ^cRatio determined by GC. ^dYield determined by GC analysis with respect to **111** (dodecane as internal standard).

Currently, only a speculative discussion of the reaction mechanism is possible. The most probable mechanism involves the ruthenium(II) carboxylate complex **144** which is formed from of [RuCl₂(*p*-cymene)]₂ and KOPiv. Thus, intermediate **145** is formed by cyclometalation with **92**. Subsequent concerted metalation deprotonation (CMD) via transition state **146** delivers ruthenium(II) complex **147**. The following oxidative addition of the aryl halide to the ruthenium(IV) species **148** and final reductive elimination yields product **116** and ruthenium(II) complex **144**. The regenerated complex **144** can now reenter the next catalytic cycle (Scheme 43).



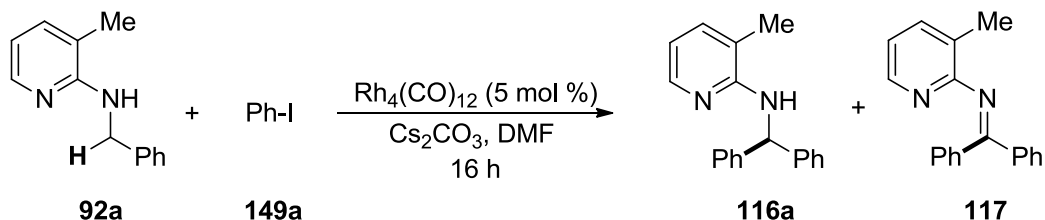
Scheme 43 Proposed mechanism for the ruthenium(II)-catalyzed reaction.

4.1.12 Rh System

In Table 18 it was shown that besides the ruthenium(II) complexes, rhodium complexes such as $[\text{RhCl}(\text{cod})]_2$ showed conversion, albeit to the undesired imine product **117**. If these complexes preferentially form the dehydrogenated imine product **117** it should be possible to shift the equilibrium by changing the reaction parameters such as temperature and the atmosphere. The investigations started with $\text{Rh}_4(\text{CO})_{12}$ (5 mol%), iodobenzene (1.5

equivalent), and Cs_2CO_3 (3 equivalents) in DMF. The reaction mixture was stirred for 16h at different temperatures under argon and hydrogen atmosphere. The results are summarized in Table 28. Excitingly, the ratio of **116a**:**117** could be changed completely from 0.07 to 7 by increasing the temperature and changing the atmosphere to hydrogen. This indicates that the formed imine represents the kinetic product, whereas the amine is the thermodynamic product.

Table 28 Rhodium-catalyzed direct arylation of **92a** under argon and hydrogen at different temperatures.



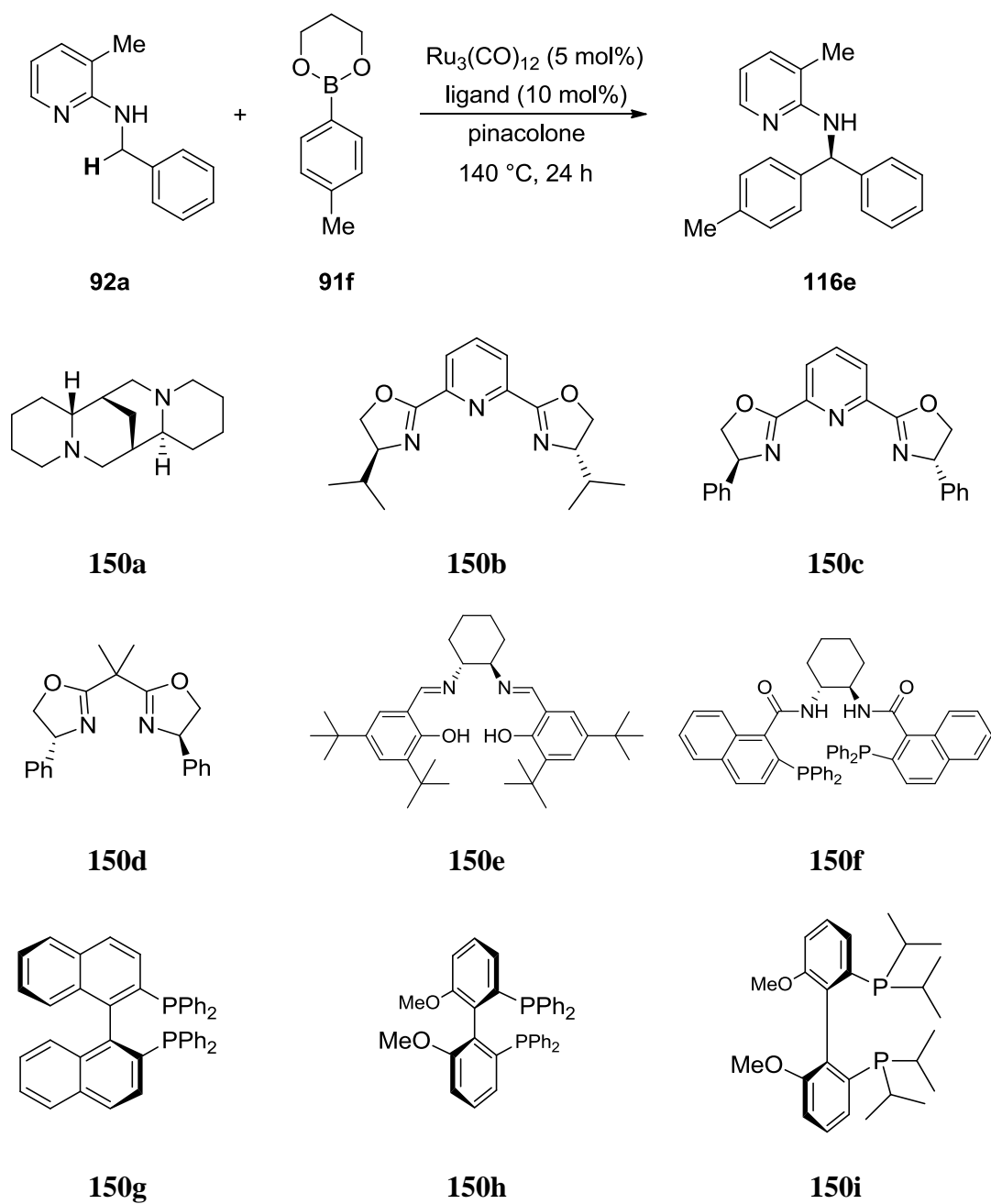
entry	atmosphere	t [°C]	conv	116a : 117 ^c
1	argon	80	52	0.07
2	argon	110	57	0.1
3	argon	140	58	0.6
4	H ₂	80	12	0.8
5	H ₂	110	26	1.2
6	H ₂	140	48	7

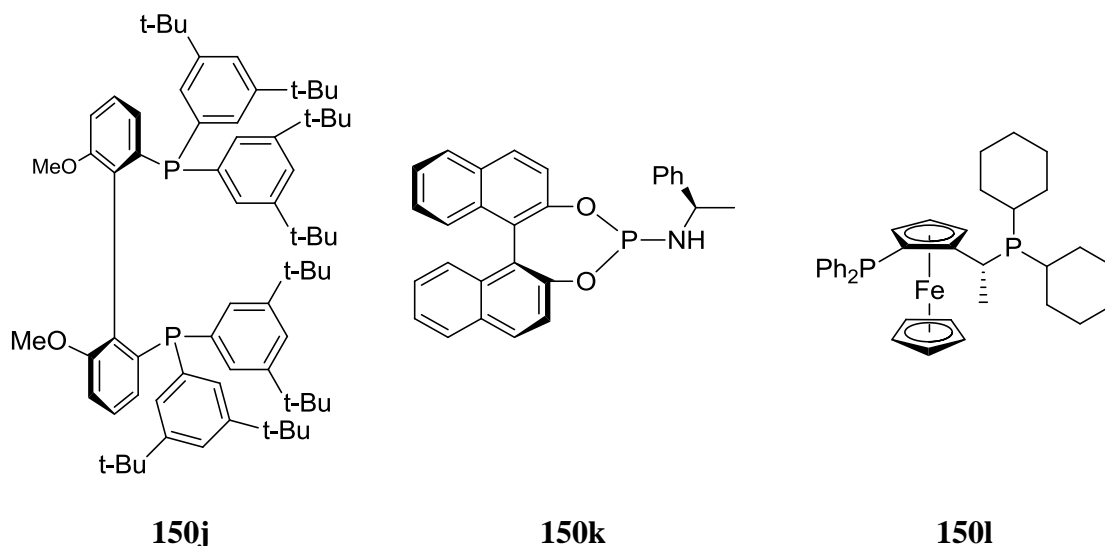
^aReaction conditions: **92a** (0.5 mmol), **149a** (0.75 mmol), $\text{Rh}_4(\text{CO})_{12}$ (5 mol%), Cs_2CO_3 (1.5 mmol), and DMF (2 mL). ^bConversion determined by GC analysis with respect to **92a**.

^cRatio determined by GC.

4.1.13 Asymmetric Catalysis

The C–H bond functionalization of the prochiral CH_2 group results in two enantiomers. It was anticipated that the presence of chiral ligands potentially induces stereopreference in favor of one enantiomer. The chiral environment of the catalyst allows distinguishing between both C–H bonds and activating the favored one. Therefore, different chiral ligands were tested for the ruthenium(0) and ruthenium(II) catalyst. In the first series of experiments, the influence of different chiral amine and phosphine ligands on the ruthenium(0) catalyzed transformation was examined. Some of the ligands are used for the ruthenium-catalyzed enantioselective hydrogenation.¹⁰⁵ Unfortunately, none of them showed good activity with respect to chiral induction as well as to chemical reactivity (Table 29, entries 2-13). The best conversion could be achieved without any ligand. The ligands are obviously binding to the active catalyst species and preventing coordination to the starting material. The stronger the coordination ability of the ligands, the lower the conversion is.

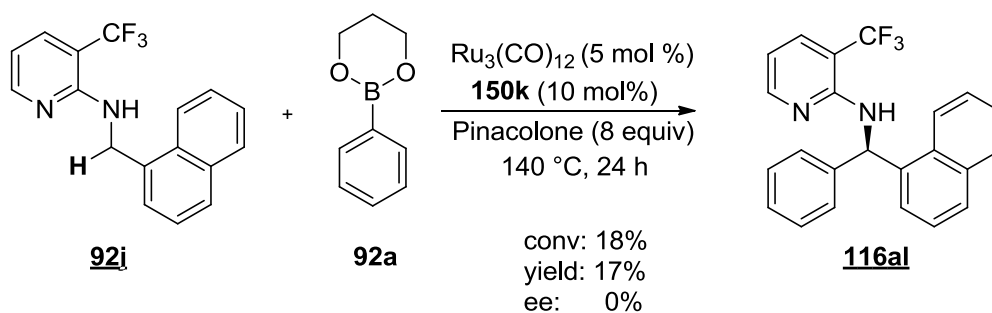
Table 29 Chiral ligand screening for the ruthenium(0)-catalyzed direct arylation of **92a**.



entry	Ligand	conv	yield	ee [%] ^d
1	No	86	64	0
2	150a	50	35	0
3	150b	5	--	--
4	150c	8	--	--
5	150d	4	--	--
6	150e	73	33	0
7	150f	3	--	--
8	150g	35	16	0
9	150h	65	44	6
10	150i	54	42	5
11	150j	55	43	0
12	150k	44	33	6
13	150l	67	42	0

^aReaction conditions: **92a** (0.5 mmol), **91f** (0.75 mmol), Ru₃(CO)₁₂ (5 mol%), ligand (10 mol%), and pinacolone (0.5 mL). ^bConversion determined by GC analysis with respect to **92a**. ^cYield determined by GC analysis with respect to **92a** (dodecane as internal standard). ^dee determined by HPLC.

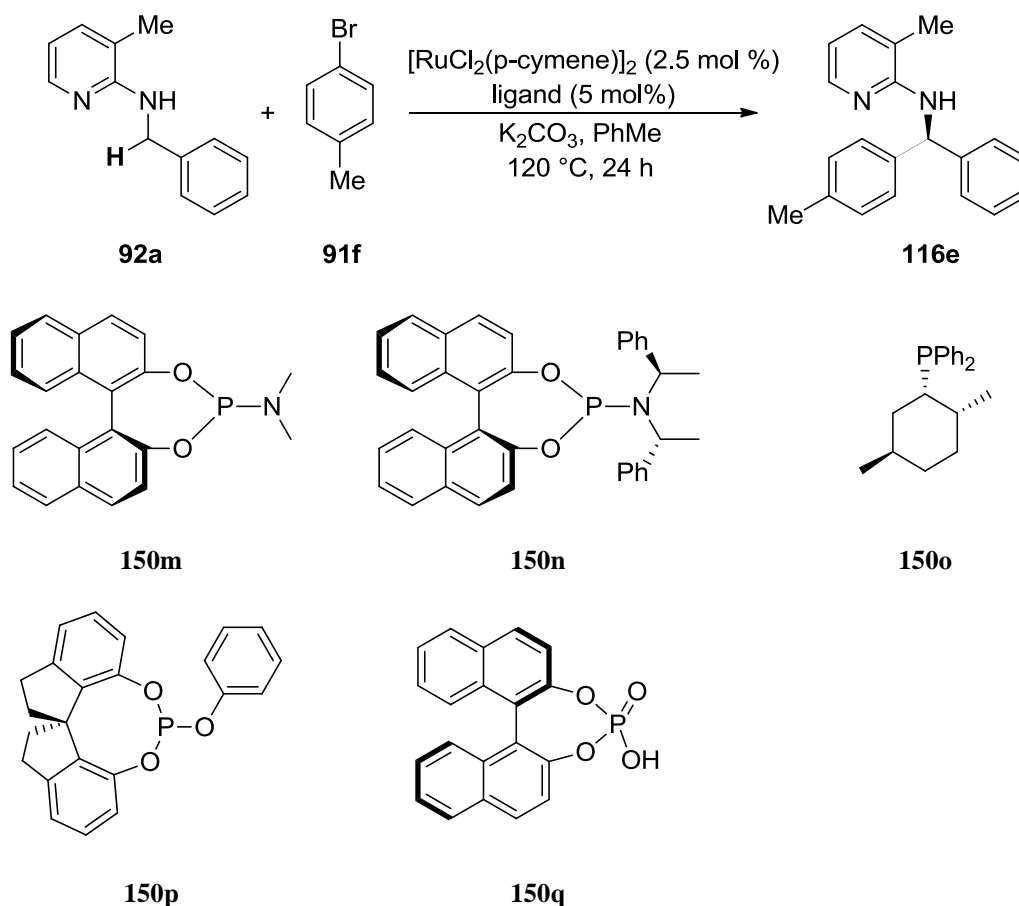
It was also tried to replace the phenyl group by a more bulky naphthyl group in order to increase the steric properties of the starting material. The reaction was conducted with ligand **150k** which showed the best activity in the previous experiments. But here, too, the reaction performed unsatisfactory (Scheme 44).



Scheme 44 Ruthenium(0)-catalyzed direct arylation of **92j** in the presence of **150k**.

As a consequence, it was decided to switch to the ruthenium(II) system, since it was known that in these reactions phosphine ligands are enhancing the conversion. The reaction was carried out in the presence of different ligands. The best result could be achieved with the phosphoramidite **150n** which showed a substantially better conversion than the catalyst alone (Table 30, entry 7). Gratifyingly, an enantiomeric excess of the product was observed even if the value is still quite low from a synthetic view. However, this promising result shows that an asymmetric C–H bond transformation can be achieved by this route, although different mechanisms are thinkable (direct sp^3 C–H activation *vs.* β -hydrid-elimination and subsequent sp^2 C–H activation).

Table 30 Chiral ligand screening for the ruthenium(II)-catalyzed direct arylation of **92a**.



entry	Ligand	conv	yield	ee [%] ^d
1	No	21	12	0
2	150b	0	--	--
3	150c	0	--	--
4	150d	0	--	--
5	150k	23	14	13
6	150m	21	14	3
7	150n	40	28	18
8	150o	9	--	--
9	150p	6	--	--
10	150q	15	--	--

^aReaction conditions: **92a** (0.5 mmol), **91f** (0.75 mmol), [RuCl₂(*p*-cymene)]₂ (2.5 mol%), KOPiv (30 mol%), K₂CO₃ (1.5 mmol), and PhMe (2 mL). ^bConversion determined by GC analysis with respect to **92a**. ^cYield determined by GC analysis with respect to **92a** (dodecane as internal standard). ^dee determined by HPLC.

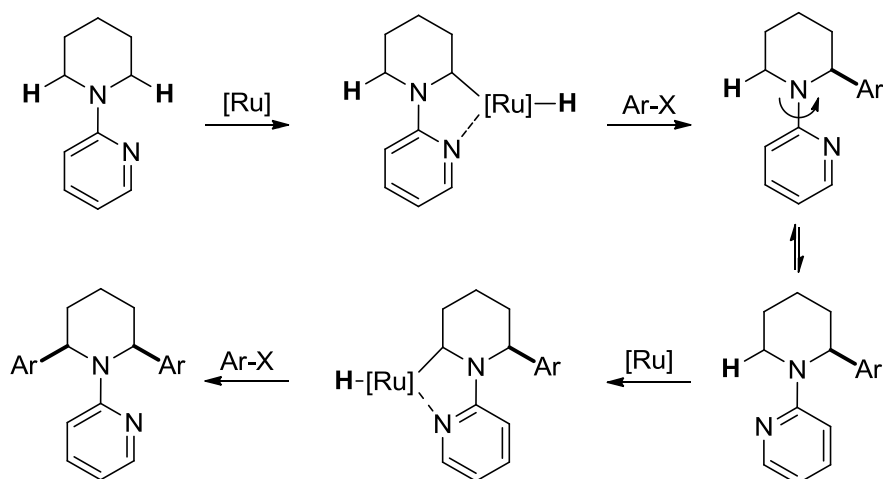
4.2 Direct Arylation of Cyclic Amines

4.2.1 Objective

Many biologically active compounds, such as alkaloids or pharmaceuticals, contain saturated amines as subunit. There are different ways for the construction of these motifs, ranging from reduction of aromatic compounds¹⁰⁶ to radical coupling reactions.⁸⁷ However, these methods are usually limited in scope and functional group tolerance (e.g., the radical coupling reaction needs strong electron withdrawing groups). The direct functionalization of small and readily accessible molecules, such as pyrrolidine and piperidine, is a very attractive pathway for the preparation of these building units. This simple method provides a powerful tool in the synthesis of those building blocks.

As one can see from the above protocols, the main problem for the direct arylation of cyclic amines is the regioselectivity. Pyrrolidine has for instance two equivalent C–H bonds in γ -position to the directing nitrogen. The arylation process would not stop after one transformation, but continues to the bis-arylated product (Scheme 45). For this reason, the Sames group used 2-substituted pyrrolidines (Scheme 18) as starting materials. The bisarylated products are often difficult to separate and reduce the yield significantly. Maes reported, for instance, in different cases a 1:1 ratio of mono and bisarylated product.

The idea was to develop a feasible method for the direct arylation of piperidine, avoiding bis-arylation products. The reason for the bis-arylation is the low energy barrier for the rotation of pyridine around the C–N bond. This free rotation allows the coordination of catalyst to the C–H bonds in both α -positions to the nitrogen, leading to the insertion of catalyst into both C–H bonds with essentially the same rate.



Scheme 45 Mechanism of bisarylation of piperidine directed by pyridine.

Based on the above experiences in governing the regioselectivity employing a suitable directing group, it was decided to use the previous findings in a way to hinder the directing effect after one transformation. The installation of a bulky group in 3-position of pyridine should avoid the rotation and subsequently metal-coordination of the pyridine nitrogen after the first arylation step (Scheme 45). This steric hindrance of the mono-arylated product should prevent the formation of the undesired bisarylated product. Fortunately, the installation of a bulky group (e.g., CF_3 , Ph) in 3-position of pyridine resulted in the formation of the mono arylated product (45%) and only traces amounts (<5%) of bisarylated product could be detected.

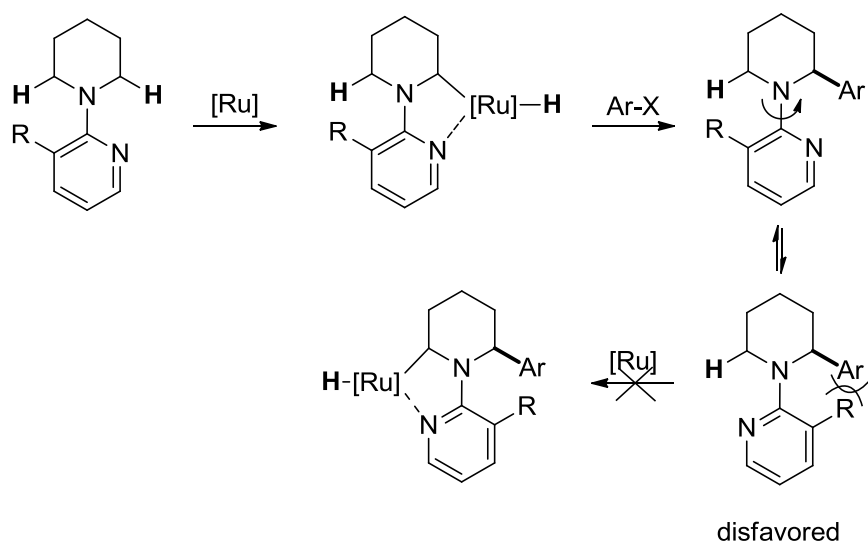
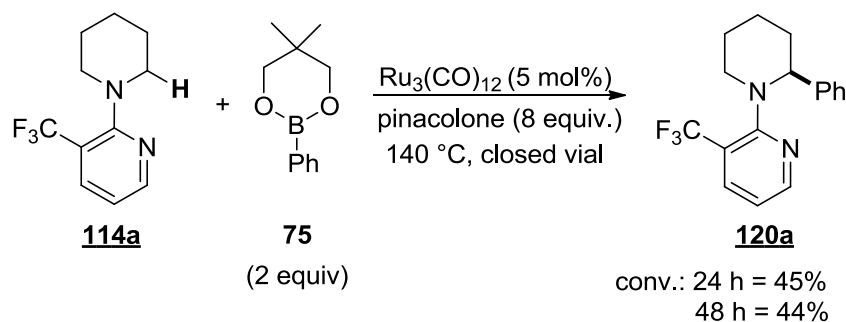


Figure 46 Avoiding bisarylation by the introduction of a bulky group in the 3-position of the pyridine directing group.

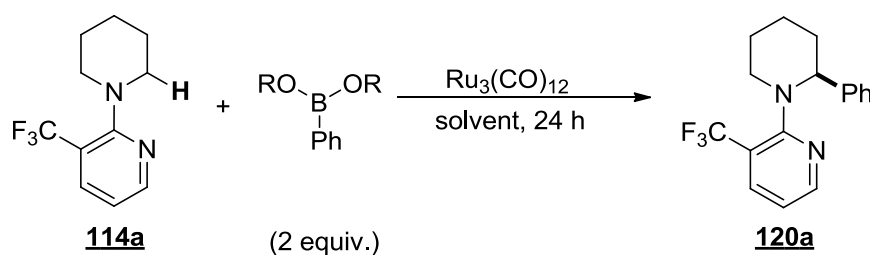
4.2.2 Screening

The experiment was carried out with conditions of the previous transformations and monitored by GC-analysis. The reaction was performed with trifluoromethyl substituted pyridine derivative **114a** in a closed vial under argon at 140 °C for 24 h. As expected, solely mono arylated product could be detected (Scheme 46). However, the conversion stopped at 45% and any further extension in reaction time (48 h = 44%) did not lead to higher conversion. In order to increase the conversion, different parameters were screened in the following.



Scheme 46 Ruthenium(0)-catalyzed direct arylation of **114a**.

The nature of the ester did not have any influence on the conversion (Table 31, entries 1-4). Thus, further optimizations continued with boronic propanediol ester because of the simple separation of these esters (they can be hydrolyzed back to the boronic acid which facilitates separation via column chromatography). Amongst the solvents, pinacolone gave the best result (45%, Table 31, entry 3). In the absence of ketone, the conversion dropped significantly (Table 31, entries 7-9). Alcohols showed also no improvement of the conversion (10%, Table 31, entries 10 and 11). Next, the concentration of the reaction was changed. An increase of solvent did not affect the reaction (42%), but a decrease resulted in lower conversion (19%, Table 31, entries 12 and 13). By increasing the catalyst loading, better results were obtained (58%, Table 31, entries 14-16). The best conditions were achieved with phenylboronic acid 1,3-propanediol ester, 10 mol% $\text{Ru}_3(\text{CO})_{12}$, and 8 equivalents pinacolone at 140 °C (58%, Table 31, entry 16). However, with the intention to develop a catalytic method, higher catalyst loadings were avoided and further reactions were carried out with 7 mol% catalyst loading. Finally, the temperature was increased which did not have any significant effect (Table 31, entries 17-20).

Table 31 Optimization studies for the ruthenium(0)-catalyzed direct arylation of **114a**.

entry	ester	solvent	catalyst [mol%]	t [°C]	conv
1	<i>neo</i> -pentanediol	pinacolone (8 equiv)	5	140	45
2	pinacol	pinacolone (8 equiv)	5	140	44
3	propanediol	pinacolone (8 equiv)	5	140	45
4	ethylene glycol	pinacolone (8 equiv)	5	140	41
5	propandiol	acetophenon (8 equiv)	5	140	26
6	propandiol	cyclohexanon (8 equiv)	5	140	23
7	propandiol	<i>o</i> -xylene	5	140	39
8	propandiol	NMP	5	140	28
9	propandiol	DMA	5	140	14
10	propandiol	<i>t</i> -BuOH	5	140	10
11	propandiol	3-ethyl-3-pentanol	5	140	11
12	propandiol	pinacolone (4 equiv)	5	140	19
13	propandiol	pinacolone (16 equiv)	5	140	42
14	propandiol	pinacolone (8 equiv)	2.5	140	19
15	propandiol	pinacolone (8 equiv)	7	140	50
16	propandiol	pinacolone (8 equiv)	10	140	58
17	propandiol	pinacolone (8 equiv)	5	120	15
18	propandiol	pinacolone (8 equiv)	5	130	38
19	propandiol	pinacolone (8 equiv)	5	150	47
20	propandiol	pinacolone (8 equiv)	5	160	46

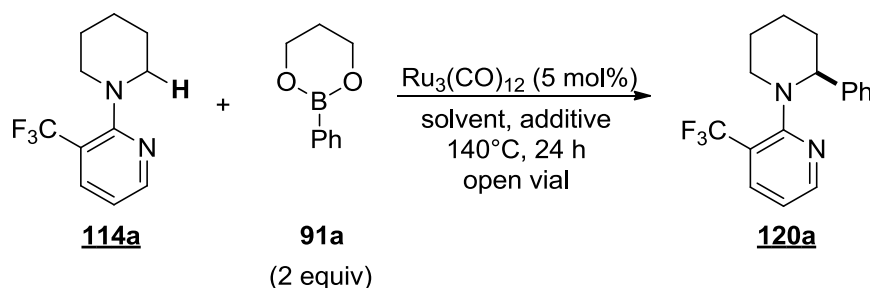
^aReaction conditions: **114a** (0.5 mmol), PhB(OR)₂ (1.5 mmol), Ru₃(CO)₁₂, and solvent (0.5 mL).

^bConversion determined by GC analysis with respect to **114a**.

According to Maes, the reaction could be enhanced by performing the transformation in an open vial experiment to release the generated hydrogen.⁹⁴ Thus, no ketone is necessary, but an alcohol to catch the formed boron species after transmetalation. In this context, it was also tried to perform the reaction in an open vial (the reaction was performed with a septum cap and argon balloon). Table 32 shows the results of the optimization. Under the open vial conditions, an increased side reaction, the deborylation of the phenylboronic acid ester, was detected. The catalyst is obviously inserting into the C–B bond and forming a new C–H bond with hydrogen. Therefore, the phenylboronic acid ester amount had to be increased to 3 equivalents. Different alcohols were tested for the transformation. The higher boiling alcohols, such as propanediol and *neo*-pentanediol, gave the best results (58%, Table 32, entries 1-4). 1 Equivalent of 3-ethyl-3-pentanol and *t*-BuOH, but only 0.5 equivalent of the diol to keep the

number of hydroxy groups constant, were used. Increasing the amount of diol to 1 equivalent resulted in decreased conversion of 32% (results not shown). In the next step, different solvents were examined (Table 32, entries 5-8). The best result could be achieved with *o*-xylene (65%, Table 32, entry 6). The addition of 1 equivalent base, which is commonly used in Suzuki reactions in order to catch the formed boron species, was tried out. However, the presence of base inhibited the reaction (Table 32, entries 9-14).

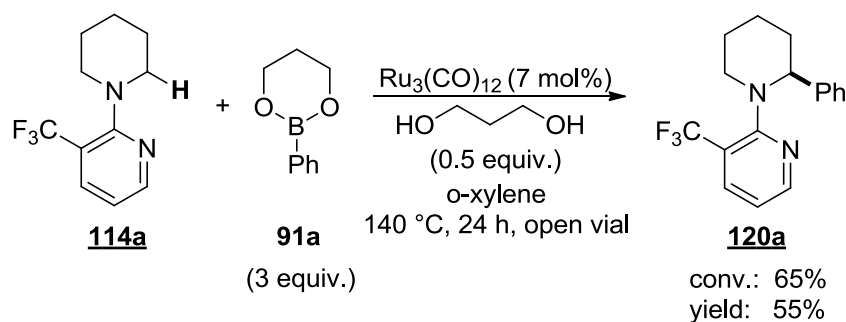
Table 32 Optimization studies for the ruthenium(0)-catalyzed direct arylation of **114a** with an open vial.



entry	alcohol	solvent	additive	conv
1	3-ethyl-3-pentanol			36
2	<i>t</i> -BuOH			28
3	propanediol			58
4	<i>neo</i> -pentanediol			54
5		<i>o</i> -xylene		39
6	propanediol	<i>o</i>-xylene		65
7	propanediol	NMP		26
8	propanediol	DMA		12
9	propanediol	<i>o</i> -xylene	NaOt-Bu	0
10	propanediol	<i>o</i> -xylene	K ₂ CO ₃	0
11	propanediol	<i>o</i> -xylene	Cs ₂ CO ₃	0
12		<i>o</i> -xylene	NaOt-Bu	0
13		<i>o</i> -xylene	K ₂ CO ₃	0
14		<i>o</i> -xylene	Cs ₂ CO ₃	0

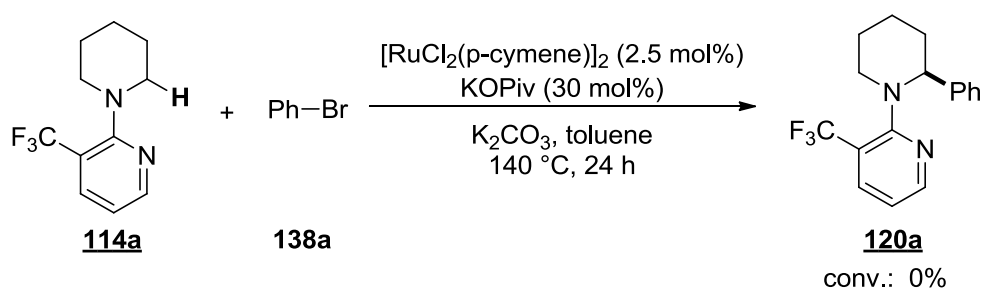
^aReaction conditions: **114a** (0.5 mmol), **91a** (1.5 mmol), Ru₃(CO)₁₂ (7 mol%), alcohol (0.5 mmol), additive (1 mmol), and solvent (0.5 mL). ^bConversion determined by GC analysis with respect to **114a**.

The best results for **114a** could be accomplished with 3 equivalents phenylboronic propanediol acid ester **91a**, 0.5 equivalent propanediol, 7 mol% Ru₃(CO)₁₂, and 1 mL *o*-xylene for 24 h at 140 °C (Scheme 47).



Scheme 47 Optimized conditions for the mono arylation of **114a**.

The $[\text{RuCl}_2(p\text{-cymene})]_2$ /aryl halide system was not suitable for this transformation (Scheme 48).



Scheme 48 Rutneum(II)-catalyzed direct arylation of **114a**.

4.2.3 Directing group

In the next step, the steric and electronic influences of the substituent in 3-position were investigated. Therefore different compounds with different groups in this position were synthesized (Figure 46) and reacted under optimized conditions. The trifluoromethyl group emerged to be the most suitable one. The methyl and phenyl substituents **151** and **152** reacted in the same range. Increasing the size of the substituent to phenyl did not lead to any increase of the conversion. The chloro substituent slowed down the reaction, but also gave only mono arylated product. In the case of the iodo substituent, pronounced dehalogenation of the compound was observed. The catalyst is obviously inserting into the weak C–I bond and forming a new C–H bond. The electron withdrawing ethoxycarbonyl substrate **155** showed a relatively high conversion. This indicates that the electronic effects of the substituent play a secondary role. The nitrogen is still electron rich enough to coordinate the metal. In the case of compound **156**, the methyl group in 6-position might disturb this coordination.

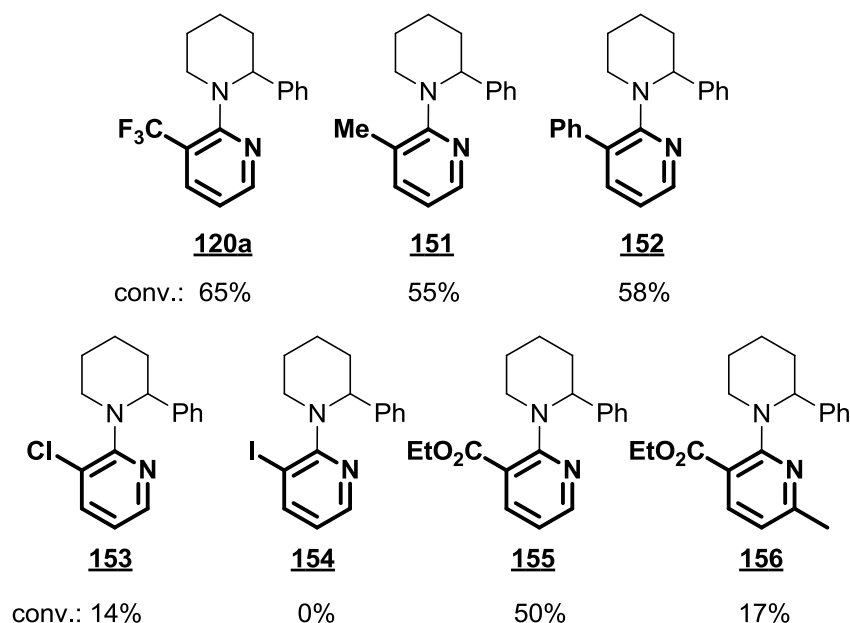
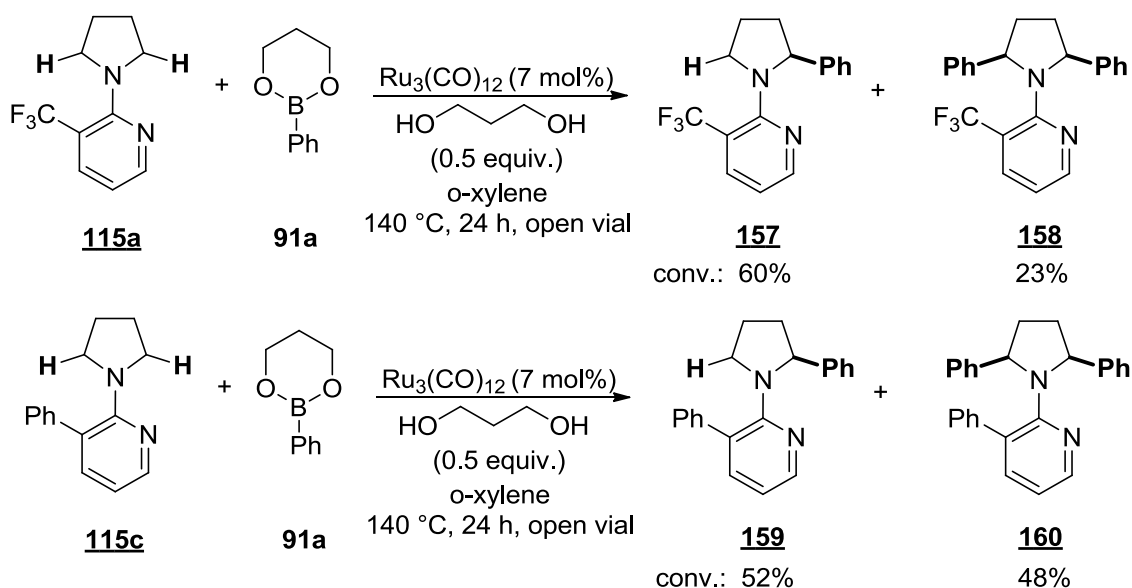


Figure 47 Screening of different directing groups.

Since the five-membered pyrrolidine and the six-membered piperidine have completely different conformations, it was investigated how pyrrolidine behaves with this directing group. Unfortunately, in the case of the more reactive pyrrolidine **115a**, high amounts of bisarylated product **158** were detected (Scheme 49). Changing the trifluoromethyl substituent to the phenyl group **115c** did not affect this behavior. The rotation barrier around the C–N bond is obviously not high enough for the five-membered pyrrolidine ring. The pyridine directing group can apparently rotate without any hindrance around the C–N bond and coordinate the ruthenium metal into both C–H bonds.



Scheme 49 The 3-substituted pyridine directing group for the direct arylation of pyrrolidine.

4.2.4 Scope

As known from the literature, the catalyst is sensitive to the electronic and steric properties of the aryl donor species (Figure 47). Reactions generally proceed in lower yields than for the acyclic compounds. The reaction performed moderately with electron donating aryl-substituents (e.g., 4-Me 44% and 4-*t*-Bu 43% conversion), but poorer with electron withdrawing substituents (e.g. Cl 34% and CF₃ 35% conversion).¹⁰⁷

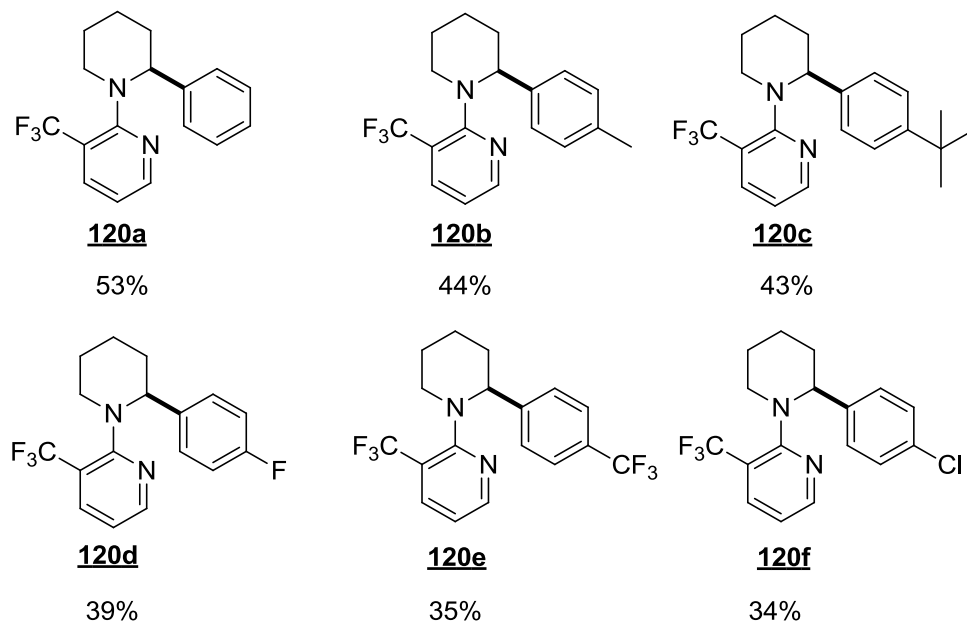


Figure 47 Scope of the direct arylation of **114a**.

5. Final Conclusion

In conclusion, cyclic and acyclic sp^3 C–H bonds adjacent to a free N–H group were readily arylated via cyclometalation with $Ru_3(CO)_{12}$ and $[RuCl_2(p\text{-cymene})]_2$. Depending on the catalyst, the reaction could be performed with arylboronic acid esters or aryl halides as aryl donor. The synthetic utility of this approach was demonstrated by the synthesis of various arylated benzylic amines. This is an unprecedented direct functionalization of benzylic amines that allows an exceedingly convenient route to diarylmethanamines.

Pyridine was found to be the most suitable directing group for these transformations. A bulky group in 3-position of the pyridine was also crucial for high conversions in these reactions. Various bulky groups (CH_3 , CF_3 , Ph) were applied and usually led to the desired products in good yield. Solely chlorine was less efficient as bulky group. Furthermore, it could be confirmed by DFT calculations that the bulky group in 3-position hinders the benzylic amine to rotate around the C–N bond and subsequently allows the insertion of the metal into the C–H bond. Finally, a protocol for the cleavage of the pyridine directing group, delivering the free diarylmethylamine, was established. Although a two-step protocol is required, deprotection is achieved in high overall yield, significantly expanding the general applicability of this approach.

Different substituents on the benzylic amine were tested with both protocols. The electronic nature of the substituents affects the electron density of the benzylic C–H bond which has a significant impact on the C–H functionalization rate. Both electron withdrawing and donating substituents were inhibiting the reaction. Amongst both protocols, $Ru_3(CO)_{12}$ turned out to be more sensitive towards the nature of the benzylic amine and the aryl donor. It should be noted that the rigorous exclusion of air/moisture is not required in any of these transformations, and comparable results are obtained in the presence and absence of air, as well as in freshly distilled versus commercial solvents.

The N–H group could also be replaced by CH_2 without a significant decrease in yield with the $Ru_3(CO)_{12}$ protocol. The benzylic nature of the CH_2 group to be arylated proved to be more important since a non-benzylic CH_2 group performed significantly worse. The arylation also occurred with C–H bonds adjacent to a N–R bond, but the conversion was decreasing significantly. However, a free N–H was mandatory for the $[RuCl_2(p\text{-cymene})]_2$ protocol, indicating the different mechanistic pathway of both catalysts. The imine formation observed with $[RuCl_2(p\text{-cymene})]_2$ seems to be a crucial intermediate in this reaction. Furthermore, the $[RuCl_2(p\text{-cymene})]_2$ protocol could be expanded to cheaper aryl chlorides by using phosphines as ligands and secondary alcohols as hydrogen source.

Preliminary mechanistic experiments were undertaken and support the mechanism proposed by Kakiuchi et al for the $Ru_3(CO)_{12}$ protocol. The KIE experiments indicate that the oxidative addition step might be the rate limiting step of the reaction. The reaction could be performed

under air and was even pushed under hydrogen where obviously a more active ruthenium(II) species is formed. The KIE experiments of the Ru(II) protocol revealed that the oxidative addition step is not the rate determining step. The improvement of the conversion in the presence of carboxylate can be explained by a CMD mechanism.

Finally, the 3-substituted pyridine directing group could also be used for the direct mono arylation of piperidines, again displaying superior selectivities for the single C-H activation event. However, this protocol has still to be optimized to afford higher yields of the product.

The establishment of these conditions should provide a valuable starting point to those wishing to examine the use of direct arylation in C–C bond synthesis and to facilitate the discovery of other novel cross-coupling partners in this type of chemistry

Publications:

1.) M. Schnürch, N. Dastbaravardeh, M. Ghobrial, B. Mrozek, M. D. Mihovilovic “Functionalization of Saturated and Unsaturated Heterocycles via Transition Metal Catalyzed C–H Activation Reactions” *Curr. Org. Chem.* **2011**, *15*, 2694.

2.) N. Dastbaravardeh, M. Schnürch, M. D. Mihovilovic “Ruthenium(0)-Catalyzed sp^3 C–H Bond Arylation of Benzylic Amines Using Arylboronates” *Org. Lett.* **2012**, *14*, 1930.

3.) N. Dastbaravardeh, M. Schnürch, M. D. Mihovilovic “Ruthenium(II)-Catalyzed sp^3 C–H Bond Arylation of Benzylic Amines Using Aryl Halides” *Org. Lett.* **2012**, *14*, 3792.

4.) N. Dastbaravardeh, M. Schnürch, M. D. Mihovilovic „Mechanistic Investigations and Substrate Scope Evaluation of Ruthenium-Catalyzed Direct sp^3 Arylation of Benzylic Positions Directed by 3-Substituted Pyridines“ *J. Org. Chem.* **2013**, *78*, 658.

5.) N. Dastbaravardeh, M. Schnürch, M. D. Mihovilovic „ Aryl Bromides and Aryl Chlorides for the Direct Arylation of Benzylic Amines Mediated by Ruthenium(II) “ *Eur. J. Org. Chem.* **2013**, in press.

6.) Maria C. Schwarz, Navid Dastbaravardeh, Karl Kirchner, Michael Schnürch, Marko D. Mihovilovic „ First Selective Direct Mono-Arylation of Piperidines Using Ruthenium Catalyzed C-H Activation” *Monatshefte für Chemie*, **2013**, in press.

6. Experimental Section

6.1. General Notes

All reactions were carried out under argon, unless otherwise noted. Argon was purified by passage through Drierite. Unless otherwise noted, chemicals were purchased from commercial suppliers and used without further purification. Pinacolone (98%) was purchased from Aldrich and stored over 4 Å molecular sieves. Toluene was dried using a Pure Solv Innovative Technology solvent purification system. For thin layer chromatography (TLC) aluminium backed silica gel was used. Boronic esters were purchased from Aldrich and used as received. All arylation reactions were carried out in capped glass vials (VWR, 8 mL) and heated in a 34-well reaction block.

Microwave Reactions were performed on a BIOTAGE Initiator™ sixty microwave unit.

Chromatography

Flash column chromatography was performed on silica gel 60 from Merck (40-63µm) whereas most separations were carried out using a Büchi Sepacore™ MPLC system with 45g column. For thin layer chromatography (TLC) aluminum backed silica gel was used.

Melting points were determined by using an automated melting point system (MPA100) of Stanford Research Systems.

HR-MS: were carried out by E. Rosenberg at Vienna University of Technology, Institute for Chemical Technologies and Analytics.

Analytical method:

All samples were analysed by LC-IT-TOF-MS in only positive ion detection mode with the recording of MS and MS/MS spectra. For the evaluation in the following, only positive ionization spectra were used (where the quasi-molecular ion is the one of $[M+H]^+$), and further data or information were not taken into consideration.

Instrumental parameters:

Shimadzu Prominence HPLC, consisting of: solvent degassing unit (DGU-20 A3), binary gradient Pump (2 x LC-20AD), auto-injector (SIL-20A), column oven (CTO-20AC), control module (CBM-20A), and diode array detector (SPD-M20A).

MS System: Shimadzu IT-TOF-MS with electrospray interface.

Chromatography (parameters: Short Col PI NI MS2):

Column: Phenomenex Prodigy ODS(3), 30 mm x 4.6 mm, 3 μ m particles, operated at 40°C; Gradient: 0 min: 70% A, 30% B (1 min); linear gradient to 5 min to 10% A, 90% B (hold 2 min); at 7.01 min back to 70% A, 30% B, hold until 8.0 min);. A: acetonitril+0.1% formic acid, B: H₂O + 0.1% formic acid. Column flow: 0.5 ml/min; injection volume: 2 μ l.

MS Parameters:

MS parameters as in auto tune. Data recorded with detector voltage at auto tune value. Scan range: 50-1000 amu for both, MS and MS/MS (PI) detection. ES ionization.

GC-MS

GC-MS runs were performed on a Thermo Finnigan Focus GC / DSQ II using a standard capillary column BGB 5 (30m x 0.32 mm ID).

NMR-spectroscopy

NMR-spectra were recorded either in CDCl₃ solution using TMS as internal standard or DMSO-d₆ or in CD₃OD on a Bruker AC 200 (200MHz) spectrometer and chemical shifts are reported in ppm

Abbreviation

BINAP = 2,2'-Bis(diphenylphosphino)-1,1'-binaphthyl

n-BuOH = *n*-Butanol

dba = Dibenzylidenacetone

DCM = Dichloromethane

DCPTPB = 2-Dicyclohexyl-phosphino-2',4',6'-triisopropylbiphenyl

DIPEA = Diisopropylethylamine

DMS = Dimethyl sulfate

DPPP = 1,3-Bis(diphenylphosphino)propane

EtOAc = Ethylacetate

EtOH = Ethanol

HRMS = High resolution mass spectrometry

m-CPBA = *meta*-Chloroperoxybenzoic acid

MPLC = Medium pressure liquid chromatography

Mp = Melting point

NMR = Nuclear magnetic resonance

PE = Petrol ether

i-PrOH = iso-Propanol

r.t. = Room temperature

rpm = round per minute

THF = Tetrahydrofuran

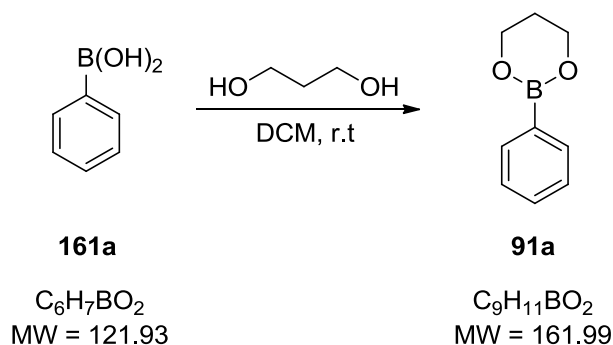
TLC = Thin layer chromatography

6.2 Synthesis of Arylboronate Esters

General procedure I:

A 50 mL round-bottomed flask was charged with arylboronic acid (1 equiv), propane-1,3-diol (1.1 equiv), and CH_2Cl_2 . The reaction mixture was stirred under air at r.t. until the arylboronic acid was consumed completely (1-3 h, monitored by TLC). The crude reaction mixture was dried over Na_2SO_4 , filtered through silica and evaporated to dryness. Subsequently, the product was dried in high vacuum. Compounds **91a-n** were prepared according to this procedure.

6.2.1 2-Phenyl-1,3,2-dioxaborinane (**91a**)



Phenylboronic acid **161a** (610 mg, 5 mmol, 1 equiv) and propane-1,3-diol (418 mg, 5.5 mmol, 1.1 equiv) were reacted in 5 mL of CH_2Cl_2 according to general procedure I.

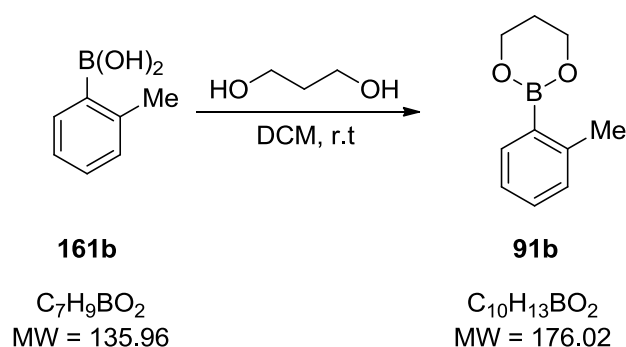
Yield: 99% (806 mg, 4.95 mmol)

Appearance: colorless oil

TLC: 0.7 (PE/EtOAc 5:1)

^1H NMR (CDCl_3 , 200MHz): δ = 2.06 (quint, J = 5.5 Hz, 2H, H4), 4.17 (t, J = 5.5 Hz, 4H, H3), 7.30-7.43 (m, 3H, H3' & H4'), 7.75-7.80 (m, 2H, H2').

^{13}C NMR (CDCl_3 , 50MHz): δ = 27.6 (t, C4), 62.1 (t, C3), 127.7 (d, C3' & C4'), 130.7 (s, C1'), 133.7 (d, C2').

6.2.2 2-(2-Methylphenyl)-1,3,2-dioxaborinane (**91b**)

2-Methylphenylboronic acid **161b** (680 mg, 5 mmol, 1 equiv) and propane-1,3-diol (418 mg, 5.5 mmol, 1.1 equiv) were reacted in 5 mL of CH_2Cl_2 according to general procedure I.

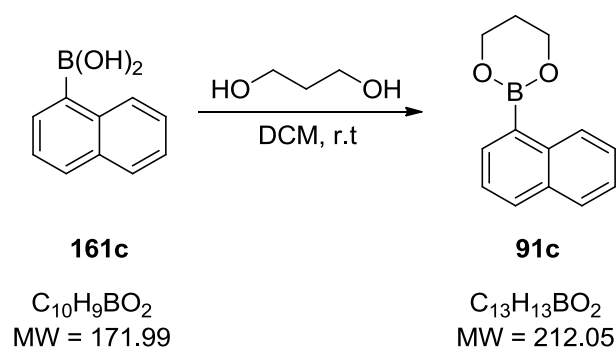
Yield: 97% (853 mg, 4.85 mmol)

Appearance: colorless oil

TLC: 0.7 (PE/EtOAc 5:1)

^1H NMR (CDCl_3 , 200MHz): δ = 2.06 (quint, J = 5.5 Hz, 2H, H4), 2.51 (s, 3H, CH_3), 4.17 (t, J = 5.5 Hz, 4H, H3), 7.11-7.18 (m, 2H, PhH), 7.24-7.28 (m, 1H, PhH), 7.70-7.74 (m, 1H, H6').

^{13}C NMR (CDCl_3 , 50MHz): δ = 22.5 (q, $\underline{\text{C}}\text{H}_3$), 27.5 (t, C4), 61.9 (t, C3), 124.7 (d, C5'), 130.0 (d, C3' & C4'), 134.8 (d, C6'), 144.0 (s, C2').

6.2.3 2-(Naphthalen-1-yl)-1,3,2-dioxaborinane (**91c**)

Naphthalen-1-ylboronic acid **161c** (860 mg, 5 mmol, 1 equiv) and propane-1,3-diol (418 mg, 5.5 mmol, 1.1 equiv) were reacted in 5 mL of CH_2Cl_2 according to general procedure I.

Yield: 94% (997 mg, 4.7 mmol)

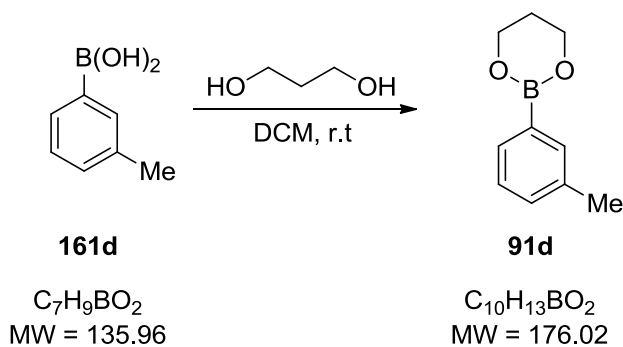
Appearance: colorless oil

TLC: 0.8 (PE/EtOAc 5:1)

^1H NMR (CDCl₃, 200MHz): δ = 2.15 (quint, J = 5.5 Hz, 2H, H₄), 4.29 (t, J = 5.5 Hz, 4H, H₃), 7.42-7.55 (m, 3H, NaphH), 7.81-7.92 (m, 2H, NaphH), 8.00-8.04 (m, 1H, NaphH), 8.74-8.80 (m, 1H, NaphH).

^{13}C NMR (CDCl₃, 50MHz): δ = 27.5 (t, C₄), 62.3 (t, C₃), 125.1 (d), 125.3 (d), 126.0 (d), 128.4 (d), 128.5 (d), 131.0 (d), 133.5 (s, C_{5'}), 134.4 (d), 136.8 (s, C_{10'}).

6.2.4 2-(3-Methylphenyl)-1,3,2-dioxaborinane (91d)



3-Methylphenylboronic acid **161d** (680 mg, 5 mmol, 1 equiv) and propane-1,3-diol (418 mg, 5.5 mmol, 1.1 equiv) were reacted in 5 mL of CH₂Cl₂ according to general procedure I.

Yield: 97% (852 mg, 4.85 mmol)

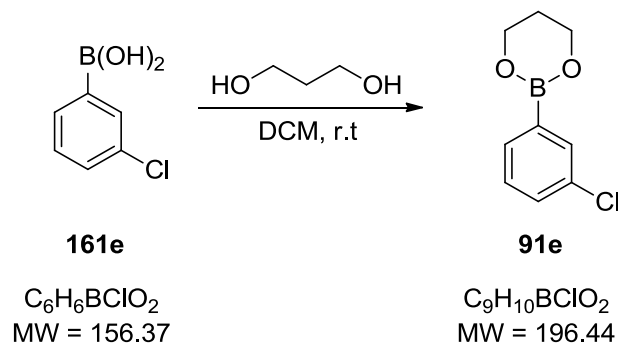
Appearance: colorless oil

TLC: 0.7 (PE/EtOAc 5:1)

^1H NMR (CDCl₃, 200MHz): δ = 2.06 (quint, J = 5.5 Hz, 2H, H₄), 2.35 (s, 3H, CH₃), 4.17 (t, J = 5.5 Hz, 4H, H₃), 7.23-7.26 (m, 2H, PhH), 7.56-7.60 (m, 2H, PhH).

^{13}C NMR (CDCl₃, 50MHz): δ = 21.5 (q, C_{CH₃}), 27.6 (t, C₄), 62.1 (t, C₃), 127.6 (d, C_{5'}), 130.8 (d, C_{4'}), 131.5 (d, C_{6'}), 134.4 (d, C_{2'}), 137.0 (s, C_{3'}).

6.2.5 2-(3-Chlorophenyl)-1,3,2-dioxaborinane (91e)



(3-Chlorophenyl)boronic acid **161e** (780 mg, 5 mmol, 1 equiv) and propane-1,3-diol (418 mg, 5.5 mmol, 1.1 equiv) were reacted in 5 mL of CH_2Cl_2 according to general procedure I.

Yield: 95% (930 mg, 4.75 mmol)

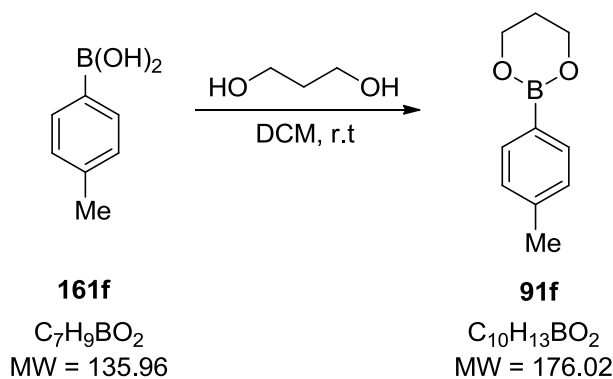
Appearance: colorless oil

TLC: 0.6 (PE/EtOAc 5:1)

^1H NMR (CDCl_3 , 200MHz): δ = 2.05 (quint, J = 5.5 Hz, 2H, H4), 4.15 (t, J = 5.5 Hz, 4H, H3), 7.22-7.40 (m, 2H, PhH), 7.60-7.64 (d, J = 7.1 Hz, 1H, H6'), 7.73 (s, 1H, H2').

^{13}C NMR (CDCl_3 , 50MHz): δ = 27.5 (t, C4), 62.2 (t, C3), 129.1 (d, C4'), 130.7 (d, C2'), 131.7 (d, C5'), 133.7 (d, C6'), 134.0 (s, C3').

6.2.6 2-(4-Methylphenyl)-1,3,2-dioxaborinane (91f)



4-Methylphenylboronic acid **161f** (680 mg, 5 mmol, 1 equiv) and propane-1,3-diol (418 mg, 5.5 mmol, 1.1 equiv) were reacted in 5 mL of CH_2Cl_2 according to general procedure I.

Yield: 96% (843 mg, 4.8 mmol)

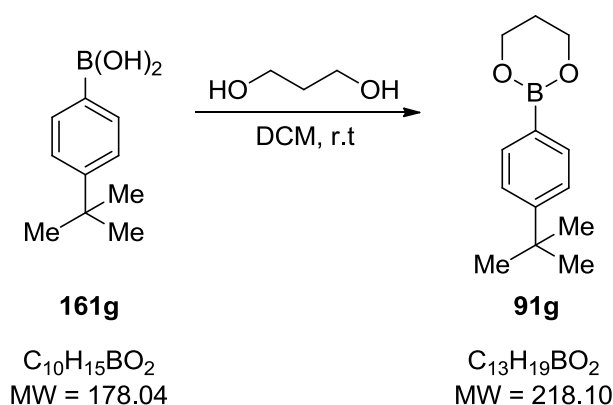
Appearance: colorless solid

Mp: 37-38 °C

TLC: 0.7 (PE/EtOAc 5:1)

^1H NMR (CDCl_3 , 200MHz): δ = 2.05 (quint, J = 5.5 Hz, 2H, H4), 2.36 (s, 3H, CH_3), 4.16 (t, J = 5.5 Hz, 4H, H3), 7.17 (d, J = 7.9 Hz, 2H, H3'), 7.67 (d, J = 7.9 Hz, 2H, H2').

^{13}C NMR (CDCl_3 , 50MHz): δ = 21.8 (q, $\underline{\text{C}}\text{H}_3$), 27.6 (t, C4), 62.1 (t, C3), 128.5 (d, C3'), 133.8 (d, C2'), 140.7 (s, C4').

6.2.7 2-(4-(1,1-Dimethylethyl)phenyl)-1,3,2-dioxaborinane (**91g**)

(4-(1,1-Dimethylethyl)phenyl)boronic acid **161g** (890 mg, 5 mmol, 1 equiv) and propane-1,3-diol (418 mg, 5.5 mmol, 1.1 equiv) were reacted in 5 mL of CH_2Cl_2 according to general procedure I.

Yield: 94% (1.02 g, 4.7 mmol)

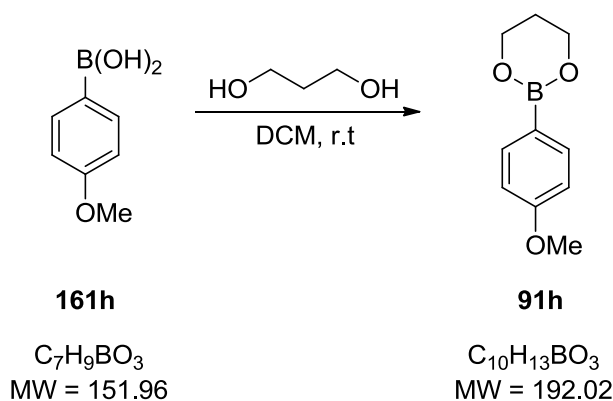
Appearance: colorless solid

Mp: 84-86 °C

TLC: 0.8 (PE/EtOAc 5:1)

^1H NMR (CDCl_3 , 200MHz): δ = 1.33 (s, 9H, $\text{C}(\text{CH}_3)_3$), 2.05 (quint, J = 5.5 Hz, 2H, H4), 4.16 (t, J = 5.5 Hz, 4H, H3), 7.39 (d, J = 8.3 Hz, 2H, H3'), 7.72 (d, J = 8.3 Hz, 2H, H2').

^{13}C NMR (CDCl_3 , 50MHz): δ = 27.6 (q, $\text{C}(\text{CH}_3)_3$), 31.4 (s, $\text{C}(\text{CH}_3)_3$), 34.9 (t, C4), 62.1 (t, C3), 124.7 (d, C3'), 133.7 (d, C2'), 153.8 (s, C4').

6.2.8 2-(4-Methoxyphenyl)-1,3,2-dioxaborinane (**91h**)

(4-Methoxyphenyl)boronic acid **161h** (760 mg, 5 mmol, 1 equiv) and propane-1,3-diol (418 mg, 5.5 mmol, 1.1 equiv) were reacted in 5 mL of CH_2Cl_2 according to general procedure I.

Yield: 97% (932 mg, 4.85 mmol)

Appearance: colorless solid

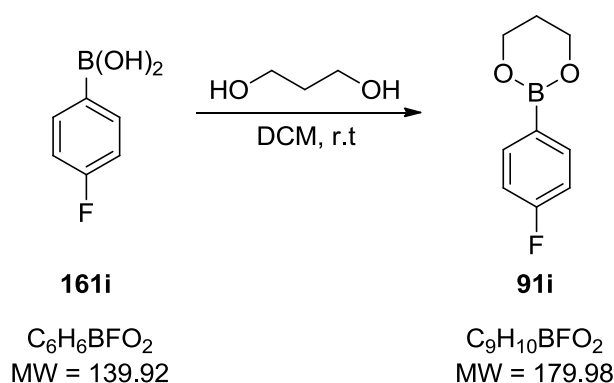
Mp: 31-32 °C

TLC: 0.6 (PE/EtOAc 5:1)

¹H NMR (CDCl₃, 200MHz): δ = 2.04 (quint, J = 5.5 Hz, 2H, H₄), 3.82 (s, 3H, OCH₃), 4.15 (t, J = 5.5 Hz, 4H, H₃), 6.88 (d, J = 8.7 Hz, 2H, H_{3'}), 7.71 (d, J = 8.7 Hz, 2H, H_{2'}).

¹³C NMR (CDCl₃, 50MHz): δ = 27.6 (t, C₄), 55.2 (q, OCH₃), 62.0 (t, C₃), 113.2 (d, C_{3'}), 135.4 (d, C_{2'}), 161.8 (s, C_{4'}).

6.2.9 2-(4-Fluorophenyl)-1,3,2-dioxaborinane (91i)



(4-Fluorophenyl)boronic acid **161i** (700 mg, 5 mmol, 1 equiv) and propane-1,3-diol (418 mg, 5.5 mmol, 1.1 equiv) were reacted in 5 mL of CH₂Cl₂ according to general procedure I.

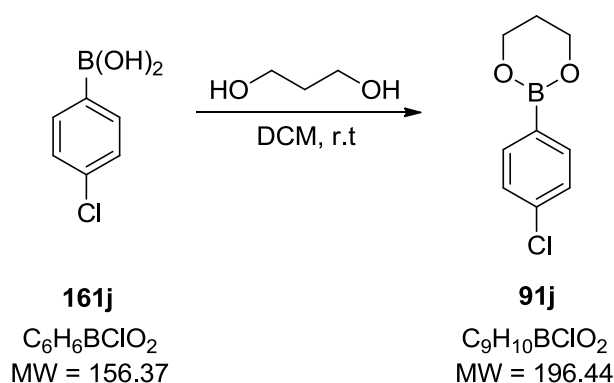
Yield: 99% (898 mg, 4.95 mmol)

Appearance: pale yellow oil

TLC: 0.7 (PE/EtOAc 5:1)

¹H NMR (CDCl₃, 200MHz): δ = 2.05 (quint, J = 5.5 Hz, 2H, H₄), 4.15 (t, J = 5.5 Hz, 4H, H₃), 6.97-7.06 (m, 2H, H_{3'}), 7.71-7.79 (m, 2H, H_{2'}).

¹³C NMR (CDCl₃, 50MHz): δ = 27.6 (t, C₄), 62.1 (t, C₃), 114.7 (d, J_{CF} = 20.0 Hz, C_{3'}), 135.9 (d, J_{CF} = 8.1 Hz, C_{2'}), 164.9 (s, J_{CF} = 248.9 Hz, C_{4'}).

6.2.10 2-(4-Chlorophenyl)-1,3,2-dioxaborinane (**91j**)

(4-Chlorophenyl)boronic acid **161j** (780 mg, 5 mmol, 1 equiv) and propane-1,3-diol (418 mg, 5.5 mmol, 1.1 equiv) were reacted in 5 mL of CH_2Cl_2 according to general procedure I.

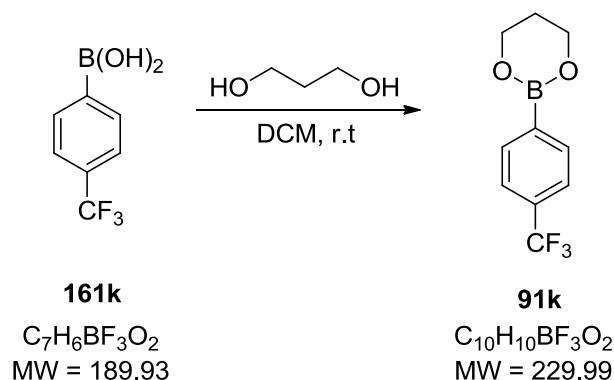
Yield: 97% (949 mg, 4.85 mmol)

Appearance: colorless oil

TLC: 0.6 (PE/EtOAc 5:1)

^1H NMR (CDCl_3 , 200MHz): δ = 2.05 (quint, J = 5.5 Hz, 2H, H4), 4.15 (t, J = 5.5 Hz, 4H, H3), 7.31 (d, J = 8.3 Hz, 2H, H3'), 7.69 (d, J = 8.3 Hz, 2H, H2').

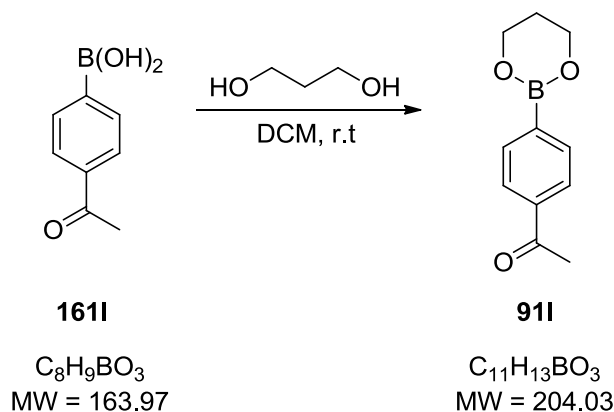
^{13}C NMR (CDCl_3 , 50MHz): δ = 27.5 (t, C4), 62.1 (t, C3), 127.9 (d, C3'), 135.3 (d, C2'), 136.9 (s, C4').

6.2.11 2-(4-(Trifluoromethyl)phenyl)-1,3,2-dioxaborinane (**91k**)

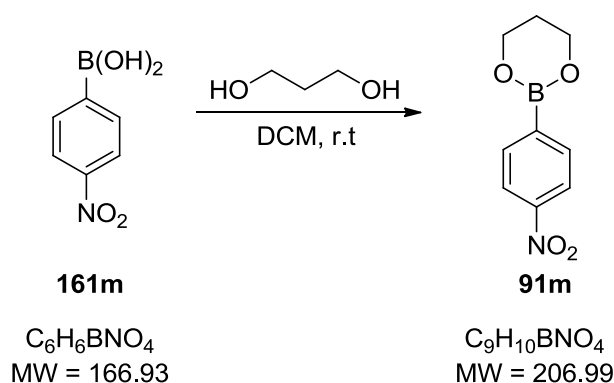
(4-(Trifluoromethyl)phenyl)boronic acid **161k** (950 mg, 5 mmol, 1 equiv) and propane-1,3-diol (418 mg, 5.5 mmol, 1.1 equiv) were reacted in 5 mL of CH_2Cl_2 according to general procedure I.

Yield: 98% (1.13 g, 4.9 mmol)

Appearance: colorless solid

Mp: 82-84 °C**TLC:** 0.7 (PE/EtOAc 5:1)**¹H NMR (CDCl₃, 200MHz):** δ = 2.07 (quint, J = 5.5 Hz, 2H, H₄), 4.17 (t, J = 5.5 Hz, 4H, H₃), 7.58 (d, J = 7.9 Hz, 2H, H_{3'}), 7.86 (d, J = 7.9 Hz, 2H, H_{2'}).**¹³C NMR (CDCl₃, 50MHz):** δ = 27.5 (t, C₄), 62.2 (t, C₃), 124.3 (d, J_{CF} = 3.9 Hz, C_{3'}), 124.5 (s, J_{CF} = 272.0 Hz, CF₃), 132.3 (s, J_{CF} = 32.2 Hz, C_{4'}), 134.1 (d, C_{2'}).**6.2.12 1-(4-(1,3,2-Dioxaborinan-2-yl)phenyl)ethanone (91I)**(4-Acetylphenyl)boronic acid **161I** (820 mg, 5 mmol, 1 equiv) and propane-1,3-diol (418 mg, 5.5 mmol, 1.1 equiv) were reacted in 5 mL of CH₂Cl₂ according to general procedure I.**Yield:** 97% (990 mg, 4.85 mmol)**Appearance:** colorless solid**Mp:** 80-82 °C**TLC:** 0.5 (PE/EtOAc 5:1)**¹H NMR (CDCl₃, 200MHz):** δ = 2.07 (quint, J = 5.5 Hz, 2H, H₄), 2.60 (s, 3H, CH₃), 4.18 (t, J = 5.5 Hz, 4H, H₃), 7.82-7.93 (m, 4H, PhH).**¹³C NMR (CDCl₃, 50MHz):** δ = 26.9 (q, CH₃), 27.5 (t, C₄), 62.2 (t, C₃), 127.3 (d, C_{3'}), 133.9 (d, C_{2'}), 138.6 (s, C_{4'}), 198.8 (s, CO).

6.2.13 2-(4-Nitrophenyl)-1,3,2-dioxaborinane (91m)



(4-Nitrophenyl)boronic acid **161m** (835 mg, 5 mmol, 1 equiv) and propane-1,3-diol (418 mg, 5.5 mmol, 1.1 equiv) were reacted in 5 mL of CH_2Cl_2 according to general procedure I.

Yield: 97% (949 mg, 4.85 mmol)

Appearance: yellow solid

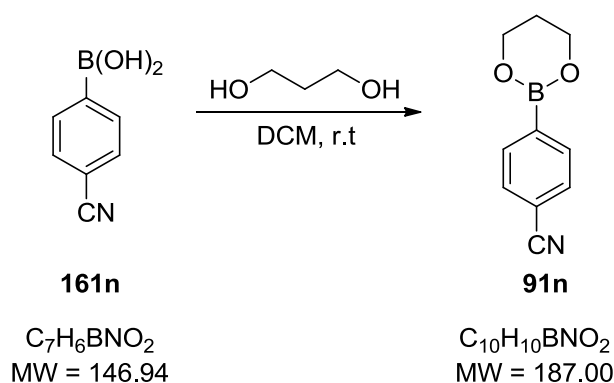
Mp: 136-137 °C

TLC: 0.4 (PE/EtOAc 5:1)

^1H NMR (CDCl_3 , 200MHz): δ = 2.09 (quint, J = 5.5 Hz, 2H, H4), 4.19 (t, J = 5.5 Hz, 4H, H3), 7.90 (d, J = 8.6 Hz, 2H, H3'), 8.15 (d, J = 8.6 Hz, 2H, H2').

^{13}C NMR (CDCl_3 , 50MHz): δ = 27.4 (t, C4), 62.3 (t, C3), 127.4 (d, C3'), 134.7 (d, C2'), 149.6 (s, C4').

6.2.14 4-(1,3,2-Dioxaborinan-2-yl)benzotrile (91n)



(4-Cyanophenyl)boronic acid **161n** (735 mg, 5 mmol, 1 equiv) and propane-1,3-diol (418 mg, 5.5 mmol, 1.1 equiv) were reacted in 5 mL of CH_2Cl_2 according to general procedure I.

Yield: 99% (931 mg, 4.95 mmol)

Appearance: yellow solid

Mp: 87-89 °C

TLC: 0.4 (PE/EtOAc 5:1)

¹H NMR (CDCl₃, 200MHz): δ = 2.07 (quint, J = 5.5 Hz, 2H, H4), 4.17 (t, J = 5.5 Hz, 4H, H3), 7.60 (d, J = 8.3 Hz, 2H, H3'), 7.78 (d, J = 8.3 Hz, 2H, H2').

¹³C NMR (CDCl₃, 50MHz): δ = 27.4 (t, C4), 62.3 (t, C3), 113.9 (s, C4'), 119.3 (s, CN), 131.1 (d, C3'), 134.2 (d, C2').

6.3 Synthesis of Precursors

General procedure II:

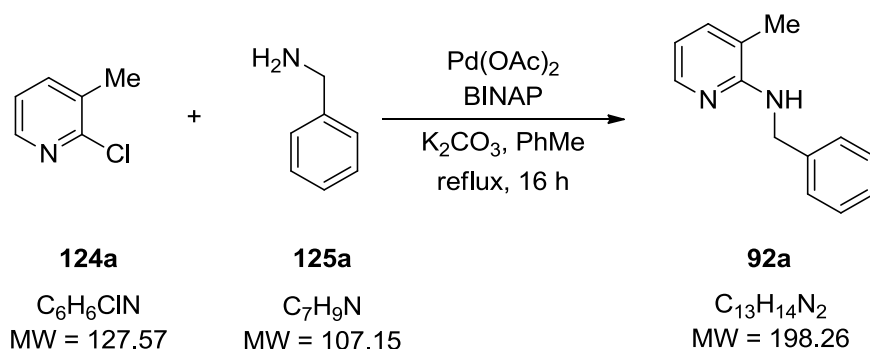
2-Chloro-3-substituted pyridine (1 equiv), amine (1.2 equiv), K₂CO₃ (3.5 equiv) Pd(OAc)₂ (2 mol%), and BINAP (2 mol%) were placed in an oven-dried 6 mL-vial with septum screw cap and a magnetic stirring bar. The vial was evacuated and flushed with argon (three times). After adding dry toluene to the reaction mixture, the vial was closed with a fully covered solid Teflon lined cap. The reaction vial was then heated in a reaction block at 130 °C for 16 h. After cooling to r.t., the solid material was removed by filtration and washed with 10mL of CH₂Cl₂. The combined organic layers were evaporated and the resulting crude product was purified by flash column chromatography (SiO₂ 200:1; PE:EtOAc = 15:1/10:1/5:1). The product was dried in high vacuum. Compounds **92a-n** were prepared according to this procedure.

General procedure III:

2-Bromo-3-substituted pyridine (1 equiv), amine (1.4 equiv), NaOtBu (2 equiv), Pd₂(dba)₂ (2 mol%) and DPPP (2 mol%) were placed in an oven-dried 6 mL-vial with septum screw cap and a magnetic stirring bar. The vial was evacuated and flushed with argon (three times). After adding dry toluene to the reaction mixture, the vial was closed with a fully covered solid Teflon lined cap. The reaction vial was then heated in a reaction block at 75 °C for 16 h. After cooling to r.t., the solid material was removed by filtration and washed with 10mL of CH₂Cl₂. The combined organic layers were evaporated and the resulting crude product was purified by flash column chromatography (SiO₂ 200:1; PE:EtOAc = 15:1/10:1/5:1). The product was dried in high vacuum. Compounds **97a-98b** were prepared according to this procedure.

General procedure IV:

A 3M solution of CH_3MgCl in THF (1.2 equiv) was added dropwise to a solution of *N*-benzyl-pyridin-2-amine (1 equiv) in dry THF (5 mL) at r.t., and the mixture was stirred for 10 min at that temperature. The acyl chloride (3 equiv) was dissolved in 2 mL THF and then added slowly to the solution. Stirring was continued at r.t. for 1 h (or full conversion, monitored by TLC). Then the reaction was quenched with H_2O , and the resulting solution was extracted with Et_2O (3 x 5 mL). The combined organic layers were washed with NaHCO_3 (2x), brine (2x), dried over Na_2SO_4 , filtered, and concentrated in vacuo. The product was dried in high vacuum. Compounds **99a-f** were prepared according to this procedure.

6.3.1 *N*-Benzyl-3-methylpyridin-2-amine (92a)

2-Chloro-3-methylpyridine **124a** (128 mg, 1 mmol, 1 equiv), benzylamine **125a** (128 mg, 1.2 mmol, 1.2 equiv), K_2CO_3 (483 mg, 3.5 mmol, 3.5 equiv), $\text{Pd}(\text{OAc})_2$ (4 mg, 0.02 mmol, 2 mol%), and BINAP (12 mg, 0.02 mmol, 2 mol%) in 2.5 mL of dry toluene were converted according to general procedure II. Analytical data is in accordance with the literature.⁹¹

Yield: 92% (182 mg, 0.92 mmol)

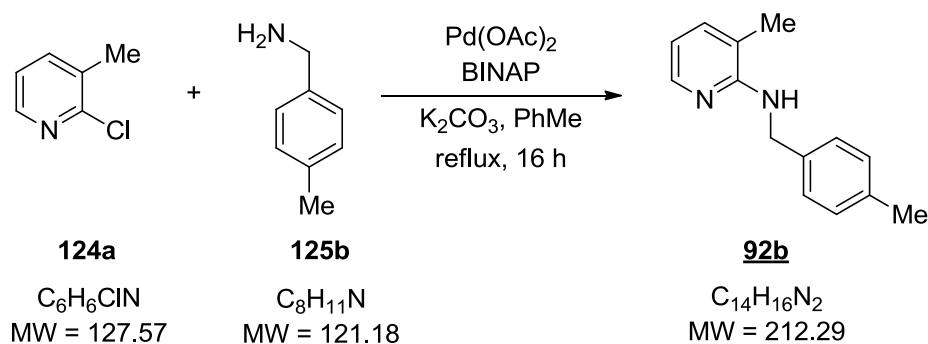
Appearance: colorless solid

Mp: 48-49 °C

TLC: 0.6 (PE/EtOAc 5:1)

^1H NMR (CDCl_3 , 200MHz): δ = 2.09 (s, 3H, CH_3), 4.36 (s, 1H, NH), 4.70 (d, 3J = 5.3 Hz, 2H, CH_2), 6.57 (dd, 3J = 7.1, 3J = 5.1 Hz, 1H, H5), 7.23-7.43 (m, 6H, PhH & H4), 8.06 (dd, 3J = 5.0, 4J = 1.3 Hz, 1H, H6).

^{13}C NMR (CDCl_3 , 50MHz): δ = 17.1 (q, $\underline{\text{C}}\text{H}_3$), 45.9 (t, $\underline{\text{C}}\text{H}_2$), 113.0 (d, C5), 116.6 (s, C3), 127.3 (d, C4'), 128.0 (d, C2'), 128.7 (d, C3'), 136.9 (d, C4), 140.1 (s, C1'), 145.6 (d, C6), 156.8 (s, C2).

6.3.2 3-Methyl-N-(4-methylbenzyl)pyridin-2-amine (**92b**)

2-Chloro-3-methylpyridine **124a** (128 mg, 1 mmol, 1 equiv), 4-methylbenzylamine **125b** (145 mg, 1.2 mmol, 1.2 equiv), K_2CO_3 (483 mg, 3.5 mmol, 3.5 equiv), $Pd(OAc)_2$ (4 mg, 0.02 mmol, 2 mol%), and BINAP (12 mg, 0.02 mmol, 2 mol%) in 2.5 mL of dry toluene were converted according to general procedure II.

Yield: 88% (188 mg, 0.88 mmol)

Appearance: colorless solid

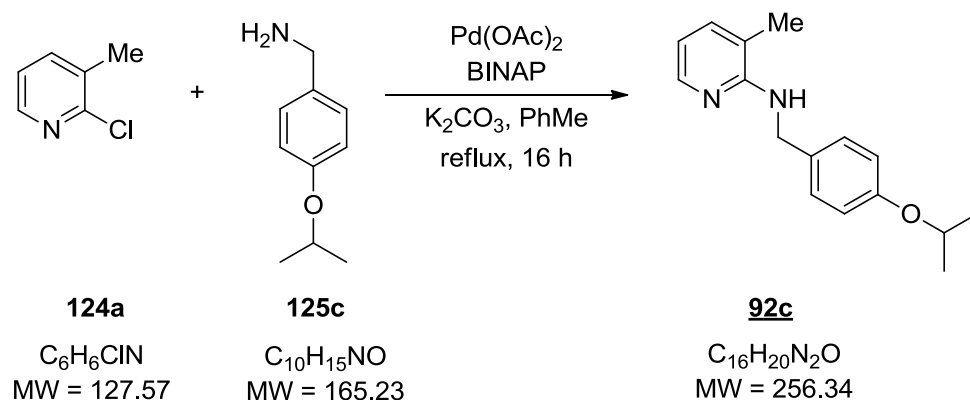
Mp: 46-47 °C

TLC: 0.6 (PE/EtOAc 5:1)

1H NMR (CDCl₃, 200MHz): δ = 2.01 (s, 3H, 3-CH₃), 2.30 (s, 3H, 4'-CH₃), 4.26 (s, 1H, NH), 4.59 (d, 3J = 5.2 Hz, 2H, CH₂), 6.50 (dd, 3J = 7.1, 3J = 5.1 Hz, 1H, H5), 7.08-7.26 (m, 5H, H4 & PhH), 8.00 (dd, 3J = 5.0, 4J = 1.3 Hz, 1H, H6).

^{13}C NMR (CDCl₃, 50MHz): δ = 17.1 (q, 3-CH₃), 21.2 (q, 4'-CH₃), 45.8 (t, CH₂), 112.9 (d, C5), 116.6 (s, C3), 128.0 (d, C2'), 129.4 (d, C3'), 136.8 (s, C1'), 136.9 (s, C4'), 137.0 (d, C4), 145.5 (d, C6), 156.8 (s, C2).

HRMS: calculated for $C_{14}H_{16}N_2$: $[M+H]^+$ 213.1386, found $[M+H]^+$ 213.1380; Δ = 2.82 ppm.

6.3.3 N-(4-Isopropoxybenzyl)-3-methylpyridin-2-amine (**92c**)

2-Chloro-3-methylpyridine **124a** (128 mg, 1 mmol, 1 equiv), **125c** (4-isopropoxyphenyl)methanamine (198 mg, 1.2 mmol, 1.2 equiv), K₂CO₃ (483 mg, 3.5 mmol, 3.5 equiv), Pd(OAc)₂ (4 mg, 0.02 mmol, 2 mol%), and BINAP (12 mg, 0.02 mmol, 2 mol%) in 2.5 mL of dry toluene were converted according to general procedure II.

Yield: 72% (185 mg, 0.72 mmol)

Appearance: colorless oil

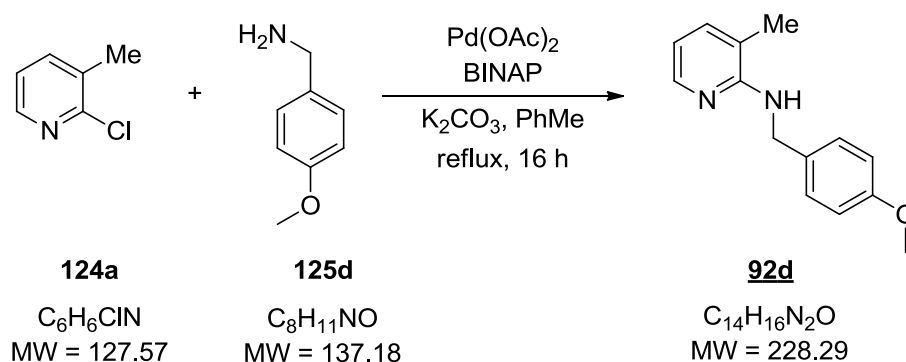
TLC: 0.5 (PE/EtOAc 5:1)

¹H NMR (CDCl₃, 200MHz): δ = 1.33 (d, ³J = 6.0 Hz, 6H, CH(CH₃)₂), 2.06 (s, 3H, CH₃), 4.27 (s, 1H, NH), 4.51 (sep, ³J = 6.0 Hz, 1H, CH), 4.59 (d, ³J = 5.2 Hz, 2H, CH₂), 6.54 (dd, ³J = 7.1, ³J = 5.1 Hz, 1H, H5), 6.86 (d, ³J = 8.6 Hz, 2H, H2'), 7.20-7.32 (m, 3H, H4 & H3'), 8.05 (dd, ³J = 5.1, ⁴J = 1.3 Hz, 1H, H6).

¹³C NMR (CDCl₃, 50MHz): δ = 17.1 (q, CH₃), 21.2 (q, CH(CH₃)₂), 45.5 (t, CH₂), 70.0 (d, CH(CH₃)₂), 112.9 (d, C5), 116.0 (d, C2'), 116.6 (s, C3), 129.3 (d, C3'), 131.9 (s, C4'), 136.9 (d, C4), 145.6 (d, C6), 156.8 (s, C1'), 157.3 (s, C2).

HRMS: calculated for C₁₆H₂₀N₂O⁺: [M+H]⁺ 257.1648, found [M+H]⁺ 257.1642; Δ = 2.33 ppm.

6.3.4 *N*-(4-Methoxybenzyl)-3-methylpyridin-2-amine (**92d**)



2-Chloro-3-methylpyridine **124a** (128 mg, 1 mmol, 1 equiv), 4-methoxybenzylamine **125d** (164 mg, 1.2 mmol, 1.2 equiv), K₂CO₃ (414 mg, 3 mmol, 3 equiv), Pd(OAc)₂ (4 mg, 0.02 mmol, 2 mol%), and BINAP (12 mg, 0.02 mmol, 2 mol%) in 2.5 mL of dry toluene were converted according to general procedure II.

Yield: 80% (183 mg, 0.8 mmol)

Appearance: yellow oil

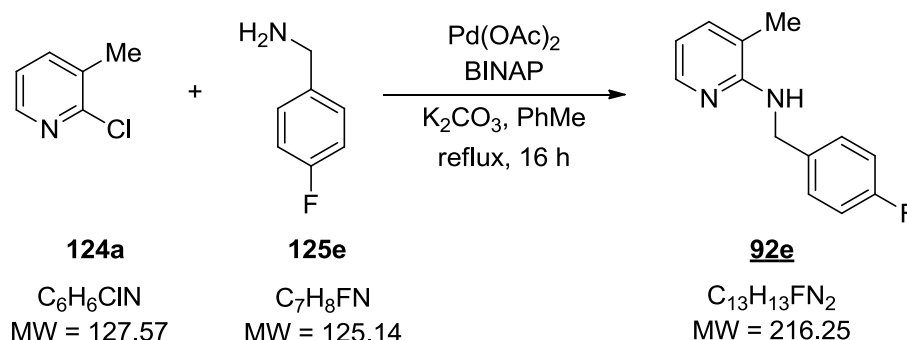
TLC: 0.5 (PE/EtOAc 5:1)

¹H NMR (CDCl₃, 200MHz): δ = 2.07 (s, 3H, CH₃), 3.80 (s, 3H, OCH₃), 4.30 (s, 1H, NH), 4.61 (d, ³J = 5.2 Hz, 2H, CH₂), 6.55 (dd, ³J = 7.1, ³J = 5.1 Hz, 1H, H5), 6.88 (d, ³J = 8.6 Hz, 2H, H2'), 7.21-7.34 (m, 3H, H4 & H3'), 8.06 (dd, ³J = 4.9, ⁴J = 1.0 Hz, 1H, H6).

¹³C NMR (CDCl₃, 50MHz): δ = 17.1 (q, CH₃), 45.4 (t, CH₂), 55.4 (q, OCH₃), 112.9 (d, C5), 114.1 (d, C2'), 116.6 (s, C3), 129.3 (d, C3'), 132.1 (s, C4'), 136.9 (d, C4), 145.5 (d, C6), 156.8 (s, C1'), 158.9 (s, C2).

HRMS: calculated for C₁₄H₁₆N₂O⁺: [M+H]⁺ 229.1335, found [M+H]⁺ 229.1338; Δ = 1.31 ppm.

6.3.5 *N*-(4-Fluorobenzyl)-3-methylpyridin-2-amine (**92e**)



2-Chloro-3-methylpyridine **124a** (128 mg, 1 mmol, 1 equiv), (4-fluorophenyl)methanamine **125e** (150 mg, 1.2 mmol, 1.2 equiv), K₂CO₃ (483 mg, 3.5 mmol, 3.5 equiv), Pd(OAc)₂ (4 mg, 0.02 mmol, 2 mol%), and BINAP (12 mg, 0.02 mmol, 2 mol%) in 2.5 mL of dry toluene were converted according to general procedure II.

Yield: 73% (158 mg, 0.73 mmol)

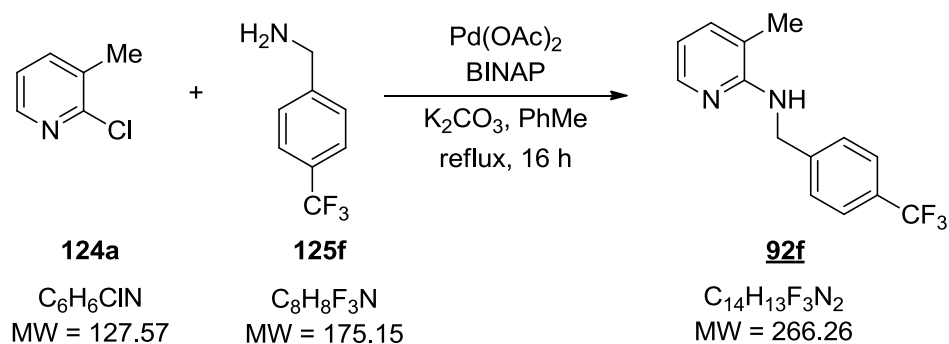
Appearance: colorless oil

TLC: 0.7 (PE/EtOAc 5:1)

¹H NMR (CDCl₃, 200MHz): δ = 2.08 (s, 3H, CH₃), 4.36 (s, 1H, NH), 4.65 (d, ³J = 5.4 Hz, 2H, CH₂), 6.56 (dd, ³J = 7.1, ³J = 5.1 Hz, 1H, H5), 6.96-7.05 (m, 2H, H3'), 7.21-7.37 (m, 3H, H4 & H2'), 8.03 (dd, ³J = 5.0, ⁴J = 1.2 Hz, 1H, H6).

¹³C NMR (CDCl₃, 50MHz): δ = 17.1 (q, CH₃), 45.1 (t, CH₂), 113.2 (d, C5), 115.5 (d, *J*_{CF} = 21.3 Hz, C3'), 116.6 (s, C3), 129.5 (d, *J*_{CF} = 8.0 Hz, C2'), 135.9 (s, *J*_{CF} = 3.1 Hz, C1'), 137.1 (d, C4), 145.6 (d, C6), 156.6 (s, C2), 162.2 (s, *J*_{CF} = 244.9 Hz, C4').

HRMS: calculated for C₁₃H₁₃N₂F⁺: [M+H]⁺ 217.1136, found [M+H]⁺ 217.1125; Δ = 5.07 ppm.

6.3.6 3-Methyl-N-[4-(trifluoromethyl)benzyl]pyridin-2-amine (**92f**)

2-Chloro-3-methylpyridine **124a** (128 mg, 1 mmol, 1 equiv), (4-(trifluoromethyl)phenyl)methanamine **125f** (210 mg, 1.2 mmol, 1.2 equiv), K_2CO_3 (483 mg, 3.5 mmol, 3.5 equiv), Pd(OAc)_2 (4 mg, 0.02 mmol, 2 mol%), and BINAP (12 mg, 0.02 mmol, 2 mol%) in 2.5 mL of dry toluene were converted according to general procedure II.

Yield: 73% (195 mg, 0.73 mmol)

Appearance: colorless solid

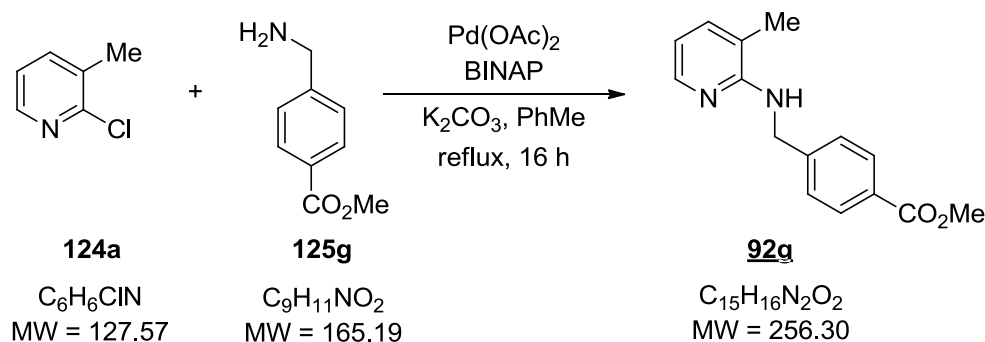
Mp: 54-55 °C

TLC: 0.7 (PE/EtOAc 5:1)

^1H NMR (CDCl_3 , 200MHz): δ = 2.14 (s, 3H, CH_3), 4.50 (s, 1H, NH), 4.78 (d, $^3J = 5.7$ Hz, 2H, CH_2), 6.58 (dd, $^3J = 7.1$, $^3J = 5.1$ Hz, 1H, H5), 7.25-7.29 (m, 1H, H4), 7.53 (d, $^3J = 9.7$ Hz, 4H, H2' & H3'), 8.03 (dd, $^3J = 5.0$, $^4J = 1.2$ Hz, 1H, H6).

^{13}C NMR (CDCl_3 , 50MHz): δ = 17.1 (q, CH_3), 45.2 (t, CH_2), 113.5 (d, C5), 116.7 (s, C3), 124.4 (s, $J_{\text{CF}} = 271.9$ Hz, CF_3), 125.6 (d, $J_{\text{CF}} = 3.9$ Hz, C3'), 127.9 (d, C2'), 129.4 (s, $J_{\text{CF}} = 32.3$ Hz, C4'), 137.2 (d, C4), 144.6 (s, C1'), 145.6 (d, C6), 156.4 (s, C2).

HRMS: calculated for $\text{C}_{14}\text{H}_{13}\text{N}_2\text{F}_3$: $[\text{M}+\text{H}]^+$ 267.1104, found $[\text{M}+\text{H}]^+$ 267.1090; $\Delta = 5.24$ ppm.

6.3.7 Methyl 4-[[3-methylpyridin-2-yl]amino]methyl]benzoate (**92g**)

2-Chloro-3-methylpyridine **124a** (128 mg, 1 mmol, 1 equiv), methyl 4-(aminomethyl)benzoate **125g** (198 mg, 1.2 mmol, 1.2 equiv), K_2CO_3 (414 mg, 3 mmol, 3 equiv), $Pd(OAc)_2$ (4 mg, 0.02 mmol, 2 mol%), and BINAP (12 mg, 0.02 mmol, 2 mol%) in 2.5 mL of dry toluene were converted according to general procedure II.

Yield: 87% (223 mg, 0.87 mmol)

Appearance: colorless solid

Mp: 122-123 °C

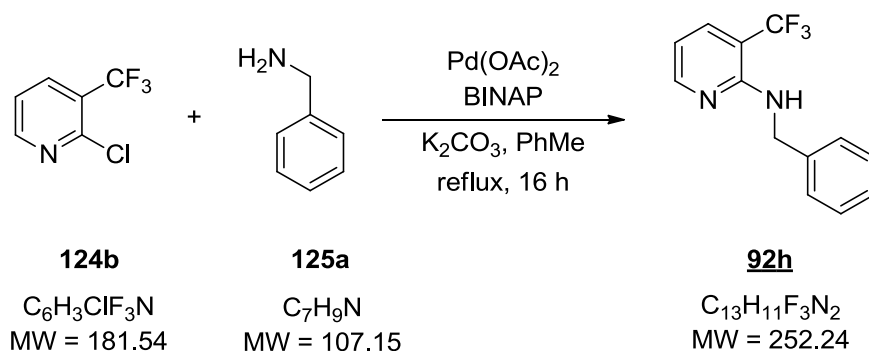
TLC: 0.6 (PE/EtOAc 5:1)

1H NMR (CDCl₃, 200MHz): δ = 2.12 (s, 3H, CH₃), 3.90 (s, 3H, OCH₃), 4.48 (s, 1H, NH), 4.77 (d, 3J = 5.7 Hz, 2H, CH₂), 6.56 (dd, 3J = 7.1, 3J = 5.1 Hz, 1H, H5), 7.23-7.27 (m, 1H, H4), 7.43 (d, 3J = 8.2 Hz, 2H, H3'), 7.97-8.02 (m, 3H, H2' & H6).

^{13}C NMR (CDCl₃, 50MHz): δ = 17.1 (q, CH₃), 45.3 (t, CH₂), 52.2 (q, OCH₃), 113.3 (d, C5), 116.6 (s, C3), 127.5 (d, C3'), 129.0 (s, C1'), 130.0 (d, C2'), 137.1 (d, C4), 145.6 (s, C4'), 145.8 (d, C6), 156.5 (s, C2), 167.1 (s, CO).

HRMS: calculated for C₁₅H₁₆N₂O₂⁺: [M+H]⁺ 257.1285, found [M+H]⁺ 257.1296; Δ = 4.28 ppm.

6.3.8 *N*-Benzyl-3-(trifluoromethyl)pyridin-2-amine (**92h**)



2-Chloro-3-(trifluoromethyl)pyridine **124b** (182 mg, 1 mmol, 1 equiv), benzylamine **125a** (128 mg, 1.2 mmol, 1.2 equiv), K_2CO_3 (483 mg, 3.5 mmol, 3.5 equiv), $Pd(OAc)_2$ (4 mg, 0.02 mmol, 2 mol%), and BINAP (12 mg, 0.02 mmol, 2 mol%) in 2.5 mL of dry toluene were converted according to general procedure II.

Yield: 95% (238 mg, 0.92 mmol)

Appearance: colorless oil

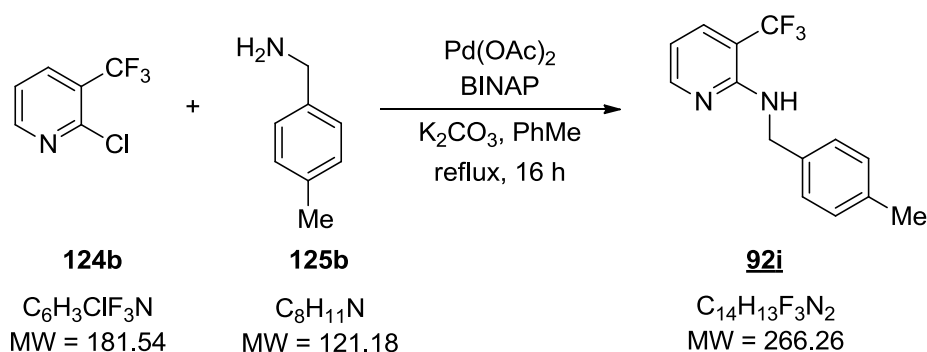
TLC: 0.8 (PE/EtOAc 5:1)

¹H NMR (CDCl₃, 200MHz): δ = 4.66 (d, ³*J* = 5.3 Hz, 2H, CH₂), 5.11 (s, 1H, NH), 6.56 (dd, ³*J* = 7.5, ³*J* = 5.0 Hz, 1H, H5), 7.16-7.28 (m, 5H, PhH), 7.59 (dd, ³*J* = 7.6, ⁴*J* = 0.8 Hz, 1H, H4), 8.20 (d, ³*J* = 4.4 Hz, 1H, H6).

¹³C NMR (CDCl₃, 50MHz): δ = 45.4 (t, CH₂), 108.7 (s, *J*_{CF} = 31.3 Hz, C3), 118.8 (d, C5), 124.6 (s, *J*_{CF} = 271.5 Hz, CF₃) 127.4 (d, C4'), 127.6 (d, C2'), 128.8 (d, C3'), 135.1 (d, *J*_{CF} = 5.1 Hz, C4), 139.2 (s, C1'), 151.9 (d, C6), 154.4 (s, C2).

HRMS: calculated for C₁₃H₁₁F₃N₂⁺: [M+H]⁺ 253.0947, found [M+H]⁺ 253.0955; Δ = 3.16 ppm.

6.3.9 *N*-(4-Methylbenzyl)-3-(trifluoromethyl)pyridin-2-amine (**92i**)



2-Chloro-3-(trifluoromethyl)pyridine **124b** (182 mg, 1 mmol, 1 equiv), methylbenzylamine **125b** (145 mg, 1.2 mmol, 1.2 equiv), K₂CO₃ (483 mg, 3.5 mmol, 3.5 equiv), Pd(OAc)₂ (4 mg, 0.02 mmol, 2 mol%), and BINAP (12 mg, 0.02 mmol, 2 mol%) in 2.5 mL of dry toluene were converted according to general procedure II.

Yield: 98% (260 mg, 0.98 mmol)

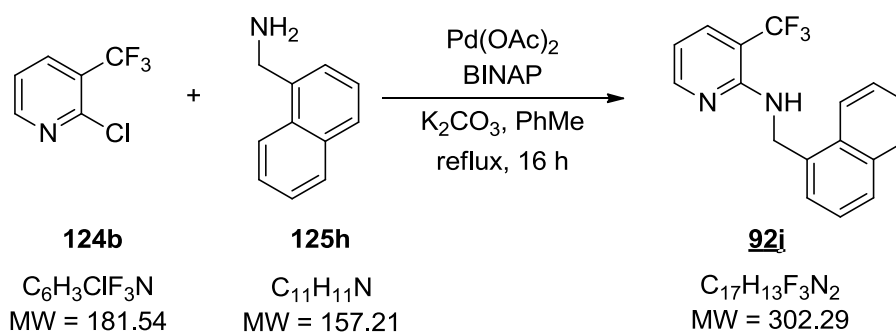
Appearance: colorless oil

TLC: 0.8 (PE/EtOAc 5:1)

¹H NMR (CDCl₃, 200MHz): δ = 2.33 (s, 3H, CH₃), 4.67 (d, ³*J* = 5.2 Hz, 2H, CH₂), 5.13 (s, 1H, NH), 6.62 (dd, ³*J* = 7.5, ³*J* = 5.0 Hz, 1H, H5), 7.12-7.26 (m, 4H, PhH), 7.65 (dd, ³*J* = 7.6, ⁴*J* = 0.8 Hz, 1H, H4), 8.27 (d, ³*J* = 4.4 Hz, 1H, H6).

¹³C NMR (CDCl₃, 50MHz): δ = 21.2 (q, CH₃), 45.2 (t, CH₂), 108.6 (q, *J* = 31.3 Hz, C3), 111.6 (d, C5), 124.6 (q, *J* = 271.5 Hz, CF₃) 127.6 (d, C2'), 129.4 (d, C3'), 135.1 (q, *J* = 5.1 Hz, C4), 136.1 (s, C4'), 137.0 (s, C1'), 151.8 (d, C6), 154.5 (s, C2).

HRMS: calculated for C₁₄H₁₃F₃N₂⁺: [M+H]⁺ 267.1104, found [M+H]⁺ 267.1093; Δ = 4.12 ppm.

6.3.10 *N*-(Naphthalen-2-ylmethyl)-3-(trifluoromethyl)pyridin-2-amine (**92j**)

2-Chloro-3-(trifluoromethyl)pyridine **124b** (182 mg, 1 mmol, 1 equiv), naphthalen-1-ylmethanamine **125h** (188 mg, 1.2 mmol, 1.2 equiv), K_2CO_3 (483 mg, 3.5 mmol, 3.5 equiv), $\text{Pd}(\text{OAc})_2$ (4 mg, 0.02 mmol, 2 mol%), and BINAP (12 mg, 0.02 mmol, 2 mol%) in 2.5 mL of dry toluene were converted according to general procedure II.

Yield: 99% (298 mg, 0.99 mmol)

Appearance: colorless solid

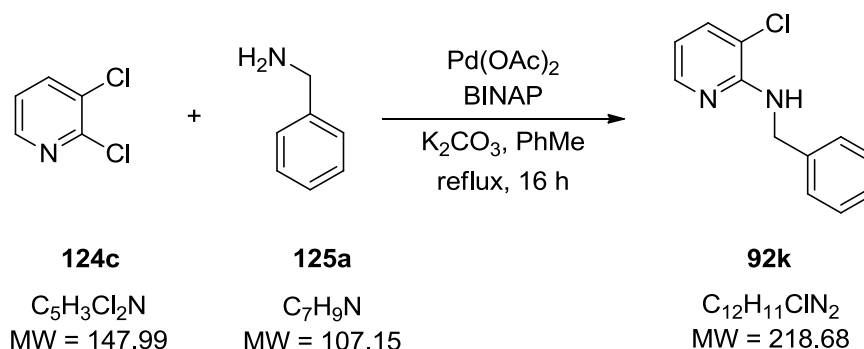
Mp: 70-71 °C

TLC: 0.9 (PE/EtOAc 5:1)

^1H NMR (CDCl_3 , 200MHz): δ = 5.19 (s, 3H, CH_2 & NH), 6.70 (dd, $^3J = 7.5$, $^3J = 5.0$ Hz, 1H, H5), 7.42-7.59 (m, 4H), 7.71 (d, $^3J = 7.5$ Hz, 1H, H4), 7.82-7.94 (m, 2H), 8.06-8.11 (m, 1H, H9), 8.36 (d, $^3J = 4.5$ Hz, 1H, H6).

^{13}C NMR (CDCl_3 , 50MHz): δ = 43.7 (t, CH_2), 108.8 (s, $J_{\text{CF}} = 31.4$ Hz, C3), 111.8 (d, C5), 123.5, 124.6 (s, $J_{\text{CF}} = 273.4$ Hz, CF_3) 125.6, 126.0, 126.5, 128.4, 128.9, 131.7, 134.0, 134.2, 135.2 (d, $J_{\text{CF}} = 5.2$ Hz, C4), 151.9 (d, C6), 154.4 (s, C2).

HRMS: calculated for $\text{C}_{17}\text{H}_{13}\text{F}_3\text{N}_2$: $[\text{M}+\text{H}]^+$ 303.1104, found $[\text{M}+\text{H}]^+$ 303.1105; $\Delta = 0.33$ ppm.

6.3.11 *N*-Benzyl-3-chloropyridin-2-amine (**92k**)

2,3-Dichloropyridine **124c** (148 mg, 1 mmol, 1 equiv), benzylamine **125a** (128 mg, 1.2 mmol, 1.2 equiv), K_2CO_3 (483 mg, 3.5 mmol, 3.5 equiv), $Pd(OAc)_2$ (4 mg, 0.02 mmol, 2 mol%), and BINAP (12 mg, 0.02 mmol, 2 mol%) in 2.5 mL of dry toluene were converted according to general procedure II. Analytical data is in accordance with the literature.¹⁰⁸

Yield: 91% (200 mg, 0.91 mmol)

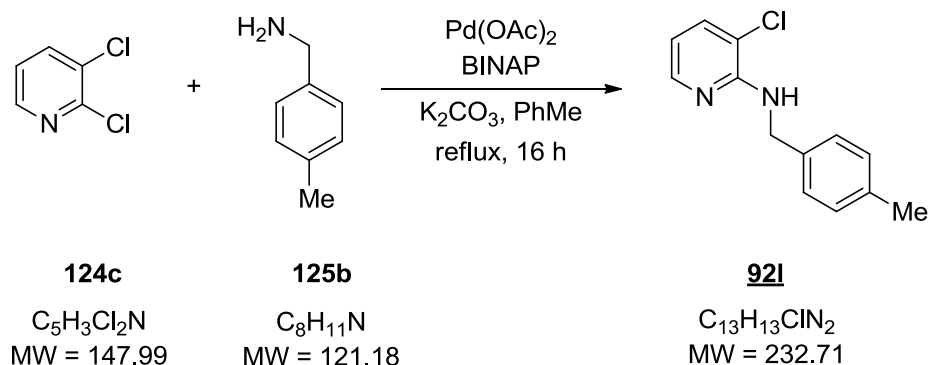
Appearance: yellow oil

TLC: 0.7 (PE/EtOAc 5:1)

1H NMR (CDCl₃, 200MHz): δ = 4.68 (d, 3J = 5.6 Hz, 2H, CH₂), 5.26 (s, 1H, NH), 6.54 (dd, 3J = 7.6, 3J = 4.9 Hz, 1H, H5), 7.23-7.39 (m, 5H, PhH), 7.45 (dd, 3J = 7.6, 4J = 1.6 Hz, 1H, H4) 8.04 (dd, 3J = 4.9, 4J = 1.6 Hz, 1H, H6).

^{13}C NMR (CDCl₃, 50MHz): δ = 45.6 (t, CH₂), 113.2 (d, C5), 115.4 (s, C3), 127.4 (d, C4'), 127.8 (d, C2'), 128.7 (d, C3'), 136.2 (d, C4), 139.4 (s, C1'), 146.2 (d, C6), 154.0 (s, C2).

6.3.12 3-Chloro-N-(4-methylbenzyl)pyridin-2-amine (**92l**)



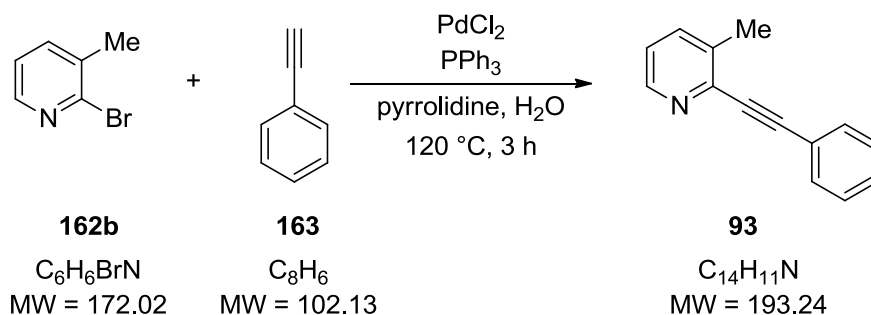
2,3-Dichloropyridine **124c** (148 mg, 1 mmol, 1 equiv), 4-methylbenzylamine **125b** (145 mg, 1.2 mmol, 1.2 equiv), K_2CO_3 (483 mg, 3.5 mmol, 3.5 equiv), $Pd(OAc)_2$ (4 mg, 0.02 mmol, 2 mol%), and BINAP (12 mg, 0.02 mmol, 2 mol%) in 2.5 mL of dry toluene were converted according to general procedure II.

Yield: 86% (201 mg, 0.86 mmol)

Appearance: colorless oil

TLC: 0.7 (PE/EtOAc 5:1)

1H NMR (CDCl₃, 200MHz): δ = 2.35 (s, 3H, CH₃), 4.65 (d, 3J = 5.4 Hz, 2H, CH₂), 5.23 (s, 1H, NH), 6.54 (dd, 3J = 7.6, 4.9 Hz, 1H, H5), 7.14-.30 (m, 4H, PhH), 7.45 (dd, 3J = 7.6, 4J = 1.6 Hz, 1H, H4), 8.04 (dd, 3J = 4.9, 4J = 1.6 Hz, 1H, H6).

6.3.15 3-Methyl-2-(phenylethynyl)pyridine (**93**)

2-Bromo-3-methylpyridine **162b** (172 mg, 1 mmol, 1 equiv), phenylacetylene **163** (122 mg, 1.2 mmol, 1.2 equiv), pyrrolidine (142 mg, 2 mmol, 2 equiv), PdCl₂ (4 mg, 0.02 mmol, 2 mol%), PPh₃ (10 mg, 0.04 mmol, 4 mol%) in 2 mL degassed water were reacted at 120 °C for 3 h. After cooling to r.t., the reaction mixture was extracted with diethyl ether (4 x 5 mL). The combined organic layers were dried over Na₂SO₄, filtered and concentrated. The residue was purified by flash chromatography (SiO₂ 200:1; PE:EtOAc = 9:1) to give the pure product. Analytical data is in accordance with the literature.¹⁰⁹

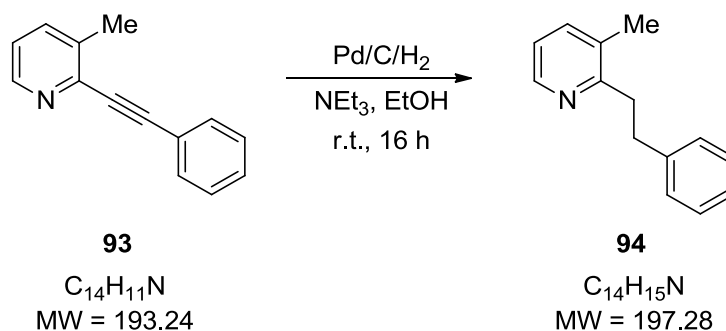
Yield: 72% (139 mg, 0.72 mmol)

Appearance: red oil

TLC: 0.8 (PE/EtOAc 5:1)

¹H NMR (CDCl₃, 200MHz): δ = 2.52 (s, 3H, CH₃), 7.15 (dd, ³J = 7.7, ³J = 4.8 Hz, 1H, H5), 7.33-7.40 (m, H3' & H4'), 7.51-7.63 (m, 3H, H4 & H2'), 8.45 (dd, ³J = 4.7, ⁴J = 1.0 Hz, 1H, H6).

¹³C NMR (CDCl₃, 50MHz): δ = 19.6 (q, C_{CH₃}), 87.6 (s, PhCC), 93.2 (s, PhCC), 122.6 (d, C5), 122.8 (s, C1'), 128.5 (d, C3'), 129.0 (d, C4'), 132.1 (d, C2'), 136.0 (d, C4), 137.1 (s, C3), 143.2 (s, C2), 147.5 (d, C6).

6.3.16 3-Methyl-2-phenethylpyridine (**94**)

3-Methyl-2-(phenylethynyl)pyridine **93** from the above protocol (193 mg, 1 mmol, 1 equiv), triethylamine (253 mg, 2.5 mmol, 2.5 equiv), 10 % palladium on carbon (30 mg), and 30 mL

EtOH were reacted at r.t. under atmospheric H₂ pressure for 16 h. The solvent was removed under reduced pressure and the residue dissolved in 25 mL Et₂O. The solid material was removed by filtration. The organic layer was washed with saturated NaHCO₃ and brine, dried over Na₂SO₄, filtered and concentrated. The product was dried in high vacuum (according to GC & NMR purity > 95%). Analytical data is in accordance with the literature.¹¹⁰

Yield: 99% (196 mg, 0.99 mmol)

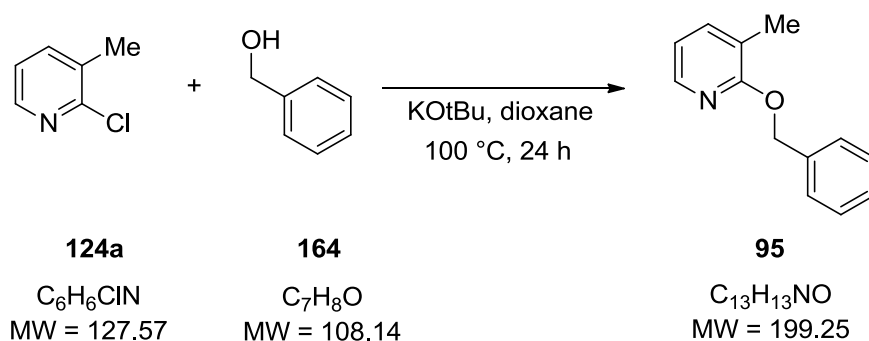
Appearance: pale yellow oil

TLC: 0.7 (PE/EtOAc 5:1)

¹H NMR (CDCl₃, 200MHz): δ = 2.23 (s, 3H, CH₃), 3.02-3.10 (m, 4H), 7.05 (dd, ³J = 7.6, ³J = 4.8 Hz, 1H, H5), 7.19-7.42 (m, 6H), 8.42 (d, ³J = 3.7 Hz, 1H, H6).

¹³C NMR (CDCl₃, 50MHz): δ = 18.8 (q, CH₃), 35.1 (t, PhCH₂), 37.5 (t, CH₂Py), 121.4 (d, C5), 126.0 (d, C4'), 128.5 (d, C2'), 128.6 (d, C3'), 131.3 (s, C3), 137.7 (d, C4), 142.1 (s, C1'), 146.8 (d, C6), 159.6 (s, C2).

6.3.17 2-(Benzyloxy)-3-methylpyridine (95)



2-Chloro-3-methylpyridine **124a** (128 mg, 1 mmol, 1 equiv), phenylmethanol **164** (140 mg, 1.3 mmol, 1.3 equiv), KOtBu (224 mg, 2 mmol, 2 equiv), and 5 mL of dioxane were refluxed for 24 h. After cooling to r.t., 2 mL of H₂O were added to the solution and the aq. phase was extracted with EtOAc (3x5mL). The combined organic layer was washed with saturated NaHCO₃, brine, dried over Na₂SO₄, filtered and concentrated. The residue was purified by flash chromatography (SiO₂ 200:1; PE:EtOAc = 19:1) to give the pure product. Analytical data is in accordance with the literature.¹¹¹

Yield: 70% (140 mg, 0.70 mmol)

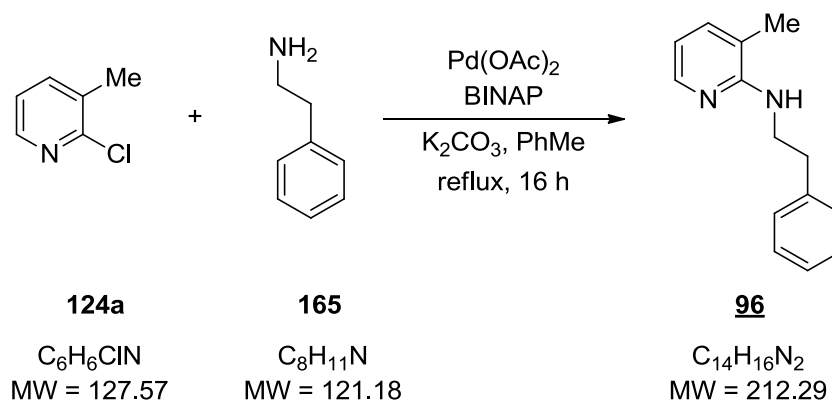
Appearance: colorless oil

TLC: 0.7 (PE/EtOAc 5:1)

^1H NMR (CDCl₃, 200MHz): δ = 2.26 (s, 3H, CH₃), 5.44 (s, 2H, CH₂), 6.82 (dd, 3J = 7.1, 3J = 5.1 Hz, 1H, H5), 7.31-7.52 (m, 6H, PhH & H4'), 8.03 (dd, 3J = 5.0, 4J = 1.3 Hz, 1H, H6).

^{13}C NMR (CDCl₃, 50MHz): δ = 16.0 (q, CH₃), 67.3 (t, CH₂), 116.9 (d, C5), 121.1 (s, C3), 127.6 (d, C2'), 127.7 (d, C4'), 128.5 (d, C3'), 138.0 (s, C1'), 138.7 (d, C4), 144.1 (d, C6), 162.0 (s, C2).

6.3.18 3-Methyl-N-phenethylpyridin-2-amine (**96**)



2-Chloro-3-methylpyridine **124a** (128 mg, 1 mmol, 1 equiv), 2-phenylethanamine **165** (145 mg, 1.2 mmol, 1.2 equiv), K₂CO₃ (483 mg, 3.5 mmol, 3.5 equiv), Pd(OAc)₂ (4 mg, 0.02 mmol, 2 mol%), and BINAP (12 mg, 0.02 mmol, 2 mol%) in 2.5 mL of dry toluene were converted according to the general procedure II.

Yield: 86% (183 mg, 0.86 mmol)

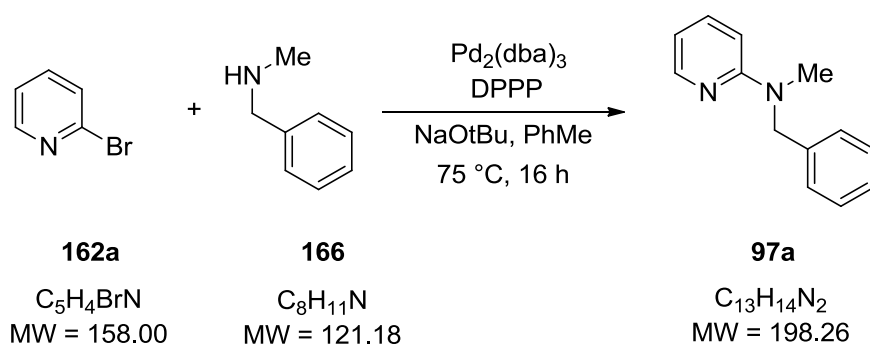
Appearance: pale yellow oil

TLC: 0.6 (PE/EtOAc 5:1)

^1H NMR (CDCl₃, 200MHz): δ = 1.98 (s, 3H, CH₃), 2.98 (t, 3J = 6.7 Hz, 2H, PhCH₂), 3.78 (q, 3J = 6.4 Hz, 2H, CH₂N), 4.13 (s, 1H, NH), 6.54 (dd, 3J = 7.1, 5.1 Hz, 1H, H5), 7.20-7.38 (m, 6H, PhH & H4), 8.07 (dd, 3J = 5.0, 4J = 1.1 Hz, 1H, H6).

^{13}C NMR (CDCl₃, 50MHz): δ = 16.9 (q, CH₃), 35.8 (t, PhCH₂), 42.8 (t, CH₂N), 112.7 (d, C5), 116.7 (s, C3), 126.4 (d, C4'), 128.6 (d, C2'), 129.0 (d, C3'), 136.8 (d, C4), 139.9 (s, C1'), 145.6 (d, C6), 156.8 (s, C2).

HRMS: calculated for C₁₄H₁₆N₂⁺: [M+H]⁺ 213.1386, found [M+H]⁺ 213.1395; Δ = 4.22 ppm.

6.3.19 *N*-Benzyl-*N*-methylpyridin-2-amine (**97a**)

2-Bromopyridine **162a** (158 mg, 1 mmol, 1 equiv), *N*-methyl-1-phenylmethanamine **166** (169 mg, 1.4 mmol, 1.4 equiv), NaOtBu (192 mg, 2 mmol, 2 equiv), Pd₂(dba)₃ (18 mg, 0.02 mmol, 2 mol%), and DPPP (16 mg, 0.04 mmol, 4 mol%) in 4 mL of dry toluene were converted according to general procedure III. Analytical data is in accordance with the literature.¹¹²

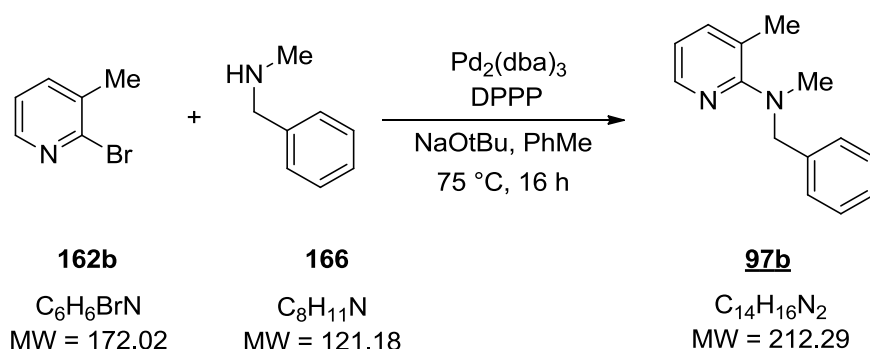
Yield: 94% (186 mg, 0.94 mmol)

Appearance: yellow oil

TLC: 0.5 (PE/EtOAc 9:1)

¹H NMR (CDCl₃, 200MHz): δ = 3.05 (s, 3H, CH₃), 4.79 (s, 2H, CH₂), 6.46-6.57 (m, 2H, H3 & H5), 7.19-7.45 (m, 6H, PhH & H4), 8.16-8.20 (m, 1H, H6).

¹³C NMR (CDCl₃, 50MHz): δ = 36.2 (q, CH₃), 53.3 (t, CH₂), 105.8 (d, C3), 111.9 (d, C5), 127.0 (d, C4'), 127.1 (d, C2'), 128.6 (d, C3'), 137.4 (d, C4), 138.8 (s, C1'), 148.1 (d, C6), 159.0 (s, C2).

6.3.20 *N*-Benzyl-*N*,3-dimethylpyridin-2-amine (**97b**)

2-Bromo-3-methylpyridine **162b** (172 mg, 1 mmol, 1 equiv), *N*-methyl-1-phenylmethanamine **166** (169 mg, 1.4 mmol, 1.4 equiv), NaOtBu (192 mg, 2 mmol, 2 equiv), Pd₂(dba)₃ (18 mg, 0.02 mmol, 2 mol%), and DPPP (16 mg, 0.04 mmol, 4 mol%) in 4 mL of dry toluene were converted according to general procedure III.

Yield: 88% (186 mg, 0.88 mmol)

Appearance: colorless oil

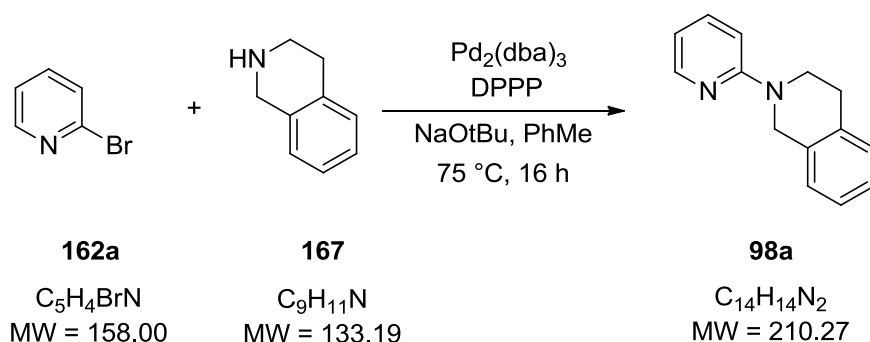
TLC: 0.5 (PE/EtOAc 9:1)

¹H NMR (CDCl₃, 200MHz): δ = 2.32 (s, 3H, CH₃), 2.75 (s, 3H, NCH₃), 4.33 (s, 2H, CH₂), 6.82 (dd, ³J = 7.3, ³J = 4.9 Hz, 1H, H5), 7.24-7.40 (m, 6H, PhH & H4), 8.16 (dd, ³J = 4.8, ⁴J = 1.5 Hz, 1H, H6).

¹³C NMR (CDCl₃, 50MHz): δ = 19.0 (q, CH₃), 39.1 (q, NCH₃), 57.8 (t, CH₂), 117.4 (d, C5), 124.5 (s, C3), 126.9 (d, C4'), 128.0 (d, C2'), 128.4 (d, C3'), 139.3 (d, C4), 139.5 (s, C1'), 145.2 (d, C6), 162.6 (s, C2).

HRMS: calculated for C₁₄H₁₆N₂⁺: [M+H]⁺ 213.1386, found [M+H]⁺ 213.1385; Δ = 0.47 ppm.

6.3.21 2-(Pyridin-2-yl)-1,2,3,4-tetrahydroisoquinoline (98a)



2-Bromopyridine **162a** (158 mg, 1 mmol, 1 equiv), 1,2,3,4-tetrahydroisoquinoline **167** (186 mg, 1.4 mmol, 1.4 equiv), NaOtBu (192 mg, 2 mmol, 2 equiv), Pd₂(dba)₃ (18 mg, 0.02 mmol, 2 mol%), and DPPP (16 mg, 0.04 mmol, 4 mol%) in 4 mL of dry toluene were converted according to general procedure III. Analytical data is in accordance with the literature.¹¹³

Yield: 95% (199 mg, 0.95 mmol)

Appearance: colorless solid

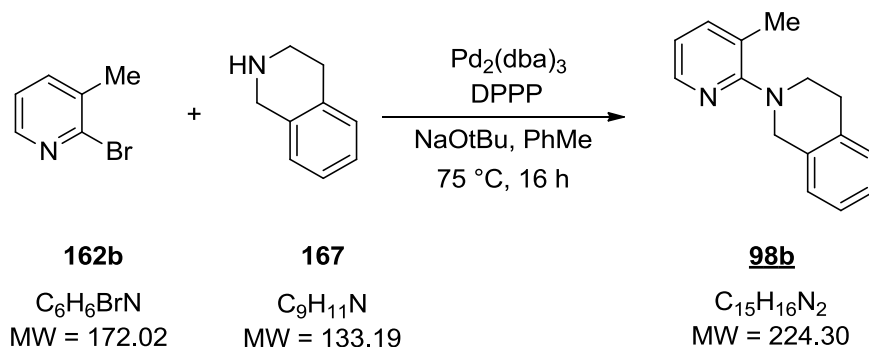
Mp: 47-49 °C

TLC: 0.5 (PE/EtOAc 9:1)

¹H NMR (CDCl₃, 200MHz): δ = 2.98 (t, ³J = 5.9 Hz, 2H, H4'), 3.86 (t, ³J = 5.9 Hz, 2H, H3'), 4.72 (s, 2H, H1'), 6.59-6.71 (m, 2H, H3 & H5), 7.21 (q, ³J = 3.1 Hz, 4H, PhH), 7.46-7.55 (m, 1H, H4), 8.25 (dd, ³J = 4.9, ⁴J = 1.2 Hz, 1H, H6).

^{13}C NMR (CDCl_3 , 50MHz): δ = 29.1 (t, C4'), 42.6 (t, C3'), 47.2 (t, C1'), 106.7 (d, C3), 112.6 (d, C5), 126.3 (d, C8'), 126.5 (d, C7'), 126.7 (d, C6'), 128.5 (d, C9'), 134.5 (s, C5'), 135.5 (s, C10'), 137.5 (d, C4), 148.1 (d, C6), 158.8 (s, C2).

6.3.22 2-(3-Methylpyridin-2-yl)-1,2,3,4-tetrahydroisoquinoline (**98b**)



2-Bromo-3-methylpyridine **162b** (172 mg, 1 mmol, 1 equiv), 1,2,3,4-tetrahydroisoquinoline **167** (186 mg, 1.4 mmol, 1.4 equiv), NaOtBu (192 mg, 2 mmol, 2 equiv), $\text{Pd}_2(\text{dba})_3$ (18 mg, 0.02 mmol, 2 mol%), and DPPP (16 mg, 0.04 mmol, 4 mol%) in 4 mL of dry toluene were converted according to general procedure III.

Yield: 91% (203 mg, 0.91 mmol)

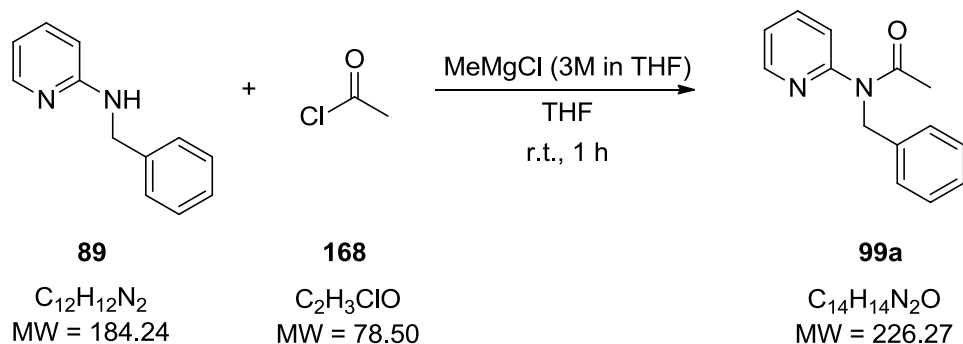
Appearance: yellow oil

TLC: 0.5 (PE/EtOAc 9:1)

^1H NMR (CDCl_3 , 200MHz): δ = 2.35 (s, 3H, CH_3), 3.07 (t, $^3J = 5.8$ Hz, 2H, H4'), 3.41 (t, $^3J = 5.8$ Hz, 2H, H3'), 4.45 (s, 2H, H1'), 6.88 (dd, $^3J = 7.3$, $^3J = 4.9$ Hz, 1H, H5), 7.19 (s, 4H, PhH), 7.42-7.46 (m, 1H, H4), 8.22 (dd, $^3J = 4.8$, $^4J = 1.8$ Hz, 1H, H6).

^{13}C NMR (CDCl_3 , 50MHz): δ = 18.5 (q, CH_3), 29.9 (t, C4'), 48.5 (t, C3'), 51.6 (t, C1'), 117.8 (d, C5), 124.9 (s, C3), 125.9 (d, C8'), 126.2 (d, C7'), 126.9 (d, C6'), 128.9 (d, C9'), 134.6 (s, C5'), 135.4 (s, C10'), 139.4 (d, C4), 145.3 (d, C6), 161.9 (d, C2).

HRMS: calculated for $\text{C}_{15}\text{H}_{16}\text{N}_2^+$: $[\text{M}+\text{H}]^+$ 225.1386, found $[\text{M}+\text{H}]^+$ 225.1378; $\Delta = 3.55$ ppm.

6.3.23 *N*-Benzyl-*N*-(pyridin-2-yl)acetamide (**99a**)

N-Benzylpyridin-2-amine **89** (184 mg, 1 mmol, 1 equiv), acetyl chloride **168** (237 mg, 3 mmol, 3 equiv), and MeMgCl (3M in THF, 0.4 mL, 1.2 mmol, 1.2 equiv) in 7 mL of THF were converted according to general procedure IV. Analytical data is in accordance with the literature.¹¹⁴

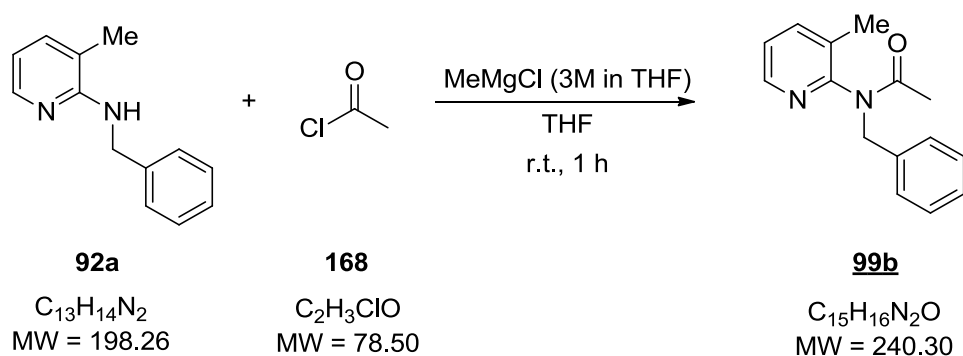
Yield: 94% (213 mg, 0.94 mmol)

Appearance: yellow oil

TLC: 0.3 (PE/EtOAc 1:1)

¹H NMR (CDCl₃, 200MHz): δ = 2.07 (s, 3H, COCH₃), 5.10 (s, 2H, CH₂), 7.08-7.30 (m, 7H), 7.61-7.70 (m, 1H, H₄), 8.49 (d, ³*J* = 4.3 Hz, 1H, H₆).

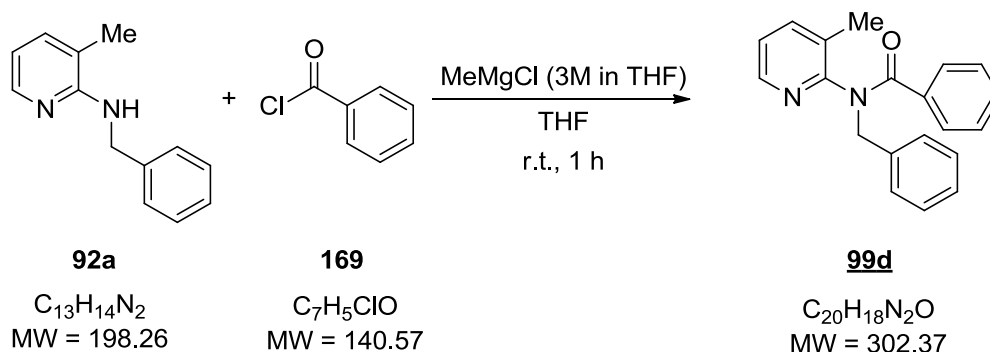
¹³C NMR (CDCl₃, 50MHz): δ = 23.2 (q, COCH₃), 51.1 (t, CH₂), 121.7 (d, C₃), 122.1 (d, C₅), 127.2 (d, C_{4'}), 127.8 (d, C_{2'}), 128.4 (d, C_{3'}), 137.6 (s, C_{1'}), 138.1 (d, C₄), 149.2 (d, C₆), 155.2 (s, C₂), 170.5 (s, CO).

6.3.24 *N*-Benzyl-*N*-(3-methylpyridin-2-yl)acetamide (**99b**)

N-Benzyl-3-methylpyridin-2-amine **92a** (198 mg, 1 mmol, 1 equiv), acetyl chloride **168** (237 mg, 3 mmol, 3 equiv), and MeMgCl (3M in THF, 0.4 mL, 1.2 mmol, 1.2 equiv) in 7 mL of THF were converted according to general procedure IV. The resulting crude product was purified by flash column chromatography (SiO₂ 200:1; PE:EtOAc = 1:1).

HRMS: calculated for $C_{19}H_{16}N_2O$: $[M+H]^+$ 289.1335, found $[M+H]^+$ 289.1327; $\Delta = 2.77$ ppm.

6.3.26 *N*-Benzyl-*N*-(3-methylpyridin-2-yl)benzamide (**99d**)



N-Benzyl-3-methylpyridin-2-amine **92a** (198 mg, 1 mmol, 1 equiv), benzoyl chloride **169** (420 mg, 3 mmol, 3 equiv), and MeMgCl (3M in THF, 0.4 mL, 1.2 mmol, 1.2 equiv) in 7 mL of THF were converted according to general procedure IV. The resulting crude product was purified by flash column chromatography (SiO₂ 200:1; PE:EtOAc = 1:1).

Yield: 83% (251 mg, 0.83 mmol)

Appearance: colorless solid

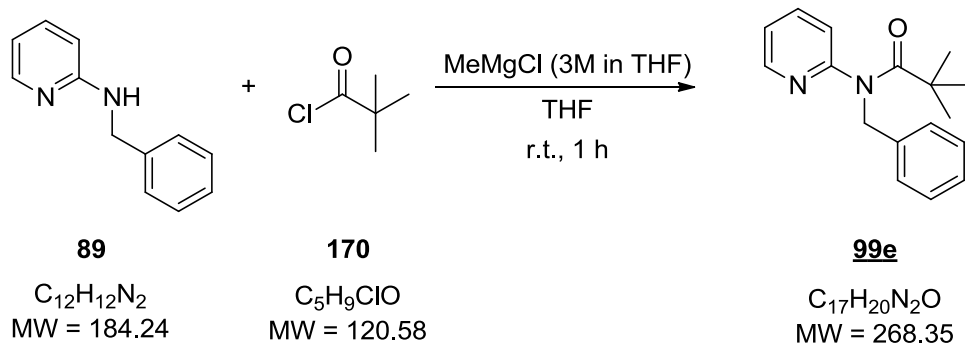
Mp: 114-116 °C

TLC: 0.3 (PE/EtOAc 5:1)

¹H NMR (CDCl₃, 200MHz): $\delta = 1.41$ (s, 3H, CH₃), 4.82 (d, ²*J* = 13.8 Hz, 1H, CH₂), 5.50 (d, ²*J* = 13.8 Hz, 1H, CH₂), 6.93-7.29 (m, 12H), 8.36 (dd, ³*J* = 4.6, ⁴*J* = 1.7 Hz, 1H, H6).

¹³C NMR (CDCl₃, 50MHz): $\delta = 17.1$ (q, CH₃), 52.4 (t, CH₂), 122.8 (d, C5), 127.5 (d, C3), 127.6 (d, C4'), 128.3 (d, C2'), 128.8 (d, C2'), 129.4 (d, C3'), 130.2 (d, C3'), 131.4 (d, C4'), 136.1 (s, C1'), 137.0 (s, C1'), 140.0 (d, C4), 147.1 (d, C6), 154.4 (s, C2), 169.7 (s, CO).

HRMS: calculated for $C_{20}H_{18}N_2O$: $[M+H]^+$ 303.1492, found $[M+H]^+$ 303.1492; $\Delta = 0.00$ ppm.

6.3.27 *N*-Benzyl-*N*-(pyridin-2-yl)pivalamide (**99e**)

N-benzylpyridin-2-amine **89** (184 mg, 1 mmol, 1 equiv), pivaloyl chloride **170** (363 mg, 3 mmol, 3 equiv), and MeMgCl (3M in THF, 0.4 mL, 1.2 mmol, 1.2 equiv) in 7 mL of THF were converted according to general procedure IV.

Yield: 79% (211 mg, 0.79 mmol)

Appearance: colorless solid

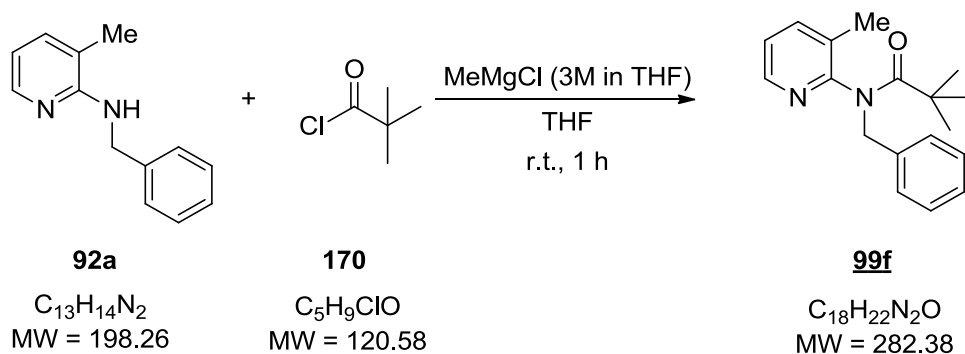
Mp: 69-71 °C

TLC: 0.3 (PE/EtOAc 5:1)

1H NMR (CDCl₃, 200MHz): δ = 1.06 (s, 9H, C(CH₃)₃), 4.95 (s, 2H, CH₂), 6.92 (dd, 3J = 7.9, 4J = 0.8 Hz, 1H, H3), 7.17-7.24 (m, 6H, PhH & H5), 7.57-7.65 (m, 1H, H4), 8.49-8.52 (m, 1H, H6).

^{13}C NMR (CDCl₃, 50MHz): δ = 29.3 (q, C(CH₃)₃), 41.4 (s, C(CH₃)₃), 54.6 (t, CH₂), 122.8 (d, C3), 123.5 (d, C5), 127.2 (d, C4'), 128.4 (d, C2'), 137.9 (d, C3'), 138.0 (s, C1'), 149.2 (d, C4), 156.5 (d, C6), 178.9 (s, C2).

HRMS: calculated for C₁₇H₂₀N₂O+: [M+H]⁺ 269.1648, found [M+H]⁺ 269.1645; Δ = 1.11 ppm.

6.3.28 *N*-Benzyl-*N*-(3-methylpyridin-2-yl)pivalamide (**99f**)

N-Benzyl-3-methylpyridin-2-amine **92a** (198 mg, 1 mmol, 1 equiv), pivaloyl chloride **170** (363 mg, 3 mmol, 3 equiv), and MeMgCl (3M in THF, 0.4 mL, 1.2 mmol, 1.2 equiv) in 7 mL of THF were converted according to general procedure IV. The resulting crude product was purified by flash column chromatography (SiO₂ 200:1; PE:EtOAc = 6:1).

Yield: 78% (221 mg, 0.78 mmol)

Appearance: colorless solid

Mp: 67- 69 °C

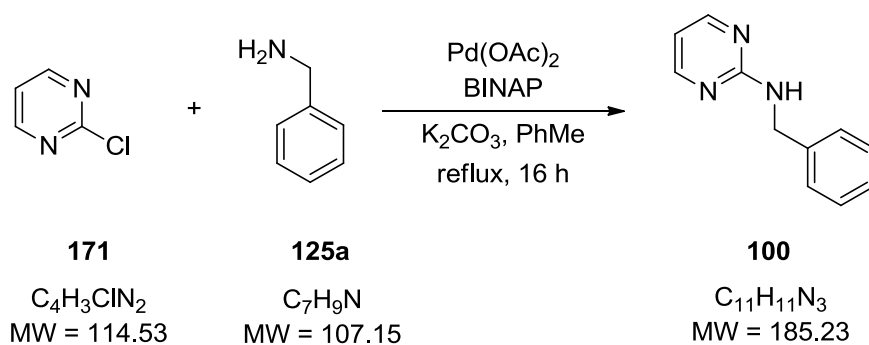
TLC: 0.2 (PE/EtOAc 5:1)

¹H NMR (CDCl₃, 200MHz): δ = 1.03 (s, 9H, C(CH₃)₃), 2.11 (s, 3H, CH₃), 4.61 (s, 1H, CH₂), 4.97 (s, 1H, CH₂), 7.14-7.31 (m, 6H, PhH & H5), 7.54 (d, ³J = 7.4 Hz, 1H, H4), 8.33 (dd, ³J = 4.7, ⁴J = 1.7 Hz, 1H, H6).

¹³C NMR (CDCl₃, 50MHz): δ = 17.8 (q, C(CH₃)), 28.7 (q, C(CH₃)₃), 41.2 (s, C(CH₃)₃), 54.1 (t, CH₂), 123.6 (d, C5), 127.2 (s, C3), 128.3 (d, C4), 128.7 (d, C2), 131.7 (d, C3), 137.5 (s, C1), 140.0 (d, C4), 146.6 (d, C6), 155.4 (s, C2), 178.6 (s, CO).

HRMS: calculated for C₁₈H₂₂N₂O⁺: [M+H]⁺ 283.1805, found [M+H]⁺ 283.1807; Δ = 0.71 ppm.

6.3.29 *N*-Benzylpyrimidin-2-amine (**100**)



2-Chloropyrimidine **171** (115 mg, 1 mmol, 1 equiv), benzylamine **125a** (128 mg, 1.2 mmol, 1.2 equiv), K₂CO₃ (483 mg, 3.5 mmol, 3.5 equiv), Pd(OAc)₂ (4 mg, 0.02 mmol, 2 mol%), and BINAP (12 mg, 0.02 mmol, 2 mol%) in 2.5 mL of dry toluene were converted according to general procedure II. Analytical data is in accordance with the literature.¹¹⁵

Yield: 25% (46 mg, 0.25 mmol)

Appearance: colorless solid

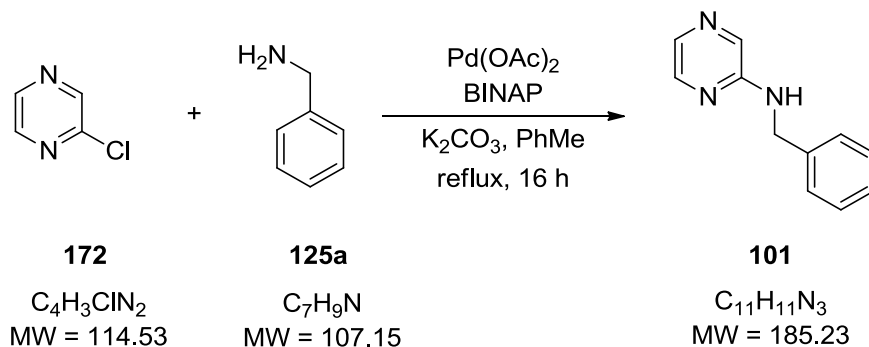
Mp: 74-76 °C (lit. 74-76 °C)

TLC: 0.5 (PE/EtOAc 5:1)

¹H NMR (CDCl₃, 200MHz): δ = 4.56 (d, J = 5.8 Hz, 2H, CH₂), 5.91 (s, 1H, NH), 6.43 (t, 3J = 4.7 Hz, 1H, H5), 7.16-7.31 (m, 5H, PhH), 8.12 (d, 3J = 4.7 Hz, 2H, H4).

¹³C NMR (CDCl₃, 50MHz): δ = 45.6 (t, CH₂), 110.8 (d, C5), 127.3 (d, C4'), 127.7 (d, C2'), 128.7 (d, C3'), 139.2 (s, C1'), 158.1 (d, C4), 162.4 (s, C2).

6.3.30 *N*-Benzylpyrazin-2-amine (101)



2-Chloropyrazine **172** (115 mg, 1 mmol, 1 equiv), benzylamine **125a** (128 mg, 1.2 mmol, 1.2 equiv), K₂CO₃ (483 mg, 3.5 mmol, 3.5 equiv), Pd(OAc)₂ (4 mg, 0.02 mmol, 2 mol%), and BINAP (12 mg, 0.02 mmol, 2 mol%) in 2.5 mL of dry toluene were converted according to general procedure II. Analytical data is in accordance with the literature.¹¹⁶

Yield: 21% (39 mg, 0.21 mmol)

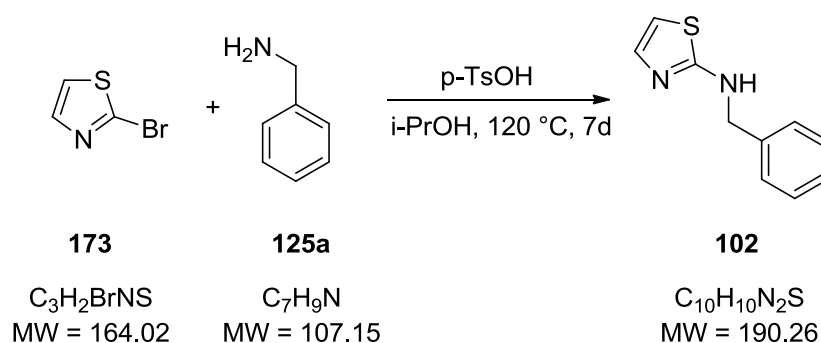
Appearance: colorless solid

Mp: 64-66 °C (lit. 69-71 °C)

TLC: 0.5 (PE/EtOAc 5:1)

¹H NMR (CDCl₃, 200MHz): δ = 4.46 (d, 3J = 5.7 Hz, 2H, CH₂), 5.06 (s, 1H, NH), 7.17-7.27 (m, 5H, PhH), 7.72 (d, 3J = 2.7 Hz, 1H, H6), 7.79 (d, 4J = 1.4 Hz, 1H, H3), 7.89 (dd, 3J = 2.7, 4J = 1.4 Hz, 1H, H5).

¹³C NMR (CDCl₃, 50MHz): δ = 45.6 (t, CH₂), 127.6 (d, C4'), 127.7 (d, C2'), 128.8 (d, C3'), 132.2 (d, C6), 133.1 (d, C3), 138.5 (s, C1'), 142.1 (d, C5), 154.6 (s, C2).

6.3.31 *N*-Benzylthiazol-2-amine (**102**)

2-Bromothiazole **173** (328 mg, 2 mmol, 1.0 equiv), benzylamine **125a** (321 mg, 3 mmol, 1.5 equiv), *p*-toluenesulfonic acid monohydrate (190 mg, 1 mmol, 0.5 equiv) in 4mL *i*-PrOH were reacted at 120 °C for 7 days, cooled to ambient temperature and concentrated *in vacuo*. The crude product was purified by flash column chromatography (SiO₂ 100:1; PE:EtOAc = 4:1). Analytical data is in accordance with the literature.¹¹⁷

Yield: 24% (90 mg, 0.48 mmol)

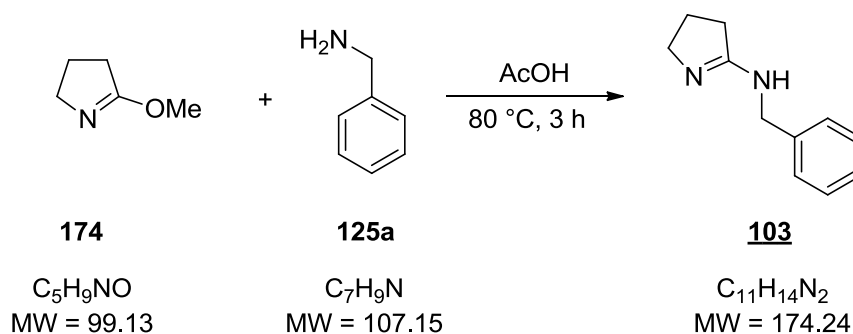
Appearance: yellow solid

Mp: 126-128 °C (lit. 126-127 °C)

TLC: 0.6 (PE/EtOAc 1:1)

¹H NMR (CDCl₃, 200MHz): δ = 4.46 (s, 2H, CH₂), 6.38 (s, 1H, NH), 6.46 (d, ³*J* = 3.6 Hz, 1H, H5), 6.99 (d, ³*J* = 3.6 Hz, 1H, H4), 7.29-7.40 (m, 5H, PhH).

¹³C NMR (CDCl₃, 50MHz): δ = 50.2 (t, C_{CH₂}), 106.6 (d, C5), 127.8 (d, C4'), 127.9 (d, C2'), 128.8 (d, C3'), 137.7 (s, C4), 139.1 (d, C1'), 170.5 (s, C2).

6.3.32 *N*-Benzyl-3,4-dihydro-2H-pyrrol-5-amine (**103**)

Benzylamine **125a** (535 mg, 5 mmol, 1.0 equiv), 2-methoxy-1-pyrroline **174** (545 g, 5.5 mmol, 1.1 equiv) and 6 μ L of acetic acid (2 mol%) were reacted at 80 °C for 3 h, cooled to ambient temperature and then 0.5 mL of 1M NaOH and a few mL of ether were added to the

vial. The layers were separated and the aqueous layer was extracted with Et₂O (2 x 5 mL). The organic layers were combined, dried over K₂CO₃, filtered, and concentrated *in vacuo*. The product was used without further purification (according to GC & NMR purity > 95%).

Yield: 99% (867 mg, 4.95 mmol)

Appearance: colorless solid

TLC: 0.3 (EE/MeOH/NEt₃ 4:1:1)

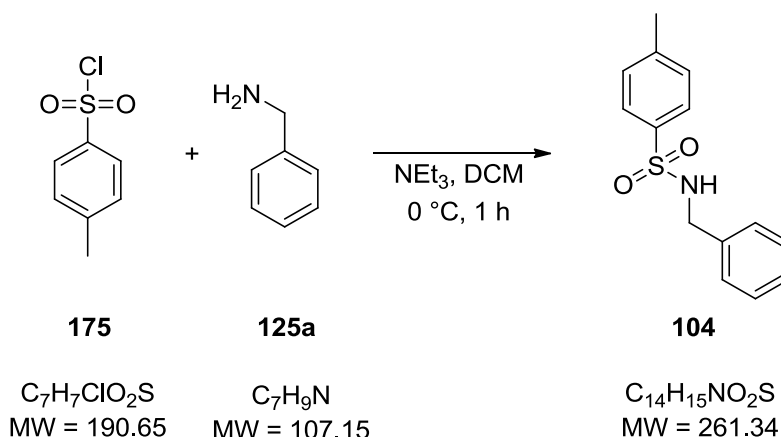
Mp: 76-78 °C

¹H NMR (CDCl₃, 200MHz): δ = 1.86-2.01 (m, 2H, H4), 2.40 (t, ³J = 8.1 Hz, 2H, H3), 3.65 (t, J = 6.8 Hz, 2H, H5), 4.29 (s, 1H, NH), 4.40 (s, 2H, CH₂), 7.22-7.30 (m, 5H, PhH).

¹³C NMR (CDCl₃, 50MHz): δ = 23.6 (t, C4), 32.8 (t, C3), 47.4 (t, CH₂), 77.4 (t, C5), 127.4 (d, C4'), 127.9 (d, C2'), 128.7 (d, C3'), 139.3 (s, C1'), 166.5 (s, C2).

HRMS: calculated for C₁₁H₁₄N₂⁺: [M+H]⁺ 175.1230, found [M+H]⁺ 175.1226; Δ = 2.28 ppm.

6.3.33 *N*-Benzyl-4-methylbenzenesulfonamide (104)



4-Methylbenzene-1-sulfonyl chloride **175** (3.82 g, 20 mmol, 1 equiv) and triethylamine (2.42 g, 24 mmol, 1.2 equiv) were dissolved in 20 mL DCM. The reaction flask was placed in an ice-bath. A solution of benzylamine **125a** (2.16 g, 20 mmol, 1.0 equiv) in 20 mL DCM was added for about 10 minutes. After TLC analysis showed the reaction to be complete, the reaction mixture was washed with 20 mL H₂O and 20 mL brine. The organic layer was dried over Na₂SO₄, filtered, and concentrated *in vacuo*. The crude product was purified by recrystallization from 95% ethanol. Analytical data is in accordance with the literature.¹¹⁸

Yield: 76% (3.95 g, 15.1 mmol)

Appearance: colorless solid

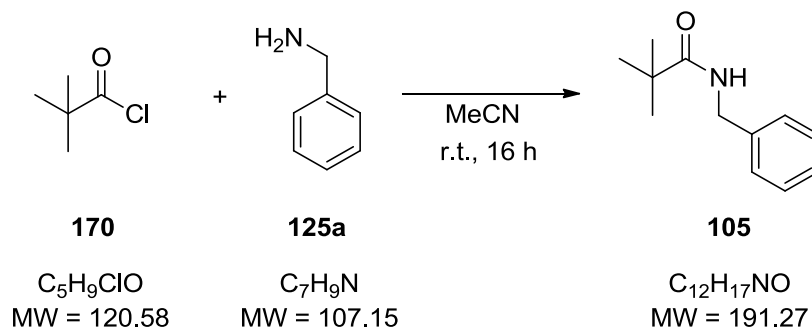
Mp: 111-113 °C (lit. 112-114 °C)

TLC: 0.5 (PE/EtOAc 5:1)

^1H NMR (CDCl₃, 200MHz): δ = 2.44 (s, 3H, CH₃), 4.12 (d, 3J = 4.0 Hz, 2H, CH₂), 4.68 (s, 1H, NH), 7.16-7.33 (m, 7H), 7.76 (d, 3J = 8.2 Hz, 2H, H₂).

^{13}C NMR (CDCl₃, 50MHz): δ = 21.7 (q, C_{CH₃}), 47.4 (t, C_{CH₂}), 127.3 (d, C_{4'}), 128.0 (d, C_{2'}), 128.8 (d, C₂), 129.9 (d, C_{3'}), 136.4 (d, C₃), 137.0 (s, C₄), 143.7 (s, C₁ & C_{1'}).

6.3.34 *N*-Benzylpivalamide (105)



Pivaloyl chloride **170** (605 mg, 5 mmol, 1 equiv) and benzylamine **125a** (1.07 g, 10 mmol, 2.0 equiv) in 5 mL MeCN were reacted at r.t. for 16 h. Subsequently, the solvent was evaporated and the residue was dissolved in 10 mL Et₂O. The organic layer was washed with H₂O (2x) and brine (2x), dried over Na₂SO₄, filtered, and concentrated *in vacuo*. The product was used without further purification (according to GC & NMR purity > 95%). Analytical data is in accordance with the literature.¹¹⁹

Yield: 84% (803 mg, 4.2 mmol)

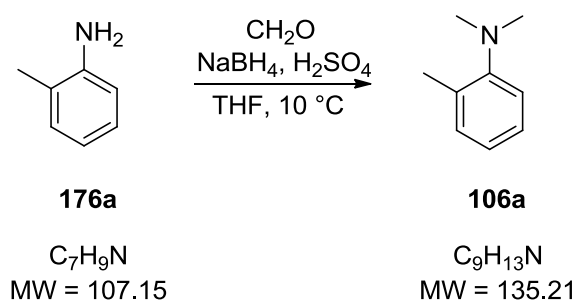
Appearance: colorless solid

Mp: 80-82 °C (lit. 80-81 °C)

TLC: 0.3 (PE/EtOAc 5:1)

^1H NMR (CDCl₃, 200MHz): δ = 1.22 (s, 9H, C(CH₃)₃), 4.42 (d, 3J = 5.6 Hz, 2H, CH₂), 6.00 (s, 1H, NH), 7.24-7.38 (m, 5H, PhH).

^{13}C NMR (CDCl₃, 50MHz): δ = 27.7 (q, C(CH₃)₃), 38.8 (s, C(CH₃)₃), 43.6 (t, C_{CH₂}), 127.4 (d, C₄), 127.6 (d, C₂), 128.7 (d, C₃), 138.8 (d, C₁), 178.4 (s, C_O).

6.3.35 *N,N*-2-Trimethylaniline (106a)

A solution of formaldehyde (37% in H_2O , 8.92 g, 110 mmol, 4.4 equiv) acidified with H_2SO_4 (3M, 7 mL) in 50 mL THF was stirred for 5 min at 10 °C. Subsequently, a solution of o-toluidine **176a** (2.67 g, 25 mmol, 1.0 equiv) and NaBH_4 (5.7 g, 150 mmol, 6 equiv) in 50 mL THF was added dropwise to the reaction mixture. After half of the addition, another 7 mL of H_2SO_4 was added to the suspension, and the dropwise addition was continued. Finally, 50 mL H_2O were added slowly to the solution, followed by addition of NaOH (2M) until the mixture was strongly basic. The mixture was extracted with Et_2O (2x) and the combined organic phases were washed with brine (2x), dried over Na_2SO_4 , filtered, and concentrated *in vacuo*. Subsequent distillation (15 mbar, 64 °C) delivered the pure product. Analytical data is in accordance with the literature.¹²⁰

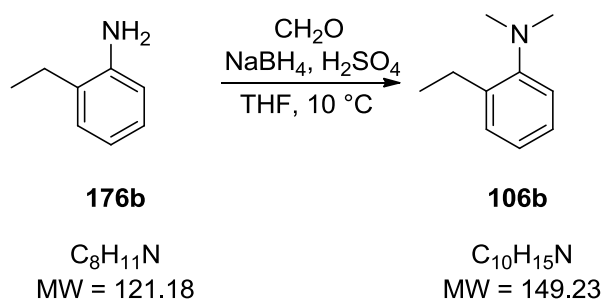
Yield: 89% (3.01 g, 22.2 mmol)

Appearance: colorless oil

TLC: 0.8 (PE/EtOAc 5:1)

^1H NMR (CDCl₃, 200MHz): δ = 2.36 (s, 3H, CH₃), 2.72 (s, 6H, N(CH₃)₂), 7.00-7.20 (m, 4H, PhH).

^{13}C NMR (CDCl₃, 50MHz): δ = 18.5 (q, CH₃), 44.4 (q, N(CH₃)₂), 118.5 (d, C6), 122.7 (d, C4), 126.6 (d, C5), 131.3 (d, C3), 132.2 (s, C2), 152.8 (s, C1).

6.3.36 2-Ethyl-*N,N*-dimethylaniline (106b)

A solution of formaldehyde (37% in H_2O , 8.92 g, 110 mmol, 4.4 equiv) acidified with H_2SO_4 (3M, 7 mL) in 50 mL THF was stirred for 5 min at 10 °C. Subsequently, a solution of 2-

ethylaniline **176b** (3.02 g, 25 mmol, 1.0 equiv) and NaBH₄ (5.7 g, 150 mmol, 6 equiv) in 50 mL THF was added dropwise to the reaction mixture. After half of the addition, another 7 mL of H₂SO₄ was added to the suspension, and the dropwise addition continued. Finally, 50 mL H₂O were added slowly to the solution, followed by addition of NaOH (2M) until the mixture was strongly basic. The mixture was extracted with Et₂O (2x) and the combined organic phases washed with brine (2x), dried over Na₂SO₄, filtered, and concentrated *in vacuo*. The product was dried in high vacuum (according to GC & NMR purity > 95%). Analytical data is in accordance with the literature.¹²¹

Yield: 89% (3.30 g, 22.2 mmol)

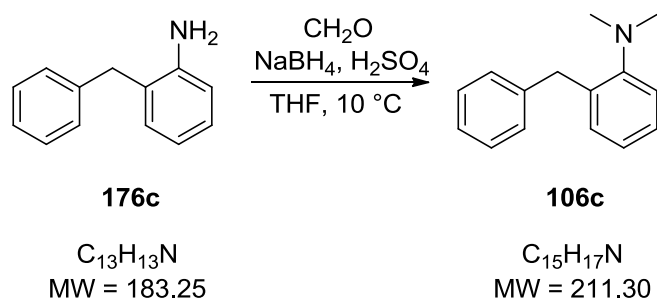
Appearance: red oil

TLC: 0.9 (PE/EtOAc 5:1)

¹H NMR (CDCl₃, 200MHz): δ = 1.18 (t, ³J = 7.5 Hz, 3H, CH₂CH₃), 2.60-2.72 (m, 8H, N(CH₃)₂ & CH₂CH₃), 6.94-7.16 (m, 4H, PhH).

¹³C NMR (CDCl₃, 50MHz): δ = 14.9 (q, CH₂CH₃), 23.6 (t, CH₂CH₃), 45.3 (q, N(CH₃)₂), 119.2 (d, C6), 123.4 (d, C4), 126.4 (d, C5), 129.0 (d, C3), 138.8 (s, C2), 152.6 (s, C1).

6.3.37 2-Benzyl-N,N-dimethylaniline (106c)



A solution of formaldehyde (37% in H₂O, 8.92 g, 110 mmol, 4.4 equiv) acidified with H₂SO₄ (3M, 7 mL) in 50 mL THF was stirred for 5 min at 10 °C. Subsequently, a solution of 2-benzylaniline **176c** (4.57 g, 25 mmol, 1.0 equiv) and NaBH₄ (5.7 g, 150 mmol, 6 equiv) in 50 mL THF was added dropwise to the reaction mixture. After half of the addition, another 7 mL of H₂SO₄ was added to the suspension, and the dropwise addition continued. Finally, 50 mL H₂O were added slowly to the solution, followed by addition of NaOH (2M) until the mixture was strongly basic. The mixture was extracted with Et₂O (2x) and the combined organic phases washed with brine (2x), dried over Na₂SO₄, filtered, and concentrated *in vacuo*. The product was dried in high vacuum (according to GC & NMR purity > 95%). Analytical data is in accordance with the literature.¹²²

Yield: 98% (5.15 g, 24.5 mmol)

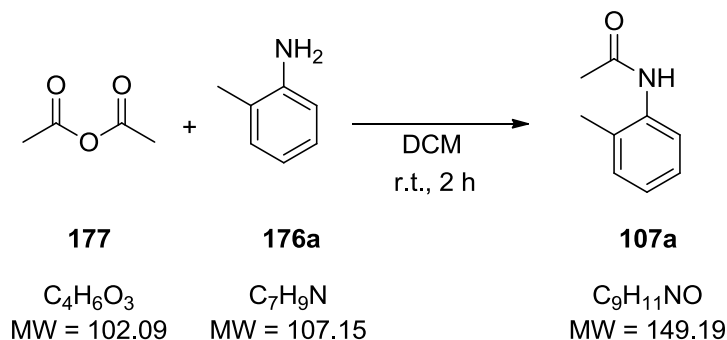
Appearance: yellow oil

TLC: 0.9 (PE/EtOAc 5:1)

¹H NMR (CDCl₃, 200MHz): δ = 2.59 (s, 6H, N(CH₃)₂), 4.02 (s, 2H, CH₂), 6.88-7.22 (m, 9H).

¹³C NMR (CDCl₃, 50MHz): δ = 36.7 (t, CH₂), 45.3 (q, N(CH₃)₂), 119.6 (d, C6), 123.5 (d, C4), 125.9 (d, C4'), 127.0 (d, C3), 128.4 (d, C5), 129.3 (d, C2'), 131.0 (d, C3'), 136.0 (s, C1'), 141.9 (s, C2), 153.0 (s, C1).

6.3.38 *N*-(2-Methylphenyl)acetamide (**107a**)



o-Toluidine **176a** (214 mg, 2 mmol, 1.0 equiv) was stirred in 5 mL DCM at r.t. Then, acetic anhydride **177** (245 mg, 2.4 mmol, 1.2 equiv) was added dropwise to the reaction mixture and stirred at r.t. for 2 h. The mixture was washed with NaHCO₃ (2x) and brine (2x), dried over Na₂SO₄, filtered, and concentrated *in vacuo*. The product was dried in high vacuum (according to GC & NMR purity > 95%). Analytical data is in accordance with the literature.¹²³

Yield: 79% (235 mg, 1.58 mmol)

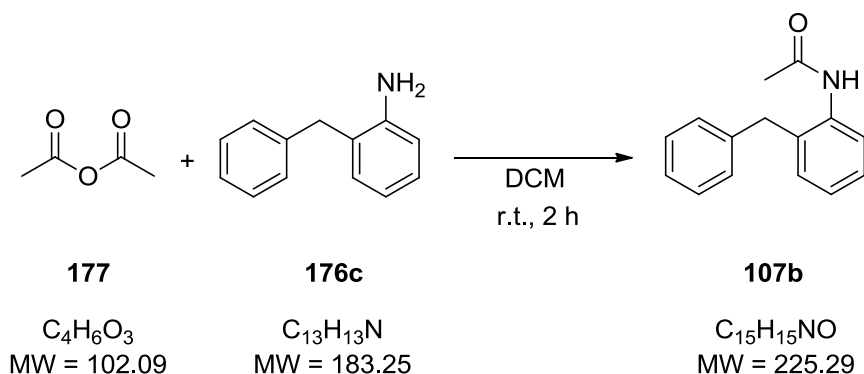
Appearance: colorless solid

Mp: 108-110 °C (lit. 109-110 °C)

TLC: 0.1 (PE/EtOAc 5:1)

¹H NMR (CDCl₃, 200MHz): δ = 2.15 (s, 3H, COCH₃), 2.22 (s, 3H, CH₃), 7.02-7.28 (m, 4H), 7.65 (d, ³J = 7.8 Hz, 1H, H3).

¹³C NMR (CDCl₃, 50MHz): δ = 17.9 (q, CH₃), 24.1 (q, COCH₃), 124.0 (d, C6), 125.6 (d, C5), 126.7 (d, C4), 130.1 (d, C3), 130.6 (s, C2), 135.7 (s, C1), 168.8 (s, CO).

6.3.39 *N*-(2-Benzylphenyl)acetamide (**107b**)

Acetic anhydride **177** (245 mg, 2.4 mmol, 1.2 equiv) was added dropwise to a solution of 2-benzylaniline **176c** (366 mg, 2 mmol, 1.0 equiv) in 5 mL DCM. The reaction mixture was stirred at r.t. for 2 h. The mixture was washed with NaHCO_3 (2x) and brine (2x), dried over Na_2SO_4 , filtered, and concentrated *in vacuo*. The product was dried in high vacuum (according to GC & NMR purity > 95%). Analytical data is in accordance with the literature.¹²⁴

Yield: 88% (398 mg, 1.76 mmol)

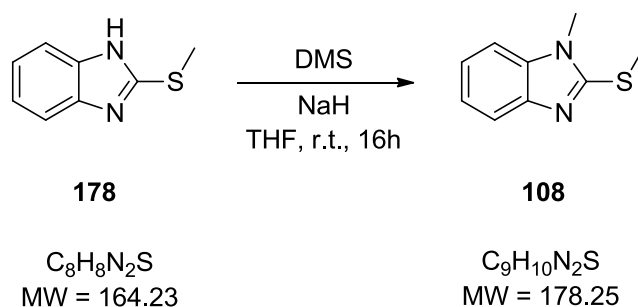
Appearance: colorless solid

Mp: 128-129 °C (lit. 124-125 °C)

TLC: 0.1 (PE/EtOAc 5:1)

^1H NMR (CDCl_3 , 200MHz): δ = 1.98 (s, 3H, CH_3), 3.98 (s, 2H, CH_2), 6.88 (s, 1H, NH), 7.13-7.35 (m, 8H), 7.78 (d, $^3J = 7.7$ Hz, 1H).

^{13}C NMR (CDCl_3 , 50MHz): δ = 24.2 (q, CH_3), 38.7 (t, CH_2), 124.5 (d, C6), 125.6 (d, C3), 126.9 (d, C5), 127.7 (d, C4'), 128.5 (d, C4), 129.1 (d, C2'), 131.0 (s, C3'), 132.0 (s, C1'), 135.9 (s, C1), 139.3 (s, C2), 168.4 (s, CO).

6.3.40 1-Methyl-2-(methylthio)-1H-benzo[d]imidazole (**108**)

2-(Methylthio)-1H-benzo[d]imidazole **178** (820 mg, 5 mmol, 1 equiv) was dissolved in 40 mL dry THF and cooled to 5 °C. Then, NaH (240 mg, 10 mmol, 2 equiv) was added in portions and the solution was stirred for 15 min. DMS (745 mg, 7.5 mmol, 1.5 equiv) was added dropwise over a period of 15 min, then the reaction mixture was warmed to r.t. and stirred for 3 hours. Subsequently, H₂O (40 mL) was added to the solution and the pH of the reaction mixture was adjusted to strong basic with NaOH. The organic phase was separated and the aqueous phase extracted two times with Et₂O (20 mL). The combined organic layers were washed with NaHCO₃ and brine, dried over Na₂SO₄, filtered and concentrated *in vacuo*. The product was dried in high vacuum (according to GC & NMR purity > 95%). Analytical data is in accordance with the literature.¹²⁵

Yield: 90% (801 mg, 4.5 mmol)

Appearance: colorless solid

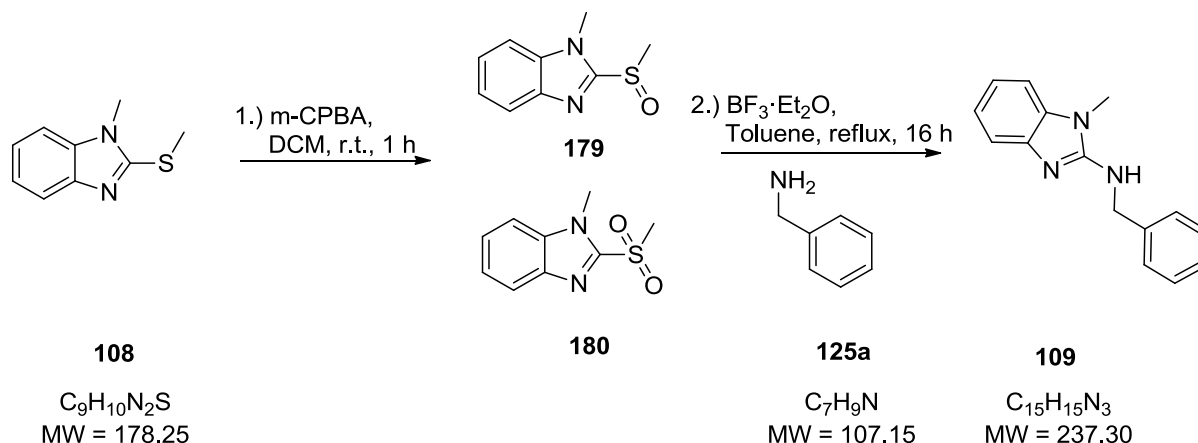
Mp: 50-53 °C (lit. 53-54 °C)

TLC: 0.3 (PE/EtOAc 5:1)

¹H NMR (CDCl₃, 200MHz): δ = 2.80 (s, 3H, SCH₃), 3.66 (s, 3H, NCH₃), 7.17-7.23 (m, 3H), 7.65-7.71 (m, 1H).

¹³C NMR (CDCl₃, 50MHz): δ = 14.7 (q, SCH₃), 30.0 (q, NCH₃), 108.4 (d, C8), 118.2 (d, C5), 121.8 (d), 121.9 (d), 137.0 (s, C9), 143.5 (s, C4), 153.3 (s, C2).

6.3.41 *N*-Benzyl-1-methyl-1H-benzo[d]imidazol-2-amine (109)



1. Step:

1-Methyl-2-(methylthio)-1H-benzo[d]imidazole **108** (356 mg, 2 mmol, 1 equiv) was dissolved in 20 mL of dry DCM and cooled to 5 °C. Then, m-CPBA (692 mg, 4 mmol, 2 equiv) was added slowly to the solution and the reaction mixture was stirred for 1 hour at r. t.. The reaction mixture was added to a NaHCO₃ solution and the organic phase was separated.

The organic layer was washed with water and brine, dried over Na_2SO_4 , filtered and concentrated *in vacuo*. The mixture of product **179** and **180** (400 mg) was recrystallized from EtOAc.

2. Step:

A mixture of **179** and **180** (400 mg), benzylamine **125a** (856 mg, 8 mmol, 4 equiv) and 6 μL of $\text{BF}_3 \cdot \text{Et}_2\text{O}$ in 5 mL dry toluene were reacted at 140°C and for 16 h. Then the vial was cooled to r.t. and the reaction mixture concentrated *in vacuo*. The product was purified by flash column chromatography (SiO_2 200:1; PE/EtOAc 4:1).

Yield: 65% (310 mg, 1.31 mmol)

Appearance: colorless solid

Mp: 164-166 $^\circ\text{C}$ (lit. 168-169 $^\circ\text{C}$)

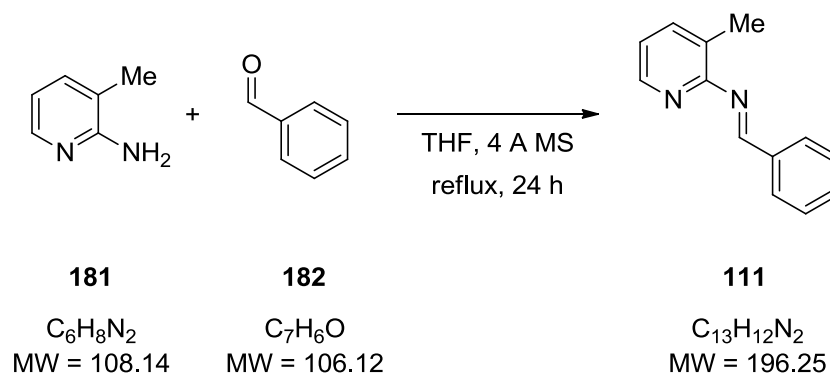
TLC: 0.1 (PE/EtOAc 2:1)

^1H NMR (CDCl_3 , 200MHz): δ = 3.46 (s, 3H, NCH_3), 4.44 (s, 1H, NH), 4.72 (d, 2H, $^3J = 5.5$ Hz, CH_2), 7.06-7.18 (m, 3H), 7.30-7.53 (m, 6H).

^{13}C NMR (CDCl_3 , 50MHz): δ = 28.4 (q, NCH_3), 47.7 (t, CH_2), 107.2 (d, C8), 116.6 (d, C5), 119.8 (d), 121.4 (d), 127.8 (d, C4'), 128.2 (d, C2'), 128.8 (d, C3'), 135.1 (s, C9), 138.7 (s, C1'), 142.2 (s, C4), 154.4 (s, C2).

HRMS: calculated for $\text{C}_{15}\text{H}_{15}\text{N}_3^+$: $[\text{M}+\text{H}]^+$ 238.1344, found $[\text{M}+\text{H}]^+$ 238.1340; $\Delta = 1.68$ ppm.

6.3.42 *N*-Benzylidene-3-methylpyridin-2-amine (111)



A solution of 2-amino-3-picoline **181** (3.24 g, 30 mmol, 1 equiv) in 15 mL of THF was prepared, and benzaldehyde **182** (4.24 g, 40 mmol, 1.3 equiv) was added in the presence of molecular sieve (4 Å). The reaction mixture was refluxed for 24 h and then cooled to r.t. The molecular sieve was removed by filtration and the solvent was evaporated *in vacuo*. Subsequently, the product was dried under high vacuum (according to GC & NMR purity > 95%). Analytical data is in accordance with the literature.¹²⁶

Yield: 50% (2.91 g, 14.8 mmol)

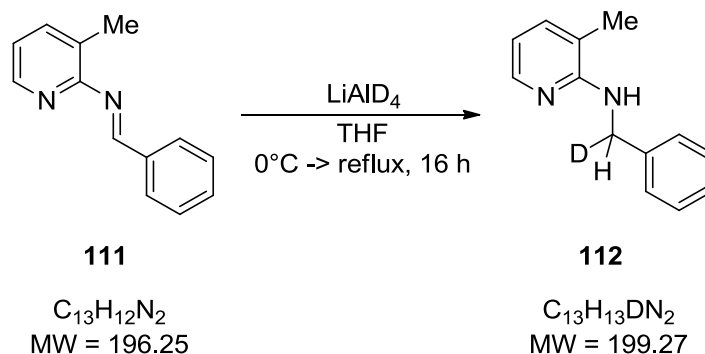
Appearance: yellow oil

TLC: 0.7 (PE/EtOAc 5:1)

^1H NMR (CDCl₃, 200MHz): δ = 2.47 (s, 3H, CH₃), 7.09 (dd, 3J = 7.5, 4.8 Hz, 1H, H5), 7.45-7.57 (m, 4H), 8.02 (dd, 3J = 6.6, 4J = 3.1 Hz, 2H, H2'), 8.31 (dd, 3J = 4.7, 4J = 1.3 Hz, 1H, H6), 9.07 (s, 1H, CH).

^{13}C NMR (CDCl₃, 50MHz): δ = 17.5 (q, CH₃), 122.0 (d, C5), 128.8 (s, C3), 128.9 (d, C3'), 129.5 (d, C2'), 131.8 (d, C4'), 136.4 (s, C1'), 139.0 (d, C4), 146.3 (d, C6), 159.7 (s, PhCHN), 161.8 (s, C2).

6.3.43 *N*-[Deuterio(phenyl)methyl]-3-methylpyridin-2-amine (112)



N-Benzylidene-3-methylpyridin-2-amine **111** (784 mg, 4 mmol, 1 equiv.) was added dropwise to a suspension of LiAlD₄ (168 mg, 4 mmol, 1 equiv.) in 2 mL THF at 0 °C. The suspension was refluxed for 16 h. Afterwards, the mixture was cooled down to 0 °C and 2 mL Et₂O were added slowly to the mixture. Subsequently, 0.5 mL H₂O and 1 mL 2N NaOH were added slowly to the reaction mixture. The mixture was extracted with Et₂O (3x). The organic phases were combined, dried over Na₂SO₄, filtered and evaporated. The product was dried in high vacuum (according to GC & NMR purity > 95%).

Yield: 80% (635 mg, 3.19 mmol)

Appearance: colorless solid

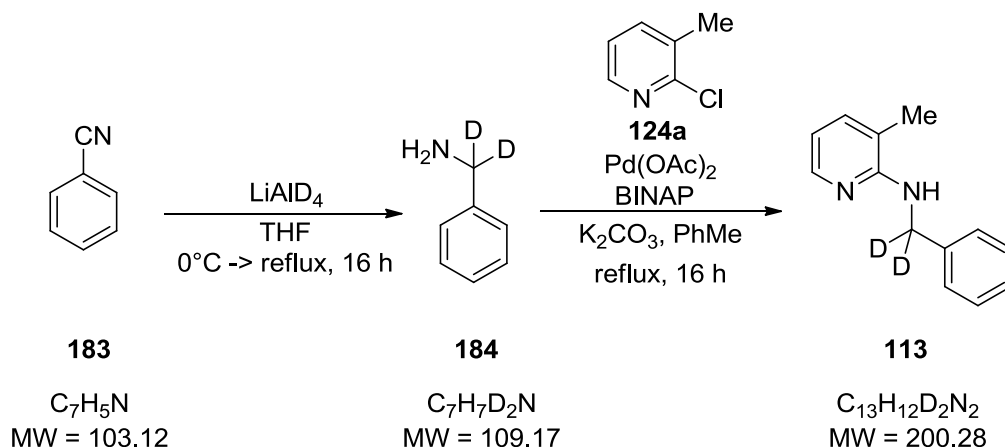
Mp: 48-49 °C

TLC: 0.6 (PE/EtOAc 5:1)

^1H NMR (CDCl₃, 200MHz): δ = 2.07 (s, 3H, CH₃), 4.34 (s, 1H, NH), 4.65-4.67 (m, 1H, CHD), 6.54 (dd, 3J = 7.1, 3J = 5.1 Hz, 1H, H5), 7.21-7.41 (m, 6H, PhH & H4), 8.04 (dd, 3J = 5.0, 4J = 1.3 Hz, 1H, H6).

^{13}C NMR (CDCl_3 , 50MHz): $\delta = 17.1$ (q, $\underline{\text{C}}\text{H}_3$), 45.6 (t, $J = 21.0$ Hz, $\underline{\text{C}}\text{HD}$), 113.0 (d, C5), 116.6 (s, C3), 127.3 (d, C4'), 128.0 (d, C2'), 128.7 (d, C3'), 136.9 (d, C4), 140.1 (s, C1'), 145.6 (d, C6), 156.8 (s, C2).

6.3.44 N-[Dideuterio(phenyl)methyl]-3-methylpyridin-2-amine (113)



1. Step:

Benzonitrile **183** (927 mg, 9 mmol, 1 equiv) was added dropwise to a suspension of LiAlD_4 (378 mg, 9 mmol, 1 equiv.) in 5 mL THF at 0 °C. The suspension was refluxed for 16 h. Afterwards, the mixture was cooled to 0 °C and 5 mL Et_2O were added slowly. Subsequently, 1 mL H_2O and 2 mL 2N NaOH were added slowly to the reaction mixture. The mixture was extracted with Et_2O (3x). The organic phases were combined, dried over Na_2SO_4 , filtered and evaporated. The crude product **184** was used without further purification for the next step.

2. Step:

2-Chloro-3-methylpyridine **124a** (256 mg, 2 mmol, 1 equiv), double deuterated benzylamine **184** (262 mg, 2.4 mmol, 1.2 equiv), K_2CO_3 (966 mg, 7 mmol, 3.5 equiv), $\text{Pd}(\text{OAc})_2$ (9 mg, 0.04 mmol, 2 mol%), and BINAP (25 mg, 0.05 mmol, 2 mol%) in 5 mL of dry toluene were converted according to general procedure II.

Yield: 49% (195 mg, 0.98 mmol)

Appearance: colorless solid

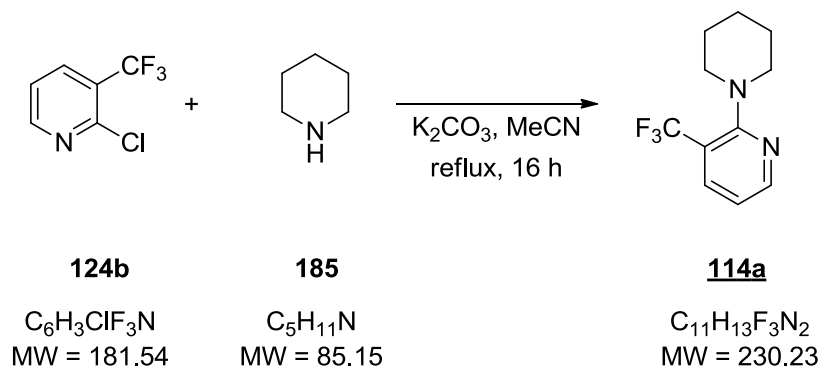
Mp: 48-49 °C

TLC: 0.6 (PE/EtOAc 5:1)

^1H NMR (CDCl_3 , 200MHz): $\delta = 2.09$ (s, 3H, CH_3), 4.36 (s, 1H, NH), 6.57 (dd, $^3J = 7.1$, $^3J = 5.1$ Hz, 1H, H5), 7.23-7.43 (m, 6H, PhH & H4), 8.06 (dd, $^3J = 5.0$, $^4J = 1.3$ Hz, 1H, H6).

^{13}C NMR (CDCl_3 , 50MHz): $\delta = 17.1$ (q, $\underline{\text{C}}\text{H}_3$), 45.4 (m, $\underline{\text{C}}\text{D}_2$), 113.0 (d, C5), 116.6 (s, C3), 127.3 (d, C4 \prime), 128.0 (d, C2 \prime), 128.7 (d, C3 \prime), 136.9 (d, C4), 140.0 (s, C1 \prime), 145.6 (d, C6), 156.8 (s, C2).

6.3.45 2-(Piperidin-1-yl)-3-(trifluoromethyl)pyridine (**114a**)



2-Chloro-3-(trifluoromethyl)pyridine **124b** (910 mg, 5 mmol, 1 equiv.), piperidine **185** (850 mg, 10 mmol, 2 equiv), and K_2CO_3 (1.38 g, 10 mmol, 2 equiv) were refluxed in 5 mL MeCN overnight. After filtration, the solvent was evaporated. The residue was dissolved in 10 mL Et_2O and subsequently washed with NaHCO_3 (2x), water, and brine. The organic layer was dried over Na_2SO_4 , filtered and concentrated *in vacuo*. The crude product was dried in high vacuum (according to GC & NMR purity > 95%).

Yield: 93% (1.07 g, 4.63 mmol)

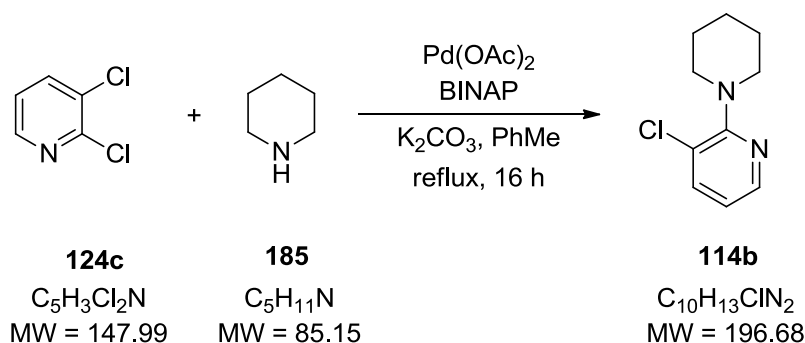
Appearance: yellow oil

TLC: 0.8 (PE/EtOAc 9:1)

^1H NMR (CDCl_3 , 200MHz): $\delta = 1.55$ -1.74 (m, 6H, H3 \prime & H4 \prime), 3.19-3.23 (m, 4H, H2 \prime), 6.91 (dd, $^3J = 7.7$, $^3J = 4.8$ Hz, 1H, H5), 7.81 (dd, $^3J = 7.7$, $^4J = 1.8$ Hz, 1H, H4), 8.39 (dd, $^3J = 4.6$, $^4J = 1.4$ Hz, 1H, H6).

^{13}C NMR (CDCl_3 , 50MHz): $\delta = 24.6$ (t, C4 \prime), 26.1 (t, C3 \prime), 52.1 (t, C2 \prime), 116.3 (d, C5), 117.1 (s, C3), 124.2 (q, $J = 272.5$ Hz, $\underline{\text{C}}\text{F}_3$), 137.3 (q, $J = 5.1$ Hz, C4), 151.0 (d, C6), 160.7 (s C2).

HRMS: calculated for $\text{C}_{11}\text{H}_{13}\text{F}_3\text{N}_2$: $[\text{M}+\text{H}]^+$ 231.1104, found $[\text{M}+\text{H}]^+$ 231.1101; $\Delta = 1.30$ ppm.

6.3.46 3-Chloro-2-(piperidin-1-yl)pyridine (**114b**)

2,3-Dichloropyridine **124c** (740 mg, 5 mmol, 1 equiv), piperidine **185** (850 mg, 10 mmol, 2 equiv), K_2CO_3 (2.41 g, 17.5 mmol, 3.5 equiv), Pd(OAc)_2 (22 mg, 0.1 mmol, 2 mol%), and BINAP (62 mg, 0.1 mmol, 2 mol%) in 15 mL of dry toluene were converted according to general procedure II. Analytical data is in accordance with the literature.¹⁰⁸

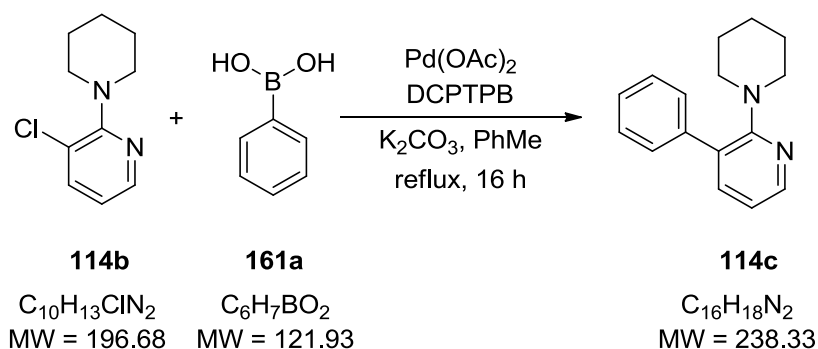
Yield: 57% (561 mg, 2.85 mmol)

Appearance: colorless oil

TLC: 0.7 (PE/EtOAc 9:1)

^1H NMR (CDCl_3 , 200MHz): δ = 1.57-1.77 (m, 6H, H3' & H4'), 3.24-3.29 (m, 4H, H2'), 6.77 (dd, $^3J = 7.7$, $^3J = 4.8$ Hz, 1H, H5), 7.55 (d, $^3J = 7.7$ Hz, 1H, H4), 8.15 (dd, $^3J = 4.7$, $^4J = 0.8$ Hz, 1H, H6).

^{13}C NMR (CDCl_3 , 50MHz): δ = 24.6 (t, C4'), 26.1 (t, C3'), 50.6 (t, C2'), 117.5 (d, C5), 123.0 (s, C3), 138.7 (d, C4), 145.8 (d, C6), 159.6 (s, C2).

6.3.47 3-Phenyl-2-(piperidin-1-yl)pyridine (**114c**)

3-Chloro-2-(piperidin-1-yl)pyridine **114b** from the above protocol (197 mg, 1 mmol, 1 equiv), phenylboronic acid **161a** (366 mg, 3 mmol, 3 equiv), K_2CO_3 (276 mg, 2 mmol, 2 equiv), Pd(OAc)_2 (4 mg, 0.02 mmol, 2 mol%), and DCPTPB (10 mg, 0.02 mmol, 2 mol%) in 2.5 mL of dry toluene were converted according to general procedure II. Analytical data is in accordance with the literature.¹⁰⁸

Yield: 55% (131 mg, 0.55 mmol)

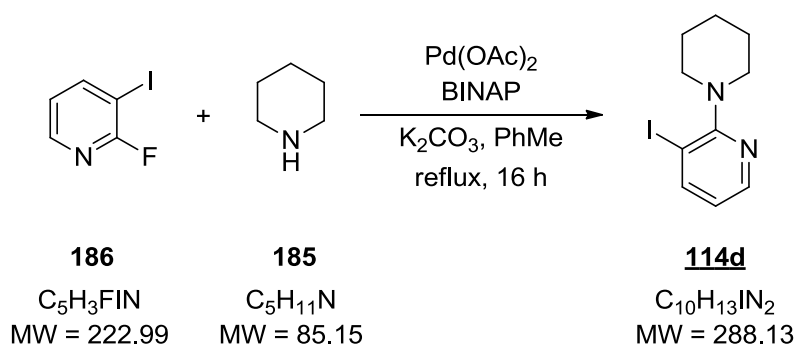
Appearance: colorless oil

TLC: 0.7 (PE/EtOAc 9:1)

¹H NMR (CDCl₃, 200MHz): δ = 1.47 (s, 6H, H3' & H4'), 3.04-3.07 (m, 4H, H2'), 6.86 (dd, ³J = 7.4, ³J = 4.9 Hz, 1H, H5), 7.26-7.45 (m, 4H, PhH), 7.56-7.62 (m, 2H, PhH & H4), 8.21 (dd, ³J = 4.9, ⁴J = 1.9 Hz, 1H, H6).

¹³C NMR (CDCl₃, 50MHz): δ = 24.6 (t, C4'), 25.8 (t, C3'), 50.3 (t, C2'), 116.5 (d, C5), 127.2 (s, C3), 127.3 (d, C2'), 127.9 (d, C4'), 128.7 (d, C3'), 139.5 (d, C4), 140.7 (s, C1'), 146.5 (d, C6), 160.8 (s, C2).

6.3.48 3-Iodo-2-(piperidin-1-yl)pyridine (**114d**)



2-Fluoro-3-iodopyridine **186** (239 mg, 1 mmol, 1 equiv), piperidine **185** (170 mg, 2 mmol, 2 equiv), K₂CO₃ (483 mg, 3.5 mmol, 3.5 equiv), Pd(OAc)₂ (4 mg, 0.02 mmol, 2 mol%), and BINAP (12 mg, 0.02 mmol, 2 mol%) in 2.5 mL of dry toluene. The reaction was carried out according to the general procedure II.

Yield: 81% (233 mg, 0.81 mmol)

Appearance: yellow oil

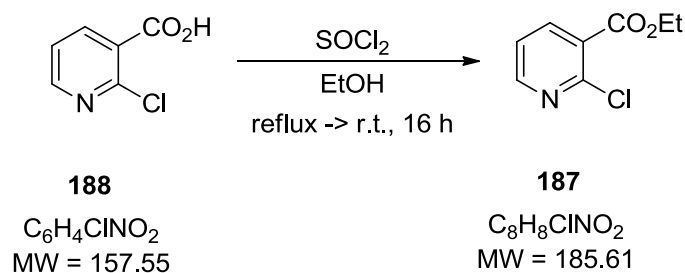
TLC: 0.7 (PE/EtOAc 5:1)

¹H NMR (CDCl₃, 200MHz): δ = 1.56-1.79 (m, 6H, H3' & H4'), 3.15-3.20 (m, 4H, H2'), 6.59 (dd, ³J = 7.6, 4.7 Hz, 1H, H5), 8.03 (dd, ³J = 7.7, ⁴J = 1.7 Hz, 1H, H4), 8.24 (dd, ³J = 4.7, ⁴J = 1.6 Hz, 1H, H6).

¹³C NMR (CDCl₃, 50MHz): δ = 24.4 (t, C4'), 26.0 (t, C3'), 51.9 (t, C2'), 89.0 (s, C3), 118.8 (d, C5), 147.3 (d, C4), 148.9 (d, C6), 163.4 (s, C2).

HRMS: calculated for C₁₀H₁₃N₂I⁺: [M+H]⁺ 289.0196, found [M+H]⁺ 289.0192; Δ = 1.38 ppm.

6.3.49 Ethyl 2-chloronicotinate (187)



2-Chloronicotinic acid **188** (1.58 g, 10 mmol, 1 equiv) was refluxed in 25 mL of thionyl chloride for 2 h. After cooling down to r.t., the thionyl chloride was distilled and 40 mL of EtOH were added to the residue. The solution was stirred overnight at r.t.. Subsequently, the solvent was evaporated and a solution of 5% K_2CO_3 (20 mL) was added to the residue. The aqueous phase was extracted with DCM (3x) and the combined organic layers washed with brine (2x), dried over Na_2SO_4 , filtered and evaporated. The product was dried under high vacuum (according to GC & NMR purity > 95%). Analytical data is in accordance with the literature.¹²⁷

Yield: 96% (1.78 g, 9.6 mmol)

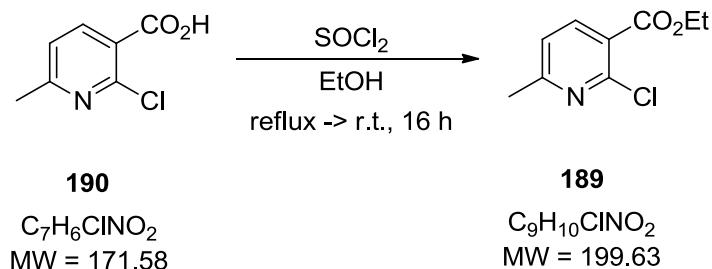
Appearance: yellow oil

TLC: 0.5 (PE/EtOAc 9:1)

^1H NMR (CDCl_3 , 200MHz): δ = 1.39 (t, 3J = 7.1 Hz, 3H, CH_3), 4.40 (q, 3J = 7.1 Hz, 2H, CH_2), 7.31 (dd, 3J = 7.7, 3J = 4.8 Hz, 1H, H5), 8.13 (dd, 3J = 7.7, 4J = 1.9 Hz, 1H, H4), 8.48 (dd, 3J = 4.8, 4J = 1.9 Hz, 1H, H6).

^{13}C NMR (CDCl_3 , 50MHz): δ = 14.2 (q, CH_3), 62.2 (t, CH_2), 122.2 (d, C4), 127.3 (s, C3), 140.3 (d, C5), 150.0 (s, C2), 151.9 (d, C6), 164.6 (s, CO).

6.3.50 Ethyl 2-chloro-6-methylnicotinate (189)



2-Chloro-6-methylnicotinic acid **190** (1.72 g, 10 mmol, 1 equiv) was refluxed in 25 mL of thionyl chloride for 2 h. After cooling down to r.t., the thionyl chloride was distilled off and 40 mL of EtOH were added to the residue. The solution was stirred overnight at r.t.. Subsequently, the solvent was evaporated and a solution of 5% K_2CO_3 (20 mL) was added to

the residue. The aqueous phase was extracted with DCM (3x) and the combined organic layers washed with brine (2x), dried over Na₂SO₄, filtered and evaporated. The product was dried in high vacuum (according to GC & NMR purity > 95%). Analytical data is in accordance with the literature.¹²⁸

Yield: 99% (1.99 g, 9.95 mmol)

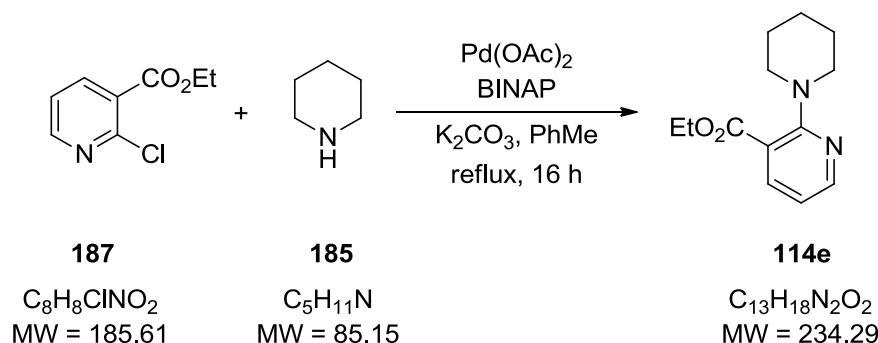
Appearance: yellow oil

TLC: 0.5 (PE/EtOAc 9:1)

¹H NMR (CDCl₃, 200MHz): δ = 1.38 (t, ³J = 7.1 Hz, 3H, CH₂CH₃), 2.56 (s, 3H, CH₃), 4.38 (q, ³J = 7.1 Hz, 2H, CH₂CH₃), 7.14 (d, ³J = 7.8 Hz, 1H, H5), 8.05 (d, ³J = 7.8 Hz, 1H, H4).

¹³C NMR (CDCl₃, 50MHz): δ = 14.3 (q, CH₂CH₃), 24.4 (q, CH₃), 62.0 (t, CH₂CH₃), 121.8 (d, C5), 124.0 (s, C3), 140.7 (d, C4), 149.4 (s, C2), 162.4 (s, CO), 164.7 (s, C6).

6.3.51 Ethyl 2-(piperidin-1-yl)nicotinate (114e)



Ethyl 2-chloronicotinate **187** (930 mg, 5 mmol, 1 equiv), piperidine **185** (1.06 g, 12.5 mmol, 2.5 equiv), K₂CO₃ (2.41 g, 17.5 mmol, 3.5 equiv), Pd(OAc)₂ (22 mg, 0.1 mmol, 2 mol%), and BINAP (62 mg, 0.1 mmol, 2 mol%) in 15 mL of dry toluene were converted according to general procedure II. Analytical data is in accordance with the literature.¹²⁹

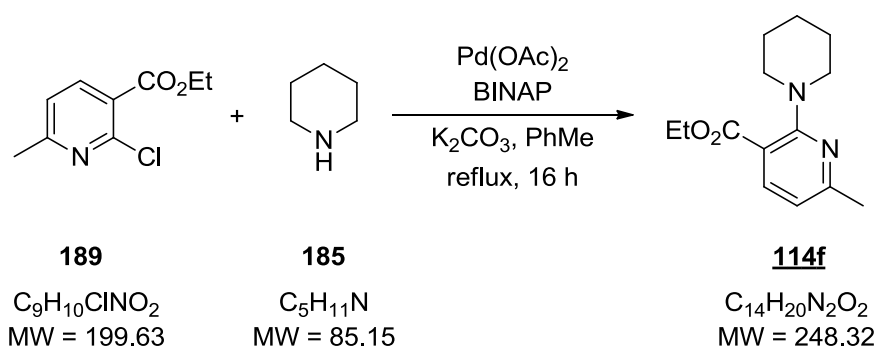
Yield: 92% (1.08 g, 4.6 mmol)

Appearance: yellow oil

TLC: 0.7 (PE/EtOAc 5:1)

¹H NMR (CDCl₃, 200MHz): δ = 1.38 (t, ³J = 7.1 Hz, 3H, CH₃), 1.65 (m, 6H, H3' & H4'), 3.40-3.37 (m, 4H, H2'), 4.35 (q, ³J = 7.1 Hz, 2H, CH₂), 6.67 (dd, ³J = 7.6, ³J = 4.7 Hz, 1H, H5), 7.92 (dd, ³J = 7.6, ⁴J = 2.0 Hz, 1H, H4), 8.25 (dd, ³J = 4.7, ⁴J = 2.0 Hz, 1H, H6).

¹³C NMR (CDCl₃, 50MHz): δ = 14.4 (q, CH₃), 24.7 (t, C4'), 26.0 (t, C3'), 50.5 (t, C2'), 61.1 (t, CH₂), 113.4 (s, C3), 114.1 (d, C5), 140.6 (d, C4), 150.4 (d, C6), 159.7 (s, C2), 167.9 (s, CO).

6.3.52 Ethyl 6-methyl-2-(piperidin-1-yl)nicotinate (**114f**)

Ethyl 2-chloro-6-methylnicotinate **189** (1 g, 5 mmol, 1 equiv), piperidine **185** (1.06 g, 12.5 mmol, 2.5 equiv), K_2CO_3 (2.41 g, 17.5 mmol, 3.5 equiv), Pd(OAc)_2 (22 mg, 0.1 mmol, 2 mol%), and BINAP (62 mg, 0.1 mmol, 2 mol%) in 15 mL of dry toluene were converted according to general procedure II.

Yield: 84% (1.04 g, 4.2 mmol)

Appearance: colorless solid

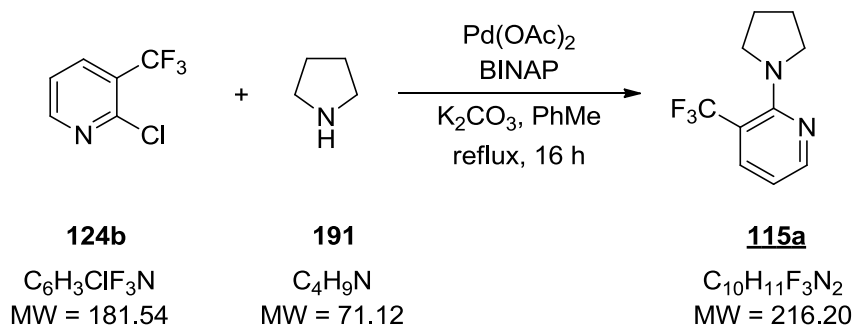
Mp: 58-60 °C

TLC: 0.9 (PE/EtOAc 5:1)

^1H NMR (CDCl_3 , 200MHz): δ = 1.36 (t, 3J = 7.1 Hz, 3H, CH_2CH_3), 1.63-1.67 (m, 6H, H3' & H4'), 2.40 (s, 3H, CH_3), 3.23-3.35 (m, 4H, H2'), 4.32 (q, 3J = 7.1 Hz, 2H, CH_2CH_3), 6.52 (d, 3J = 7.7 Hz, 1H, H5), 7.83 (d, 3J = 7.7 Hz, 1H, H4).

^{13}C NMR (CDCl_3 , 50MHz): δ = 14.5 (q, CH_2CH_3), 24.7 (q, CH_3), 24.8 (t, C4'), 26.0 (t, C3'), 50.5 (t, C2'), 60.8 (t, CH_2CH_3), 110.7 (s, C3), 113.0 (d, C5), 141.0 (d, C4), 159.4 (s, C6), 160.0 (s, C2), 168.0 (s, CO).

HRMS: calculated for $\text{C}_{14}\text{H}_{20}\text{N}_2\text{O}_2$: $[\text{M}+\text{H}]^+$ 249.1598, found $[\text{M}+\text{H}]^+$ 249.1587; Δ = 4.41 ppm.

6.3.53 2-(Pyrrolidin-1-yl)-3-(trifluoromethyl)pyridine (**115a**)

2-Chloro-3-(trifluoromethyl)pyridine **124b** (910 mg, 5 mmol, 1 equiv.), pyrrolidine **191** (888 mg, 12.5 mmol, 2.5 equiv), K₂CO₃ (2.41 g, 17.5 mmol, 3.5 equiv), Pd(OAc)₂ (22 mg, 0.1 mmol, 2 mol%), and BINAP (62 mg, 0.1 mmol, 2 mol%) in 15 mL of dry toluene were converted according to general procedure II.

Yield: 86% (929 mg, 4.3 mmol)

Appearance: colorless oil

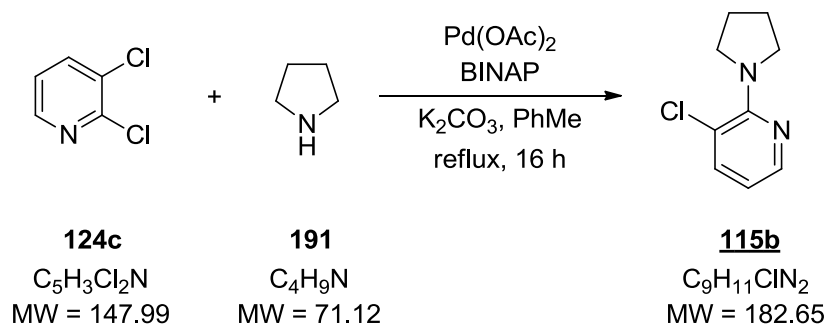
TLC: 0.8 (PE/EtOAc 9:1)

¹H NMR (CDCl₃, 200MHz): δ = 1.90-1.97 (m, 4H, H3'), 3.58 (t, ³J = 6.1 Hz, 4H, H2'), 6.61 (dd, ³J = 7.7, ³J = 4.7 Hz, 1H, H5), 7.77 (dd, ³J = 7.7, ⁴J = 1.8 Hz, 1H, H4), 8.27 (dd, ³J = 4.7, ⁴J = 1.3 Hz, 1H, H6).

¹³C NMR (CDCl₃, 50MHz): δ = 25.7 (t, C3'), 49.6 (t, J_{CF} = 3.2 Hz, C2'), 108.7 (s, J_{CF} = 32.1 Hz, C3), 111.0 (d, C5), 124.7 (s, J_{CF} = 271.2 Hz, CF₃), 137.0 (d, J_{CF} = 6.2 Hz, C4), 150.7 (d, C6), 155.1 (s, C2).

HRMS: calculated for C₁₀H₁₁F₃N₂⁺: [M+H]⁺ 217.0947, found [M+H]⁺ 217.0945; Δ = 0.92 ppm.

6.3.54 3-Chloro-2-(pyrrolidin-1-yl)pyridine (**115b**)



2,3-Dichloropyridine **124c** (740 mg, 5 mmol, 1 equiv), pyrrolidine **191** (888 mg, 12.5 mmol, 2.5 equiv), K₂CO₃ (2.41 g, 17.5 mmol, 3.5 equiv), Pd(OAc)₂ (22 mg, 0.1 mmol, 2 mol%), and BINAP (62 mg, 0.1 mmol, 2 mol%) in 15 mL of dry toluene were converted according to general procedure II.

Yield: 76% (691 mg, 3.78 mmol)

Appearance: colorless oil

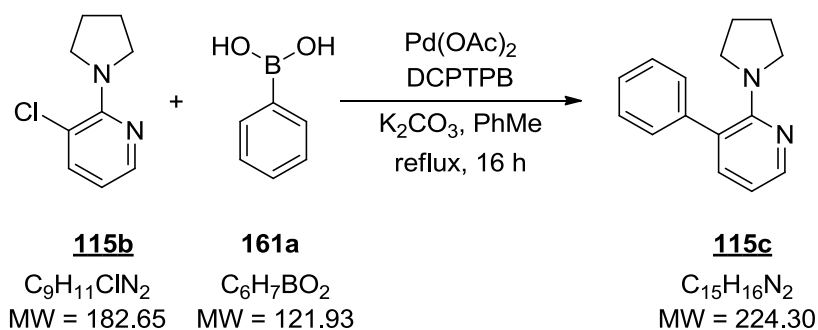
TLC: 0.7 (PE/EtOAc 5:1)

^1H NMR (CDCl₃, 200MHz): δ = 1.88-1.94 (m, 4H, H3'), 3.63-3.69 (m, 4H, H2'), 6.54 (dd, 3J = 7.6, 3J = 4.7 Hz, 1H, H5), 7.44 (dd, 3J = 7.6, 4J = 1.6 Hz, 1H, H4), 8.03 (dd, 3J = 4.7, 4J = 1.6 Hz, 1H, H6).

^{13}C NMR (CDCl₃, 50MHz): δ = 25.8 (t, C3'), 49.9 (t, C2'), 113.7 (d, C5), 116.6 (s, C3), 138.9 (d, C4), 145.5 (d, C6), 155.5 (s, C2).

HRMS: calculated for C₉H₁₁N₂Cl⁺: [M+H]⁺ 183.0684, found [M+H]⁺ 183.0678; Δ = 3.28 ppm.

6.3.55 3-Phenyl-2-(pyrrolidin-1-yl)pyridine (**115c**)



3-Chloro-2-(pyrrolidin-1-yl)pyridine **115b** from the above protocol (183 mg, 1 mmol, 1 equiv), phenylboronic acid **161a** (366 mg, 3 mmol, 3 equiv), K₂CO₃ (276 mg, 2 mmol, 2 equiv), Pd(OAc)₂ (4 mg, 0.02 mmol, 2 mol%), and DCPTPB (10 mg, 0.02 mmol, 2 mol%) in 2.5 mL of dry toluene were converted according to general procedure II.

Yield: 94% (211 mg, 0.94 mmol)

Appearance: colorless oil

TLC: 0.5 (PE/EtOAc 5:1)

^1H NMR (CDCl₃, 200MHz): δ = 1.72-1.78 (m, 4H, H3'), 3.09-3.16 (m, 4H, H2'), 6.68 (dd, 3J = 7.3, 3J = 4.9 Hz, 1H, H5), 7.24-7.38 (m, 6H, PhH & H4), 8.16 (dd, 3J = 4.9, 4J = 1.9 Hz, 1H, H6).

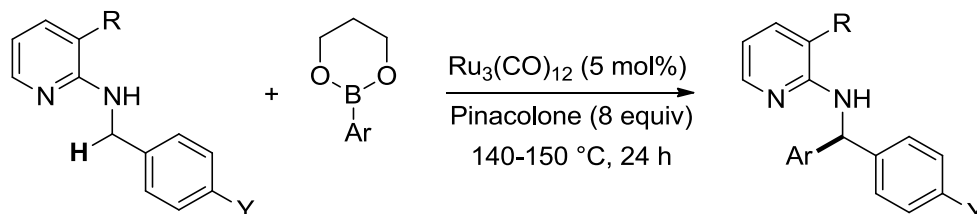
^{13}C NMR (CDCl₃, 50MHz): δ = 25.8 (t, C3'), 50.9 (t, C2'), 112.7 (d, C5), 122.9 (s, C3), 126.6 (d, C4'), 128.1 (d, C2''), 128.9 (d, C3''), 139.7 (d, C4), 141.4 (s, C1''), 146.3 (d, C6), 156.9 (s, C2).

HRMS: calculated for C₁₅H₁₆N₂⁺: [M+H]⁺ 225.1386, found [M+H]⁺ 225.1380; Δ = 2.67 ppm.

6.4 C-H Bond Functionalization

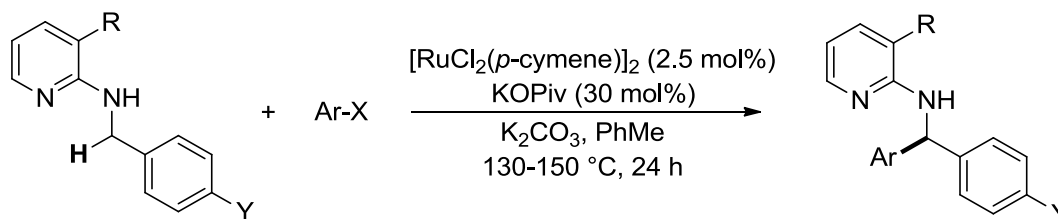
6.4.1 General Methods

Method A



Pyridine derivative (0.5 mmol, 1 equiv), arylboronic acid ester (0.75 mmol, 1.5 equiv), and $\text{Ru}_3(\text{CO})_{12}$ (0.025 mmol, 5 mol%) were placed in an oven-dried 6 mL-vial with septum screw cap and a magnetic stirring bar. The vial was evacuated and flushed with argon (3x). After adding 0.5 mL of dry pinacolone to the reaction mixture, the vial was closed with a fully covered solid Teflon lined cap. The reaction vial was then heated in a reaction block at 140 °C for 24-36 h. After cooling to r.t., 2 mL of EtOAc and 2 mL of water were added to the reaction mixture and stirred for 5 min at r.t. The reaction mixture was extracted with EtOAc (3x). The combined organic layers were dried over Na_2SO_4 , filtered and concentrated under reduced pressure. The resulting crude product was purified by flash column chromatography (SiO_2 150:1; PE:EtOAc = 49:1) and dried in high vacuum.

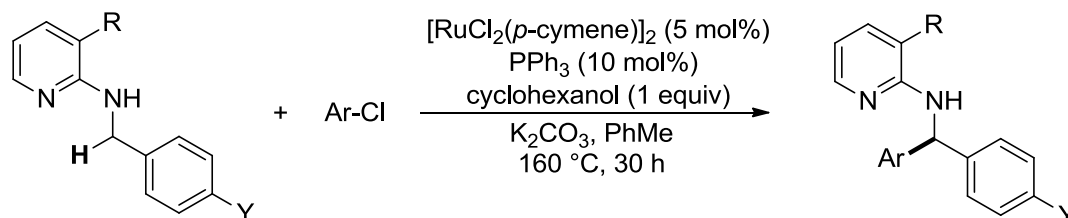
Method B



$[\text{RuCl}_2(p\text{-cymene})]_2$ (0.0125 mmol, 2.5 mol%) and KOPiv (0.15 mmol, 30 mol%) were placed in an oven-dried 6 mL-vial with septum screw cap and a magnetic stirring bar. The vial was evacuated and flushed with argon (3x). After adding 2 mL of dry toluene, the reaction mixture was stirred at r.t. for 30 min. Subsequently, the pyridine derivative (0.5 mmol, 1 equiv), aryl halide (0.75 mmol, 1.5 equiv) and K_2CO_3 (1.5 mmol, 3 equiv) were added to the mixture. The vial was again evacuated and flushed with argon, closed with a fully covered solid Teflon lined cap and heated in a reaction block at 130-150 °C for 24 h. After cooling to r.t., the suspension was filtered through a short pad of Celite®, which was further washed with DCM (2 x 5 mL). The combined organic layers were concentrated in

vacuum and the remaining residue was purified by flash column chromatography (SiO₂ 150:1; PE:EtOAc = 49:1) and dried in high vacuum.

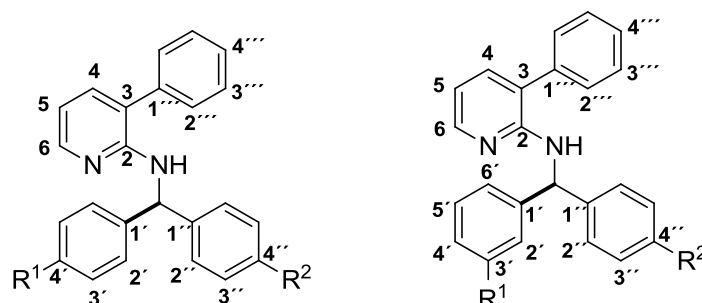
Method C

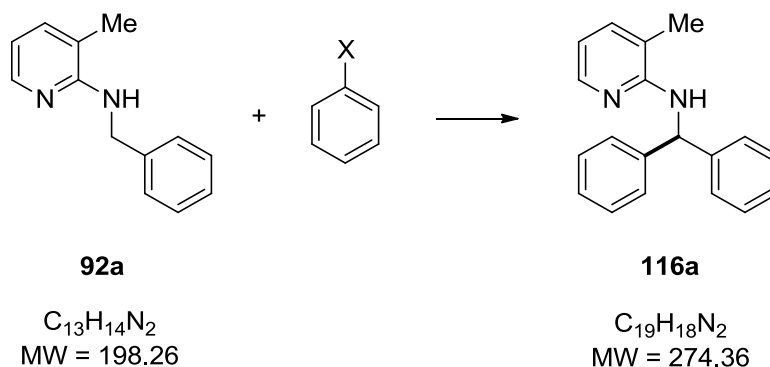


[RuCl₂(*p*-cymene)]₂ (0.025 mmol, 5 mol%) and PPh₃ (0.05 mmol, 10 mol%) were placed in an oven-dried 6 mL-vial with septum screw cap and a magnetic stirring bar. The vial was evacuated and flushed with argon (3x). After adding 2 mL of dry *o*-xylene, the reaction mixture was stirred at r.t. for 30 min. Subsequently, the pyridine derivative (0.5 mmol, 1 equiv), aryl chloride (1.5 mmol, 3 equiv), cyclohexanol (0.5 mmol, 1 equiv), and K₂CO₃ (1.5 mmol, 3 equiv) were added to the mixture. The vial was again evacuated and flushed with argon, closed with a fully covered solid Teflon lined cap and heated in a reaction block at 160 °C for 30 h. After cooling to r.t., the suspension was filtered through a short pad of Celite®, which was further washed with DCM (2 x 5 mL). The combined organic layers were concentrated in vacuum and the remaining residue was purified by flash column chromatography (SiO₂ 150:1; PE:EtOAc = 49:1) and dried in high vacuum.

General Structure

The general structure of the compounds described in this section can be represented by this general structure. The C and H of pyridine ring are annotated as C and H, where as the C and H of the aryls are annotated as C', H', C'', and H'' for assigning the NMR signals. The numbering depends on individual compound structure.



6.4.2 *N*-Benzhydryl-3-methylpyridin-2-amine (116a)Method A

N-Benzyl-3-methylpyridin-2-amine **92a** (99 mg, 0.5 mmol, 1 equiv), 2-phenyl-1,3,2-dioxaborinane **91a** (122 mg, 0.75 mmol, 1.5 equiv), and Ru₃(CO)₁₂ (16 mg, 0.025 mmol, 5 mol%) in 0.5 mL of dry pinacolone were converted according to the general protocol – method A. Analytical data is in accordance with the literature.¹³⁰

Yield: 64% (88 mg, 0.32 mmol)

Method B

N-Benzyl-3-methylpyridin-2-amine **92a** (99 mg, 0.5 mmol, 1 equiv), bromobenzene **138a** (118 mg, 0.75 mmol, 1.5 equiv), [RuCl₂(*p*-cymene)]₂ (7.6 mg, 0.0125 mmol, 2.5 mol%), KO₂Piv (21 mg, 0.15 mmol, 30 mol%), and K₂CO₃ (207 mg, 1.5 mmol, 3 equiv) in 2 mL of dry toluene were converted according to the general protocol – method B.

Yield: 69% (95 mg, 0.35 mmol)

Method C

N-Benzyl-3-methylpyridin-2-amine **92a** (99 mg, 0.5 mmol, 1 equiv), chlorobenzene **139a** (170 mg, 1.5 mmol, 3 equiv), [RuCl₂(*p*-cymene)]₂ (15 mg, 0.025 mmol, 5 mol%), PPh₃ (13 mg, 0.05 mmol, 10 mol%), cyclohexanol (50 mg, 0.5 mmol, 1 equiv), and K₂CO₃ (207 mg, 1.5 mmol, 3 equiv) in 2 mL of *o*-xylene were converted according to the general protocol – method C.

Yield: 70% (97 mg, 0.35 mmol)

Appearance: colorless solid

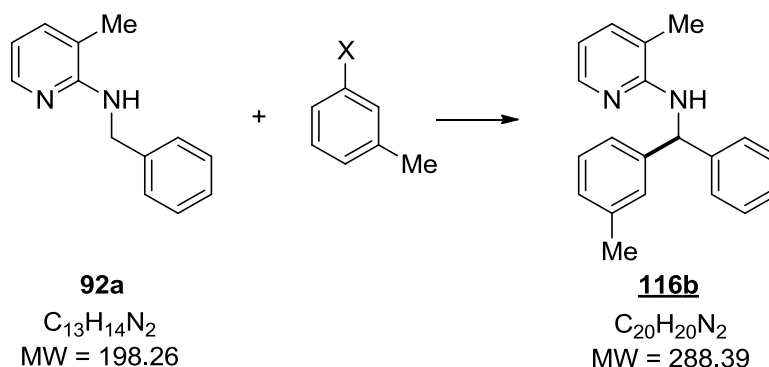
Mp: 91-93°C (lit.)

TLC: 0.5 (PE/EtOAc 9:1)

¹H NMR (CDCl₃, 200MHz): δ = 2.07 (s, 3H, CH₃), 4.60 (d, ³J = 6.8 Hz, 1H, NH), 6.42-6.48 (m, 2H, CH & H5), 7.12-7.29 (m, 11H), 7.89 (dd, ³J = 5.0, ⁴J = 1.3 Hz, 1H, H6).

^{13}C NMR (CDCl_3 , 50MHz): $\delta = 17.2$ (q, $\underline{\text{C}}\text{H}_3$), 58.6 (d, $\underline{\text{C}}\text{H}$), 113.2 (d, C5), 116.4 (s, C3), 127.1 (d, C4 \prime), 127.7 (d, C2 \prime), 128.6 (d, C3 \prime), 137.0 (d, C4), 143.6 (s, C1 \prime), 145.7 (d, C6), 155.8 (s, C2).

6.4.3 3-Methyl-N-[3-methylphenyl(phenyl)methyl]pyridin-2-amine (**116b**)



Method A

N-Benzyl-3-methylpyridin-2-amine **92a** (99 mg, 0.5 mmol, 1 equiv), 2-(3-methylphenyl)-1,3,2-dioxaborinane **91d** (132 mg, 0.75 mmol, 1.5 equiv), and $\text{Ru}_3(\text{CO})_{12}$ (16 mg, 0.025 mmol, 5 mol%) in 0.5 mL of dry pinacolone were converted according to the general protocol – method A.

Yield: 61% (88 mg, 0.30 mmol)

Method B

N-Benzyl-3-methylpyridin-2-amine **92a** (99 mg, 0.5 mmol, 1 equiv), 1-bromo-3-methylbenzene **138b** (128 mg, 0.75 mmol, 1.5 equiv), $[\text{RuCl}_2(p\text{-cymene})]_2$ (7.6 mg, 0.0125 mmol, 2.5 mol%), KOPiv (21 mg, 0.15 mmol, 30 mol%), and K_2CO_3 (207 mg, 1.5 mmol, 3 equiv) in 2 mL of dry toluene were converted according to the general protocol – method B.

Yield: 55% (79 mg, 0.28 mmol)

Method C

N-Benzyl-3-methylpyridin-2-amine **92a** (99 mg, 0.5 mmol, 1 equiv), 1-chloro-3-methylbenzene **139b** (191 mg, 1.5 mmol, 3 equiv), $[\text{RuCl}_2(p\text{-cymene})]_2$ (15 mg, 0.025 mmol, 5 mol%), PPh_3 (13 mg, 0.05 mmol, 10 mol%), cyclohexanol (50 mg, 0.5 mmol, 1 equiv), and K_2CO_3 (207 mg, 1.5 mmol, 3 equiv) in 2 mL of *o*-xylene were converted according to the general protocol – method C.

Yield: 72% (104 mg, 0.36 mmol)

Appearance: colorless oil

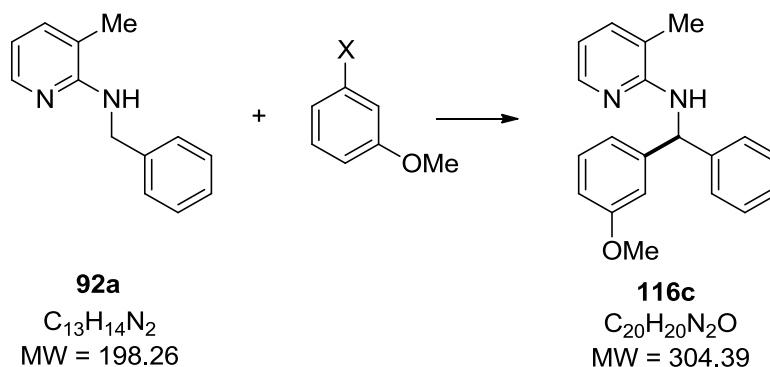
TLC: 0.5 (PE/EtOAc 9:1)

¹H NMR (CDCl₃, 200MHz): δ = 2.11 (s, 3H, PyCH₃), 2.29 (s, 3H, PhCH₃), 4.63 (d, ³J = 7.2 Hz, 1H, NH), 6.46-6.52 (m, 2H, CH & H5), 7.01-7.34 (m, 10H), 7.95 (dd, ³J = 5.0, ⁴J = 1.2 Hz, 1H, H6).

¹³C NMR (CDCl₃, 50MHz): δ = 17.2 (q, PyCH₃), 21.6 (q, PhCH₃), 58.5 (d, CH), 113.1 (d, C5), 116.4 (s, C3), 124.7 (d, C6'), 127.0 (d, C4''), 127.6 (d, C4'), 127.9 (d, C2''), 128.5 (d, C5'), 128.6 (d, C3''), 129.3 (d, C2'), 137.0 (d, C4), 138.2 (s, C3'), 143.6 (s, C1'), 143.7 (s, C1''), 145.8 (d, C6), 155.8 (s, C2).

HRMS: calculated for C₂₀H₂₀N₂⁺: [M+H]⁺ 289.1699, found [M+H]⁺ 289.1679; Δ = 6.92 ppm.

6.4.4 *N*-[(3-Methoxyphenyl)(phenyl)methyl]-3-methylpyridin-2-amine (**116c**)



Method B

N-Benzyl-3-methylpyridin-2-amine **92a** (99 mg, 0.5 mmol, 1 equiv), 1-bromo-3-methoxybenzene **138c** (140 mg, 0.75 mmol, 1.5 equiv), [RuCl₂(*p*-cymene)]₂ (7.6 mg, 0.0125 mmol, 2.5 mol%), KOPiv (21 mg, 0.15 mmol, 30 mol%), and K₂CO₃ (207 mg, 1.5 mmol, 3 equiv) in 2 mL of dry toluene were converted according to the general protocol – method B.

Yield: 60% (91 mg, 0.30 mmol)

Appearance: colorless oil

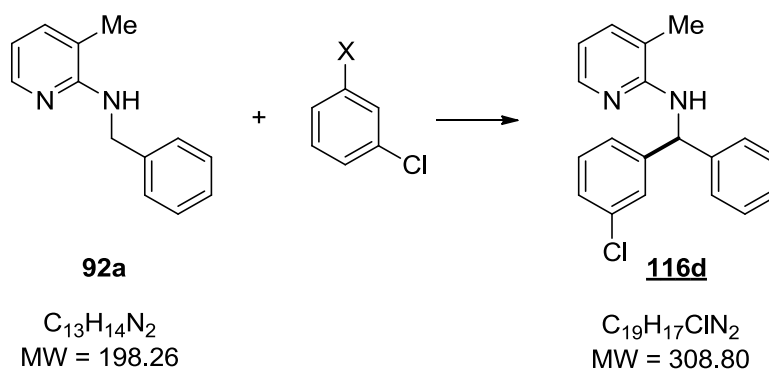
TLC: 0.5 (PE/EtOAc 9:1)

¹H NMR (CDCl₃, 200MHz): δ = 2.12 (s, 3H, CH₃), 3.73 (s, 3H, OCH₃), 4.65 (d, ³J = 7.5 Hz, 1H, NH), 6.48-6.54 (m, 2H, CH & H5), 6.74-6.80 (m, 1H, H4'), 6.89-6.93 (m, 2H), 7.18-7.37 (m, 7H), 7.96 (dd, ³J = 5.0, ⁴J = 1.2 Hz, 1H,).

¹³C NMR (CDCl₃, 50MHz): δ = 17.1 (q, CH₃), 55.2 (q, OCH₃), 58.5 (d, CH), 112.1 (d, C4'), 113.2 (d, C2'), 113.7 (d, C5), 116.4 (s, C3), 120.0 (d, C6'), 127.1 (d, C4''), 127.6 (d, C2''), 128.6 (d, C3''), 129.6 (d, C5'), 137.0 (d, C4), 143.5 (s, C1''), 145.3 (s, C1'), 145.7 (d, C6), 155.7 (s, C2), 159.8 (s, C3').

HRMS: calculated for $C_{20}H_{20}N_2O+$: $[M+H]^+$ 305.1648, found $[M+H]^+$ 305.1637; $\Delta = 3.60$ ppm.

6.4.5 *N*-[(3-Chlorophenyl)(phenyl)methyl]-3-methylpyridin-2-amine (**116d**)



Method A

N-Benzyl-3-methylpyridin-2-amine **92a** (99 mg, 0.5 mmol, 1 equiv), 2-(2-chlorophenyl)-1,3,2-dioxaborinane **91e** (147 mg, 0.75 mmol, 1.5 equiv), and $Ru_3(CO)_{12}$ (16 mg, 0.025 mmol, 5 mol%) in 0.5 mL of dry pinacolone were converted according to the general protocol – method A.

Yield: 38% (58 mg, 0.19 mmol)

Method B

N-Benzyl-3-methylpyridin-2-amine **92a** (99 mg, 0.5 mmol, 1 equiv), 1-bromo-3-chlorobenzene **138d** (143 mg, 0.75 mmol, 1.5 equiv), $[RuCl_2(p\text{-cymene})]_2$ (7.6 mg, 0.0125 mmol, 2.5 mol%), KO₂Piv (21 mg, 0.15 mmol, 30 mol%), and K_2CO_3 (207 mg, 1.5 mmol, 3 equiv) in 2 mL of dry toluene were converted according to the general protocol – method B.

Yield: 37% (58 mg, 0.19 mmol)

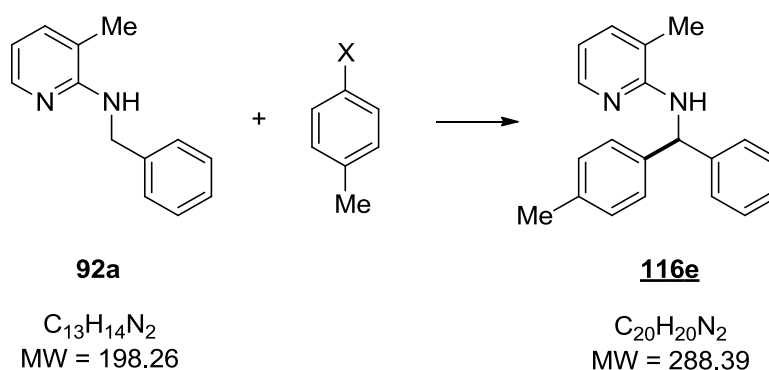
Appearance: colorless oil

TLC: 0.5 (PE/EtOAc 9:1)

1H NMR (CDCl₃, 200MHz): $\delta = 2.13$ (s, 3H, CH₃), 4.59 (d, $^3J = 6.6$ Hz, 1H, NH), 6.46-6.57 (m, 2H, CH & H5), 7.19-7.32 (m, 10H), 7.95 (dd, $^3J = 5.0$, $^4J = 1.3$ Hz, 1H, H6).

^{13}C NMR (CDCl₃, 50MHz): $\delta = 17.2$ (q, CH₃), 58.3 (d, CH), 113.6 (d, C5), 116.6 (s, C3), 125.8 (d, C6'), 127.3 (d, C4'), 127.5 (d, C4'), 127.6 (d, C2'), 127.8 (d, C2''), 128.9 (d, C3''), 129.8 (d, C5'), 134.5 (d, C3'), 137.2 (d, C4), 143.0 (s, C1'), 145.8 (d, C6 & C1'), 155.6 (s, C2).

HRMS: calculated for $C_{20}H_{20}N_2+$: $[M+H]^+$ 309.1153, found $[M+H]^+$ 309.1138; $\Delta = 4.85$ ppm.

6.4.6 3-Methyl-N-[phenyl(4-methylphenyl)methyl]pyridin-2-amine (**116e**)Method A

N-Benzyl-3-methylpyridin-2-amine **92a** (99 mg, 0.5 mmol, 1 equiv), 2-(4-methylphenyl)-1,3,2-dioxaborinane **91f** (132 mg, 0.75 mmol, 1.5 equiv), and $Ru_3(CO)_{12}$ (16 mg, 0.025 mmol, 5 mol%) in 0.5 mL of dry pinacolone were converted according to the general protocol – method A.

Yield: 62% (89 mg, 0.31 mmol)

Method B

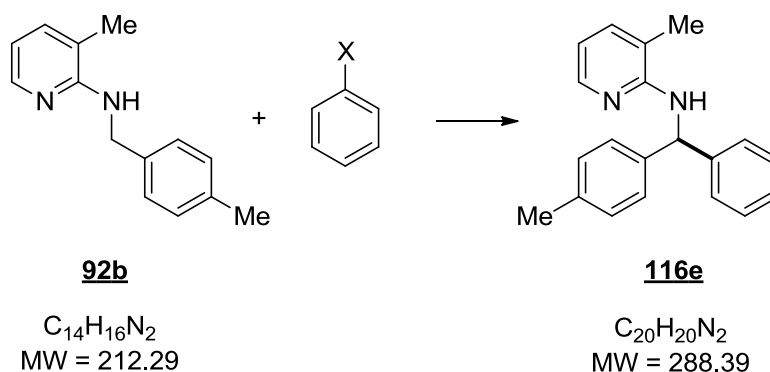
N-Benzyl-3-methylpyridin-2-amine **92a** (99 mg, 0.5 mmol, 1 equiv), 1-bromo-4-methylbenzene **138e** (128 mg, 0.75 mmol, 1.5 equiv), $[RuCl_2(p\text{-cymene})]_2$ (7.6 mg, 0.0125 mmol, 2.5 mol%), $KOPiv$ (21 mg, 0.15 mmol, 30 mol%), and K_2CO_3 (207 mg, 1.5 mmol, 3 equiv) in 2 mL of dry toluene were converted according to the general protocol – method B.

Yield: 65% (94 mg, 0.33 mmol)

Method C

N-Benzyl-3-methylpyridin-2-amine **92a** (99 mg, 0.5 mmol, 1 equiv), 1-chloro-4-methylbenzene **139c** (191 mg, 1.5 mmol, 3 equiv), $[RuCl_2(p\text{-cymene})]_2$ (15 mg, 0.025 mmol, 5 mol%), PPh_3 (13 mg, 0.05 mmol, 10 mol%), cyclohexanol (50 mg, 0.5 mmol, 1 equiv), and K_2CO_3 (207 mg, 1.5 mmol, 3 equiv) in 2 mL of *o*-xylene were converted according to the general protocol – method C.

Yield: 79% (114 mg, 0.40 mmol)

**Method A**

3-Methyl-*N*-(4-methylbenzyl)pyridin-2-amine **92b** (106 mg, 0.5 mmol, 1 equiv), 2-phenyl-1,3,2-dioxaborinane **91a** (122 mg, 0.75 mmol, 1.5 equiv), and Ru₃(CO)₁₂ (16 mg, 0.025 mmol, 5 mol%) in 0.5 mL of dry pinacolone were converted according to the general protocol – method A.

Yield: 76% (109 mg, 0.38 mmol)

Method B

3-Methyl-*N*-(4-methylbenzyl)pyridin-2-amine **92b** (106 mg, 0.5 mmol, 1 equiv), bromobenzene **138a** (118 mg, 0.75 mmol, 1.5 equiv), [RuCl₂(*p*-cymene)]₂ (7.6 mg, 0.0125 mmol, 2.5 mol%), KOPiv (21 mg, 0.15 mmol, 30 mol%), and K₂CO₃ (207 mg, 1.5 mmol, 3 equiv) in 2 mL of dry toluene were converted according to the general protocol – method B.

Yield: 48% (69 mg, 0.24 mmol)

Appearance: colorless solid

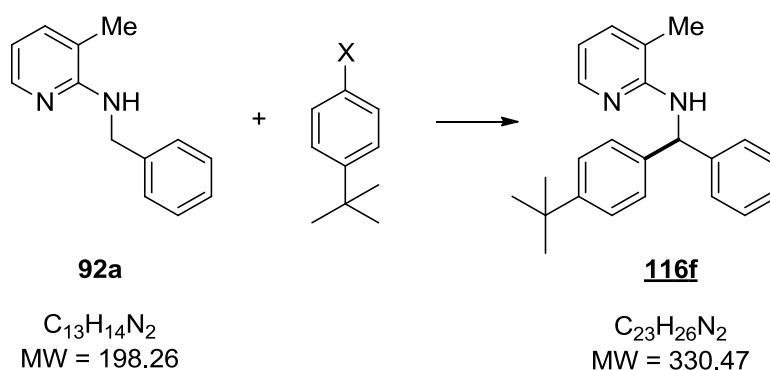
Mp: 103-105 °C

TLC: 0.5 (PE/EtOAc 9:1)

¹H NMR (CDCl₃, 200MHz): δ = 2.13 (s, 3H, PyCH₃), 2.32 (s, 3H, PhCH₃), 4.64 (d, ³J = 6.8 Hz, 1H, NH), 6.46-6.54 (m, 2H, CH & H5), 7.09-7.32 (m, 10H), 7.96 (dd, ³J = 5.0, ⁴J = 1.3 Hz, 1H, H6).

¹³C NMR (CDCl₃, 50MHz): δ = 17.2 (q, PhCH₃), 21.2 (q, PyCH₃), 58.3 (d, CH), 113.1 (d, C5), 116.4 (s, C3), 127.0 (d, C4''), 127.6 (d, C2''), 127.7 (d, C2'), 128.6 (d, C3''), 129.3 (d, C3'), 136.8 (s, C4'), 137.0 (d, C4), 140.7 (s, C1'), 143.7 (s, C1''), 145.8 (d, C6), 155.8 (s, C2).

HRMS: calculated for C₂₀H₂₀N₂⁺: [M+H]⁺ 289.1699, found [M+H]⁺ 289.1699; Δ = 0.00 ppm.

6.4.7 *N*-[4-(1,1-Dimethylethyl)phenyl](phenyl)methyl]-3-methylpyridin-2-amine (**116f**)Method A

N-Benzyl-3-methylpyridin-2-amine **92a** (99 mg, 0.5 mmol, 1 equiv), 2-(4-(1,1-dimethylethyl)phenyl)-1,3,2-dioxaborinane **91g** (164 mg, 0.75 mmol, 1.5 equiv), and $Ru_3(CO)_{12}$ (16 mg, 0.025 mmol, 5 mol%) in 0.5 mL of dry pinacolone were converted according to the general protocol – method A.

Yield: 64% (106 mg, 0.32 mmol)

Method B

N-Benzyl-3-methylpyridin-2-amine **92a** (99 mg, 0.5 mmol, 1 equiv), 1-bromo-4-(1,1-dimethylethyl)benzene **138f** (160 mg, 0.75 mmol, 1.5 equiv), $[RuCl_2(p\text{-cymene})]_2$ (7.6 mg, 0.0125 mmol, 2.5 mol%), KO₂Piv (21 mg, 0.15 mmol, 30 mol%), and K_2CO_3 (207 mg, 1.5 mmol, 3 equiv) in 2 mL of dry toluene were converted according to the general protocol – method B.

Yield: 64% (106 mg, 0.32 mmol)

Appearance: colorless solid

Mp: 120-122 °C

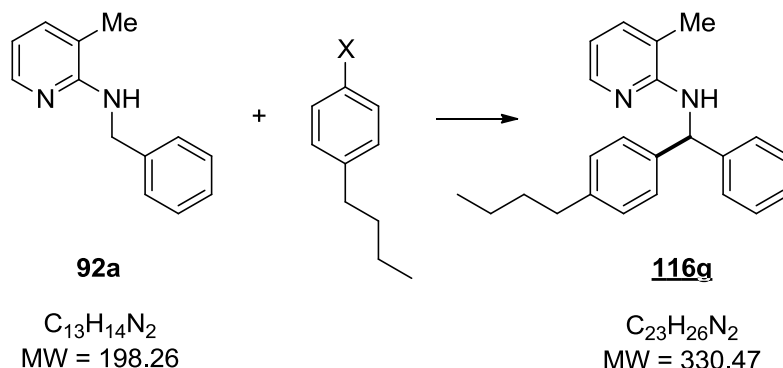
TLC: 0.6 (PE/EtOAc 9:1)

¹H NMR (CDCl₃, 200MHz): δ = 1.29 (s, 9H, C(CH₃)₃), 2.13 (s, 3H, CH₃), 4.66 (d, ³*J* = 6.8 Hz, 1H, NH), 6.48-6.53 (m, 2H, CH & H5), 7.20-7.34 (m, 10H), 7.96 (dd, ³*J* = 5.0, ⁴*J* = 1.3 Hz, 1H, H6).

¹³C NMR (CDCl₃, 50MHz): δ = 17.3 (q, C-CH₃), 31.5 (q, C(C-CH₃)₃), 34.6 (s, C(CH₃)₃), 58.2 (d, C-H), 113.1 (d, C5), 116.4 (s, C3), 125.6 (d, C3'), 127.0 (d, C4'), 127.4 (d, C2'), 127.6 (d, C2''), 128.5 (d, C3''), 137.0 (d, C4), 140.6 (s, C1'), 143.7 (s, C1''), 145.8 (d, C6), 150.0 (s, C4'), 155.9 (s, C2).

HRMS: calculated for $C_{23}H_{26}N_2$: $[M+H]^+$ 331.2169, found $[M+H]^+$ 331.2178; $\Delta = 2.72$ ppm.

6.4.8 *N*-[(4-Butylphenyl)(phenyl)methyl]-3-methylpyridin-2-amine (**116g**)



Method B

N-Benzyl-3-methylpyridin-2-amine **92a** (99 mg, 0.5 mmol, 1 equiv), 1-bromo-4-butylbenzene **138g** (160 mg, 0.75 mmol, 1.5 equiv), $[RuCl_2(p\text{-cymene})]_2$ (7.6 mg, 0.0125 mmol, 2.5 mol%), KO₂Piv (21 mg, 0.15 mmol, 30 mol%), and K_2CO_3 (207 mg, 1.5 mmol, 3 equiv) in 2 mL of dry toluene were converted according to the general protocol – method B.

Yield: 67% (111 mg, 0.34 mmol)

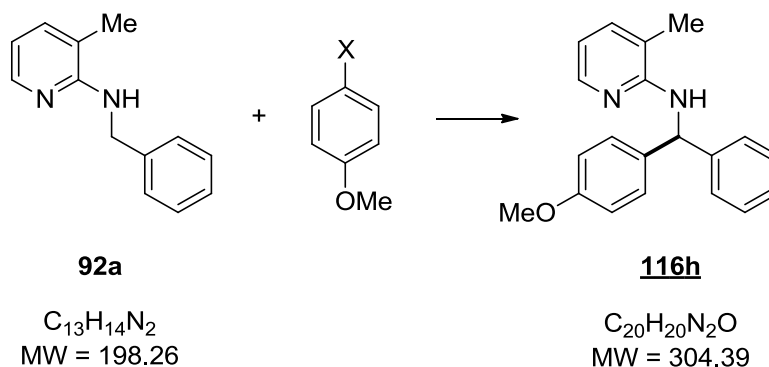
Appearance: colorless oil

TLC: 0.5 (PE/EtOAc 9:1)

¹H NMR (CDCl₃, 200MHz): δ = 0.89 (t, $^3J = 7.2$ Hz, 3H, CH₂CH₃), 1.23-1.41 (m, 2H, CH₂CH₂CH₃), 1.48-1.63 (m, 2H, CH₂CH₂CH₂), 2.08 (s, 3H, CH₃), 2.55 (t, $^3J = 7.7$ Hz, 2H, PhCH₂CH₂), 4.62 (d, $^3J = 7.0$ Hz, 1H, NH), 6.43-6.50 (m, 2H), 7.06-7.33 (m, 10H), 7.93 (dd, $^3J = 5.0$, $^4J = 1.3$ Hz, 1H, H₆).

¹³C NMR (CDCl₃, 50MHz): δ = 14.1 (q, CH₂CH₃), 17.2 (q, CH₃), 22.5 (t, CH₂CH₂CH₃), 33.7 (t, CH₂CH₂CH₂), 35.4 (t, PhCH₂CH₂), 58.3 (d, CH), 113.1 (d, C₅), 116.4 (s, C₃), 127.0 (d, C₄''), 127.5 (d, C₂''), 127.6 (d, C₂'), 128.5 (d, C₃''), 128.6 (d, C₃'), 137.0 (d, C₄'), 140.9 (s, C₁''), 141.7 (s, C₄'), 143.8 (s, C₁''), 145.8 (d, C₆), 155.9 (s, C₂).

HRMS: calculated for $C_{23}H_{26}N_2$: $[M+H]^+$ 331.2169, found $[M+H]^+$ 331.2156; $\Delta = 3.92$ ppm.

6.4.9 *N*-[(4-Methoxyphenyl)(phenyl)methyl]-3-methylpyridin-2-amine (**116h**)Method A

N-Benzyl-3-methylpyridin-2-amine **92a** (99 mg, 0.5 mmol, 1 equiv), 2-(4-methoxyphenyl)-1,3,2-dioxaborinane **91h** (144 mg, 0.75 mmol, 1.5 equiv), and $Ru_3(CO)_{12}$ (16 mg, 0.025 mmol, 5 mol%) in 0.5 mL of dry pinacolone were converted according to the general protocol – method A.

Yield: 39% (59 mg, 0.20 mmol)

Method B

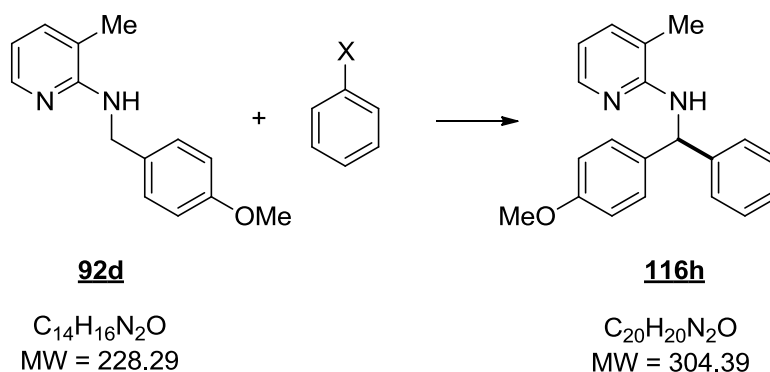
N-Benzyl-3-methylpyridin-2-amine **92a** (99 mg, 0.5 mmol, 1 equiv), 1-bromo-4-methoxybenzene **138h** (140 mg, 0.75 mmol, 1.5 equiv), $[RuCl_2(p\text{-cymene})]_2$ (7.6 mg, 0.0125 mmol, 2.5 mol%), $KOPiv$ (21 mg, 0.15 mmol, 30 mol%), and K_2CO_3 (207 mg, 1.5 mmol, 3 equiv) in 2 mL of dry toluene were converted according to the general protocol – method B.

Yield: 63% (96 mg, 0.32 mmol)

Method C

N-Benzyl-3-methylpyridin-2-amine **92a** (99 mg, 0.5 mmol, 1 equiv), 1-chloro-4-methoxybenzene **139d** (215 mg, 1.5 mmol, 3 equiv), $[RuCl_2(p\text{-cymene})]_2$ (15 mg, 0.025 mmol, 5 mol%), PPh_3 (13 mg, 0.05 mmol, 10 mol%), cyclohexanol (50 mg, 0.5 mmol, 1 equiv), and K_2CO_3 (207 mg, 1.5 mmol, 3 equiv) in 2 mL of *o*-xylene were converted according to the general protocol – method C.

Yield: 64% (97 mg, 0.32 mmol)

**Method A**

N-(4-Methoxybenzyl)-3-methylpyridin-2-amine **92d** (114 mg, 0.5 mmol, 1 equiv), 2-phenyl-1,3,2-dioxaborinane **91a** (122 mg, 0.75 mmol, 1.5 equiv), and $Ru_3(CO)_{12}$ (16 mg, 0.025 mmol, 5 mol%) in 0.5 mL of dry pinacolone were converted according to the general protocol – method A.

Yield: 32% (49 mg, 0.16 mmol)

Method B

N-(4-Methoxybenzyl)-3-methylpyridin-2-amine **92d** (114 mg, 0.5 mmol, 1 equiv), bromobenzene **138a** (118 mg, 0.75 mmol, 1.5 equiv), $[RuCl_2(p\text{-cymene})]_2$ (7.6 mg, 0.0125 mmol, 2.5 mol%), KOPiv (21 mg, 0.15 mmol, 30 mol%), and K_2CO_3 (207 mg, 1.5 mmol, 3 equiv) in 2 mL of dry toluene were converted according to the general protocol – method B.

Yield: 28% (43 mg, 0.14 mmol)

Appearance: colorless solid

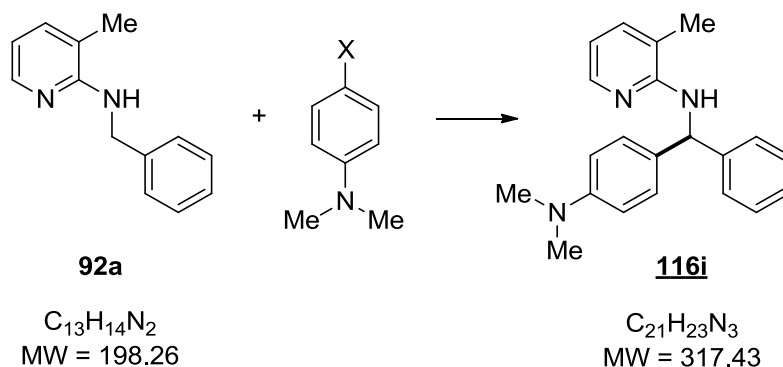
Mp: 59-61 °C

TLC: 0.5 (PE/EtOAc 9:1)

1H NMR (CDCl₃, 200MHz): δ = 2.14 (s, 3H, PyCH₃), 3.79 (s, 3H, OCH₃), 4.63 (d, 3J = 6.5 Hz, 1H, NH), 6.46-6.55 (m, 2H, CH & H5), 6.82-6.89 (m, 2H, H3'), 7.22-7.36 (m, 8H), 7.97 (dd, 3J = 5.0, 4J = 1.3 Hz, 1H, H6).

^{13}C NMR (CDCl₃, 50MHz): δ = 17.2 (q, PyCH₃), 55.4 (q, OCH₃), 58.0 (d, CH), 113.2 (d, C5), 114.0 (d, C3'), 116.4 (s, C3), 127.0 (d, C4''), 127.6 (d, C2''), 128.6 (d, C2'), 128.9 (d, C3''), 135.8 (s, C1'), 137.0 (d, C4), 143.8 (s, C1''), 145.8 (d, C6), 155.8 (s, C4'), 158.7 (s, C2).

HRMS: calculated for $C_{20}H_{20}N_2O$: $[M+H]^+$ 305.1648, found $[M+H]^+$ 305.1655; Δ = 2.29 ppm.

6.4.10 *N*-[4-(Dimethylamino)phenyl](phenyl)methyl]-3-methylpyridin-2-amine (**116i**)**Method B**

N-Benzyl-3-methylpyridin-2-amine **92a** (99 mg, 0.5 mmol, 1 equiv), 4-bromo-*N,N*-dimethylaniline **138i** (150 mg, 0.75 mmol, 1.5 equiv), [RuCl₂(*p*-cymene)]₂ (7.6 mg, 0.0125 mmol, 2.5 mol%), KOPiv (21 mg, 0.15 mmol, 30 mol%), and K₂CO₃ (207 mg, 1.5 mmol, 3 equiv) in 2 mL of dry toluene were converted according to the general protocol – method B.

Yield: 50% (79 mg, 0.25 mmol)

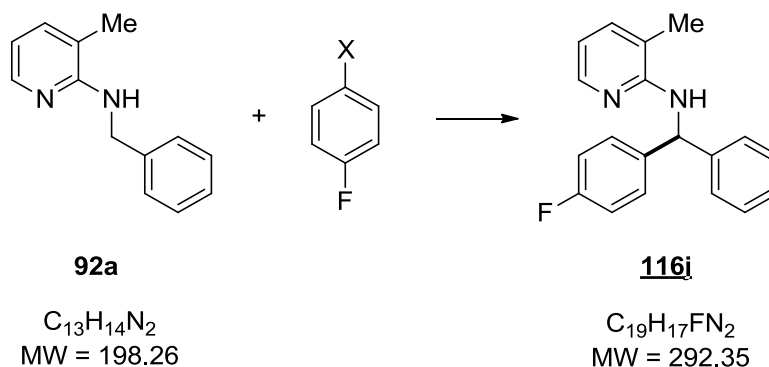
Appearance: yellow oil

TLC: 0.5 (PE/EtOAc 9:1)

¹H NMR (CDCl₃, 200MHz): δ = 2.10 (s, 3H, CH₃), 2.90 (s, 6H, N(CH₃)₂), 4.62 (d, ³*J* = 6.8 Hz, 1H, NH), 6.41-6.51 (m, 2H, CH & H5), 6.64-6.69 (m, 2H), 7.13-7.35 (m, 8H), 7.95 (dd, ³*J* = 5.0, ⁴*J* = 1.3 Hz, 1H, H6).

¹³C NMR (CDCl₃, 50MHz): δ = 17.2 (q, CH₃), 40.7 (q, N(CH₃)₂), 58.0 (d, CH), 112.7 (d, C3'), 112.9 (d, C5), 116.4 (s, C3), 126.7 (d, C4''), 127.4 (d, C2''), 128.4 (d, C2'), 128.7 (d, C3''), 131.6 (s, C1'), 136.9 (d, C4), 144.0 (s, C1''), 145.7 (d, C6), 149.8 (s, C4'), 155.9 (s, C2).

HRMS: calculated for C₂₁H₂₃N₃⁺: [M+H]⁺ 318.1965, found [M+H]⁺ 318.1955; Δ = 3.14 ppm.

6.4.11 *N*-[(4-Fluorophenyl)(phenyl)methyl]-3-methylpyridin-2-amine (**116j**)Method A

N-Benzyl-3-methylpyridin-2-amine **92a** (99 mg, 0.5 mmol, 1 equiv), 2-(4-fluorophenyl)-1,3,2-dioxaborinane **91i** (135 mg, 0.75 mmol, 1.5 equiv), and $Ru_3(CO)_{12}$ (16 mg, 0.025 mmol, 5 mol%) in 0.5 mL of dry pinacolone were converted according to the general protocol – method A.

Yield: 66% (96 mg, 0.33 mmol)

Method B

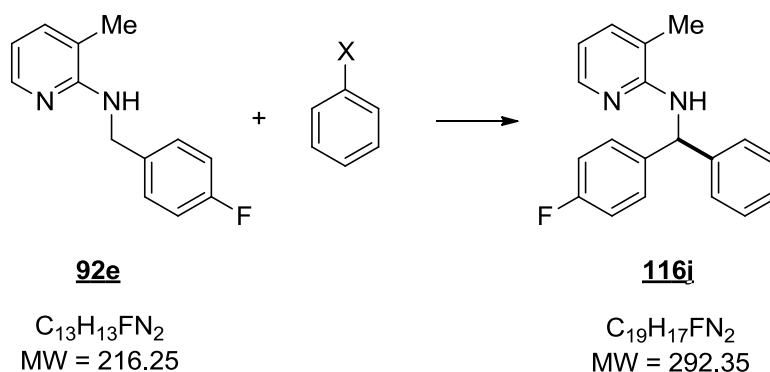
N-Benzyl-3-methylpyridin-2-amine **92a** (99 mg, 0.5 mmol, 1 equiv), 1-bromo-4-fluorobenzene **138j** (131 mg, 0.75 mmol, 1.5 equiv), $[RuCl_2(p\text{-cymene})]_2$ (7.6 mg, 0.0125 mmol, 2.5 mol%), $KOPiv$ (21 mg, 0.15 mmol, 30 mol%), and K_2CO_3 (207 mg, 1.5 mmol, 3 equiv) in 2 mL of dry toluene were converted according to the general protocol – method B.

Yield: 61% (89 mg, 0.31 mmol)

Method C

N-Benzyl-3-methylpyridin-2-amine **92a** (99 mg, 0.5 mmol, 1 equiv), 1-chloro-4-fluorobenzene **139e** (197 mg, 1.5 mmol, 3 equiv), $[RuCl_2(p\text{-cymene})]_2$ (15 mg, 0.025 mmol, 5 mol%), PPh_3 (13 mg, 0.05 mmol, 10 mol%), cyclohexanol (50 mg, 0.5 mmol, 1 equiv), and K_2CO_3 (207 mg, 1.5 mmol, 3 equiv) in 2 mL of *o*-xylene were converted according to the general protocol – method C.

Yield: 56% (82 mg, 0.28 mmol)

**Method A**

N-(4-Fluorobenzyl)-3-methylpyridin-2-amine **92e** (108 mg, 0.5 mmol, 1 equiv), 2-phenyl-1,3,2-dioxaborinane **91a** (122 mg, 0.75 mmol, 1.5 equiv), and Ru₃(CO)₁₂ (16 mg, 0.025 mmol, 5 mol%) in 0.5 mL of dry pinacolone were converted according to the general protocol – method A.

Yield: 44% (64 mg, 0.22 mmol)

Method B

N-(4-Fluorobenzyl)-3-methylpyridin-2-amine **92e** (108 mg, 0.5 mmol, 1 equiv), bromobenzene **138a** (118 mg, 0.75 mmol, 1.5 equiv), [RuCl₂(*p*-cymene)]₂ (7.6 mg, 0.0125 mmol, 2.5 mol%), KOPiv (21 mg, 0.15 mmol, 30 mol%), and K₂CO₃ (207 mg, 1.5 mmol, 3 equiv) in 2 mL of dry toluene were converted according to the general protocol – method B.

Yield: 59% (86 mg, 0.30 mmol)

Appearance: colorless solid

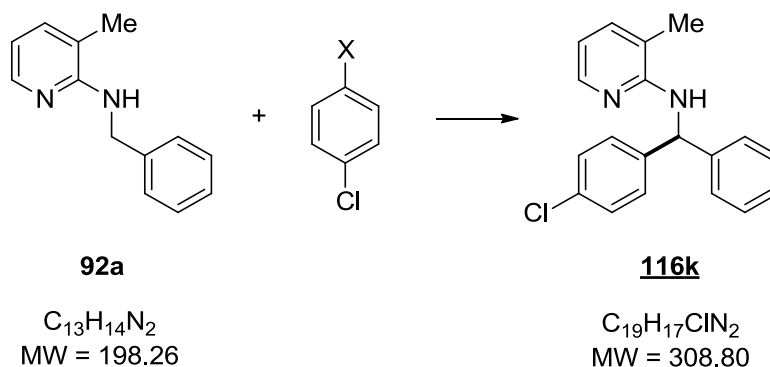
Mp: 101-103 °C

TLC: 0.5 (PE/EtOAc 9:1)

¹H NMR (CDCl₃, 200MHz): δ = 2.07 (s, 3H, CH₃), 4.55 (d, ³J = 6.7 Hz, 1H, NH), 6.42-6.50 (m, 2H, CH & H5), 6.86-6.97 (m, 2H), 7.16-7.26 (m, 8H), 7.90 (dd, ³J = 5.0, ⁴J = 1.3 Hz, 1H, H6).

¹³C NMR (CDCl₃, 50MHz): δ = 17.2 (q, C_{CH3}), 58.0 (d, C_{NH}), 113.4 (d, C5), 115.4 (d, J_{CF} = 21.3 Hz, C3'), 116.5 (s, C3), 127.3 (d, C4''), 127.7 (d, C2''), 128.7 (d, C3''), 129.2 (d, J_{CF} = 8.1 Hz, C2'), 137.2 (d, C4), 139.3 (s, J_{CF} = 3.1 Hz, C1'), 143.4 (s, C1''), 145.7 (d, C6), 155.6 (s, C2), 161.9 (s, J_{CF} = 245.0 Hz, C4').

HRMS: calculated for C₁₉H₁₇N₂F⁺: [M+H]⁺ 293.1449, found [M+H]⁺ 293.1448; Δ = 0.34 ppm.

6.4.12 *N*-[(4-Chlorophenyl)(phenyl)methyl]-3-methylpyridin-2-amine (**116k**)Method A

N-Benzyl-3-methylpyridin-2-amine **92a** (99 mg, 0.5 mmol, 1 equiv), 2-(4-chlorophenyl)-1,3,2-dioxaborinane **91j** (147 mg, 0.75 mmol, 1.5 equiv), and $Ru_3(CO)_{12}$ (16 mg, 0.025 mmol, 5 mol%) in 0.5 mL of dry pinacolone were converted according to the general protocol – method A.

Yield: 33% (51 mg, 0.17 mmol)

Method B

N-Benzyl-3-methylpyridin-2-amine **92a** (99 mg, 0.5 mmol, 1 equiv), 1-bromo-4-chlorobenzene **138k** (143 mg, 0.75 mmol, 1.5 equiv), $[RuCl_2(p\text{-cymene})]_2$ (7.6 mg, 0.0125 mmol, 2.5 mol%), $KOPiv$ (21 mg, 0.15 mmol, 30 mol%), and K_2CO_3 (207 mg, 1.5 mmol, 3 equiv) in 2 mL of dry toluene were converted according to the general protocol – method B.

Yield: 51% (79 mg, 0.26 mmol)

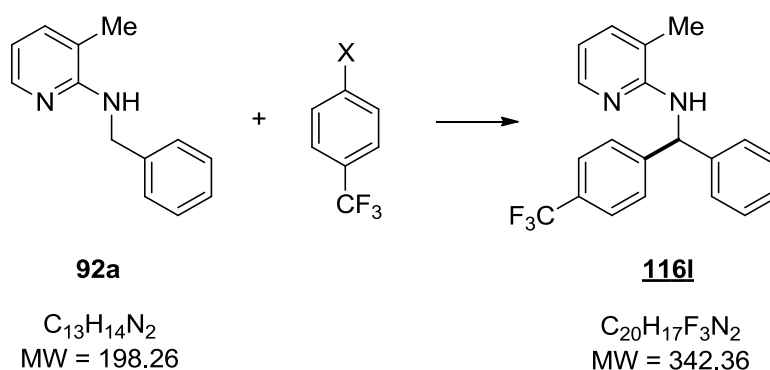
Appearance: colorless oil

TLC: 0.5 (PE/EtOAc 9:1)

1H NMR (CDCl₃, 200MHz): δ = 2.12 (s, 3H, CH₃), 4.59 (d, 3J = 6.6 Hz, 1H, NH), 6.45-6.55 (m, 2H, CH & H5), 7.21-7.32 (m, 10H), 7.94 (dd, 3J = 5.0, 4J = 1.3 Hz, 1H, H6).

^{13}C NMR (CDCl₃, 50MHz): δ = 17.1 (q, $\underline{C}H_3$), 58.2 (d, $\underline{C}H$), 113.5 (d, C5), 116.5 (s, C3), 127.5 (d, C4'), 127.8 (d, C2'), 128.7 (d, C3'), 128.8 (d, C3'), 129.0 (d, C2'), 132.7 (s, C4'), 137.1 (d, C4), 142.1 (s, C1'), 143.2 (s, C1'), 145.7 (d, C6), 155.6 (d, C2).

HRMS: calculated for $C_{19}H_{17}N_2Cl^+$: $[M+H]^+$ 309.1153, found $[M+H]^+$ 309.1138; Δ = 4.85 ppm.

6.4.13 3-Methyl-N-[phenyl(4-(trifluoromethyl)phenyl)methyl]pyridin-2-amine (**116l**)Method A

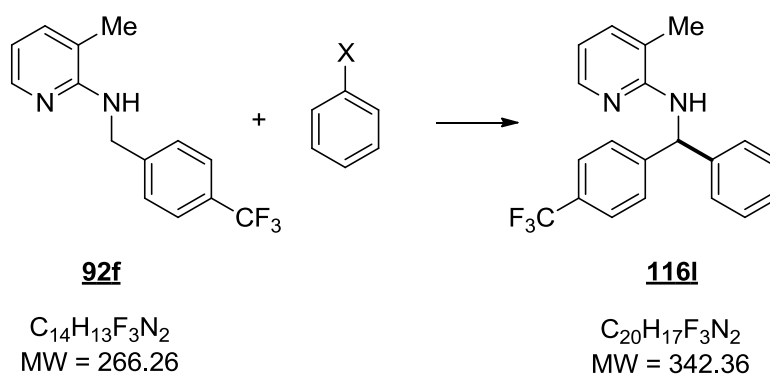
N-Benzyl-3-methylpyridin-2-amine **92a** (99 mg, 0.5 mmol, 1 equiv), 2-(4-(trifluoromethyl)phenyl)-1,3,2-dioxaborinane **91k** (173 mg, 0.75 mmol, 1.5 equiv), and Ru₃(CO)₁₂ (16 mg, 0.025 mmol, 5 mol%) in 0.5 mL of dry pinacolone were converted according to the general protocol – method A.

Yield: 41% (70 mg, 0.21 mmol)

Method C

N-Benzyl-3-methylpyridin-2-amine **92a** (99 mg, 0.5 mmol, 1 equiv), 1-chloro-4-(trifluoromethyl)benzene **139f** (272 mg, 1.5 mmol, 3 equiv), [RuCl₂(*p*-cymene)]₂ (15 mg, 0.025 mmol, 5 mol%), PPh₃ (13 mg, 0.05 mmol, 10 mol%), cyclohexanol (50 mg, 0.5 mmol, 1 equiv), and K₂CO₃ (207 mg, 1.5 mmol, 3 equiv) in 2 mL of *o*-xylene were converted according to the general protocol – method C.

Yield: 30% (51 mg, 0.15 mmol)

Method A

3-Methyl-*N*-(4-(trifluoromethyl)benzyl)pyridin-2-amine **92f** (133 mg, 0.5 mmol, 1 equiv), 2-phenyl-1,3,2-dioxaborinane **91a** (122 mg, 0.75 mmol, 1.5 equiv), and Ru₃(CO)₁₂ (16 mg, 0.025 mmol, 5 mol%) in 0.5 mL of dry pinacolone were converted according to the general protocol – method A.

Yield: 15% (26 mg, 0.08 mmol)

Method B

3-Methyl-*N*-(4-(trifluoromethyl)benzyl)pyridin-2-amine **92f** (133 mg, 0.5 mmol, 1 equiv), bromobenzene **138a** (118 mg, 0.75 mmol, 1.5 equiv), [RuCl₂(*p*-cymene)]₂ (7.6 mg, 0.0125 mmol, 2.5 mol%), KOPiv (21 mg, 0.15 mmol, 30 mol%), and K₂CO₃ (207 mg, 1.5 mmol, 3 equiv) in 2 mL of dry toluene were converted according to the general protocol – method B.

Yield: 57% (97 mg, 0.29 mmol)

Appearance: colorless solid

Mp: 56-58 °C

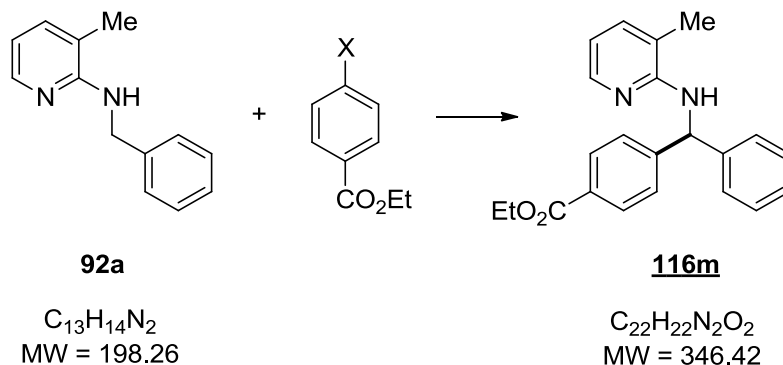
TLC: 0.5 (PE/EtOAc 9:1)

¹H NMR (CDCl₃, 200MHz): δ = 2.17 (s, 3H, CH₃), 4.65 (d, ³*J* = 6.3 Hz, 1H, NH), 6.54-6.60 (m, 2H, CH & H5), 7.26-7.60 (m, 10H), 7.97 (dd, ³*J* = 5.0, ⁴*J* = 1.3 Hz, 1H, H6).

¹³C NMR (CDCl₃, 50MHz): δ = 17.1 (q, CH₃), 58.6 (d, CH), 113.7 (d, C5), 116.6 (s, C3), 124.4 (s, *J*_{CF} = 272.7 Hz, CF₃), 125.5 (d, *J*_{CF} = 3.8 Hz, C3'), 127.7 (d, C4''), 127.8 (d, C2''), 127.9 (d, C2'), 128.9 (d, C3'), 129.2 (s, *J*_{CF} = 32.3 Hz, C4'), 137.2 (d, C4), 142.9 (s, C1'), 145.7 (d, C6), 147.6 (s, C1''), 155.5 (s, C2).

HRMS: calculated for C₂₀H₁₇F₃N₂⁺: [M+H]⁺ 343.1417, found [M+H]⁺ 343.1433; Δ = 4.66 ppm.

6.4.14 Ethyl 4-(((3-methylpyridin-2-yl)amino)(phenyl)methyl) benzoate (116m**)**



Method B

N-Benzyl-3-methylpyridin-2-amine **92a** (99 mg, 0.5 mmol, 1 equiv), ethyl 4-bromobenzoate **138l** (172 mg, 0.75 mmol, 1.5 equiv), [RuCl₂(*p*-cymene)]₂ (7.6 mg, 0.0125 mmol, 2.5 mol%), KOPiv (21 mg, 0.15 mmol, 30 mol%), and K₂CO₃ (207 mg, 1.5 mmol, 3 equiv) in 2 mL of dry toluene were converted according to the general protocol – method B.

Yield: 33% (57 mg, 0.17 mmol)

Appearance: yellow oil

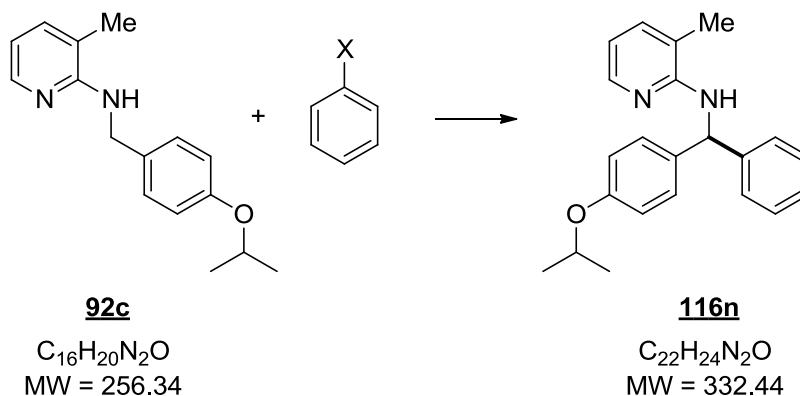
TLC: 0.5 (PE/EtOAc 9:1)

¹H NMR (CDCl₃, 200MHz): δ = 1.37 (t, ³J = 7.1 Hz, 3H, CH₂CH₃), 2.15 (s, 3H, CH₃), 4.36 (q, ³J = 7.1 Hz, 2H, CH₂CH₃), 4.66 (d, ³J = 6.6 Hz, 1H, NH), 6.51-6.57 (m, 2H, CH & H5), 7.23-7.35 (m, 6H), 7.42 (d, ³J = 8.1 Hz, 2H, H4), 7.94-8.02 (m, 3H, H3' & H6).

¹³C NMR (CDCl₃, 50MHz): δ = 14.4 (q, CH₂CH₃), 17.1 (q, CH₃), 58.7 (d, CH), 60.9 (t, CH₂CH₃), 113.5 (d, C5), 116.6 (s, C3), 127.4 (d, C4'), 127.6 (s, C4'), 127.9 (d, C2'), 128.8 (d, C2'), 129.3 (d, C3'), 129.9 (d, C3'), 137.1 (d, C4), 143.0 (s, C1'), 145.7 (d, C6), 148.7 (s, C1'), 155.6 (s, C2), 166.6 (s, CO).

HRMS: calculated for C₂₂H₂₂N₂O₂: [M+H]⁺ 347.1754, found [M+H]⁺ 347.1737; Δ = 4.90 ppm.

6.4.15 *N*-[(4-Isopropoxyphenyl)(phenyl)methyl]-3-methylpyridin-2-amine (**116n**)



Method A

N-(4-Isopropoxybenzyl)-3-methylpyridin-2-amine **92c** (128 mg, 0.5 mmol, 1 equiv), 2-phenyl-1,3,2-dioxaborinane **91a** (122 mg, 0.75 mmol, 1.5 equiv), and Ru₃(CO)₁₂ (16 mg, 0.025 mmol, 5 mol%) in 0.5 mL of dry pinacolone were converted according to the general protocol – method A.

Yield: 25% (42 mg, 0.13 mmol)

Method B

N-(4-Isopropoxybenzyl)-3-methylpyridin-2-amine **92c** (128 mg, 0.5 mmol, 1 equiv), bromobenzene **138a** (118 mg, 0.75 mmol, 1.5 equiv), [RuCl₂(*p*-cymene)]₂ (7.6 mg, 0.0125 mmol, 2.5 mol%), KOPiv (21 mg, 0.15 mmol, 30 mol%), and K₂CO₃ (207 mg, 1.5 mmol, 3 equiv) in 2 mL of dry toluene were converted according to the general protocol – method B.

Yield: 43% (71 mg, 0.22 mmol)

Appearance: colorless oil

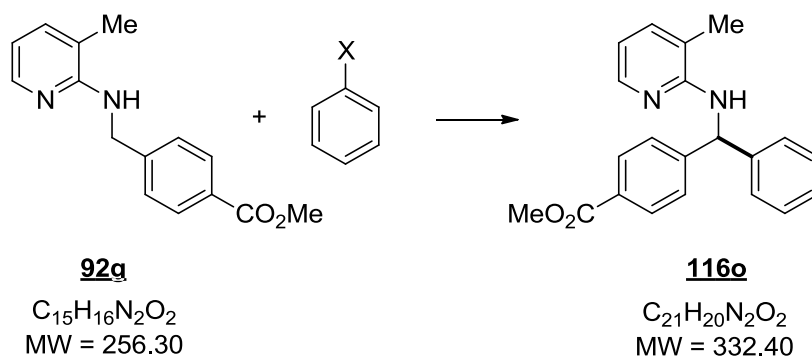
TLC: 0.7 (PE/EtOAc 9:1)

^1H NMR (CDCl₃, 200MHz): δ = 1.30 (d, 3J = 6.0 Hz, 6H, CH(CH₃)₂), 2.11 (s, 3H, CH₃), 4.49 (sep, 3J = 6.0 Hz, 1H, CH(CH₃)₂), 4.61 (d, 3J = 7.0 Hz, 1H, NH), 6.44-6.52 (m, 2H, CH & H5), 6.77-6.85 (m, 2H), 7.17-7.34 (m, 8H), 7.95 (dd, 3J = 5.0, 4J = 1.3 Hz, 1H, H6).

^{13}C NMR (CDCl₃, 50MHz): δ = 17.2 (q, CH₃), 22.2 (q, CH(CH₃)₂), 58.0 (d, CH), 69.9 (d, CH(CH₃)₂), 113.1 (d, C5), 115.8 (d, C3'), 116.4 (d, C3), 126.9 (d, C4'), 127.5 (d, C2'), 128.5 (d, C2), 128.9 (d, C3'), 135.6 (s, C1'), 137.0 (d, C4), 143.8 (s, C1'), 145.8 (d, C6), 155.8 (s, C2), 157.0 (s, C4').

HRMS: calculated for C₂₂H₂₄N₂O₂: [M+H]⁺ 333.1961, found [M+H]⁺ 333.1963; Δ = 0.60 ppm.

6.4.16 Methyl 4-(((3-methylpyridin-2-yl)amino)(phenyl)methyl)benzoate (**116o**)



Method A

Methyl 4-(((3-methylpyridin-2-yl)amino)methyl)benzoate **92g** (128 mg, 0.5 mmol, 1 equiv), 2-phenyl-1,3,2-dioxaborinane **91a** (122 mg, 0.75 mmol, 1.5 equiv), and Ru₃(CO)₁₂ (16 mg, 0.025 mmol, 5 mol%) in 0.5 mL of dry pinacolone were converted according to the general protocol – method A.

Yield: 26% (43 mg, 0.13 mmol)

Method B

Methyl 4-(((3-methylpyridin-2-yl)amino)methyl)benzoate **92g** (128 mg, 0.5 mmol, 1 equiv), bromobenzene **138a** (118 mg, 0.75 mmol, 1.5 equiv), [RuCl₂(*p*-cymene)]₂ (7.6 mg, 0.0125 mmol, 2.5 mol%), KOPiv (21 mg, 0.15 mmol, 30 mol%), and K₂CO₃ (207 mg, 1.5 mmol, 3 equiv) in 2 mL of dry toluene were converted according to the general protocol – method B.

Yield: 57% (95 mg, 0.14 mmol)

Appearance: colorless oil

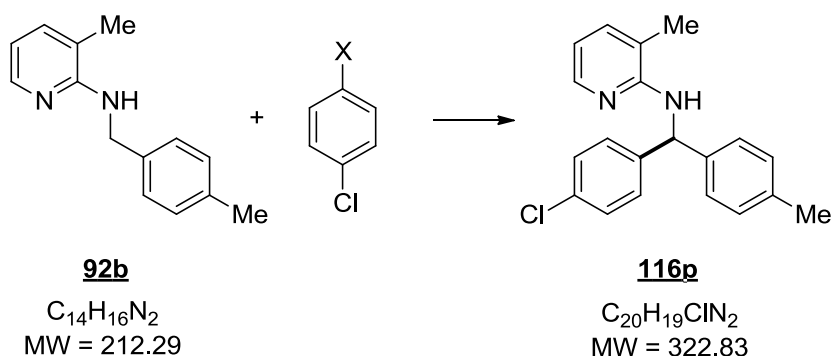
TLC: 0.6 (PE/EtOAc 9:1)

^1H NMR (CDCl₃, 200MHz): δ = 2.13 (s, 3H, CH₃), 3.86 (s, 3H, OCH₃), 4.65 (d, 3J = 6.6 Hz, 1H, NH), 6.49-6.55 (m, 2H, CH & H5), 7.21-7.33 (m, 6H, PhH & H4), 7.41 (d, 3J = 8.2 Hz, 2H, H3'), 7.92-7.99 (m, 3H).

^{13}C NMR (CDCl₃, 50MHz): δ = 17.1 (q, CH₃), 52.1 (q, OCH₃), 58.7 (d, CH), 113.5 (d, C5), 116.5 (s, C3), 127.4 (d, C4'), 127.5 (d, C4'), 127.9 (d, C2' & C2''), 128.8 (d, C3'), 129.9 (d, C3'), 137.1 (d, C4), 142.9 (s, C1'), 145.7 (d, C6), 148.8 (s, C1'), 155.5 (s, C2), 167.1 (s, CO).

HRMS: calculated for C₂₁H₂₀N₂O₂⁺: [M+H]⁺ 333.1598, found [M+H]⁺ 333.1587; Δ = 3.30 ppm.

6.4.17 *N*-[(4-Chlorophenyl)(4-methylphenyl)methyl]-3-methylpyridin-2-amine (**116p**)



Method A

3-Methyl-*N*-(4-methylbenzyl)pyridin-2-amine **92b** (106 mg, 0.5 mmol, 1 equiv), 2-(4-chlorophenyl)-1,3,2-dioxaborinane **91j** (147 mg, 0.75 mmol, 1.5 equiv), and Ru₃(CO)₁₂ (16 mg, 0.025 mmol, 5 mol%) in 0.5 mL of dry pinacolone were converted according to the general protocol – method A.

Yield: 50% (81 mg, 0.25 mmol)

Appearance: colorless oil

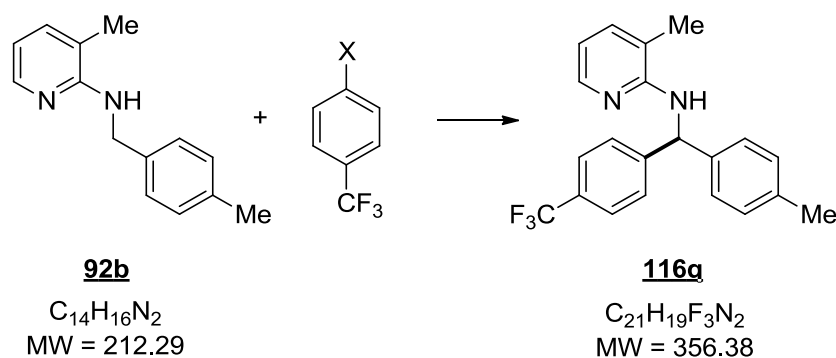
TLC: 0.7 (PE/EtOAc 9:1)

^1H NMR (CDCl₃, 200MHz): δ = 2.03 (s, 3H, PyCH₃), 2.23 (s, 3H, PhCH₃), 4.49 (d, 3J = 6.6 Hz, 1H, NH), 6.34 (d, 3J = 6.7 Hz, 1H, CH), 6.43 (dd, 3J = 7.1, 3J = 5.1 Hz, 1H, H5), 7.01-7.16 (m, 9H), 7.86 (dd, 3J = 5.0, 4J = 1.3 Hz, 1H, H6).

^{13}C NMR (CDCl_3 , 50MHz): $\delta = 17.2$ (q, PyCH_3), 21.2 (q, PhCH_3), 57.9 (d, CH), 113.4 (d, C5), 116.5 (s, C3), 127.7 (d, C2 \prime), 128.6 (d, C3 \prime), 128.9 (d, C2 $\prime\prime$), 129.5 (d, C3 $\prime\prime$), 132.6 (s, C4 $\prime\prime$), 137.1 (s, C4 \prime), 137.2 (d, C4), 140.2 (s, C1 \prime), 142.2 (s, C1 $\prime\prime$), 145.7 (d, C6), 155.6 (s, C2).

HRMS: calculated for $\text{C}_{20}\text{H}_{19}\text{N}_2\text{Cl}^+$: $[\text{M}+\text{H}]^+$ 323.1310, found $[\text{M}+\text{H}]^+$ 323.1317; $\Delta = 2.17$ ppm.

6.4.18 3-Methyl-N-[4-methylphenyl(4-(trifluoromethyl)phenyl)methyl]pyridin-2-amine (116g)



Method A

3-Methyl-N-(4-methylbenzyl)pyridin-2-amine **92b** (106 mg, 0.5 mmol, 1 equiv), 2-(4-(trifluoromethyl)phenyl)-1,3,2-dioxaborinane **91k** (173 mg, 0.75 mmol, 1.5 equiv), and $\text{Ru}_3(\text{CO})_{12}$ (16 mg, 0.025 mmol, 5 mol%) in 0.5 mL of dry pinacolone were converted according to the general protocol – method A.

Yield: 33% (58 mg, 0.17 mmol)

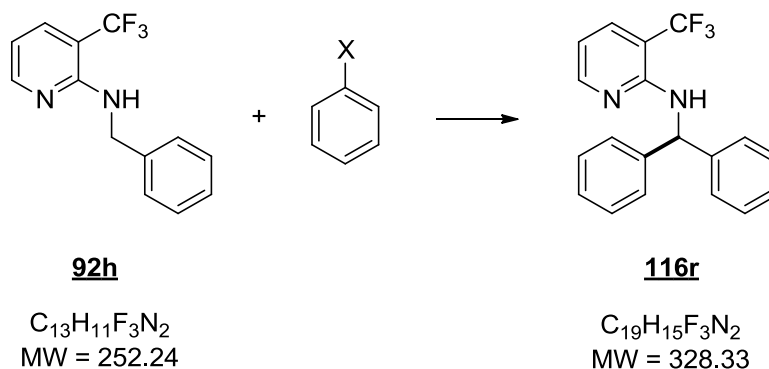
Appearance: colorless oil

TLC: 0.7 (PE/EtOAc 9:1)

^1H NMR (CDCl_3 , 200MHz): $\delta = 2.16$ (s, 3H, PyCH_3), 2.35 (s, 3H, PhCH_3), 4.63 (d, $^3J = 6.3$ Hz, 1H, NH), 6.49-6.59 (m, 2H, CH & H5), 7.14-7.29 (m, 5H), 7.52 (q, $^3J = 9.7$ Hz, 4H), 7.97 (dd, $^3J = 5.0$, $^4J = 1.3$ Hz, 1H, H6).

^{13}C NMR (CDCl_3 , 50MHz): $\delta = 17.2$ (q, PyCH_3), 21.2 (q, PhCH_3), 58.4 (d, CH), 113.6 (d, C5), 116.6 (d, C3), 124.4 (s, $J_{\text{CF}} = 272.0$ Hz, CF_3), 125.4 (d, $J_{\text{CF}} = 3.8$ Hz, C3 \prime), 127.7 (d, C2 $\prime\prime$), 127.8 (d, C2 \prime), 129.1 (s, $J_{\text{CF}} = 32.3$ Hz, C4 \prime), 129.7 (d, C3 $\prime\prime$), 137.2 (s, C4 $\prime\prime$), 137.4 (d, C4), 140.0 (s, C1 $\prime\prime$), 145.7 (s, C6), 147.8 (d, C1 \prime), 155.6 (s, C2).

HRMS: calculated for $\text{C}_{21}\text{H}_{19}\text{N}_2\text{F}_3^+$: $[\text{M}+\text{H}]^+$ 357.1573, found $[\text{M}+\text{H}]^+$ 357.1587; $\Delta = 3.92$ ppm.

6.4.19 *N*-Benzhydryl-3-(trifluoromethyl)pyridin-2-amine (**116r**)Method A

N-Benzyl-3-(trifluoromethyl)pyridin-2-amine **92h** (126 mg, 0.5 mmol, 1 equiv), 2-phenyl-1,3,2-dioxaborinane **91a** (122 mg, 0.75 mmol, 1.5 equiv), and $Ru_3(CO)_{12}$ (16 mg, 0.025 mmol, 5 mol%) in 0.5 mL of dry pinacolone were converted according to the general protocol – method A.

Yield: 78% (128 mg, 0.39 mmol)

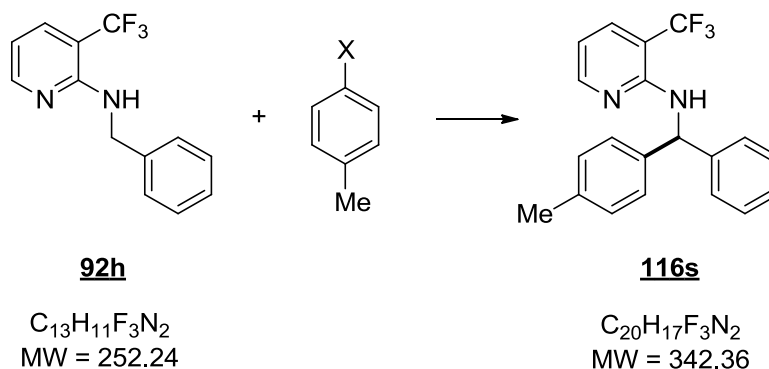
Appearance: colorless oil

TLC: 0.6 (PE/EtOAc 9:1)

1H NMR (CDCl₃, 200MHz): δ = 5.45 (d, 3J = 6.7 Hz, 1H, NH), 6.54-6.63 (m, 2H, CH & H5), 7.19-7.32 (m, 10H), 7.66 (d, 3J = 7.3 Hz, 1H, H4), 8.19 (d, 3J = 4.6, 1H, H6).

^{13}C NMR (CDCl₃, 50MHz): δ = 58.5 (d, \underline{CH}), 108.8 (s, J_{CF} = 31.2 Hz, C3), 112.1 (d, C5), 124.6 (s, J_{CF} = 271.3 Hz, $\underline{CF_3}$), 127.4 (d, C4'), 127.6 (d, C2'), 128.8 (d, C3'), 135.1 (d, J_{CF} = 5.1 Hz, C4), 142.7 (s, C1'), 151.9 (d, C6), 153.6 (s, C2).

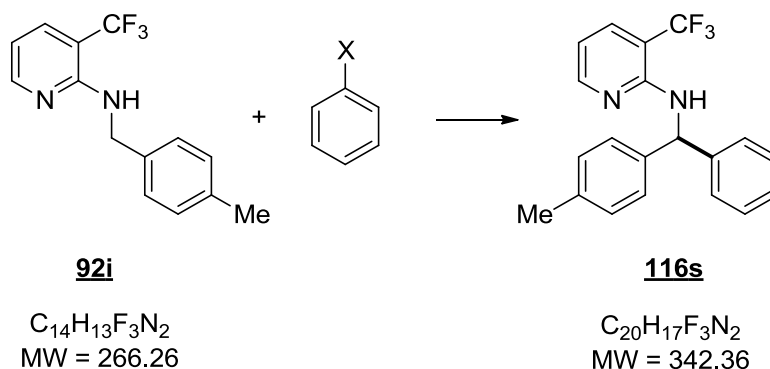
HRMS: calculated for $C_{19}H_{15}F_3N_2$: $[M+H]^+$ 329.1260, found $[M+H]^+$ 329.1271; Δ = 3.34 ppm.

6.4.20 *N*-[4-Methylphenyl(phenyl)methyl]-3-(trifluoromethyl)pyridin-2-amine (**116s**)

Method A

N-Benzyl-3-(trifluoromethyl)pyridin-2-amine **92h** (126 mg, 0.5 mmol, 1 equiv), 2-(4-methylphenyl)-1,3,2-dioxaborinane **91f** (132 mg, 0.75 mmol, 1.5 equiv), and Ru₃(CO)₁₂ (16 mg, 0.025 mmol, 5 mol%) in 0.5 mL of dry pinacolone were converted according to the general protocol – method A.

Yield: 77% (132 mg, 0.39 mmol)

Method A

N-(4-Methylbenzyl)-3-(trifluoromethyl)pyridin-2-amine **92i** (133 mg, 0.5 mmol, 1 equiv), 2-phenyl-1,3,2-dioxaborinane **91a** (122 mg, 0.75 mmol, 1.5 equiv), and Ru₃(CO)₁₂ (16 mg, 0.025 mmol, 5 mol%) in 0.5 mL of dry pinacolone were converted according to the general protocol – method A.

Yield: 80% (136 mg, 0.40 mmol)

Appearance: colorless oil

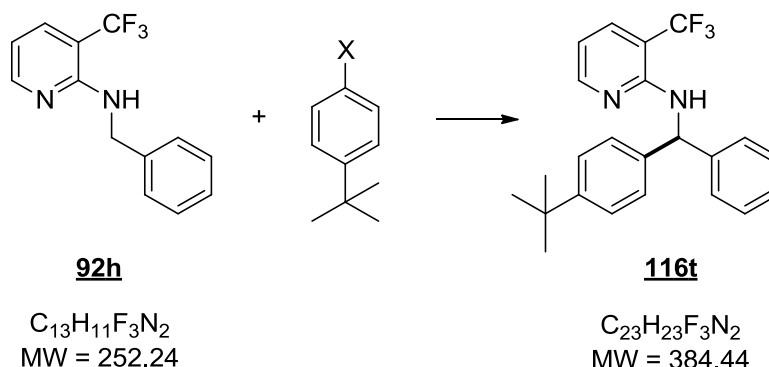
TLC: 0.6 (PE/EtOAc 9:1)

¹H NMR (CDCl₃, 200MHz): δ = 2.32 (s, 3H, CH₃), 5.44 (d, ³*J* = 6.2 Hz, 1H, NH), 6.51 (d, ³*J* = 7.1 Hz, 1H, CH), 6.60 (dd, ³*J* = 7.6, ³*J* = 5.0 Hz, 1H, H5), 7.10-7.36 (m, 9H), 7.66 (d, ³*J* = 7.5 Hz, 1H, H4), 8.19 (d, ³*J* = 4.7, 1H, H6).

¹³C NMR (CDCl₃, 50MHz): δ = 21.2 (q, CH₃), 58.3 (d, CH), 108.7 (s, *J*_{CF} = 31.3 Hz, C3), 112.0 (d, C5), 124.6 (s, *J*_{CF} = 271.6 Hz, CF₃), 127.3 (d, C4''), 127.4 (d, C2''), 127.5 (d, C2'), 128.7 (d, C3'), 129.4 (d, C3'), 135.0 (d, *J*_{CF} = 5.1 Hz, C4), 137.0 (s, C4'), 139.8 (s, C1'), 142.9 (s, C1''), 152.0 (d, C6), 153.6 (s, C2).

HRMS: calculated for C₂₀H₁₇F₃N₂⁺: [M+H]⁺ 343.1417, found [M+H]⁺ 343.1429; Δ = 3.50 ppm.

6.4.21 *N*-[4-(1,1-Dimethylethyl)phenyl](phenyl)methyl]-3-(trifluoromethyl)pyridin-2-amine (116t**)**



Method A

N-Benzyl-3-(trifluoromethyl)pyridin-2-amine **92h** (126 mg, 0.5 mmol, 1 equiv), 2-(4-(1,1-dimethylethyl)phenyl)-1,3,2-dioxaborinane **91g** (164 mg, 0.75 mmol, 1.5 equiv), and $Ru_3(CO)_{12}$ (16 mg, 0.025 mmol, 5 mol%) in 0.5 mL of dry pinacolone were converted according to the general protocol – method A.

Yield: 70% (134 mg, 0.35 mmol)

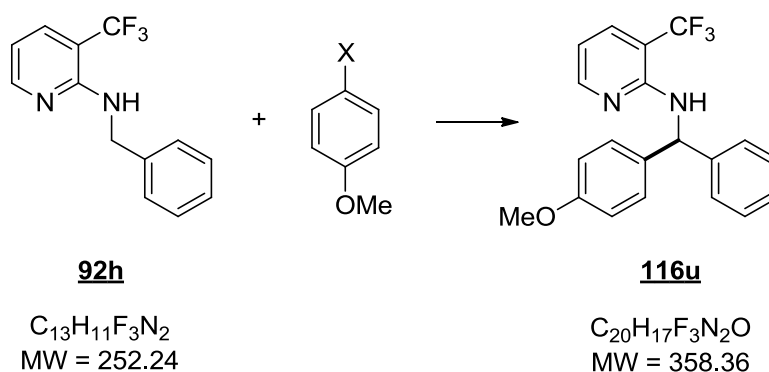
Appearance: colorless oil

TLC: 0.6 (PE/EtOAc 9:1)

1H NMR (CDCl₃, 200MHz): δ = 1.29 (s, 9H, C(CH₃)₃), 5.47 (d, 3J = 6.6 Hz, 1H, NH), 6.53-6.64 (m, 2H, CH & H5), 7.12-7.35 (m, 9H), 7.66 (d, 3J = 7.6 Hz, 1H, H4), 8.20 (d, 3J = 4.8, 1H, H6).

^{13}C NMR (CDCl₃, 50MHz): δ = 31.5 (q, C(CH₃)₃), 34.6 (s, C(CH₃)₃), 58.1 (d, CH), 108.7 (s, J_{CF} = 31.3 Hz, C3), 112.0 (d, C5), 124.7 (s, J_{CF} = 271.7 Hz, CF₃), 125.7 (d, C3'), 127.3 (d, C4'), 127.5 (d, C2'), 128.7 (d, C2''), 129.4 (d, C3''), 135.1 (d, J_{CF} = 5.1 Hz, C4), 139.6 (s, C1'), 142.9 (s, C1''), 150.2 (d, C6), 152.0 (s, C4'), 153.7 (s, C2).

HRMS: calculated for C₂₃H₂₃F₃N₂⁺: [M+H]⁺ 385.1886, found [M+H]⁺ 385.1910; Δ = 6.23 ppm.

6.4.22 *N*-[(4-Methoxyphenyl)(phenyl)methyl]-3-(trifluoromethyl)pyridin-2-amine (**116u**)Method A

N-Benzyl-3-(trifluoromethyl)pyridin-2-amine **92h** (126 mg, 0.5 mmol, 1 equiv), 2-(4-methoxyphenyl)-1,3,2-dioxaborinane **91h** (144 mg, 0.75 mmol, 1.5 equiv), and $Ru_3(CO)_{12}$ (16 mg, 0.025 mmol, 5 mol%) in 0.5 mL of dry pinacolone were converted according to the general protocol – method A.

Yield: 61% (109 mg, 0.31 mmol)

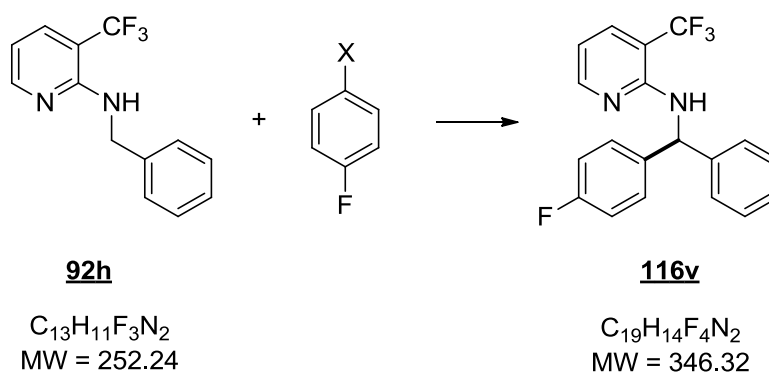
Appearance: colorless oil

TLC: 0.6 (PE/EtOAc 9:1)

1H NMR (CDCl₃, 200MHz): δ = 3.79 (s, 3H, OCH₃), 5.41 (d, 3J = 6.5 Hz, 1H, NH), 6.51 (d, 3J = 7.0 Hz, 1H, CH), 6.62 (dd, 3J = 7.6, 3J = 5.0 Hz, 1H, H5), 6.82-6.90 (m, 2H, H3'), 7.18-7.32 (m, 7H), 7.67 (d, 3J = 6.6 Hz, 1H, H4), 8.21 (d, 3J = 4.5, 1H, H6).

^{13}C NMR (CDCl₃, 50MHz): δ = 55.3 (q, OCH₃), 57.9 (d, CH), 108.7 (s, J_{CF} = 31.3 Hz, C3), 112.0 (d, C5), 114.1 (d, C3'), 124.6 (s, J_{CF} = 271.5 Hz, CF₃), 127.3 (d, C4''), 127.4 (d, C2''), 128.7 (d, C2'), 128.8 (d, C3''), 134.9 (s, C1'), 135.0 (d, J_{CF} = 5.5 Hz, C4), 142.9 (s, C1''), 152.0 (d, C6), 153.6 (s, C4'), 158.9 (s, C2).

HRMS: calculated for $C_{20}H_{17}F_3N_2O^+$: [M+H]⁺ 359.1366, found [M+H]⁺ 359.1386; Δ = 5.57 ppm.

6.4.23 *N*-[(4-Fluorophenyl)(phenyl)methyl]-3-(trifluoromethyl)pyridin-2-amine (**116v**)Method A

N-Benzyl-3-(trifluoromethyl)pyridin-2-amine **92h** (126 mg, 0.5 mmol, 1 equiv), 2-(4-fluorophenyl)-1,3,2-dioxaborinane **91i** (135 mg, 0.75 mmol, 1.5 equiv), and $Ru_3(CO)_{12}$ (16 mg, 0.025 mmol, 5 mol%) in 0.5 mL of dry pinacolone were converted according to the general protocol – method A.

Yield: 51% (88 mg, 0.26 mmol)

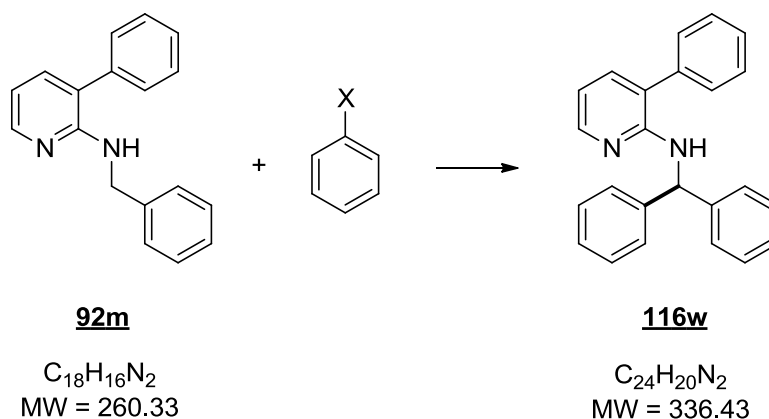
Appearance: colorless oil

TLC: 0.6 (PE/EtOAc 9:1)

1H NMR (CDCl₃, 200MHz): δ = 5.39 (d, 3J = 6.1 Hz, 1H, NH), 6.53 (d, 3J = 6.8 Hz, 1H, CH), 6.63 (dd, 3J = 7.6, 3J = 5.0 Hz, 1H, H5), 7.00-7.04 (m, 2H), 7.23-7.33 (m, 7H), 7.67 (d, 3J = 7.6 Hz, 1H, H4), 8.20 (d, 3J = 4.8, 1H, H6).

^{13}C NMR (CDCl₃, 50MHz): δ = 57.9 (d, CH), 108.9 (s, J_{CF} = 31.3 Hz, C3), 112.3 (d, C5), 115.6 (d, J_{CF} = 21.2 Hz, C3'), 124.6 (s, J_{CF} = 271.6 Hz, CF₃), 127.5 (d, C4'), 127.6 (d, C2'), 128.9 (d, C3''), 129.1 (d, J_{CF} = 8.1 Hz, C2'), 135.1 (d, J_{CF} = 5.1 Hz, C4), 138.5 (s, J_{CF} = 3.2 Hz, C1'), 142.5 (s, C1''), 151.9 (d, C6), 153.5 (s, C2), 162.1 (s, J_{CF} = 245.5 Hz, C4').

HRMS: calculated for $C_{19}H_{14}F_4N_2$: $[M+H]^+$ 347.1166, found $[M+H]^+$ 347.1178; Δ = 3.46 ppm.

6.4.24 *N*-Benzhydryl-3-phenylpyridin-2-amine (**116w**)Method A

N-Benzyl-3-phenylpyridin-2-amine **92m** (130 mg, 0.5 mmol, 1 equiv), 2-phenyl-1,3,2-dioxaborinane **91a** (122 mg, 0.75 mmol, 1.5 equiv), and $Ru_3(CO)_{12}$ (16 mg, 0.025 mmol, 5 mol%) in 0.5 mL of dry pinacolone were converted according to the general protocol – method A.

Yield: 90% (151 mg, 0.45 mmol)

Method B

N-Benzyl-3-phenylpyridin-2-amine **92m** (130 mg, 0.5 mmol, 1 equiv), bromobenzene **138a** (118 mg, 0.75 mmol, 1.5 equiv), $[RuCl_2(p\text{-cymene})]_2$ (7.6 mg, 0.0125 mmol, 2.5 mol%), KOPiv (21 mg, 0.15 mmol, 30 mol%), and K_2CO_3 (207 mg, 1.5 mmol, 3 equiv) in 2 mL of dry toluene were converted according to the general protocol – method B.

Yield: 70% (118 mg, 0.35 mmol)

Method C

N-Benzyl-3-phenylpyridin-2-amine **92m** (130 mg, 0.5 mmol, 1 equiv), chlorobenzene **139a** (170 mg, 1.5 mmol, 3 equiv), $[RuCl_2(p\text{-cymene})]_2$ (15 mg, 0.025 mmol, 5 mol%), PPh_3 (13 mg, 0.05 mmol, 10 mol%), cyclohexanol (50 mg, 0.5 mmol, 1 equiv), and K_2CO_3 (207 mg, 1.5 mmol, 3 equiv) in 2 mL of *o*-xylene were converted according to the general protocol – method C.

Yield: 48% (81 mg, 0.24 mmol)

Appearance: colorless solid

Mp: 90-92 °C

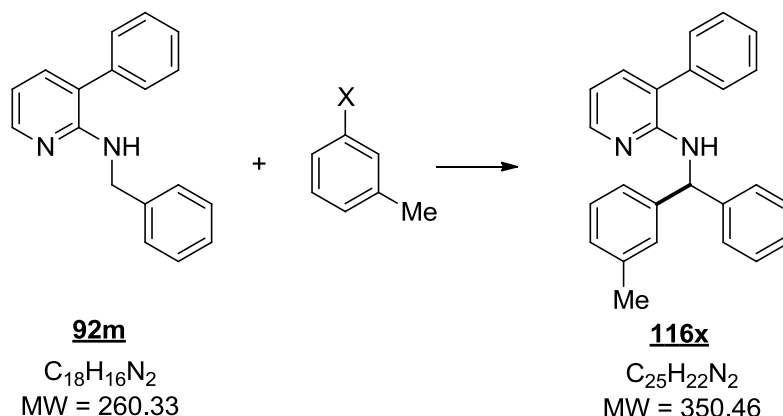
TLC: 0.7 (PE/EtOAc 9:1)

^1H NMR (CDCl₃, 200MHz): δ = 5.18 (d, 3J = 7.4 Hz, 1H, NH), 6.51 (d, 3J = 7.5 Hz, 1H, CH), 6.64 (dd, 3J = 7.2, 3J = 5.0 Hz, 1H, H5), 7.14-7.44 (m, 16H), 8.08 (dd, 3J = 5.0, 4J = 1.8 Hz, 1H, H6).

^{13}C NMR (CDCl₃, 50MHz): δ = 58.5 (d, $\underline{\text{C}}\text{H}$), 113.5 (d, C5), 122.4 (d, C3), 127.1 (d, C4'), 127.5 (d, C2''), 128.0 (d, C2'), 128.6 (d, C3'), 128.9 (d, C3''), 129.4 (d, C4''), 137.4 (d, C4), 138.1 (s, C1''), 143.5 (s, C1'), 147.4 (d, C6), 154.6 (s, C2).

HRMS: calculated for C₂₄H₂₀N₂⁺: [M+H]⁺ 337.1699, found [M+H]⁺ 337.1713; Δ = 4.15 ppm.

6.4.25 *N*-[3-Methylphenyl(phenyl)methyl]-3-phenylpyridin-2-amine (**116x**)



Method B

N-Benzyl-3-phenylpyridin-2-amine **92m** (130 mg, 0.5 mmol, 1 equiv), 1-bromo-3-methylbenzene **138b** (128 mg, 0.75 mmol, 1.5 equiv), [RuCl₂(*p*-cymene)]₂ (7.6 mg, 0.0125 mmol, 2.5 mol%), KOPiv (21 mg, 0.15 mmol, 30 mol%), and K₂CO₃ (207 mg, 1.5 mmol, 3 equiv) in 2 mL of dry toluene were converted according to the general protocol – method B.

Yield: 68% (119 mg, 0.34 mmol)

Method C

N-Benzyl-3-phenylpyridin-2-amine **92m** (130 mg, 0.5 mmol, 1 equiv), 1-chloro-3-methylbenzene **139b** (191 mg, 1.5 mmol, 3 equiv), [RuCl₂(*p*-cymene)]₂ (15 mg, 0.025 mmol, 5 mol%), PPh₃ (13 mg, 0.05 mmol, 10 mol%), cyclohexanol (50 mg, 0.5 mmol, 1 equiv), and K₂CO₃ (207 mg, 1.5 mmol, 3 equiv) in 2 mL of *o*-xylene were converted according to the general protocol – method C.

Yield: 58% (102 mg, 0.29 mmol)

Appearance: colorless oil

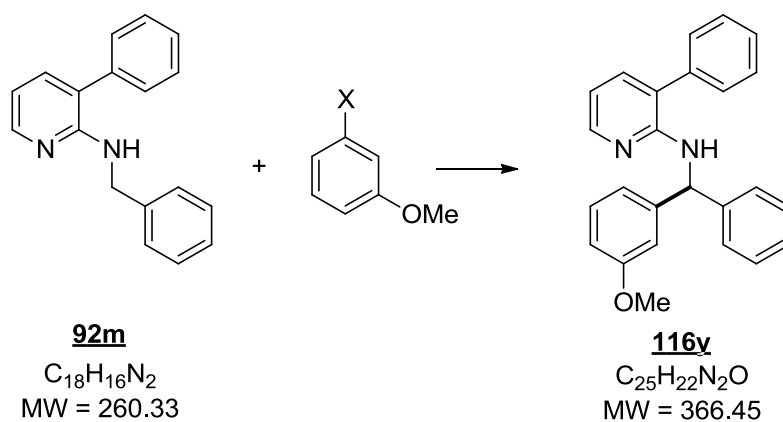
TLC: 0.7 (PE/EtOAc 9:1)

^1H NMR (CDCl₃, 200MHz): δ = 2.25 (s, 3H, CH₃), 5.18 (d, 3J = 7.5 Hz, 1H, NH), 6.49 (d, 3J = 7.5 Hz, 1H, CH), 6.61 (dd, 3J = 7.2, 3J = 5.0 Hz, 1H, H5), 6.97-7.42 (m, 15H), 8.08 (dd, 3J = 5.0, 4J = 1.8 Hz, 1H, H6).

^{13}C NMR (CDCl₃, 50MHz): δ = 21.6 (q, CH₃), 58.6 (d, CH), 113.3 (d, C5), 122.3 (s, C3), 124.5 (d, C6'), 127.0 (d, C4''), 127.5 (d, C4'), 127.8 (d, C2''), 127.9 (d, C2'), 128.3 (d, C4'''), 128.4 (d, C5'), 128.5 (d, C3'''), 128.9 (d, C3''), 129.3 (d, C2'), 137.3 (d, C4), 138.0 (s, C1'''), 138.1 (s, C3'), 143.4 (s, C1'), 143.6 (s, C1''), 147.4 (d, C6), 154.6 (s, C2).

HRMS: calculated for C₂₅H₂₂N₂: [M+H]⁺ 351.1856, found [M+H]⁺ 351.1847; Δ = 2.56 ppm.

6.4.26 *N*-[(3-Methoxyphenyl)(phenyl)methyl]-3-phenylpyridin-2-amine (**116y**)



Method B

N-Benzyl-3-phenylpyridin-2-amine **92m** (130 mg, 0.5 mmol, 1 equiv), 1-bromo-3-methoxybenzene **138c** (140 mg, 0.75 mmol, 1.5 equiv), [RuCl₂(*p*-cymene)]₂ (7.6 mg, 0.0125 mmol, 2.5 mol%), KOPiv (21 mg, 0.15 mmol, 30 mol%), and K₂CO₃ (207 mg, 1.5 mmol, 3 equiv) in 2 mL of dry toluene were converted according to the general protocol – method B.

Yield: 64% (117 mg, 0.32 mmol)

Method C

N-Benzyl-3-phenylpyridin-2-amine **92m** (130 mg, 0.5 mmol, 1 equiv), 1-chloro-3-methoxybenzene **139g** (215 mg, 1.5 mmol, 3 equiv), [RuCl₂(*p*-cymene)]₂ (15 mg, 0.025 mmol, 5 mol%), PPh₃ (13 mg, 0.05 mmol, 10 mol%), cyclohexanol (50 mg, 0.5 mmol, 1 equiv), and K₂CO₃ (207 mg, 1.5 mmol, 3 equiv) in 2 mL of *o*-xylene were converted according to the general protocol – method C.

Yield: 61% (112 mg, 0.31 mmol)

Appearance: colorless oil

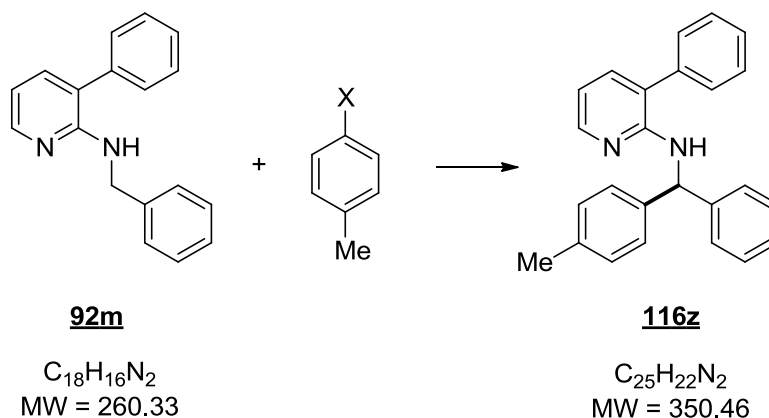
TLC: 0.7 (PE/EtOAc 9:1)

¹H NMR (CDCl₃, 200MHz): δ = 3.70 (s, 3H, CH₃), 5.18 (d, ³J = 7.5 Hz, 1H, NH), 6.48 (d, ³J = 7.5 Hz, 1H, CH), 6.63 (dd, ³J = 7.3, ³J = 5.0 Hz, 1H, H5), 6.70-6.85 (m, 3H), 7.13-7.43 (m, 12H), 8.08 (dd, ³J = 5.0, ⁴J = 1.8 Hz, 1H, H6).

¹³C NMR (CDCl₃, 50MHz): δ = 55.2 (q, CH₃), 58.6 (d, CH), 112.3 (d, C4'), 113.3 (d, C2'), 113.4 (d, C5), 119.9 (s, C3), 122.4 (d, C6'), 127.1 (d, C4''), 127.5 (d, C2'''), 127.9 (d, C2''), 128.6 (d, C4'''), 128.9 (d, C3'''), 129.3 (d, C3''), 129.6 (d, C5'), 137.3 (d, C4), 138.0 (s, C1'''), 143.3 (s, C1'), 145.1 (s, C1''), 147.4 (d, C6), 154.5 (s, C2), 159.8 (s, C3').

HRMS: calculated for C₂₅H₂₂N₂O+: [M+H]⁺ 367.1805, found [M+H]⁺ 367.1794; Δ = 3.00 ppm.

6.4.27 *N*-[4-Methylphenyl(phenyl)methyl]-3-phenylpyridin-2-amine (**116z**)



Method A

N-Benzyl-3-phenylpyridin-2-amine **92m** (130 mg, 0.5 mmol, 1 equiv), 2-(4-methylphenyl)-1,3,2-dioxaborinane **91f** (132 mg, 0.75 mmol, 1.5 equiv), and Ru₃(CO)₁₂ (16 mg, 0.025 mmol, 5 mol%) in 0.5 mL of dry pinacolone were converted according to the general protocol – method A.

Yield: 85% (149 mg, 0.43 mmol)

Method B

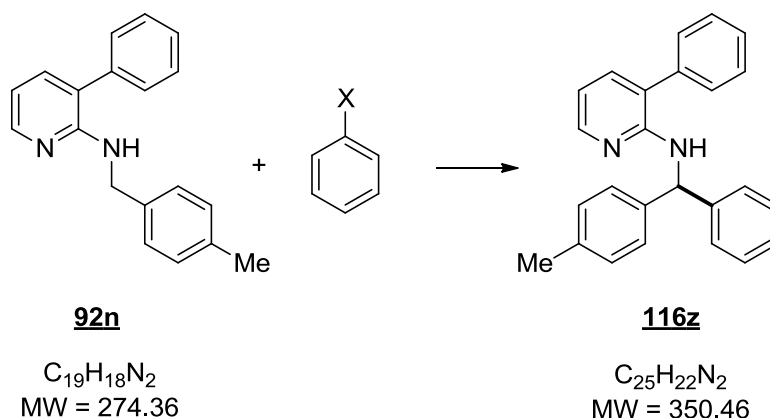
N-Benzyl-3-phenylpyridin-2-amine **92m** (130 mg, 0.5 mmol, 1 equiv), 1-bromo-4-methylbenzene **138e** (128 mg, 0.75 mmol, 1.5 equiv), [RuCl₂(*p*-cymene)]₂ (7.6 mg, 0.0125 mmol, 2.5 mol%), KOPiv (21 mg, 0.15 mmol, 30 mol%), and K₂CO₃ (207 mg, 1.5 mmol, 3 equiv) in 2 mL of dry toluene were converted according to the general protocol – method B.

Yield: 67% (117 mg, 0.34 mmol)

Method C

N-Benzyl-3-phenylpyridin-2-amine **92m** (130 mg, 0.5 mmol, 1 equiv), 1-chloro-4-methylbenzene **139c** (191 mg, 1.5 mmol, 3 equiv), [RuCl₂(*p*-cymene)]₂ (15 mg, 0.025 mmol, 5 mol%), PPh₃ (13 mg, 0.05 mmol, 10 mol%), cyclohexanol (50 mg, 0.5 mmol, 1 equiv), and K₂CO₃ (207 mg, 1.5 mmol, 3 equiv) in 2 mL of *o*-xylene were converted according to the general protocol – method C.

Yield: 39% (67 mg, 0.20 mmol)



Method A

N-(4-Methylbenzyl)-3-phenylpyridin-2-amine **92n** (137 mg, 0.5 mmol, 1 equiv), 2-phenyl-1,3,2-dioxaborinane **91a** (122 mg, 0.75 mmol, 1.5 equiv), and Ru₃(CO)₁₂ (16 mg, 0.025 mmol, 5 mol%) in 0.5 mL of dry pinacolone were converted according to the general protocol – method A.

Yield: 90% (158 mg, 0.45 mmol)

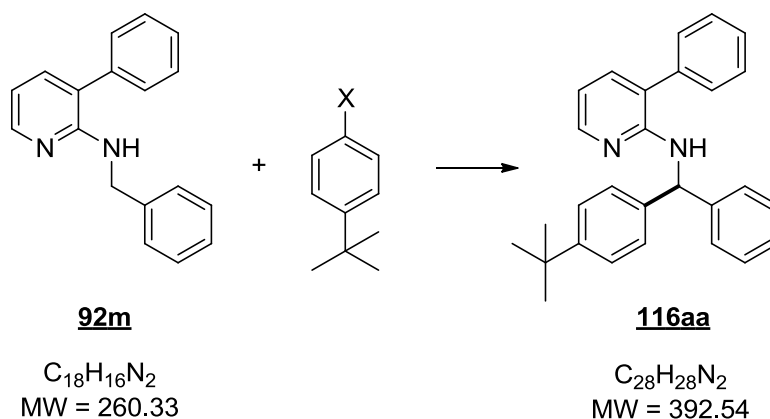
Appearance: colorless oil

TLC: 0.7 (PE/EtOAc 9:1)

¹H NMR (CDCl₃, 200MHz): δ = 2.29 (s, 3H, CH₃), 5.17 (d, ³J = 7.4 Hz, 1H, NH), 6.47 (d, ³J = 7.5 Hz, 1H, CH), 6.63 (dd, ³J = 7.2, ³J = 5.0 Hz, 1H, H5), 7.04-7.44 (m, 15H), 8.08 (dd, ³J = 5.0, ⁴J = 1.8 Hz, 1H, H6).

¹³C NMR (CDCl₃, 50MHz): δ = 21.2 (q, C_H3), 58.4 (d, C_H), 113.3 (d, C5), 122.3 (s, C3), 126.9 (d, C4'), 127.4 (d, C2''), 127.5 (d, C2'), 127.9 (d, C2'), 128.5 (d, C4''), 129.0 (d, C3''), 129.3 (d, C3'), 129.4 (d, C3'), 136.6 (d, C4), 137.3 (s, C4'), 138.1 (s, C1''), 140.5 (s, C1'), 143.6 (s, C1'), 147.4 (d, C6), 154.6 (s, C2).

HRMS: calculated for C₂₅H₂₂N₂⁺: [M+H]⁺ 351.1856, found [M+H]⁺ 351.1873; Δ = 4.84 ppm.

6.4.28 *N*-[4-(1,1-Dimethylethyl)phenyl](phenyl)methyl]-3-phenylpyridin-2-amine (**116aa**)Method A

N-Benzyl-3-phenylpyridin-2-amine **92m** (130 mg, 0.5 mmol, 1 equiv), 2-(4-(1,1-dimethylethyl)phenyl)-1,3,2-dioxaborinane **91g** (164 mg, 0.75 mmol, 1.5 equiv), and $Ru_3(CO)_{12}$ (16 mg, 0.025 mmol, 5 mol%) in 0.5 mL of dry pinacolone were converted according to the general protocol – method A.

Yield: 96% (189 mg, 0.48 mmol)

Method B

N-Benzyl-3-phenylpyridin-2-amine **92m** (130 mg, 0.5 mmol, 1 equiv), 1-bromo-4-(*tert*-butyl)benzene **138f** (160 mg, 0.75 mmol, 1.5 equiv), $[RuCl_2(p\text{-cymene})]_2$ (7.6 mg, 0.0125 mmol, 2.5 mol%), KOPiv (21 mg, 0.15 mmol, 30 mol%), and K_2CO_3 (207 mg, 1.5 mmol, 3 equiv) in 2 mL of dry toluene were converted according to the general protocol – method B.

Yield: 72% (141 mg, 0.36 mmol)

Method C

N-Benzyl-3-phenylpyridin-2-amine **92m** (130 mg, 0.5 mmol, 1 equiv), 1-(*tert*-butyl)-4-chlorobenzene **139h** (254 mg, 1.5 mmol, 3 equiv), $[RuCl_2(p\text{-cymene})]_2$ (15 mg, 0.025 mmol, 5 mol%), PPh_3 (13 mg, 0.05 mmol, 10 mol%), cyclohexanol (50 mg, 0.5 mmol, 1 equiv), and K_2CO_3 (207 mg, 1.5 mmol, 3 equiv) in 2 mL of *o*-xylene were converted according to the general protocol – method C.

Yield: 55% (107 mg, 0.28 mmol)

Appearance: colorless solid

Mp: 74-76 °C

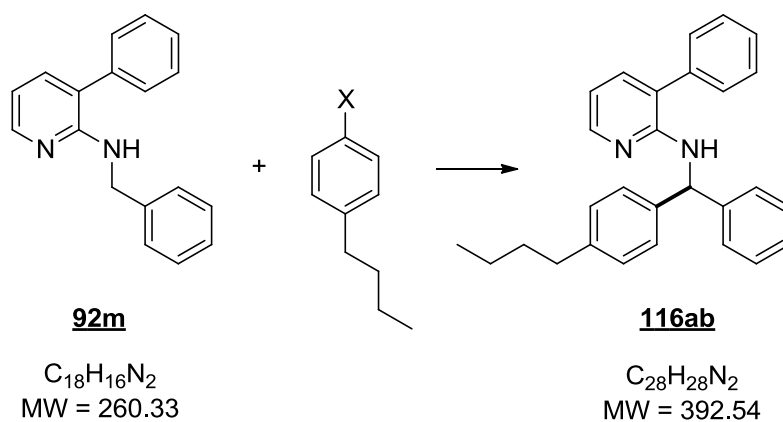
TLC: 0.7 (PE/EtOAc 9:1)

^1H NMR (CDCl₃, 200MHz): δ = 1.27 (s, 9H, C(CH₃)₃), 5.20 (d, 3J = 7.5 Hz, 1H, NH), 6.50 (d, 3J = 7.6 Hz, 1H, CH), 6.62 (dd, 3J = 7.2, 3J = 5.0 Hz, 1H, H5), 7.12-7.44 (m, 15H), 8.08 (dd, 3J = 5.0, 4J = 1.8 Hz, 1H, H6).

^{13}C NMR (CDCl₃, 50MHz): δ = 31.5 (q, C(CH₃)₃), 34.5 (s, C(CH₃)₃), 58.2 (d, CH), 113.2 (d, C5), 122.3 (s, C3), 125.5 (d, C3'), 126.9 (d, C4''), 127.2 (d, C2'''), 127.5 (d, C2'), 127.9 (d, C2''), 128.5 (d, C4'''), 129.0 (d, C3'''), 129.4 (d, C3''), 137.3 (d, C4), 138.1 (s, C1'''), 140.4 (s, C1'), 143.7 (s, C1''), 147.4 (d, C6), 149.8 (s, C4'), 154.6 (s, C2).

HRMS: calculated for C₂₈H₂₈N₂⁺: [M+H]⁺ 393.2325, found [M+H]⁺ 393.2349; Δ = 6.10 ppm.

6.4.29 *N*-[(4-Butylphenyl)(phenyl)methyl]-3-phenylpyridin-2-amine (**116ab**)



Method B

N-Benzyl-3-phenylpyridin-2-amine **92m** (130 mg, 0.5 mmol, 1 equiv), 1-bromo-4-butylbenzene **138g** (160 mg, 0.75 mmol, 1.5 equiv), [RuCl₂(*p*-cymene)]₂ (7.6 mg, 0.0125 mmol, 2.5 mol%), KOPiv (21 mg, 0.15 mmol, 30 mol%), and K₂CO₃ (207 mg, 1.5 mmol, 3 equiv) in 2 mL of dry toluene were converted according to the general protocol – method B.

Yield: 69% (135 mg, 0.35 mmol)

Method C

N-Benzyl-3-phenylpyridin-2-amine **92m** (130 mg, 0.5 mmol, 1 equiv), 1-butyl-4-chlorobenzene **139i** (254 mg, 1.5 mmol, 3 equiv), [RuCl₂(*p*-cymene)]₂ (15 mg, 0.025 mmol, 5 mol%), PPh₃ (13 mg, 0.05 mmol, 10 mol%), cyclohexanol (50 mg, 0.5 mmol, 1 equiv), and K₂CO₃ (207 mg, 1.5 mmol, 3 equiv) in 2 mL of *o*-xylene were converted according to the general protocol – method C.

Yield: 47% (92 mg, 0.24 mmol)

Appearance: colorless oil

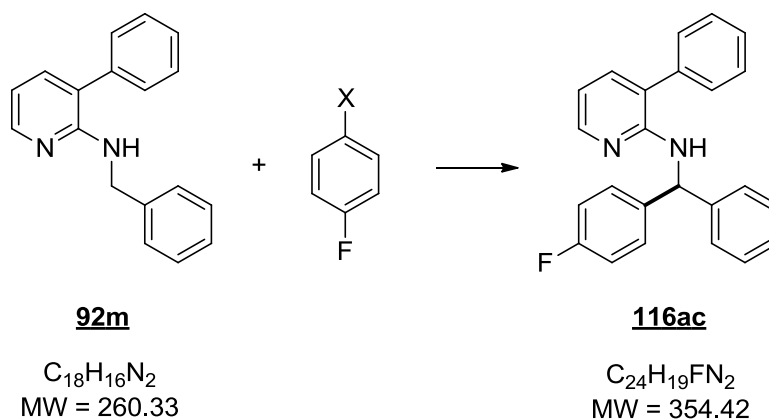
TLC: 0.7 (PE/EtOAc 9:1)

^1H NMR (CDCl₃, 200MHz): δ = 0.89 (t, 3J = 7.2 Hz, 3H, CH₃), 1.23-1.40 (m, 2H, CH₂CH₂CH₃), 1.47-1.62 (m, 2H, CH₂CH₂CH₂), 2.54 (t, 3J = 7.7 Hz, 2H, PhCH₂CH₂), 5.18 (d, 3J = 7.5 Hz, 1H, NH), 6.50 (d, 3J = 7.5 Hz, 1H, CH), 6.61 (dd, 3J = 7.2, 3J = 5.0 Hz, 1H, H5), 7.04-7.42 (m, 15H), 8.07 (dd, 3J = 5.0, 4J = 1.8 Hz, 1H, H6).

^{13}C NMR (CDCl₃, 50MHz): δ = 14.1 (q, CH₃), 22.5 (t, CH₂CH₂CH₃), 33.6 (t, CH₂CH₂CH₂), 35.4 (t, PhCH₂CH₂), 58.4 (d, CH), 113.2 (d, C5), 122.3 (s, C3), 126.9 (d, C4''), 127.4 (d, C2''), 127.5 (d, C2'), 127.9 (d, C2'), 128.5 (d, C4'''), 128.6 (d, C3'), 128.9 (d, C3'''), 129.3 (d, C3'), 137.3 (d, C4), 138.1 (s, C1'''), 140.7 (s, C1'), 141.6 (s, C4'), 143.7 (s, C1'), 147.4 (d, C6), 154.6 (s, C2).

HRMS: calculated for C₂₈H₂₈N₂⁺: [M+H]⁺ 393.2325, found [M+H]⁺ 393.2323; Δ = 0.51 ppm.

6.4.30 *N*-[(4-Fluorophenyl)(phenyl)methyl]-3-phenylpyridin-2-amine (**116ac**)



Method A

N-Benzyl-3-phenylpyridin-2-amine **92m** (130 mg, 0.5 mmol, 1 equiv), 2-(4-fluorophenyl)-1,3,2-dioxaborinane **91i** (135 mg, 0.75 mmol, 1.5 equiv), and Ru₃(CO)₁₂ (16 mg, 0.025 mmol, 5 mol%) in 0.5 mL of dry pinacolone were converted according to the general protocol – method A.

Yield: 72% (128 mg, 0.36 mmol)

Appearance: colorless solid

Mp: 79-81 °C

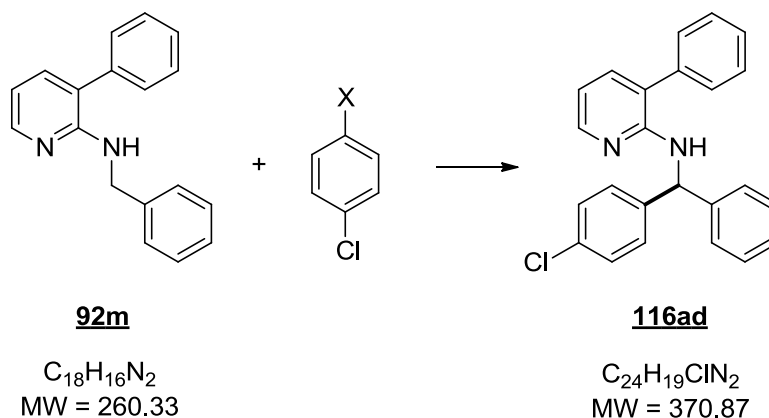
TLC: 0.7 (PE/EtOAc 9:1)

^1H NMR (CDCl₃, 200MHz): δ = 5.12 (d, 3J = 7.3 Hz, 1H, NH), 6.48 (d, 3J = 7.3 Hz, 1H, CH), 6.65 (dd, 3J = 7.3, 3J = 5.0 Hz, 1H, H5), 6.90-6.99 (m, 2H), 7.14-7.44 (m, 13H), 8.08 (dd, 3J = 5.0, 4J = 1.8 Hz, 1H, H6).

^{13}C NMR (CDCl₃, 50MHz): δ = 58.1 (d, $\underline{\text{C}}\text{H}$), 113.5 (d, C5), 115.3 (d, J_{CF} = 21.3 Hz, C3'), 122.4 (s, C3), 127.2 (d, C4''), 127.5 (d, C2'''), 128.1 (d, C2''), 128.7 (d, C4'''), 128.9 (d, C3'''), 129.1 (d, J_{CF} = 8.0 Hz, C3'), 129.4 (d, C3''), 137.4 (d, C4), 138.0 (s, C1'''), 139.2 (s, J_{CF} = 3.2 Hz, C1'), 143.2 (s, C1''), 147.3 (d, C6), 154.4 (s, C2), 161.9 (s, J_{CF} = 245.1 Hz, C4').

HRMS: calculated for C₂₄H₁₉N₂F⁺: [M+H]⁺ 355.1605, found [M+H]⁺ 355.1621; Δ = 4.51 ppm.

6.4.31 *N*-[(4-Chlorophenyl)(phenyl)methyl]-3-phenylpyridin-2-amine (**116ad**)



Method B

N-Benzyl-3-phenylpyridin-2-amine **92m** (130 mg, 0.5 mmol, 1 equiv), 1-bromo-4-chlorobenzene **138k** (143 mg, 0.75 mmol, 1.5 equiv), [RuCl₂(*p*-cymene)]₂ (7.6 mg, 0.0125 mmol, 2.5 mol%), KO_{Piv} (21 mg, 0.15 mmol, 30 mol%), and K₂CO₃ (207 mg, 1.5 mmol, 3 equiv) in 2 mL of dry toluene were converted according to the general protocol – method B.

Yield: 59% (109 mg, 0.30 mmol)

Appearance: colorless oil

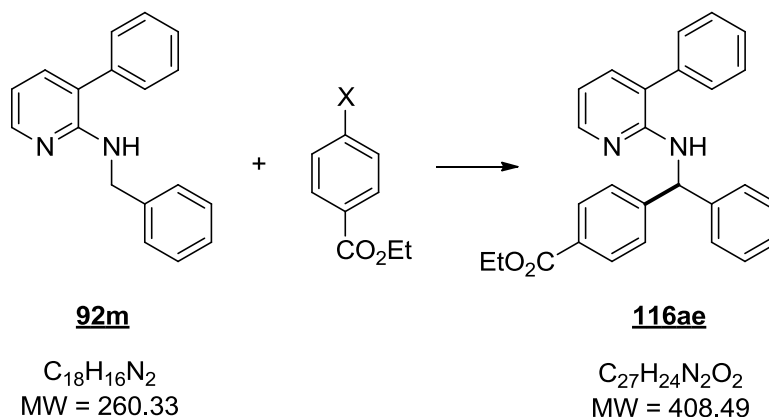
TLC: 0.7 (PE/EtOAc 9:1)

^1H NMR (CDCl₃, 200MHz): δ = 5.12 (d, 3J = 7.2 Hz, 1H, NH), 6.47 (d, 3J = 7.3 Hz, 1H, CH), 6.64 (dd, 3J = 7.2, 3J = 5.0 Hz, 1H, H5), 7.15-7.42 (m, 15H), 8.07 (dd, 3J = 5.0, 4J = 1.8 Hz, 1H, H6).

^{13}C NMR (CDCl₃, 50MHz): δ = 58.2 (d, $\underline{\text{C}}\text{H}$), 113.6 (d, C5), 122.4 (s, C3), 127.3 (d, C4''), 127.5 (d, C2'''), 128.0 (d, C2''), 128.6 (d, C4'''), 128.7 (d, C3'''), 128.9 (d, C3'), 129.4 (d, C3''), 132.7 (d, C3'), 137.4 (d, C4), 137.9 (s, C1'''), 142.0 (s, C1'), 142.9 (s, C1''), 147.3 (d, C6), 154.3 (s, C2, one phenyl-carbon is overlapping).

HRMS: calculated for $C_{24}H_{19}N_2Cl+$: $[M+H]^+$ 371.1310, found $[M+H]^+$ 371.1294; $\Delta = 4.31$ ppm.

6.4.32 Ethyl 4-[phenyl((3-phenylpyridin-2-yl)amino)methyl]benzoate (**116ae**)



Method B

N-Benzyl-3-phenylpyridin-2-amine **92m** (130 mg, 0.5 mmol, 1 equiv), ethyl 4-bromobenzoate **138i** (172 mg, 0.75 mmol, 1.5 equiv), $[RuCl_2(p\text{-cymene})]_2$ (7.6 mg, 0.0125 mmol, 2.5 mol%), KO₂Piv (21 mg, 0.15 mmol, 30 mol%), and K_2CO_3 (207 mg, 1.5 mmol, 3 equiv) in 2 mL of dry toluene were converted according to the general protocol – method B.

Yield: 42% (86 mg, 0.21 mmol)

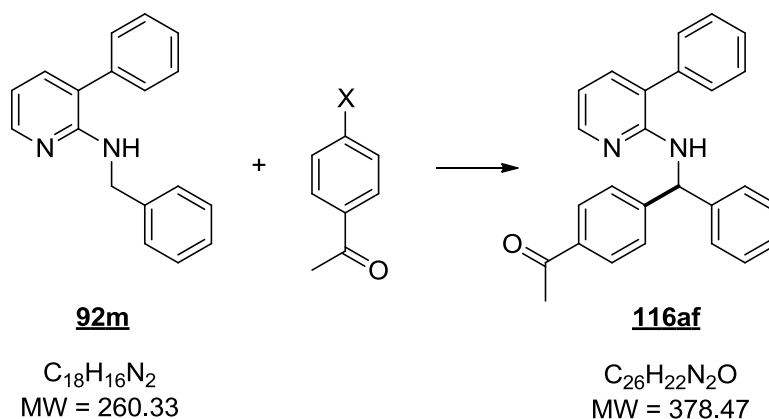
Appearance: colorless oil

TLC: 0.6 (PE/EtOAc 9:1)

1H NMR (CDCl₃, 200MHz): $\delta = 1.35$ (t, $^3J = 7.1$ Hz, 3H, CH₃), 4.33 (q, $^3J = 7.1$ Hz, 2H, CH₂), 5.17 (d, $^3J = 7.2$ Hz, 1H, NH), 6.53 (d, $^3J = 7.2$ Hz, 1H, CH), 6.66 (dd, $^3J = 7.2$, $^3J = 5.0$ Hz, 1H, H5), 7.16-7.45 (m, 13H), 7.96 (d, $^3J = 8.3$ Hz, 2H, H3'), 8.06 (dd, $^3J = 5.0$, $^4J = 1.8$ Hz, 1H, H6).

^{13}C NMR (CDCl₃, 50MHz): $\delta = 14.4$ (q, $\underline{C}H_3$), 58.7 (d, $\underline{C}H$), 60.9 (t, $\underline{C}H_2$), 113.7 (d, C5), 122.5 (s, C3), 127.3 (d, C4''), 127.4 (d, C2''), 127.6 (s, C4'), 128.0 (d, C2'), 128.8 (d, C4'''), 128.9 (d, C3'''), 129.2 (d, C3'), 129.4 (d, C3''), 129.9 (d, C3'), 137.4 (d, C4), 137.9 (s, C1'''), 142.7 (s, C1'), 147.3 (s, C6), 148.6 (d, C1'), 154.3 (s, C2), 166.6 (s, $\underline{C}O$).

HRMS: calculated for $C_{27}H_{24}N_2O_2+$: $[M+H]^+$ 409.1911, found $[M+H]^+$ 409.1907; $\Delta = 0.98$ ppm.

6.4.33 1-[4-(Phenyl((3-phenylpyridin-2-yl)amino)methyl)phenyl]ethanone (**116af**)**Method B**

N-Benzyl-3-phenylpyridin-2-amine **92m** (130 mg, 0.5 mmol, 1 equiv), 1-(4-bromophenyl)ethanone **138m** (149 mg, 0.75 mmol, 1.5 equiv), [RuCl₂(*p*-cymene)]₂ (7.6 mg, 0.0125 mmol, 2.5 mol%), KO₂Piv (21 mg, 0.15 mmol, 30 mol%), and K₂CO₃ (207 mg, 1.5 mmol, 3 equiv) in 2 mL of dry toluene were converted according to the general protocol – method B.

Yield: 41% (76 mg, 0.21 mmol)

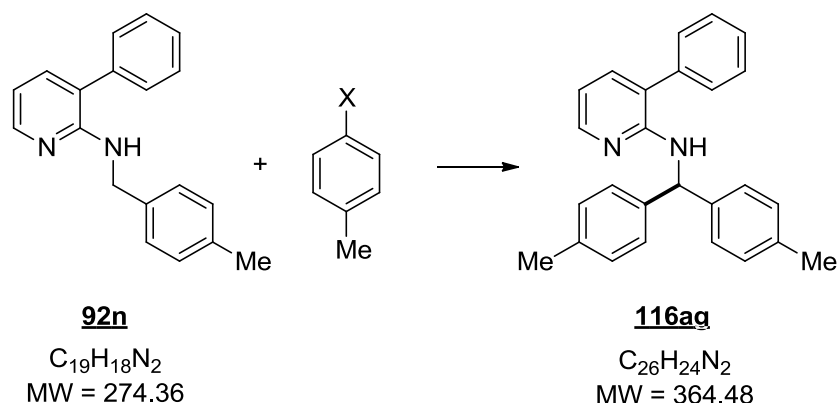
Appearance: colorless oil

TLC: 0.6 (PE/EtOAc 9:1)

¹H NMR (CDCl₃, 200MHz): δ = 2.53 (s, 3H, CH₃), 5.18 (d, ³J = 7.1 Hz, 1H, NH), 6.52 (d, ³J = 7.1 Hz, 1H, CH), 6.66 (dd, ³J = 7.2, ³J = 5.0 Hz, 1H, H5), 7.19-7.44 (m, 13H), 7.87 (d, ³J = 8.2 Hz, 2H, H3'), 8.06 (dd, ³J = 5.0, ⁴J = 1.7 Hz, 1H, H6).

¹³C NMR (CDCl₃, 50MHz): δ = 26.7 (q, CH₃), 58.7 (d, CH), 113.7 (d, C5), 122.4 (s, C3), 127.4 (d, C4'), 127.5 (d, C2''), 127.6 (s, C4'), 128.0 (d, C2''), 128.7 (d, C4''), 128.8 (d, C3''), 128.9 (d, C3'), 129.4 (d, C3'), 135.9 (d, C3'), 137.4 (d, C4), 137.8 (s, C1''), 142.6 (s, C1'), 147.3 (s, C6), 149.0 (d, C1'), 154.3 (s, C2), 197.8 (s, CO).

HRMS: calculated for C₂₆H₂₂N₂O+: [M+H]⁺ 379.1805, found [M+H]⁺ 379.1799; Δ = 1.58 ppm.

6.4.34 *N*-(Di-4-methylphenylmethyl)-3-phenylpyridin-2-amine (**116ag**)Method A

N-(4-Methylbenzyl)-3-phenylpyridin-2-amine **92n** (137 mg, 0.5 mmol, 1 equiv), 2-(4-methylphenyl)-1,3,2-dioxaborinane **91f** (132 mg, 0.75 mmol, 1.5 equiv), and $Ru_3(CO)_{12}$ (16 mg, 0.025 mmol, 5 mol%) in 0.5 mL of dry pinacolone were converted according to the general protocol – method A.

Yield: 73% (133 mg, 0.37 mmol)

Appearance: colorless solid

Mp: 127-129 °C

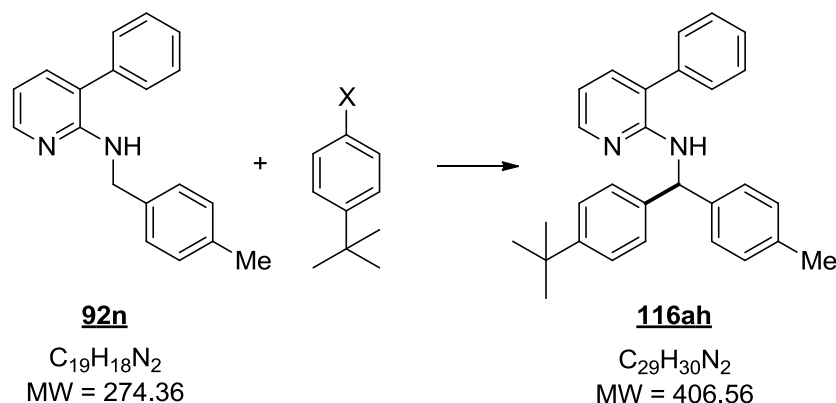
TLC: 0.8 (PE/EtOAc 9:1)

1H NMR (CDCl₃, 200MHz): δ = 2.19 (s, 6H, CH₃), 5.08 (d, 3J = 7.4 Hz, 1H, NH), 6.35 (d, 3J = 7.5 Hz, 1H, CH), 6.52 (dd, 3J = 7.2, 3J = 5.0 Hz, 1H, H5), 7.95-7.34 (m, 14H), 7.99 (dd, 3J = 5.0, 4J = 1.8 Hz, 1H, H6).

^{13}C NMR (CDCl₃, 50MHz): δ = 21.2 (q, CH₃), 58.1 (d, CH), 113.2 (d, C5), 122.3 (s, C3), 127.4 (d, C2''), 127.9 (d, C2'), 128.9 (d, C4''), 129.2 (d, C3''), 129.3 (d, C3'), 136.5 (d, C4), 137.2 (s, C4'), 138.1 (s, C1''), 140.7 (s, C1'), 147.4 (d, C6), 154.6 (s C2).

HRMS: calculated for $C_{26}H_{24}N_2$: [M+H]⁺ 365.2012, found [M+H]⁺ 365.2043; Δ = 8.48 ppm.

6.4.35 *N*-[4-(1,1-Dimethylethyl)phenyl](4-methylphenyl)methyl]-3-phenylpyridin-2-amine (116ah**)**



Method A

N-(4-Methylbenzyl)-3-phenylpyridin-2-amine **92n** (137 mg, 0.5 mmol, 1 equiv), 2-(4-(1,1-dimethylethyl)phenyl)-1,3,2-dioxaborinane **91g** (164 mg, 0.75 mmol, 1.5 equiv), and $Ru_3(CO)_{12}$ (16 mg, 0.025 mmol, 5 mol%) in 0.5 mL of dry pinacolone were converted according to the general protocol – method A.

Yield: 67% (137 mg, 0.34 mmol)

Appearance: colorless solid

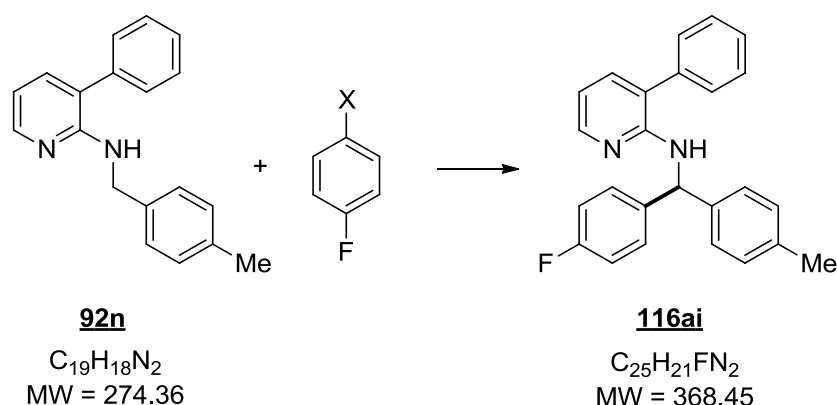
Mp: 97-99 °C

TLC: 0.8 (PE/EtOAc 9:1)

1H NMR (CDCl₃, 200MHz): δ = 1.18, (s, 9H, C(CH₃)₃), 2.20 (s, 3H, CH₃), 5.11 (d, 3J = 7.5 Hz, 1H, NH), 6.38 (d, 3J = 7.6 Hz, 1H, CH), 6.53 (dd, 3J = 7.2, 3J = 5.0 Hz, 1H, H5), 6.96-7.36 (m, 14H), 8.00 (dd, 3J = 5.0, 3J = 1.8 Hz, 1H, H6).

^{13}C NMR (CDCl₃, 50MHz): δ = 21.2 (q, C(CH₃)), 31.5 (q, C(CH₃)₃), 34.5 (s, C(CH₃)₃), 57.9 (d, CH), 113.1 (d, C5), 122.3 (s, C3), 125.4 (d, C3'), 127.1 (d, C2''), 127.4 (d, C2'), 127.9 (d, C2''), 129.0 (d, C4''), 129.2 (d, C3''), 129.3 (d, C3'), 136.5 (d, C4), 137.3 (s, C4'), 138.2 (s, C1''), 140.6 (s, C1'), 140.8 (s, C1'), 147.4 (d, C6), 149.7 (s, C4'), 154.7 (s, C2).

HRMS: calculated for $C_{29}H_{30}N_2$: [M+H]⁺ 407.2482, found [M+H]⁺ 407.2515; Δ = 8.10 ppm.

6.4.36 *N*-[(4-Fluorophenyl)(4-methylphenyl)methyl]-3-phenylpyridin-2-amine (**116ai**)Method A

N-(4-Methylbenzyl)-3-phenylpyridin-2-amine **92n** (137 mg, 0.5 mmol, 1 equiv), 2-(4-fluorophenyl)-1,3,2-dioxaborinane **91i** (135 mg, 0.75 mmol, 1.5 equiv), and $Ru_3(CO)_{12}$ (16 mg, 0.025 mmol, 5 mol%) in 0.5 mL of dry pinacolone were converted according to the general protocol – method A.

Yield: 60% (110 mg, 0.30 mmol)

Appearance: colorless solid

Mp: 100-102 °C

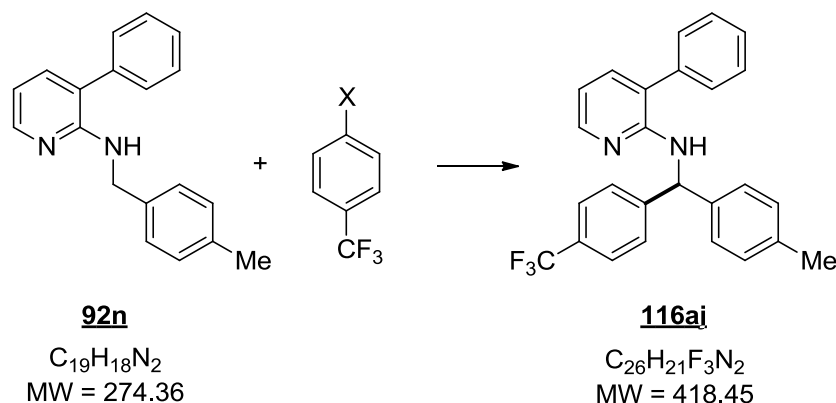
TLC: 0.8 (PE/EtOAc 9:1)

1H NMR (CDCl₃, 200MHz): δ = 2.29 (s, 3H, CH₃), 5.11 (d, 3J = 7.2 Hz, 1H, NH), 6.43 (d, 3J = 7.3 Hz, 1H, CH), 6.64 (dd, 3J = 7.3, 5.0 Hz, 1H, H5), 6.90-7.45 (m, 14H), 8.07 (dd, 3J = 5.0, 4J = 1.8 Hz, 1H, H6).

^{13}C NMR (CDCl₃, 50MHz): δ = 21.2 (q, CH₃), 57.8 (d, CH), 113.4 (d, C5), 115.3 (d, J_{CF} = 21.3 Hz, C3'), 122.4 (s, C3), 127.4 (d, C2'''), 128.0 (d, C2''), 128.9 (d, C4'), 129.1 (d, C3'''), 129.4 (d, C3''), 136.9 (d, C4), 137.4 (s, C4'), 138.0 (s, C1'''), 139.4 (s, J_{CF} = 3.1 Hz, C1'), 140.3 (s, C1''), 147.4 (d, C6), 154.5 (s, C2), 161.9 (s, J_{CF} = 244.9 Hz, C4') (C2' is overlapping).

HRMS: calculated for C₂₅H₂₁N₂F⁺: [M+H]⁺ 369.1762, found [M+H]⁺ 369.1787; Δ = 6.77 ppm.

6.4.37 3-Phenyl-N-[4-methylphenyl(4-(trifluoromethyl)phenyl)methyl]pyridin-2-amine (116aj)



Method A

N-(4-Methylbenzyl)-3-phenylpyridin-2-amine **92n** (137 mg, 0.5 mmol, 1 equiv), 2-(4-(trifluoromethyl)phenyl)-1,3,2-dioxaborinane **91k** (173 mg, 0.75 mmol, 1.5 equiv), and $Ru_3(CO)_{12}$ (16 mg, 0.025 mmol, 5 mol%) in 0.5 mL of dry pinacolone were converted according to the general protocol – method A.

Yield: 33% (69 mg, 0.17 mmol)

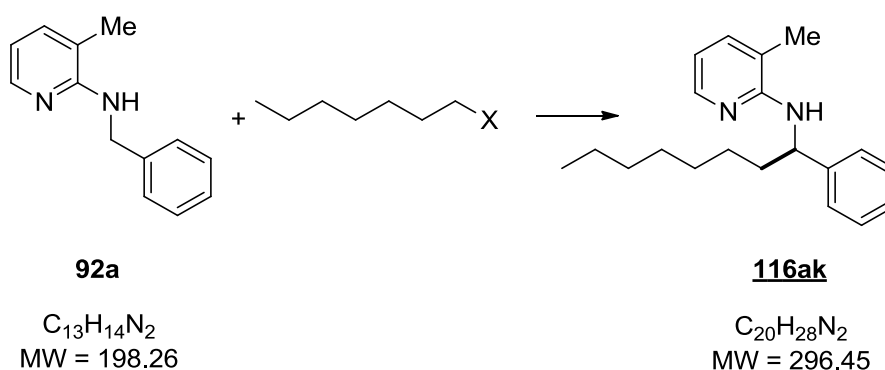
Appearance: colorless oil

TLC: 0.8 (PE/EtOAc 9:1)

1H NMR (CDCl₃, 200MHz): δ = 2.21 (s, 3H), 5.06 (d, 3J = 6.9 Hz, 1H), 6.39 (d, 3J = 6.9 Hz, 1H), 6.58 (dd, 3J = 7.3, 3J = 5.0 Hz, 1H), 7.00 (s, 4H), 7.14-7.46 (m, 10H), 7.98 (dd, 3J = 5.0, 4J = 1.8 Hz, 1H).

^{13}C NMR (CDCl₃, 50MHz): δ = 21.2 (q, \underline{CH}_3), 53.4 (d, \underline{CH}), 113.7 (d, C5), 122.5 (s, C3), 125.5 (d, J_{CF} = 3.8 Hz, C3'), 127.5 (d, C2''), 127.6 (d, C2'), 128.1 (d, C2'), 128.9 (d, C4''), 129.4 (d, C3''), 129.6 (d, C3'), 137.3 (d, C4), 137.4 (s, C4'), 137.9 (s, C1''), 139.7 (s, C1'), 147.3 (s, C1'), 147.9 (d, C6), 154.3 (s, C2) (\underline{CF}_3 and C4' are overlapping with other peaks).

HRMS: calculated for $C_{26}H_{21}N_2F_3$: $[M+H]^+$ 419.1735, found $[M+H]^+$ 419.1765; Δ = 7.16 ppm.

6.4.38 3-Methyl-N-(1-phenyloctyl)pyridin-2-amine (**116ak**)Method C

N-Benzyl-3-methylpyridin-2-amine **92a** (99 mg, 0.5 mmol, 1 equiv), 1-chlorooctane **139g** (203 mg, 1.5 mmol, 3 equiv), $[RuCl_2(p\text{-cymene})]_2$ (15 mg, 0.025 mmol, 5 mol%), PPh_3 (13 mg, 0.05 mmol, 10 mol%), cyclohexanol (50 mg, 0.5 mmol, 1 equiv), and K_2CO_3 (207 mg, 1.5 mmol, 3 equiv) in 2 mL of *o*-xylene were converted according to the general protocol – method C.

Yield: 39% (57 mg, 0.20 mmol)

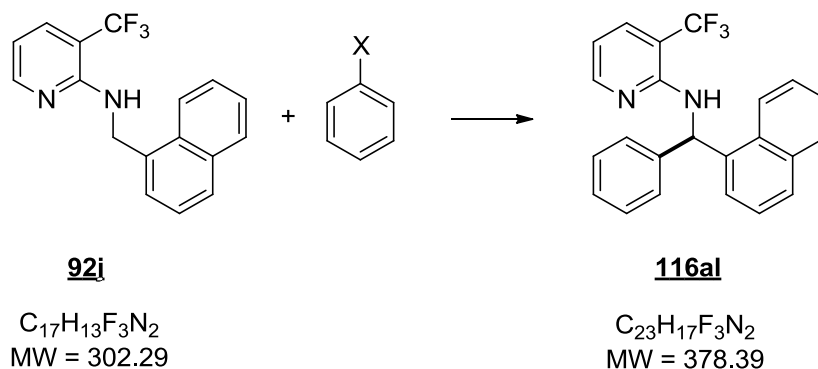
Appearance: colorless oil

TLC: 0.7 (PE/EtOAc 9:1)

1H NMR (CDCl₃, 200MHz): δ = 0.82-0.88 (m, 3H, CH₂CH₃), 1.23 (s, 10H), 1.80-1.94 (m, 2H, PhCH₂CH₂), 2.09 (s, 3H, CH₃), 4.36 (d, 3J = 7.6 Hz, 1H, NH), 5.23 (q, 3J = 7.3 Hz, 1H, CH), 6.45 (dd, 3J = 7.1, 3J = 5.1 Hz, 1H, H5), 7.14-7.39 (m, 6H, PhH & H4), 7.94 (dd, 3J = 5.0, 4J = 1.3 Hz, 1H, H6).

^{13}C NMR (CDCl₃, 50MHz): δ = 14.2 (q, C7'), 17.2 (q, CH₃), 22.7 (t, C6'), 26.5 (t, C2'), 29.3 (t, C4'), 29.7 (t, C3'), 31.9 (t, C5'), 37.6 (t, C1'), 54.7 (d, CH), 112.6 (d, C5), 116.2 (s, C3), 126.6 (d, C4''), 126.8 (d, C2''), 128.5 (d, C3''), 136.8 (d, C4), 144.7 (d, C1''), 145.7 (d, C6), 156.3 (s, C2).

HRMS: calculated for $C_{20}H_{28}N_2$: $[M+H]^+$ 297.2325, found $[M+H]^+$ 297.2319; Δ = 2.02 ppm.

6.4.39 *N*-[Naphthalen-1-yl(phenyl)methyl]-3-(trifluoromethyl)pyridin-2-amine (**116al**)Method A

N-(naphthalen-1-ylmethyl)-3-(trifluoromethyl)pyridin-2-amine **92i** (151 mg, 0.5 mmol, 1 equiv), 2-phenyl-1,3,2-dioxaborinane **91a** (122 mg, 0.75 mmol, 1.5 equiv), and $Ru_3(CO)_{12}$ (16 mg, 0.025 mmol, 5 mol%) in 0.5 mL of dry pinacolone were converted according to the general protocol – method A.

Yield: 17% (32 mg, 0.09 mmol)

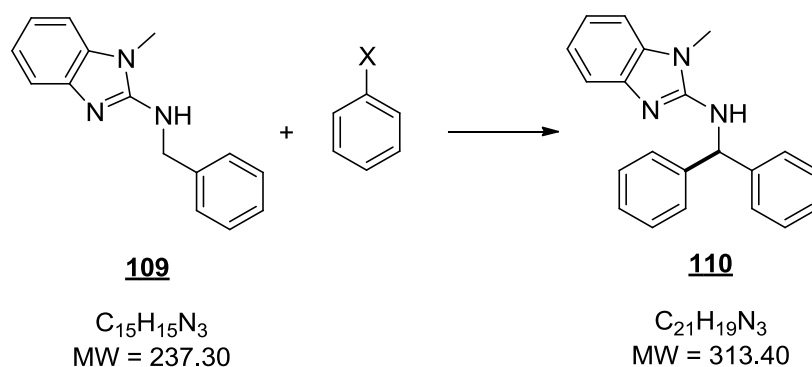
Appearance: colorless oil

TLC: 0.8 (PE/EtOAc 9:1)

1H NMR (CDCl₃, 200MHz): δ = 5.47 (d, 3J = 6.7 Hz, 1H, NH), 6.62 (dd, 3J = 7.5, 3J = 5.0 Hz, 1H, H5), 7.23-7.50 (m, 10H), 7.67 (d, 3J = 7.6 Hz, 1H), 7.77-7.91 (m, 2H), 8.03-8.08 (m, 1H), 8.20 (d, 3J = 4.3 Hz, 1H, H6).

^{13}C NMR (CDCl₃, 50MHz): δ = 55.3 (d, $\underline{C}H$), 108.7 (s, J_{CF} = 31.4 Hz, C3), 112.1 (d, C5), 124.0 (d), 124.6 (s, J_{CF} = 271.2 Hz, $\underline{C}F_3$), 125.5 (d, C2'), 125.9 (d), 126.5 (d), 127.4 (d), 127.8 (d, C3'), 128.4 (d), 128.8 (d, 2 peaks overlapping), 128.9 (d), 131.6 (s), 134.1 (s), 135.2 (d, J_{CF} = 5.1 Hz, C4), 138.1 (s, C1'), 142.3 (s, C1'), 152.1 (d, C6), 153.4 (s, C2).

HRMS: calculated for $C_{23}H_{17}N_2F_3^+$: $[M+H]^+$ 379.1422, found $[M+H]^+$ 379.1408; Δ = 3.69 ppm.

6.4.40 *N*-Benzhydryl-1-methyl-1H-benzo[d]imidazol-2-amine (**110**)Method A

N-Benzyl-1-methyl-1H-benzo[d]imidazol-2-amine **109** (119 mg, 0.5 mmol, 1 equiv), 2-phenyl-1,3,2-dioxaborinane **91a** (122 mg, 0.75 mmol, 1.5 equiv), and Ru₃(CO)₁₂ (16 mg, 0.025 mmol, 5 mol%) in 0.5 mL of dry pinacolone were converted according to the general protocol – method A.

Yield: 45% (70 mg, 0.23 mmol)

Appearance: yellow solid

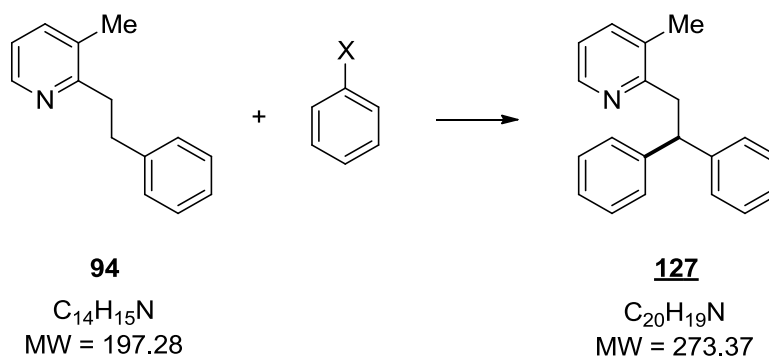
Mp: 189-191 °C

TLC: 0.3 (PE/EtOAc 2:1)

¹H NMR (CDCl₃, 200MHz): δ = 3.54 (s, 3H, CH₃, NCH₃), 4.62 (d, ³J = 6.6Hz, 1H, NH), 6.49 (d, ³J = 6.8Hz, 1H, CH), 7.07-7.10 (m, 3H), 7.29-7.49 (m, 11H).

¹³C NMR (CDCl₃, 50MHz): δ = 28.5 (q, C_{H3}), 60.5 (d, CH), 107.2 (d, C8), 117.0 (d, C5), 119.8 (d), 121.3 (d), 127.5 (d, C4'), 127.6 (d, C2'), 128.8 (d, C3'), 135.1 (s, C9), 142.2 (s, C1'), 142.4 (s, C4), 153.4 (s, C2).

HR-MS: calculated for C₂₁H₁₉N₃⁺: [M+H]⁺ 314.1652, found [M+H]⁺ 314.1660; Δ = 2.55 ppm.

6.4.41 2-(2,2-Diphenylethyl)-3-methylpyridine (**127**)

Method A

3-Methyl-2-phenethylpyridine **94** (99 mg, 0.5 mmol, 1 equiv), 2-phenyl-1,3,2-dioxaborinane **91a** (122 mg, 0.75 mmol, 1.5 equiv), and $\text{Ru}_3(\text{CO})_{12}$ (16 mg, 0.025 mmol, 5 mol%) in 0.5 mL of dry pinacolone were converted according to the general protocol – method A.

Yield: 75% (102 mg, 0.38 mmol)

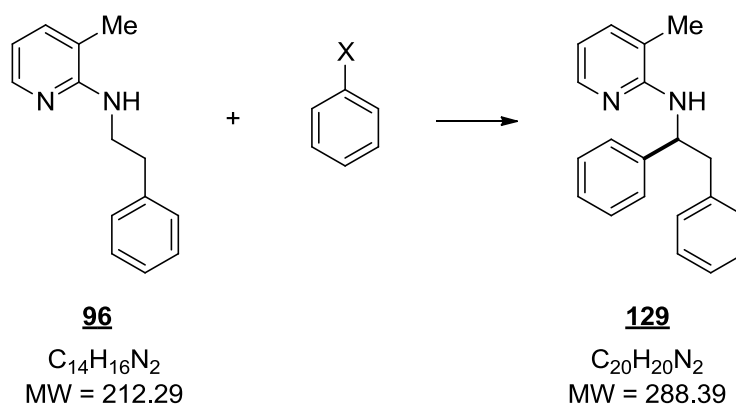
Appearance: colorless oil

TLC: 0.6 (PE/EtOAc 9:1)

^1H NMR (CDCl₃, 200MHz): δ = 2.01 (s, 3H, CH₃), 3.51 (d, 3J = 7.8 Hz, 2H, CH₂), 4.74 (t, 3J = 7.8 Hz, 1H, CH), 6.97 (dd, 3J = 7.6, 3J = 4.8 Hz, 1H, H5), 7.11-7.29 (m, 11H), 8.38 (d, 3J = 4.5 Hz, 1H, H6).

^{13}C NMR (CDCl₃, 50MHz): δ = 18.8 (q, CH₃), 40.8 (t, CH₂), 50.5 (d, CH), 121.2 (d, C5), 126.2 (d, C4'), 128.2 (d, C2'), 128.3 (d, C3'), 131.8 (s, C3), 137.6 (d, C4), 144.7 (s, C1'), 146.7 (d, C6), 158.4 (s, C2).

HRMS: calculated for C₂₀H₁₉N⁺: [M+H]⁺ 274.1590, found [M+H]⁺ 274.1601; Δ = 4.01 ppm.

6.4.42 *N*-(1,2-Diphenylethyl)-3-methylpyridin-2-amine (**129**)Method A

3-Methyl-*N*-phenethylpyridin-2-amine **96** (106 mg, 0.5 mmol, 1 equiv), 2-phenyl-1,3,2-dioxaborinane **91a** (122 mg, 0.75 mmol, 1.5 equiv), and $\text{Ru}_3(\text{CO})_{12}$ (16 mg, 0.025 mmol, 5 mol%) in 0.5 mL of dry pinacolone were converted according to the general protocol – method A.

Yield: 39% (56 mg, 0.20 mmol)

Appearance: colorless oil

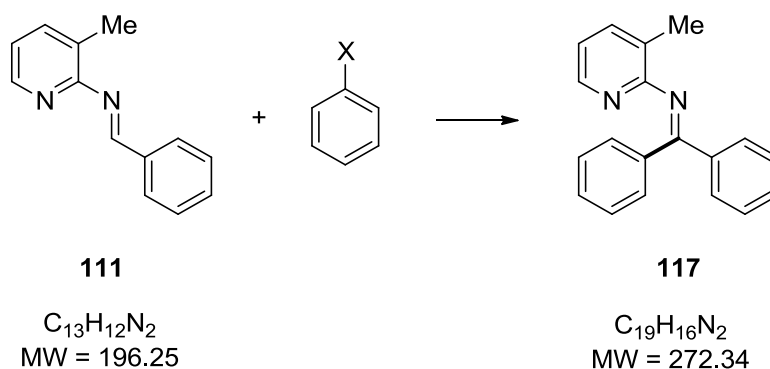
TLC: 0.6 (PE/EtOAc 9:1)

¹H NMR (CDCl₃, 200MHz): δ = 2.05 (s, 3H, CH₃), 3.21 (d, ³J = 6.6 Hz, 2H, CH₂), 4.48 (d, ³J = 7.0 Hz, 1H, NH), 5.55 (t, ³J = 6.8 Hz, 1H, CH), 6.49 (dd, ³J = 7.1, ³J = 5.1 Hz, 1H, H5), 7.06-7.35 (m, 11H), 7.96 (dd, ³J = 5.0, ⁴J = 1.3 Hz, 1H, H6).

¹³C NMR (CDCl₃, 50MHz): δ = 17.0 (q, CH₃), 43.7 (t, CH₂), 55.6 (d, CH), 112.9 (d, C5), 116.7 (s, C3), 126.5 (d, C4'), 126.7 (d, C4'), 126.9 (d, C2'), 128.3 (d, C2''), 128.4 (d, C3'), 129.6 (d, C3''), 136.9 (d, C4), 138.0 (s, C1'), 143.5 (s, C1'), 145.7 (d, C6), 156.0 (s, C2).

HRMS: calculated for C₂₀H₂₀N₂⁺: [M+H]⁺ 289.1699, found [M+H]⁺ 289.1708; Δ = 3.11 ppm.

6.4.43 *N*-(Diphenylmethylene)-3-methylpyridin-2-amine (117)



Method B

N-benzylidene-3-methylpyridin-2-amine **111** (98 mg, 0.5 mmol, 1 equiv), bromobenzene **138a** (118 mg, 0.75 mmol, 1.5 equiv), [RuCl₂(*p*-cymene)]₂ (7.6 mg, 0.0125 mmol, 2.5 mol%), KOPiv (21 mg, 0.15 mmol, 30 mol%), and K₂CO₃ (207 mg, 1.5 mmol, 3 equiv) in 2 mL of dry toluene were converted according to the general protocol – method B. Analytical data is in accordance with the literature.¹³⁰

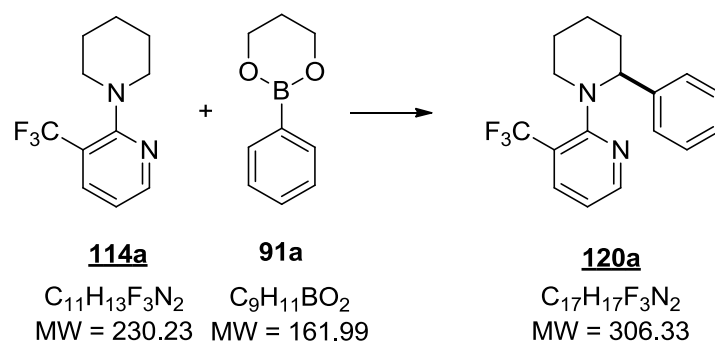
Yield: 67% (91 mg, 0.34 mmol)

Appearance: yellow oil

TLC: 0.6 (PE/EtOAc 9:1)

¹H NMR (CDCl₃, 200MHz): δ = 2.08 (s, 3H, CH₃), 6.76 (dd, ³J = 7.4, ³J = 4.9 Hz, 1H, H5), 7.20-7.42 (m, 9H), 7.82 (d, ³J = 6.5 Hz, 2H), 8.09 (d, ³J = 4.8 Hz, 1H, H6).

¹³C NMR (CDCl₃, 50MHz): δ = 17.5 (q, CH₃), 118.8 (d, C5), 122.8 (s, C3), 127.8 (d, C3'), 128.1 (d, C2'), 128.9 (d, C4'), 129.7 (s, C1'), 138.1 (d, C4), 145.7 (d, C6), 162.3 (s, C2), 169.4 (s, (Ph)₂C=N).

6.4.44 2-(2-Phenylpiperidin-1-yl)-3-(trifluoromethyl)pyridine (**120a**)Method A

2-(Piperidin-1-yl)-3-(trifluoromethyl)pyridine **114a** (115 mg, 0.5 mmol, 1 equiv), 2-phenyl-1,3,2-dioxaborinane **91a** (243 mg, 1.5 mmol, 3 equiv), and $\text{Ru}_3(\text{CO})_{12}$ (16 mg, 0.025 mmol, 5 mol%) in 0.5 mL of dry pinacolone were converted according to the general protocol – method A. The product was purified by flash column chromatography (SiO_2 900:1; PE:EtOAc = 49:1) and dried in high vacuum.

Yield: 53% (81 mg, 0.27 mmol)

Appearance: colorless solid

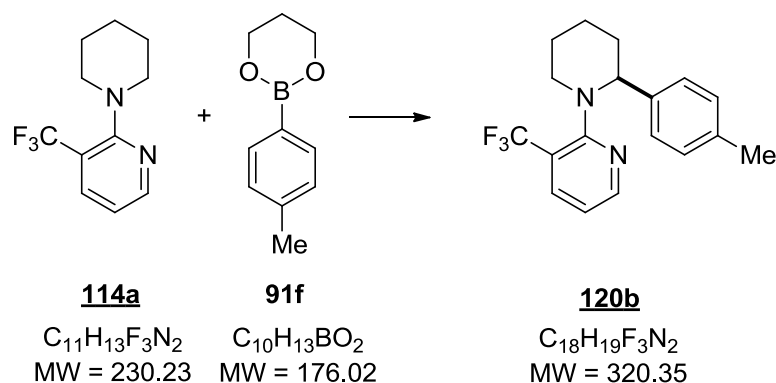
Mp: 89-91 °C

TLC: 0.8 (PE/EtOAc 9:1)

^1H NMR (CDCl_3 , 200MHz): δ = 1.43-1.96 (m, 6H), 2.77 (td, 2J = 11.2, 3J = 3.1 Hz, 1H, H6^a), 3.32-3.39 (m, 1H, H6^b), 4.46 (dd, 3J = 9.3, 3J = 3.4 Hz, 1H, H2'), 6.89 (dd, 3J = 7.8, 3J = 4.8 Hz, 1H, H5), 6.96-7.14 (m, 3H), 7.29-7.34 (m, 2H), 7.75 (dd, 3J = 7.8, 4J = 1.8 Hz, 1H, H4), 8.32 (dd, 3J = 4.6, 4J = 1.5 Hz, 1H, H6).

^{13}C NMR (CDCl_3 , 50MHz): δ = 25.0 (t, C4'), 26.2 (t, C5'), 35.7 (t, C3'), 56.8 (t, C6'), 64.4 (d, C2'), 119.1 (d, C5), 121.8 (d, J = 30.9 Hz, C3), 123.6 (s, J = 272.7 Hz, CF_3), 126.3 (d, C4'), 127.8 (d, C2''), 128.0 (d, C3''), 136.4 (q, J = 5.2 Hz, C4), 144.5 (s, C1'), 151.2 (d, C6), 162.6 (s, C2).

HR-MS: calculated for $\text{C}_{17}\text{H}_{17}\text{F}_3\text{N}_2$: $[\text{M}+\text{H}]^+$ 307.1417, found $[\text{M}+\text{H}]^+$ 307.1409; Δ = 2.60 ppm.

6.4.45 2-[2-(4-methylphenyl)piperidin-1-yl]-3-(trifluoromethyl)pyridine (**120b**)Method A

2-(Piperidin-1-yl)-3-(trifluoromethyl)pyridine **114a** (115 mg, 0.5 mmol, 1 equiv), 2-(4-methylphenyl)-1,3,2-dioxaborinane **91f** (264 mg, 1.5 mmol, 3 equiv), and $Ru_3(CO)_{12}$ (16 mg, 0.025 mmol, 5 mol%) in 0.5 mL of dry pinacolone were converted according to the general protocol – method A. The product was purified by flash column chromatography (SiO₂ 900:1; PE:EtOAc = 49:1) and dried in high vacuum.

Yield: 44% (70 mg, 0.22 mmol)

Appearance: colorless solid

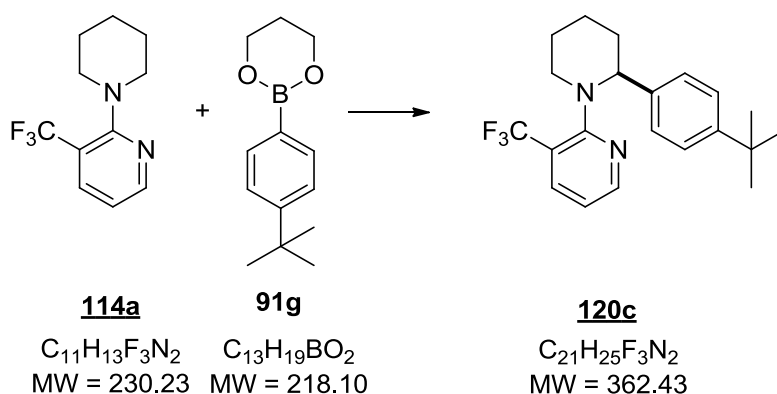
Mp: 54-56 °C

TLC: 0.8 (PE/EtOAc 9:1)

¹H NMR (CDCl₃, 200MHz): δ = 1.51-1.95 (m, 6H), 2.19 (s, 3H, CH₃), 2.78 (td, ²J = 11.2, ³J = 3.1 Hz, 1H, H6^a), 3.22-3.39 (m, 1H, H6^b), 4.45 (dd, ³J = 8.9, ³J = 3.9 Hz, 1H, H2[∘]), 6.87-6.94 (m, 3H), 7.22 (d, ³J = 8.0 Hz, 2H, H2[∘]'), 7.77 (dd, ³J = 7.8, ⁴J = 1.3 Hz, 1H, H4), 8.36 (dd, ³J = 4.7, ⁴J = 1.4 Hz, 1H, H6).

¹³C NMR (CDCl₃, 50MHz): δ = 21.1 (q, C_{CH₃}), 25.0 (t, C4[∘]), 26.2 (t, C5[∘]), 35.7 (t, C3[∘]), 56.8 (t, C6[∘]), 64.1 (d, C2[∘]), 119.0 (d, C5), 121.8 (s, J = 30.8 Hz, C3), 123.7 (s, J = 272.6 Hz, C_{F₃}), 127.9 (d, C2[∘]'), 128.6 (d, C3[∘]'), 135.7 (s, C4[∘]'), 136.4 (d, J = 5.2 Hz, C4), 141.4 (s, C1[∘]'), 151.2 (d, C6), 162.8 (s, C2).

HR-MS: calculated for C₁₈H₁₉F₃N₂⁺: [M+H]⁺ 321.1557, found [M+H]⁺ 321.1564; Δ = 2.18 ppm.

6.4.46 2-[2-(4-(1,1-Dimethylethyl)phenyl)piperidin-1-yl]-3-(trifluoromethyl)pyridine (**120c**)Method A

2-(Piperidin-1-yl)-3-(trifluoromethyl)pyridine **114a** (115 mg, 0.5 mmol, 1 equiv), 2-(4-(1,1-dimethylethyl)phenyl)-1,3,2-dioxaborinane **91g** (327 mg, 1.5 mmol, 3 equiv), and $Ru_3(CO)_{12}$ (16 mg, 0.025 mmol, 5 mol%) in 0.5 mL of dry pinacolone were converted according to the general protocol – method A. The product was purified by flash column chromatography (SiO_2 900:1; PE:EtOAc = 49:1) and dried in high vacuum.

Yield: 43% (78 mg, 0.22 mmol)

Appearance: colorless solid

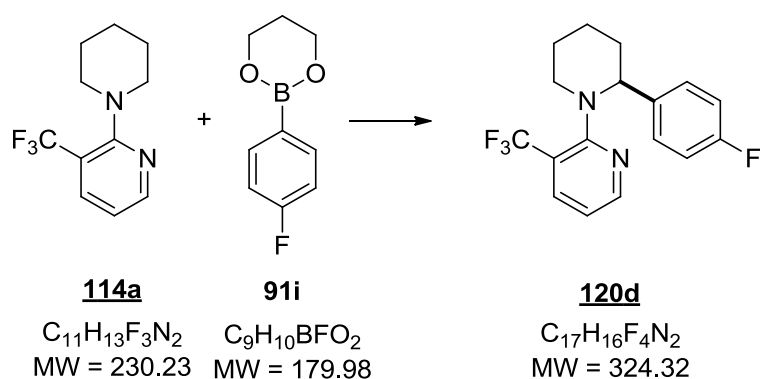
Mp: 86-88 °C

TLC: 0.8 (PE/EtOAc 9:1)

1H NMR ($CDCl_3$, 200MHz): δ = 1.20 (s, 9H, $C(CH_3)_3$), 1.51-1.90 (m, 6H), 2.81 (td, 2J = 11.1, 3J = 3.1 Hz, 1H, $H6^{a}$), 3.29-3.36 (m, 1H, $H6^{b}$), 4.50 (dd, 3J = 8.5, 3J = 4.3 Hz, 1H, $H2'$), 6.87 (dd, 3J = 7.8, 3J = 4.8 Hz, 1H, $H5$), 7.11 (d, 3J = 8.5 Hz, 2H, $H2''$), 7.22 (d, 3J = 8.5 Hz, 2H, $H3''$), 7.75 (dd, 3J = 7.8, 4J = 1.8 Hz, 1H, $H4$), 8.34 (dd, 3J = 4.8, 4J = 1.3 Hz, 1H, $H6$).

^{13}C NMR ($CDCl_3$, 50MHz): δ = 24.8 (t, $C4'$), 26.2 (t, $C5'$), 31.4 (q, $C(CH_3)_3$), 34.4 (s, $C(CH_3)_3$), 35.4 (t, $C3'$), 56.4 (t, $C6'$), 63.7 (d, $C2'$), 118.7 (d, $C5$), 121.3 (s, J = 30.8 Hz, $C3$), 123.7 (s, J = 272.6 Hz, $C(F)_3$), 124.7 (d, $C3''$), 127.5 (d, $C2''$), 136.5 (d, J = 5.2 Hz, $C4$), 141.1 (s, $C1''$), 148.8 (d, $C4'$), 151.2 (s, $C6$), 162.6 (s, $C2$).

HR-MS: calculated for $C_{21}H_{25}F_3N_2$: $[M+H]^+$ 363.2043, found $[M+H]^+$ 363.2036; Δ = 1.93 ppm.

6.4.47 2-[2-(4-Fluorophenyl)piperidin-1-yl]-3-(trifluoromethyl)pyridine (**120d**)**Method A**

2-(Piperidin-1-yl)-3-(trifluoromethyl)pyridine **114a** (115 mg, 0.5 mmol, 1 equiv), 2-(4-fluorophenyl)-1,3,2-dioxaborinane **91i** (270 mg, 1.5 mmol, 3 equiv), and $\text{Ru}_3(\text{CO})_{12}$ (16 mg, 0.025 mmol, 5 mol%) in 0.5 mL of dry pinacolone were converted according to the general protocol – method A. The product was purified by flash column chromatography (SiO_2 900:1; PE:EtOAc = 49:1) and dried in high vacuum.

Yield: 39% (62 mg, 0.20 mmol)

Appearance: pale yellow solid

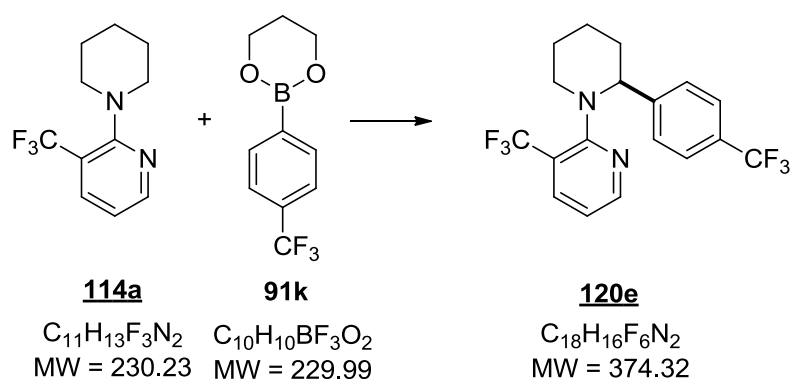
Mp: 70-72 °C

TLC: 0.4 (PE/EtOAc 9:1)

^1H NMR (CDCl_3 , 200MHz): δ = 1.46-1.94 (m, 6H), 2.75 (td, 2J = 11.2, 3J = 3.1 Hz, 1H, H6^a), 3.28-3.38 (m, 1H, H6^b), 4.43 (dd, 2J = 9.7, 3J = 3.3 Hz, 1H, H2'), 6.73-6.83 (m, 2H), 6.95 (dd, 3J = 7.8, 3J = 4.8 Hz, 1H, H5), 7.23-7.30 (m, 2H), 7.78 (dd, 3J = 7.8, 3J = 1.6 Hz, 1H, H4), 8.35 (dd, 3J = 4.7, 4J = 1.4 Hz, 1H, H6).

^{13}C NMR (CDCl_3 , 50MHz): δ = 24.8 (t, C4'), 26.0 (t, C5'), 35.6 (t, C3'), 56.8 (t, C6'), 63.6 (d, C2'), 114.4 (d, J = 21.4 Hz, C3''), 119.2 (d, C5), 121.9 (q, J = 30.8 Hz, C3), 123.4 (q, J = 272.7 Hz, $\underline{\text{C}}\text{F}_3$), 129.4 (d, J = 7.7 Hz, C2'), 136.2 (q, J = 5.3 Hz, C4), 140.0 (d, J = 3.2 Hz, C1'), 151.1 (d, C6), 161.2 (d, J = 243.7 Hz, C4''), 162.5 (s, C2).

HR-MS: calculated for $\text{C}_{17}\text{H}_{16}\text{F}_4\text{N}_2$: $[\text{M}+\text{H}]^+$ 325.1322, found $[\text{M}+\text{H}]^+$ 325.1317; Δ = 1.54 ppm.

6.4.48 3-(Trifluoromethyl)-2-[2-(4-(trifluoromethyl)phenyl)piperidin-1-yl]pyridine (**120e**)Method A

2-(Piperidin-1-yl)-3-(trifluoromethyl)pyridine **114a** (115 mg, 0.5 mmol, 1 equiv), 2-(4-(trifluoromethyl)phenyl)-1,3,2-dioxaborinane **91k** (345 mg, 1.5 mmol, 3 equiv), and $Ru_3(CO)_{12}$ (16 mg, 0.025 mmol, 5 mol%) in 0.5 mL of dry pinacolone were converted according to the general protocol – method A. The product was purified by flash column chromatography (SiO_2 900:1; PE:EtOAc = 49:1) and dried in high vacuum.

Yield: 35% (65 mg, 0.18 mmol)

Appearance: pale yellow solid

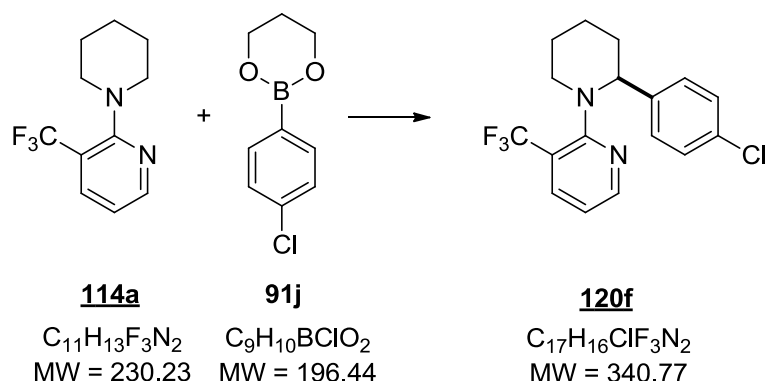
Mp: 60-62 °C

TLC: 0.5 (PE/EtOAc 9:1)

1H NMR ($CDCl_3$, 200MHz): δ = 1.53-1.93 (m, 6H), 2.74 (td, 2J = 11.6, 3J = 2.5 Hz, 1H, H6^a), 3.35-3.40 (m, 1H, H6^b), 4.53 (dd, 2J = 10.9, 3J = 2.4 Hz, 1H, H2'), 6.95 (dd, 3J = 7.7, 3J = 4.9 Hz, 1H, H5), 7.35 (d, 3J = 8.3, 2H, H2''), 7.42 (d, 3J = 8.3, 2H, H3''), 7.80 (dd, 3J = 7.8, 3J = 1.7 Hz, 1H, H4), 8.32 (dd, 3J = 4.8, 4J = 1.4 Hz, 1H, H6).

^{13}C NMR ($CDCl_3$, 50MHz): δ = 24.7 (t, C4'), 26.0 (t, C5'), 35.6 (t, C3'), 56.9 (t, C6'), 64.0 (d, C2'), 119.3 (d, C5), 121.7 (q, J = 30.9 Hz, C3), 123.4 (q, J = 272.8 Hz, $\underline{C}F_3$), 124.2 (q, J = 271.8 Hz, $\underline{C}F_3$), 124.8 (d, J = 3.8 Hz, C3''), 128.1 (d, C2''), 128.4 (d, J = 32.3 Hz, C4''), 136.5 (q, J = 5.2 Hz, C4), 148.6 (s, C1''), 151.1 (d, C6), 162.0 (s, C2).

HR-MS: calculated for $C_{18}H_{16}F_6N_2$: $[M+H]^+$ 375.1290, found $[M+H]^+$ 375.1280; Δ = 2.67 ppm.

6.4.49 2-[2-(4-Chlorophenyl)piperidin-1-yl]-3-(trifluoromethyl)pyridine (**120f**)Method A

2-(Piperidin-1-yl)-3-(trifluoromethyl)pyridine **114a** (115 mg, 0.5 mmol, 1 equiv), 2-(4-chlorophenyl)-1,3,2-dioxaborinane **91j** (294 mg, 1.5 mmol, 3 equiv), and $Ru_3(CO)_{12}$ (16 mg, 0.025 mmol, 5 mol%) in 0.5 mL of dry pinacolone were converted according to the general protocol – method A. The product was purified by flash column chromatography (SiO₂ 900:1; PE:EtOAc = 49:1) and dried in high vacuum.

Yield: 34% (58 mg, 0.17 mmol)

Appearance: colourless oil

TLC: 0.4 (PE/EtOAc 9:1)

¹H NMR (CDCl₃, 200MHz): δ = 1.48-1.91 (m, 6H), 2.73 (td, 2J = 11.6, 3J = 2.5 Hz, 1H, H6^a), 3.31-3.36 (m, 1H, H6^b), 4.42 (dd, 3J = 10.8, 3J = 2.5 Hz, 1H, H2'), 6.94 (dd, 3J = 7.7, 3J = 4.9 Hz, 1H, H5), 7.06 (d, 3J = 8.3 Hz, 2H, H2''), 7.24 (d, 3J = 8.3 Hz, 2H, H3''), 7.78 (dd, 3J = 7.8, 4J = 1.7 Hz, 1H, H4), 8.34 (dd, 3J = 4.7, 4J = 1.5 Hz, 1H, H6).

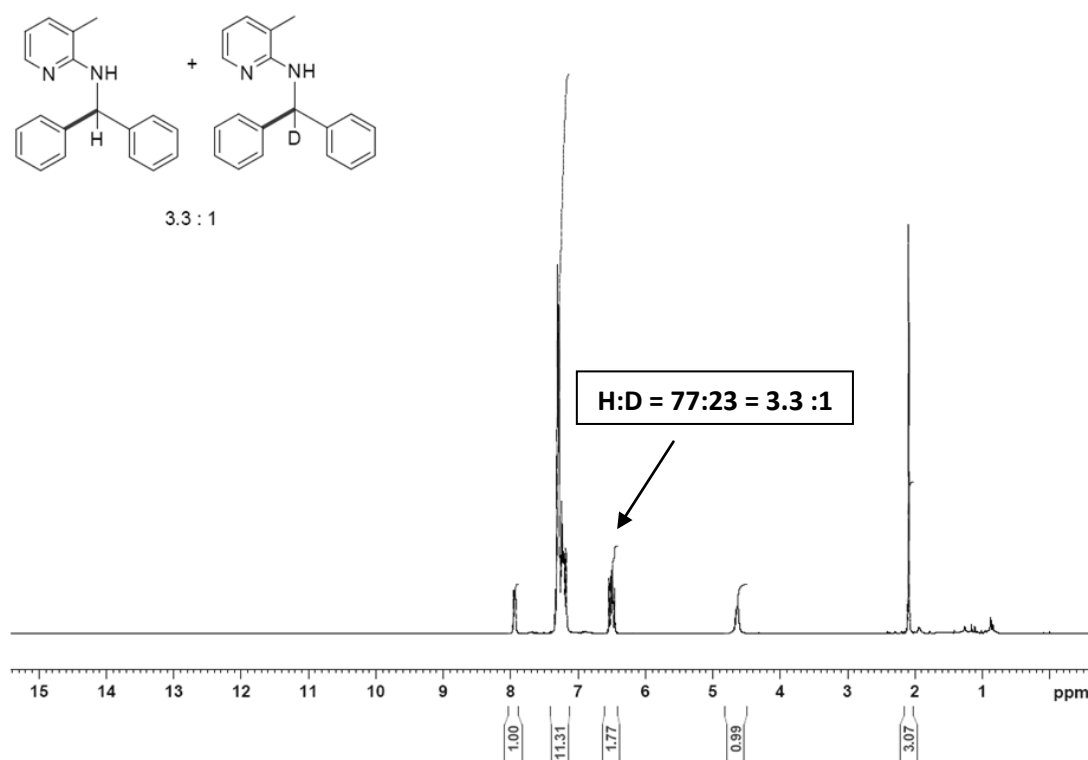
¹³C NMR (CDCl₃, 50MHz): δ = 24.8 (t, C4'), 26.0 (t, C5'), 35.6 (t, C3'), 56.9 (t, C6'), 63.7 (d, C2'), 119.2 (d, C5), 121.8 (q, J = 30.9 Hz, C3), 123.4 (q, J = 272.7 Hz, $\underline{C}F_3$), 127.9 (d, C2''), 239.3 (d, C3''), 131.7 (s, C4''), 136.3 (d, J = 5.2 Hz, C4), 142.9 (s, C1''), 151.2 (d, C6), 162.3 (s, C2).

HR-MS: calculated for $C_{17}H_{16}F_3N_2Cl$: $[M+H]^+$ 341.1027, found $[M+H]^+$ 341.1035; Δ = 2.35 ppm.

6.5 KIE Experiments

6.5.1 Ru(0) Intermolecular Competition Experiment

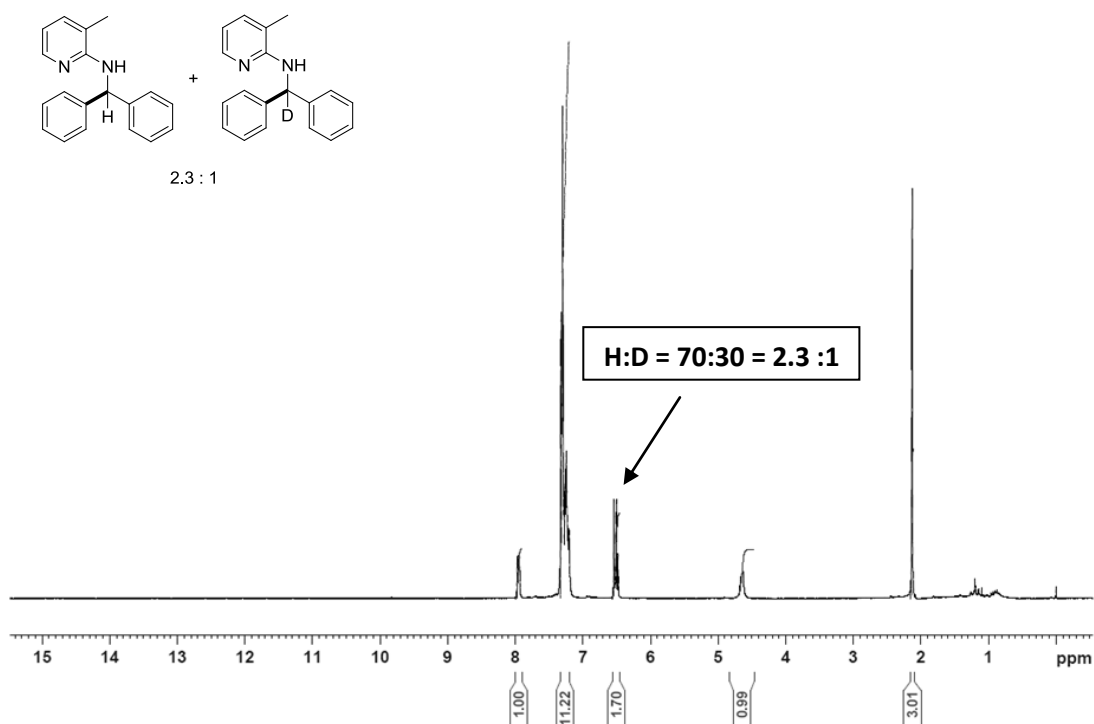
N-Benzyl-3-methylpyridin-2-amine **92a** (99 mg, 0.5 mmol, 1 equiv), double deuterated *N*-benzyl-3-methylpyridin-2-amine **113** (100 mg, 0.5 mmol, 1 equiv), 2-phenyl-1,3,2-dioxaborinane **91a** (81 mg, 0.5 mmol, 1 equiv), Ru₃(CO)₁₂ (16 mg, 0.025 mmol, 5 mol%), and 0.5 mL dry pinacolone were placed in an oven-dried 6 mL-vial with septum screw cap and a magnetic stirring bar. The reaction was carried out according to the general method A. The mixture of products was isolated and analyzed by ¹H-NMR. The proton of the corresponding C–H is overlapping with the H5 of the pyridine group. Therefore, the value of the integral is 0.77 which corresponds to a H:D mixture of 77:33 = 3.3:1. → **KIE = 3.3**.



6.5.2 Ru(0) Intramolecular Competition Experiment

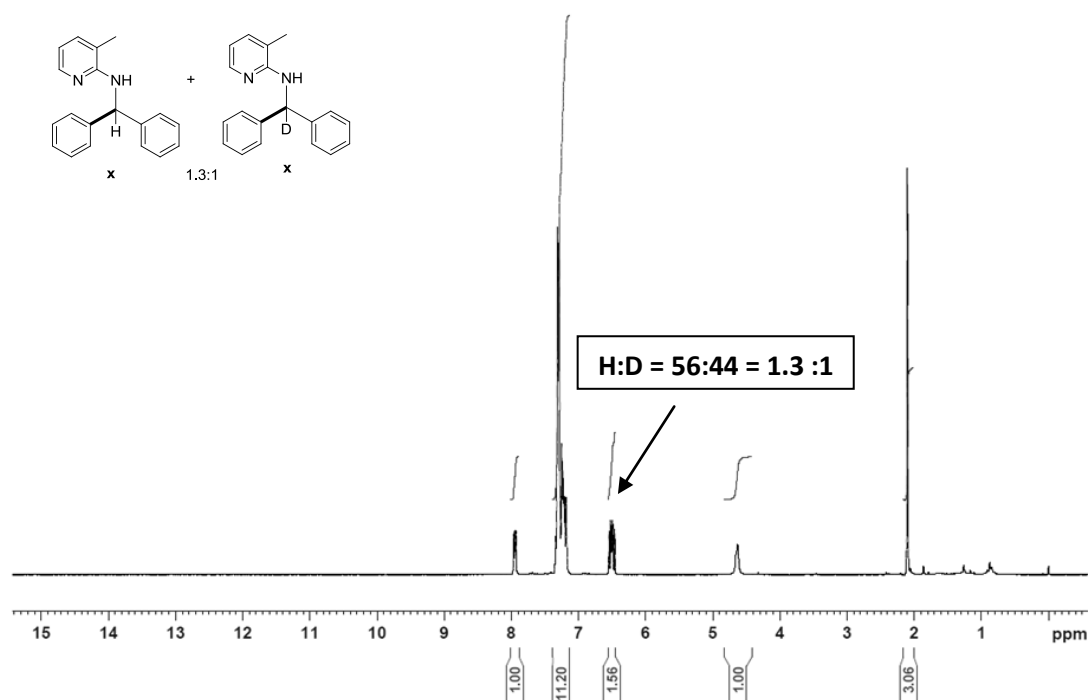
The single deuterated *N*-benzyl-3-methylpyridin-2-amine **112** (99 mg, 0.5 mmol, 1 equiv), 2-phenyl-1,3,2-dioxaborinane **91a** (81 mg, 0.5 mmol, 1 equiv), Ru₃(CO)₁₂ (16 mg, 0.025 mmol, 5 mol%) and 0.5 mL dry pinacolone were converted according to the general protocol - method A. The mixture of products was isolated and analyzed by ¹H-NMR. The proton of the

corresponding C–H is overlapping with the H5 of the pyridine group. Therefore, the value of the integral is 0.70 which corresponds to a H:D mixture of 70:30 = 2.3:1. → **KIE = 2.3**



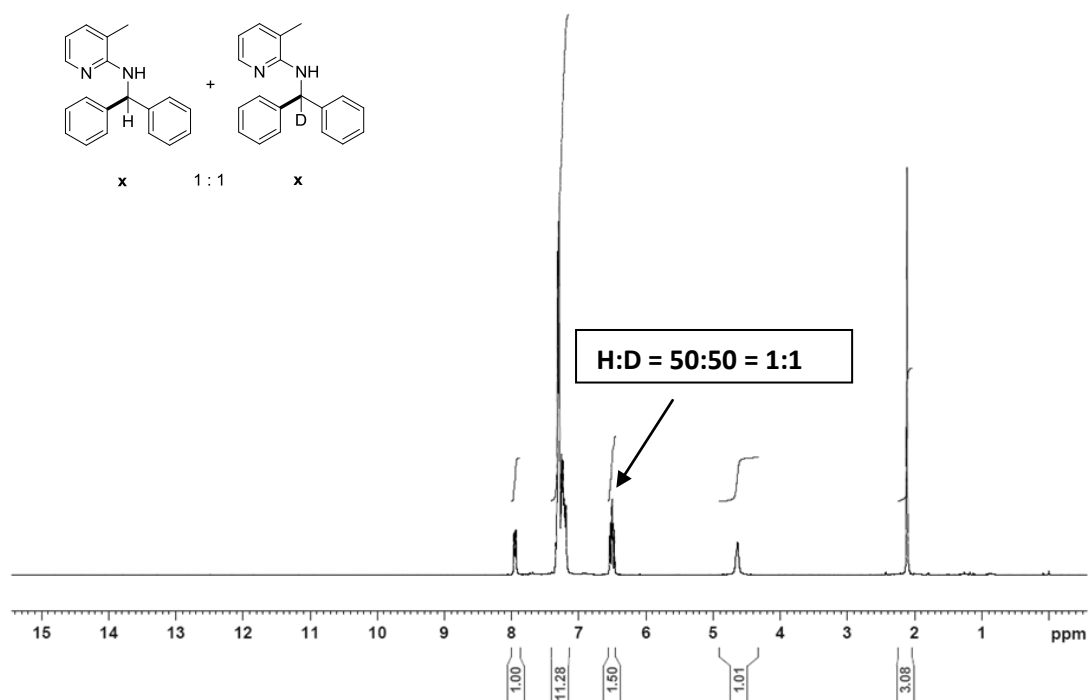
6.5.3 Ru(II) Intermolecular Competition Experiment

N-Benzyl-3-methylpyridin-2-amine **92a** (99 mg, 0.5 mmol, 1 equiv), the double deuterated *N*-benzyl-3-methylpyridin-2-amine **113** (100 mg, 0.5 mmol, 1 equiv), bromobenzene **138a** (79 mg, 0.5 mmol, 1 equiv), [RuCl₂(*p*-cymene)]₂ (7.6 mg, 0.0125 mmol, 2.5 mol%), KOPiv (21 mg, 0.15 mmol, 30 mol%), and K₂CO₃ (207 mg, 1.5 mmol, 3 equiv) in 2 mL of dry toluene were converted according to the general protocol - method B. The mixture of products was isolated and analyzed by ¹H-NMR. The proton of the corresponding C–H is overlapping with the H5 of the pyridine group. Therefore, the value of the integral is 0.56 which corresponds to a H:D mixture of 56:44 = 1.3:1. → **KIE = 1.3**



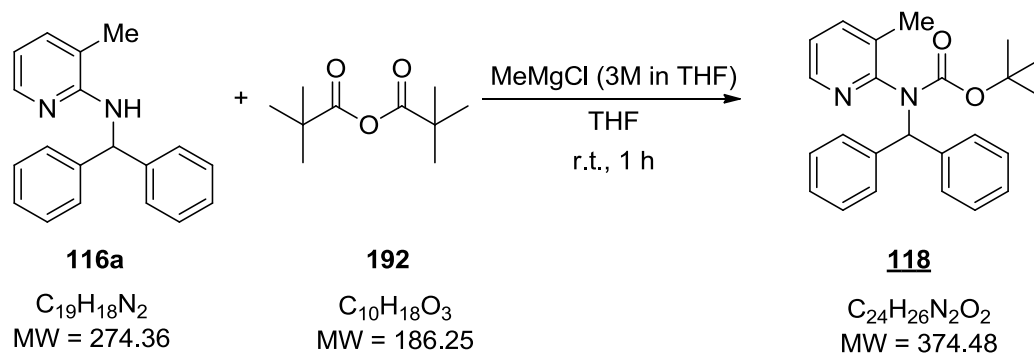
6.5.4 Ru(II) Intramolecular Competition Experiment

The single deuterated *N*-benzyl-3-methylpyridin-2-amine **112** (99 mg, 0.5 mmol, 1 equiv), bromobenzene **138a** (79 mg, 0.5 mmol, 1 equiv), [RuCl₂(*p*-cymene)]₂ (7.6 mg, 0.0125 mmol, 2.5 mol%), KOPiv (21 mg, 0.15 mmol, 30 mol%), and K₂CO₃ (207 mg, 1.5 mmol, 3 equiv) in 2 mL of dry toluene were converted according to the general protocol - method B. The mixture of products was isolated and analyzed by ¹H-NMR. The proton of the corresponding C–H is overlapping with the H5 of the pyridine group. Therefore, the value of the integral is 0.50 which corresponds to a H:D mixture of 50:50 = 1:1. → **KIE = 1**



6.6 Directing Group Cleavage

6.6.1 *tert*-Butyl benzhydryl(3-methylpyridin-2-yl)carbamate (**118**)



A 3M solution of CH_3MgCl in THF (1.2 mL, 3.6 mmol, 1.2 equiv) was added dropwise to a solution of *N*-benzhydryl-3-methylpyridin-2-amine **116a** (822 mg, 3 mmol, 1 equiv) in dry THF (20 mL) at r.t., and the mixture was stirred for 10 min at that temperature. Di-*tert*-butyl dicarbonate **192** (1.96 g, 9 mmol, 3 equiv) was dissolved in 10 mL THF and then added slowly to the solution. The stirring was continued at r.t. for 1 h. Then the reaction was quenched with H_2O , and the resulting solution was extracted with DCM (3 x 50 mL). The combined organic layers were washed with brine, dried over Na_2SO_4 , and concentrated *in*

vacuo. The resulting crude product was purified by flash column chromatography (SiO₂ 100:1; PE:EtOAc = 19:1).

Yield: 92% (1.03 g, 2.76 mmol)

Appearance: colorless solid

Mp: 114-115 °C

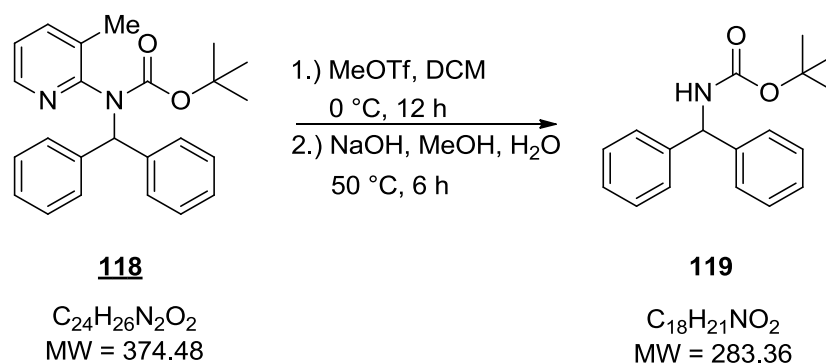
TLC: 0.4 (PE/EtOAc 5:1)

¹H NMR (CDCl₃, 200MHz): δ = 1.27 (s, 9H), 2.03 (s, 3H), 6.56 (s, 1H), 6.92-7.30 (m, 10 H), 7.69 (s; 2H), 8.29 (d, *J* = 4.4 Hz, 1H).

¹³C NMR (CDCl₃, 50MHz): δ = 17.7, 28.1, 67.0, 80.7, 122.3, 126.9, 127.8, 129.9, 132.2, 138.8, 139.6, 146.0, 153.2, 153.9.

HRMS: calculated for C₂₄H₂₆N₂O₂: [M+H]⁺ 375.2067, found [M+H]⁺ 375.2057.

6.6.2 *tert*-Butyl benzhydrylcarbamate (**119**)



Methyl trifluoromethanesulfonate (45 mg, 0.275 mmol, 1.1 equiv.) was added dropwise to a solution of **118** (94 mg, 0.25 mmol, 1 equiv) in DCM (6 mL) at 0 °C, and the resulting solution was stirred for 12 h at that temperature. Then the solvent was removed under vacuum, and the residue was dissolved in MeOH (3 mL). A 2M aq NaOH solution (1.5 mL) was added, and stirring was continued at 50 °C for 6 h. The solvents were removed, and the resulting residue was extracted with DCM (3 x 5 mL). The combined organic layers were washed with brine, dried over Na₂SO₄, and concentrated *in vacuo*. The residue was recrystallized from MeOH-water to give the desired product. Analytical data is in accordance with the literature.¹³¹

Yield: 91% (64 mg, 0.23 mmol)

Appearance: colorless solid

Mp: 121-122 °C (lit. 121-123 °C)

TLC: 0.5 (PE/EtOAc 5:1)

¹H NMR (CDCl₃, 200MHz): δ = 1.43 (s, 9H), 5.17 (s, 1H), 5.90 (s, 1H), 7.22-7.36 (m, 10 H).

¹³C NMR (CDCl₃, 50MHz): δ = 28.3, 58.4, 79.8, 127.2, 127.3, 128.6, 142.1, 155.0.

6.7 DFT Calculation

Computational Details. All calculations were performed using the Gaussian 03 software package,¹³² and the PBE1PBE functional without symmetry constraints. That functional uses a hybrid generalized gradient approximation (GGA), including 25 % mixture of Hartree-Fock¹³³ exchange with DFT exchange-correlation, given by Perdew, Burke and Ernzerhof functional (PBE).¹³⁴ The optimized geometries were obtained with the 6-31G(d,p) basis sets. Frequency calculations were performed to confirm the nature of the stationary points, yielding one imaginary frequency for the transition states and none for the minima. Each transition state was further confirmed by following its vibrational mode downhill on both sides and obtaining the minima presented on the energy profiles.

7. Literature

¹ For an insightful perspective on the historical development of cross-coupling reactions, see: Johansson Seechurn, C. C. C.; Kitching, M. O.; Colacot, T. J.; Snieckus, V. *Angew. Chem., Int. Ed.* **2012**, *51*, 5062-5085.

² Heck, R. F.; Nolley, J. P. *J. Org. Chem.* **1972**, *37*, 2320-2322.

³ For Nobel Lecture, see: Negishi, E. *Angew. Chem.* **2011**, *123*, 6870-6897; *Angew. Chem., Int. Ed.* **2011**, *50*, 6738-6764.

⁴ For Nobel Lecture, see: Suzuki, A. *Angew. Chem.* **2011**, *123*, 6854-6869; *Angew. Chem., Int. Ed.* **2011**, *50*, 6722-6737.

⁵ L. Ackermann in *Modern Arylation Methods* (Ed.: L. Ackermann), Wiley-VCH, Weinheim, **2009**, pp. 1 – 24.

⁶ Larsen, R. D.; King, A. O.; Chen, C. Y.; Corley, E. G.; Foster, B. S.; Roberts, F. E.; Yang, C.; Lieberman, D. R.; Reamer, R. A.; et al. *J. Org. Chem.* **1994**, *59*, 6391-4.

⁷ King, A. O.; Corley, E. G.; Anderson, R. K.; Larsen, R. D.; Verhoeven, T. R.; Reider, P. J.; Xiang, Y. B.; Belley, M.; Leblanc, Y.; et al. *J. Org. Chem.* **1993**, *58*, 3731-5.

⁸ O. Loiseleur, D. Kaufmann, S. Abel, H. M. Buerger, M. Meisenbach, B. Schmitz, G. Sedelmeier, WO-Patent 03066613, 2003.

⁹ R. H. Crabtree in *The Organometallic Chemistry of the Transition Metals*, 5th ed., John Wiley & Sons, Hoboken, NJ, **2009**, p. 227.

¹⁰ Miyaura N.; Suzuki, A. *J. Chem. Soc. Chem. Commun.* **1979**, 866-867.

¹¹ Negishi, E.; King, A. O.; Okukado, N. *J. Org. Chem.* **1977**, *42*, 1821-1823.

¹² Scott, W. J.; Crisp, G. T.; Stille, J. K. *J. Am. Chem. Soc.* **1984**, *106*, 4630-4632.

¹³ For recent reviews on C–H activation, see (a) Ackermann, L. *Chem. Rev.* **2011**, *111*, 1315-1345. (b) Yeung, C. S.; Dong, V. M. *Chem. Rev.* **2011**, *111*, 1215-1292. (c) Baudoin, O. *Chem. Soc. Rev.* **2011**, *40*, 4902-4911. (d) Cho, S. H.; Kim, J. Y.; Kwak, J.; Chang, S. *Chem. Soc. Rev.* **2011**, *40*, 5068-5083. (e) Schnürch, M.; Dastbaravardeh, N.; Ghobrial, M.; Mrozek, B.; Mihovilovic, M. D. *Curr. Org. Chem.* **2011**, *15*, 2694-2730. (f) Colby, D. A.; Bergman, R. G.; Ellman, J. A. *Chem. Rev.* **2010**, *110*, 624-655. (g) Daugulis, O. *Top. Curr. Chem.* **2010**, *292*, 57–84. (h) Fagnou, K. *Top. Curr. Chem.* **2010**, *292*, 35–56. (i) Ackermann, L., Vicente, R., Kapdi, A.R. *Angew. Chem. Int. Ed.* **2009**, *48*, 9792-9826. (j) McGlacken, G. P.; Bateman, L. M. *Chem. Soc. Rev.* **2009**, *38*, 2447-2464.

¹⁴ Dyker, G.; Editor *Handbook of C–H Transformations: Applications in Organic Synthesis, Volume 2*, 2005.

¹⁵ For recent papers on sp² C-H bond functionalization, see (a) Ackermann, L.; Diers, E.; Manvar, A. *Org. Lett.* **2012**, *14*, 1154-1157. (b) Ackermann, L.; Pospesch, J.; Graczyk, K.; Rauch, K. *Org. Lett.* **2012**, *14*, 930-933. (c) Wencel-Delord, J.; Nimphius, C.; Patureau, F. W.; Glorius, F. *Angew. Chem., Int. Ed.* **2012**, *51*, 2247-2251. (d) Tauchert, M. E.; Incarvito, C. D.; Rheingold, A. L.; Bergman, R. G.; Ellman, J. A. *J. Am. Chem. Soc.* **2012**, *134*, 1482-1485. (e) Flegeau, E. F.; Bruneau, C.; Dixneuf, P. H.; Jutand, A. *J. Am. Chem. Soc.* **2011**, *133*, 10161-10170. (f) Shiota, H.; Ano, Y.; Aihara, Y.; Fukumoto, Y.; Chatani, N. *J. Am. Chem. Soc.* **2011**, *133*, 14952-14955.

¹⁶ For selected papers on sp³ C-H bond functionalization, see (a) Sundararaju, B.; Achard, M.; Sharma, G. V. M.; Bruneau, C. *J. Am. Chem. Soc.* **2011**, *133*, 10340-10343. (b) Pan, S.; Endo, K.; Shibata, T. *Org. Lett.* **2011**, *13*,

4692-4695. (c) Ghobrial, M.; Harhammer, K.; Mihovilovic, M. D.; Schnürch, M. *Chem. Commun.* **2010**, 46, 8836-8838. (d) Rousseaux, S.; Gorelsky, S. I.; Chung, B. K. W.; Fagnou, K. *J. Am. Chem. Soc.* **2010**, 132, 10692-10705. (e) Jazzar, R.; Hitce, J.; Renaudat, A.; Sofack-Kreutzer, J.; Baudoin, O. *Chem. Eur. J.* **2010**, 16, 2654-2672. (f) Shabashov, D.; Daugulis, O. *Org. Lett.* **2005**, 7, 3657-3659.

¹⁷ For selected papers on diarylmethylamines, see (a) McCauley, J. P., Jr.; Dantzman, C. L.; King, M. M.; Ernst, G. E.; Wang, X.; Brush, K.; Palmer, W. E.; Frieze, W.; Andisik, D. W.; Hoesch, V.; Doring, K.; Hulsizer, J.; Bui, K. H.; Liu, J.; Hudzik, T. J.; Wesolowski, S. S. *Bioorg. Med. Chem. Lett.* **2012**, 22, 1169-1173. (b) Jolidon, S.; Alberati, D.; Dowle, A.; Fischer, H.; Hainzl, D.; Narquizian, R.; Norcross, R.; Pinard, E. *Bioorg. Med. Chem. Lett.* **2008**, 18, 5533-5536. (c) Song, K.-S.; Lee, S.-H.; Chun, H. J.; Kim, J. Y.; Jung, M. E.; Ahn, K.; Kim, S.-U.; Kim, J.; Lee, J. *Bioorg. Med. Chem.* **2008**, 16, 4035-4051.

¹⁸ Gillard, M.; Van Der Perren, C.; Moguilevsky, N.; Massingham, R.; Chatelain, P. *Mol. Pharm.* **2002**, 61, 391-399.

¹⁹ Lowes, D. J.; Guiguemde, W. A.; Connelly, M. C.; Zhu, F.; Sigal, M. S.; Clark, J. A.; Lemoff, A. S.; Derisi, J. L.; Wilson, E. B.; Guy, R. K. *J. Med. Chem.* **2011**, 54, 7477-7485.

²⁰ Bilge, S. S.; Bozkurt, A.; Ilkaya, F.; Ciftcioglu, E.; Kesim, Y.; Uzbay, T. I. *Eur. J. Pharm.* **2012**, 681, 44-49.

²¹ For reviews, see (a) Marques, C. S.; Burke, A. J. *ChemCatChem* **2011**, 3, 635-645. (b) Nugent, T. C.; El-Shazly, M. *Adv. Synth. Catal.* **2010**, 352, 753-819. (c) Schmidt, F.; Stemmler, R. T.; Rudolph, J.; Bolm, C. *Chem. Soc. Rev.* **2006**, 35, 454-470.

²² For selected books, see (a) L. Ackermann in *Modern Arylation Methods* (Ed.: L. Ackermann), Wiley-VCH, Weinheim, **2009**. (b) Dyker, G.; Editor *Handbook of C-H Transformations: Applications in Organic Synthesis, Volume 2*, 2005. (c) R. H. Crabtree in *The Organometallic Chemistry of the Transition Metals*, 5th ed., John Wiley & Sons, Hoboken, NJ, **2009**. (d) J. Hartwig in *Organotransition Metal Chemistry – from bonding to catalysis*, University Science Books, Sausalito, CA, **2010**.

²³ J. Hartwig in *Organotransition Metal Chemistry – from bonding to catalysis*, University Science Books, Sausalito, CA, **2010**, p. 540.

²⁴ J. Hartwig in *Organotransition Metal Chemistry – from bonding to catalysis*, University Science Books, Sausalito, CA, **2010**, p. 541.

²⁵ R. H. Crabtree in *The Organometallic Chemistry of the Transition Metals*, 5th ed., John Wiley & Sons, Hoboken, NJ, **2009**, pp. 88-93.

²⁶ M. Bochmann in *Organometallics 1*, Oxford University Press, Oxford, **1994**.

²⁷ J. Hartwig in *Organotransition Metal Chemistry – from bonding to catalysis*, University Science Books, Sausalito, CA, **2010**, p. 53.

²⁸ J. Hartwig in *Organotransition Metal Chemistry – from bonding to catalysis*, University Science Books, Sausalito, CA, **2010**, p. 33-39.

²⁹ Grubbs, R. H.; Miyashita, A. *J. Am. Chem. Soc.* **1978**, 100, 7418-20.

³⁰ R. H. Crabtree in *The Organometallic Chemistry of the Transition Metals*, 5th ed., John Wiley & Sons, Hoboken, NJ, **2009**, p. 60-61.

³¹ J. Hartwig in *Organotransition Metal Chemistry – from bonding to catalysis*, University Science Books, Sausalito, CA, **2010**, pp. 57-59.

- ³² Kobayashi, S.; Mori, Y.; Fossey, J. S.; Salter, M. M. *Chem. Rev.* **2011**, *111*, 2626-2704.
- ³³ J. Hartwig in *Organotransition Metal Chemistry – from bonding to catalysis*, University Science Books, Sausalito, CA, **2010**, p. 543.
- ³⁴ J. Hartwig in *Organotransition Metal Chemistry – from bonding to catalysis*, University Science Books, Sausalito, CA, **2010**, p. 544.
- ³⁵ J. Hartwig in *Organotransition Metal Chemistry – from bonding to catalysis*, University Science Books, Sausalito, CA, **2010**, p. 893.
- ³⁶ R. H. Crabtree in *The Organometallic Chemistry of the Transition Metals*, 5th ed., John Wiley & Sons, Hoboken, NJ, **2009**, pp. 153-156.
- ³⁷ J. Hartwig in *Organotransition Metal Chemistry – from bonding to catalysis*, University Science Books, Sausalito, CA, **2010**, p. 264.
- ³⁸ R. H. Crabtree in *The Organometallic Chemistry of the Transition Metals*, 5th ed., John Wiley & Sons, Hoboken, NJ, **2009**, p. 68.
- ³⁹ J. Hartwig in *Organotransition Metal Chemistry – from bonding to catalysis*, University Science Books, Sausalito, CA, **2010**, p. 265.
- ⁴⁰ Chatt, J.; Davidson, J. M. *J. Chem. Soc.* **1965**, 843-55.
- ⁴¹ Kakiuchi, F.; Chatani, N. *Adv. Synth. Catal.* **2003**, *345*, 1077-1101.
- ⁴² Janowicz, A. H.; Bergman, R. G. *J. Am. Chem. Soc.* **1982**, *104*, 352-4.
- ⁴³ Jones, W. D.; Feher, F. J. *Organometallics* **1983**, *2*, 562-563.
- ⁴⁴ Shilov, A. E.; Shul'pin, G. B. *Chem. Rev.* **1997**, *97*, 2879-2932.
- ⁴⁵ J. Hartwig in *Organotransition Metal Chemistry – from bonding to catalysis*, University Science Books, Sausalito, CA, **2010**, p. 895.
- ⁴⁶ J. Hartwig in *Organotransition Metal Chemistry – from bonding to catalysis*, University Science Books, Sausalito, CA, **2010**, p. 326.
- ⁴⁷ J. Hartwig in *Organotransition Metal Chemistry – from bonding to catalysis*, University Science Books, Sausalito, CA, **2010**, p. 332.
- ⁴⁸ J. Hartwig in *Organotransition Metal Chemistry – from bonding to catalysis*, University Science Books, Sausalito, CA, **2010**, p. 36.
- ⁴⁹ J. Hartwig in *Organotransition Metal Chemistry – from bonding to catalysis*, University Science Books, Sausalito, CA, **2010**, p. 550.
- ⁵⁰ Morikawa, K.; Benedict, W. S.; Taylor, H. S. *J. Am. Chem. Soc.* **1936**, *58*, 1445-1449.
- ⁵¹ Hodges, R. J.; Garnett, J. L. *J. Catal.* **1969**, *13*, 83-98.
- ⁵² Kleiman, J. P.; Dubeck, M. *J. Am. Chem. Soc.* **1963**, *85*, 1544-5.
- ⁵³ Ackermann, L. *Chem. Rev.* **2011**, *111*, 1315-1345.

- ⁵⁴ Seki, M.; Nagahama, M. *J. Org. Chem.* **2011**, *76*, 10198-10206.
- ⁵⁵ Hong, P.; Yamazaki, H.; Sonogashira, K.; Hagihara, N. *Chem. Lett.* **1978**, 535.
- ⁵⁶ Akita, Y.; Inoue, A.; Yamamoto, K.; Ohta, A.; Kurihara, T.; Shimizu, M. *Heterocycles* **1985**, *23*, 2327-33.
- ⁵⁷ Cho, S. H.; Kim, J. Y.; Kwak, J.; Chang, S. *Chem. Soc. Rev.* **2011**, *40*, 5068-5083.
- ⁵⁸ Liegault, B.; Petrov, I.; Gorelsky, S. I.; Fagnou, K. *J. Org. Chem.*, **2010**, *75*, 1047-1060.
- ⁵⁹ Ackermann, L.; Vicente, R.; Kapdi, A.R. *Angew. Chem. Int. Ed.* **2009**, *48*, 9792-9826.
- ⁶⁰ Lafrance, M.; Lapointe, D.; Fagnou, K. *Tetrahedron* **2008**, *64*, 6015-6020.
- ⁶¹ J. Hartwig in *Organotransition Metal Chemistry – from bonding to catalysis*, University Science Books, Sausalito, CA, **2010**, p. 945.
- ⁶² Yanagisawa, S.; Ueda, K.; Sekizawa, H.; Itami, K. *Programmed J. Am. Chem. Soc.*, **2009**, *131*, 14622-14623.
- ⁶³ Albrecht, M. *Chem. Rev.* **2010**, *110*, 576-623.
- ⁶⁴ R. H. Crabtree in *The Organometallic Chemistry of the Transition Metals*, 5th ed., John Wiley & Sons, Hoboken, NJ, **2009**, p. 68.
- ⁶⁵ For selected papers on palladium catalyzed cyclometalation assisted C–H activation, see (a) Shabashov, D.; Daugulis, O. *Org. Lett.* **2005**, *7*, 3657-3659. (b) Zaitsev, V. G.; Shabashov, D.; Daugulis, O. *J. Am. Chem. Soc.* **2005**, *127*, 13154-13155. (c) Daugulis, O.; Do, H.-Q.; Shabashov, D. *Acc. Chem. Res.* **2009**, *42*, 1074-1086. (d) Koley, M.; Dastbaravardeh, N.; Schnürch, M.; Mihovilovic, M. D. *ChemCatChem*, Ahead of Print.
- ⁶⁶ For selected papers on ruthenium catalyzed cyclometalation assisted C–H activation, see (a) Deng, G.; Zhao, L.; Li, C.-J. *Angew. Chem., Int. Ed.* **2008**, *47*, 6278-6282 (b) Martinez, R.; Genet, J.-P.; Darses, S. *Chem. Commun.* **2008**, 3855-3857. (c) Ackermann, L.; Althammer, A.; Born, R. *Synlett* **2007**, 2833-2836. (d) Matsuura, Y.; Tamura, M.; Kochi, T.; Sato, M.; Chatani, N.; Kakiuchi, F. *J. Am. Chem. Soc.* **2007**, *129*, 9858-9859. (e) Ackermann, L. *Org. Lett.* **2005**, *7*, 3123-3125. (f) Oi, S.; Ogino, Y.; Fukita, S.; Inoue, Y. *Org. Lett.* **2002**, *4*, 1783-1785. (g) Oi, S.; Fukita, S.; Hirata, N.; Watanuki, N.; Miyano, S.; Inoue, Y. *Org. Lett.* **2001**, *3*, 2579-2581. (h) Jun, C.-H. *Chem. Commun.* **1998**, 1405-1406.
- ⁶⁷ Murai, S.; Kakiuchi, F.; Sekine, S.; Tanaka, Y.; Kamatani, A.; Sonoda, M.; Chatani, N. *Nature* **1993**, 366, 529-31.
- ⁶⁸ Thirunavukkarasu, V. S.; Donati, M.; Ackermann, L. *Org. Lett.* **2012**, *14*, 3416-3419.
- ⁶⁹ Ueno, S.; Chatani, N.; Kakiuchi, F. *J. Am. Chem. Soc.* **2007**, *129*, 6098-6099.
- ⁷⁰ Padala, K.; Pimparkar, S.; Madasamy, P.; Jeganmohan, M. *Chem. Commun.* **2012**, *48*, 7140-7142.
- ⁷¹ Chinnagolla, R. K.; Jeganmohan, M. *Chem. Commun.* **2012**, *48*, 2030-2032.
- ⁷² Hashimoto, Y.; Hirano, K.; Satoh, T.; Kakiuchi, F.; Miura, M. *Org. Lett.* **2012**, *14*, 2058-2061.
- ⁷³ Ackermann, L.; Mulzer, M. *Org. Lett.* **2008**, *10*, 5043-5045.
- ⁷⁴ Kim, J. Y.; Park, S. H.; Ryu, J.; Cho, S. H.; Kim, S. H.; Chang, S. *J. Am. Chem. Soc.* **2012**, *134*, 9110-9113.
- ⁷⁵ Ackermann, L.; Born, R.; Alvarez-Bercedo, P. *Angew. Chem., Int. Ed.* **2007**, *46*, 6364-6367.

- ⁷⁶ Ackermann, L.; Vicente, R.; Althammer, A. *Org. Lett.* **2008**, *10*, 2299-2302.
- ⁷⁷ Wang, C.; Chen, H.; Wang, Z.; Chen, J.; Huang, Y. *Angew. Chem., Int. Ed.* **2012**, *51*, 7242-7245.
- ⁷⁸ Oi, S.; Sasamoto, H.; Funayama, R.; Inoue, Y. *Chem. Lett.* **2008**, *37*, 994-995.
- ⁷⁹ Umeda, N.; Hirano, K.; Satoh, T.; Miura, M. *J. Org. Chem.* **2009**, *74*, 7094-7099.
- ⁸⁰ Matsuura, Y.; Tamura, M.; Kochi, T.; Sato, M.; Chatani, N.; Kakiuchi, F. *J. Am. Chem. Soc.* **2007**, *129*, 9858-9859.
- ⁸¹ Li, H.; Wei, W.; Xu, Y.; Zhang, C.; Wan, X. *Chem. Commun.* **2011**, *47*, 1497-1499.
- ⁸² Chatani, N.; Asaumi, T.; Ikeda, T.; Yorimitsu, S.; Ishii, Y.; Kakiuchi, F.; Murai, S. *J. Am. Chem. Soc.* **2000**, *122*, 12882-12883.
- ⁸³ Kakiuchi, F.; Igi, K.; Matsumoto, M.; Chatani, N.; Murai, S. *Chem. Lett.* **2001**, 422-423.
- ⁸⁴ Saidi, O.; Marafie, J.; Ledger, A. E. W.; Liu, P. M.; Mahon, M. F.; Kociok-Kohn, G.; Whittlesey, M. K.; Frost, C. G. *J. Am. Chem. Soc.* **2011**, *133*, 19298-19301.
- ⁸⁵ For selected papers on CMD mechanism, see (a) Gorelsky, S. I.; Lapointe, D.; Fagnou, K. *J. Org. Chem.* **2012**, *77*, 658-668. (b) Flegeau, E. F.; Bruneau, C.; Dixneuf, P. H.; Jutand, A. *J. Am. Chem. Soc.* **2011**, *133*, 10161-10170. (c) Rousseaux, S.; Gorelsky, S. I.; Chung, B. K. W.; Fagnou, K. *J. Am. Chem. Soc.* **2010**, *132*, 10692-10705. (d) Gorelsky, S.; Lapointe, D.; Fagnou, K. *J. Am. Chem. Soc.* **2008**, *130*, 10848-10849.
- ⁸⁶ Campos, K. R. *Chem. Soc. Rev.* **2007**, *36*, 1069-1084.
- ⁸⁷ McNally, A.; Prier, C. K.; MacMillan, D. W. C. *Science* **2011**, *334*, 1114-1117.
- ⁸⁸ For selected papers on the direct functionalization of THIQ, see (a) Hari, D.-P.; König, B. *Org. Lett.* **2011**, *13*, 3852. (b) Boess, E.; Sureshkumar, D.; Sud, A.; Wirtz, C.; Fares, C.; Klussmann, M. *J. Am. Chem. Soc.* **2011**, *133*, 8106. (c) Liu, P.; Zhou, C.-Y.; Xiang, S.; Che, C.-M. *Chem. Commun.* **2010**, *46*, 2739. (d) Li, Z.; Yu, R.; Li, H. *Angew. Chem., Int. Ed.* **2008**, *47*, 7497. (e) Murahashi, S.-I.; Nakae, T.; Terai, H.; Komiyama, N. *J. Am. Chem. Soc.* **2008**, *130*, 11005.
- ⁸⁹ (a) Ghobrial, M.; Harhammer, K.; Schnürch, M.; Mihovilovic, M. D. *Chem. Commun.* **2010**, *46*, 8836-8838. (b) Ghobrial, M.; Schnürch, M.; Mihovilovic, M. D. *J. Org. Chem.* **2011**, *76*, 8781-8793.
- ⁹⁰ For selected papers on C-H activation adjacent to nitrogen, see (a) Martinez, R.; Simon, M.-O.; Chevalier, R.; Pautigny, C.; Genet, J.-P.; Darses, S. *J. Am. Chem. Soc.* **2009**, *131*, 7887-7895. (b) Simon, M.-O.; Martinez, R.; Genet, J.-P.; Darses, S. *Adv. Synth. Catal.* **2009**, *351*, 153-157. (c) Ueno, S.; Chatani, N.; Kakiuchi, F. *J. Am. Chem. Soc.* **2007**, *129*, 6098-6099.
- ⁹¹ Murai, S.; Chatani, N.; Asaumi, T.; Yorimitsu, S.; Ikeda, T.; Kakiuchi, F. *J. Am. Chem. Soc.* **2001**, *123*, 10935-10941.
- ⁹² Jun, C. H.; Hwang, D. C.; Na, S. J. *Chem. Commun.* **1998**, *13*, 1405-1406.
- ⁹³ Sames, D.; Pastine, S. J.; Gribkov, D. V. *J. Am. Chem. Soc.* **2006**, *128*, 14220-14221.
- ⁹⁴ Prokopcova, H.; Bergman, S. D.; Aelvoet, K.; Smout, V.; Herrebout, W.; Van der Veken, B.; Meerpoel, L.; Maes, B. U. W. *Chem. Eur. J.* **2010**, *16*, 13063-13067.

- ⁹⁵ Jana, K. J.; Grimme, S.; Studer, A. *Chem. Eur. J.* **2009**, *15*, 9078-9084.
- ⁹⁶ For the *N*-Boc deprotection, see (a) Norma, J. T.; Simon, W. M.; Frost, H. N.; Ewing, M. *Tetrahedron Lett.* **2004**, *45*, 905-906. (b) Srinivasan, N.; Yurek-George, A.; Ganesan, A. *Mol. Div.* **2005**, *9*, 291-293.
- ⁹⁷ Mkhaliid, I. A. I., Barnard, J. H., Marder, T. B., Murphy, J. M., Hartwig, J. F. *Chem. Rev.* **2010**, *110*, 890-931.
- ⁹⁸ Tagata, T.; Nishida, M.; Nishida, A. *Tetrahedron Lett.* **2009**, *50*, 6176-6179.
- ⁹⁹ Gribkov, D. V.; Pastine, S. J.; Schnürch, M.; Sames, D. *J. Am. Chem. Soc.* **2007**, *129*, 11750-11755.
- ¹⁰⁰ Gomez-Gallego, M.; Sierra, M. A. *Chem. Rev.* **2011**, *111*, 4857-4963.
- ¹⁰¹ Simmons, E. M.; Hartwig, J. F. *Angew. Chem., Int. Ed.* **2012**, *51*, 3066-3072.
- ¹⁰² For recent papers on [RuCl₂(p-cymene)]₂ catalyzed C-H bond functionalization, see (a) Ackermann, L.; Pospech, J.; Graczyk, K.; Rauch, K. *Org. Lett.* **2012**, *14*, 930-933. (b) Chinnagolla, R. K.; Jeganmohan, M. *Chem. Commun.* **2012**, *48*, 2030-2032. (c) Ueyama, T.; Mochida, S.; Fukutani, T.; Hirano, K.; Satoh, T.; Miura, M. *Org. Lett.* **2011**, *13*, 706-708. (d) Arockiam, P. B.; Fischmeister, C.; Bruneau, C.; Dixneuf, P. H. *Green Chem.* **2011**, *13*, 3075-3078.
- ¹⁰³ J. Hartwig in *Organotransition Metal Chemistry – from bonding to catalysis*, University Science Books, Sausalito, CA, **2010**, p. 913.
- ¹⁰⁴ Park, Y. J.; Jo, E.-A.; Jun, C.-H. *Chem. Commun.* **2005**, 1185-1187.
- ¹⁰⁵ Ohkuma, T.; Noyori, R. *Angew. Chem., Int. Ed.* **2001**, *40*, 40-73.
- ¹⁰⁶ Kamochi, Y.; Kudo, T. *Heterocycles* **1993**, *36*, 2383-96.
- ¹⁰⁷ This work was continued in the master thesis of Maria Schwarz.
- ¹⁰⁸ Koley, M.; Wimmer, L.; Schnürch, M.; Mihovilovic, M. D. *Eur. J. Org. Chem.* **2011**, 1972-1979.
- ¹⁰⁹ Beveridge R. E., A., B. A. *Synthesis* **2010**, *6*, 1000-1008.
- ¹¹⁰ Reimann, E.; Schwaetzer, I.; Zymalkowski, F. *Justus Liebigs Annalen der Chemie* **1975**, 1070-80.
- ¹¹¹ Lanni, E. L.; Bosscher, M. A.; Ooms, B. D.; Shandro, C. A.; Ellsworth, B. A.; Anderson, C. E. *J. Org. Chem.* **2008**, *73*, 6425-6428.
- ¹¹² Zhu, L.; Gao, T.-T.; Shao, L.-X. *Tetrahedron* **2011**, *67*, 5150-5155.
- ¹¹³ Toma, G.; Fujita, K.-i.; Yamaguchi, R. *Eur. J. Org. Chem.* **2009**, 4586-4588.
- ¹¹⁴ Manley, P. J.; Bilodeau, M. T. *Org. Lett.* **2002**, *4*, 3127-3129.
- ¹¹⁵ Ermolat'ev, D. S.; Alifanov, V. L.; Rybakov, V. B.; Babaev, E. V.; Van der Eycken, E. V. *Synthesis* **2008**, 2083-2088.
- ¹¹⁶ Jeanjot, P.; Bruyneel, F.; Arrault, A.; Gharbi, S.; Cavalier, J.-F.; Abels, A.; Marchand, C.; Touillaux, R.; Rees, J.-F.; Marchand-Brynaert, J. *Synthesis* **2003**, 513-522.
- ¹¹⁷ Gondi, S. R.; Son, D. Y. *Synth. Commun.* **2008**, *38*, 401-410.
- ¹¹⁸ Wang, F.; Liu, H.; Fu, H.; Jiang, Y.; Zhao, Y. *Adv. Synth. Catal.* **2009**, *351*, 246-252.

- ¹¹⁹ Taylor, J. E.; Jones, M. D.; Williams, J. M. J.; Bull, S. D. *J. Org. Chem.* **2012**, *77*, 2808-2818.
- ¹²⁰ Bennet, A. J.; Somayaji, V.; Brown, R. S.; Santarsiero, B. D. *J. Am. Chem. Soc.* **1991**, *113*, 7563-71.
- ¹²¹ Selva, M.; Perosa, A.; Tundo, P.; Brunelli, D. *J. Org. Chem.* **2006**, *71*, 5770-5773.
- ¹²² Creencia, E. C.; Taguchi, K.; Horaguchi, T. *J. Heterocycl. Chem.* **2008**, *45*, 837-843.
- ¹²³ Lee, Y. M.; Moon, M. E.; Vajpayee, V.; Filimonov, V. D.; Chi, K.-W. *Tetrahedron* **2010**, *66*, 7418-7422.
- ¹²⁴ Antonchick, A. P.; Samanta, R.; Kulikov, K.; Lategahn, J. *Angew. Chem., Int. Ed.* **2011**, *50*, 8605-8608.
- ¹²⁵ Lee, T. R.; Kim, K. *J. Heterocycl. Chem.* **1989**, *26*, 747-51.
- ¹²⁶ Marce, P.; Godard, C.; Feliz, M.; Yanez, X.; Bo, C.; Castillon, S. *Organometallics* **2009**, *28*, 2976-2985.
- ¹²⁷ Penhoat, M.; Levacher, V.; Dupas, G. *J. Org. Chem.* **2003**, *68*, 9517-9520.
- ¹²⁸ Cappelli, A.; Nannicini, C.; Gallelli, A.; Giuliani, G.; Valenti, S.; Mohr, G. P.; Anzini, M.; Mennuni, L.; Ferrari, F.; Caselli, G.; Giordani, A.; Peris, W.; Makovec, F.; Giorgi, G.; Vomero, S. *J. Med. Chem.* **2008**, *51*, 2137-2146.
- ¹²⁹ Leost, F.; Chantegrel, B.; Deshayes, C. *Tetrahedron* **1997**, *53*, 7557-7576.
- ¹³⁰ Park, Y. J.; Jo, E.-A.; Jun, C.-H. *Chem. Commun.* **2005**, 1185-1187.
- ¹³¹ Maddani, M. R.; Moorthy, S. K.; Prabhu, K. R. *Tetrahedron* **2010**, *66*, 329-333.
- ¹³² *Gaussian 03*, R. C., Frisch, M. J.; Trucks, G. W.; Schlegel, H. B.; Scuseria, G. E.; Robb, M. A.; Cheeseman, J. R.; Montgomery, Jr., J. A.; Vreven, T.; Kudin, K. N.; Burant, J. C.; Millam, J. M.; Iyengar, S.; S.; Tomasi, J. B., V.; Mennucci, B.; Cossi, M.; Scalmani, G.; Rega, N.; Petersson, G. A.; Nakatsuji, H.; Hada, M.; Ehara, M.; Toyota, K.; Fukuda, R.; Hasegawa, J.; Ishida, M.; Nakajima, T.; Honda, Y.; Kitao, O.; Nakai, H.; Klene, M.; Li, X.; Knox, J. E.; Hratchian, H. P.; Cross, J. B.; Adamo, C.; Jaramillo, J.; Gomperts, R.; Stratmann, R. E.; Yazyev, O.; Austin, A. J.; Cammi, R.; Pomelli, C.; Ochterski, J. W.; Ayala, P. Y.; Morokuma, K.; Voth, G. A.; Salvador, P.; Dannenberg, J. J.; Zakrzewski, V. G.; Dapprich, S.; Daniels, A. D.; Strain, M. C.; Farkas, O.; Malick, D. K.; Rabuck, A. D.; Raghavachari, K.; Foresman, J. B.; Ortiz, J. V.; Cui, Q.; Baboul, A. G.; Clifford, S.; Cioslowski, J.; Stefanov, B. B.; Liu, G.; Liashenko, A.; Piskorz, P.; Komaromi, I.; Martin, R. L.; Fox, D. J.; Keith, T.; Al-Laham, M. A.; Peng, C. Y.; Nanayakkara, A.; Challacombe, M.; Gill, P. M. W.; Johnson, B.; Chen, W.; Wong, M. W.; Gonzalez, C.; Pople, J. A. Gaussian, Inc.; Wallingford CT: 2004.
- ¹³³ Hehre, W. J. R., L.; Schleyer, P. v.R.; Pople, J. A. *Ab Initio Molecular Orbital Theory*; John Wiley & Sons: NY, 1986.
- ¹³⁴ Perdew, J. P.; Burke, K.; Ernzerhof, M. *Phys. Rev. Lett.* **1997**, *78*, 1396.

**NAVID
DASTBARAVARDEH**



Home: Lerchenfelderstr. 9-11/21 1070 Vienna, Austria Mobile: +43 (0) 69917102918 Email: navid@ioc.tuwien.ac.at	University: <i>Vienna University of Technology</i> Institute of Applied Synthetic Chemistry Getreidemarkt 9 1060 Vienna, Austria
--	---

Nationality: German
Date of Birth: 14.09.1982

EDUCATION

-
- | | |
|-------------------|---|
| 02/2009 – present | PhD “Transition-metal catalyzed direct arylation of sp³ C-H bonds”

<i>Vienna University of Technology (TUW)</i>
Supervisor: Prof. M. D. Mihovilovic & Dr. M. Schnürch. Funding provided by the Austrian Science Fund (FWF). |
| 10/2007-07/2008 | Master thesis “Synthesis of coatings for the automotive industry”

<i>Ludwig-Maximilians-University Munich (LMU)</i>
Supervisor: Prof. K. Karaghiosoff |
| | <ul style="list-style-type: none"> • Graduation to Dipl. Chem. (= Master of Science) in 2008. |
| 09/2006-06/2007 | Research internships at Prof. P. Knochel, Prof. P. Klüfers and Prof. T. Bein group (each 3 month, <i>LMU</i>). |
| 10/2002-07/2008 | Undergraduate studies of chemistry (<i>LMU</i>). |
| 06/2002 | German Abitur (= A Levels). |

PUBLICATIONS

-
- G. Manolikakes, N. Dastbaravardeh, P. Knochel, “Nickel-Catalyzed Cross-Coupling Reactions of Aryltitanium(IV) Alkoxides with Aryl Halides” *Synlett* **2007**, 2077.
 - M. Schnürch, N. Dastbaravardeh, M. Ghobrial, B. Mrozek, M. D. Mihovilovic “Functionalization of Saturated and Unsaturated

- Heterocycles via Transition Metal Catalyzed C–H Activation Reactions” *Curr. Org. Chem.* **2011**, *15*, 2694.
- N. Dastbaravardeh, M. Schnürch, M. D. Mihovilovic “Ruthenium(0)-Catalyzed sp^3 C–H Bond Arylation of Benzylic Amines Using Arylboronates” *Org. Lett.* **2012**, *14*, 1930.
 - N. Dastbaravardeh, M. Schnürch, M. D. Mihovilovic “Ruthenium(II)-Catalyzed sp^3 C–H Bond Arylation of Benzylic Amines Using Aryl Halides” *Org. Lett.* **2012**, *14*, 3792.
 - M. Koley, N. Dastbaravardeh, M. Schnürch, M. D. Mihovilovic “Palladium (II) catalyzed regioselective ortho arylation of sp^2 C–H bonds of N-aryl-2-amino pyridine derivatives” *ChemCatChem*, in press.
 - N. Dastbaravardeh, K. Kirchner, M. Schnürch, M. D. Mihovilovic „Mechanistic Investigations and Substrate Scope Evaluation of Ruthenium-Catalyzed Direct sp^3 Arylation of Benzylic Positions Directed by 3-Substituted Pyridines“ *J. Org. Chem.* **2013**, *78*, 658.
 - Maria C. Schwarz, Navid Dastbaravardeh, Karl Kirchner, Michael Schnürch, Marko D. Mihovilovic „ First Selective Direct Mono-Arylation of Piperidines Using Ruthenium Catalyzed C-H Activation” *Monatshefte für Chemie*, **2013**, in press.
 - N. Dastbaravardeh, M. Schnürch, M. D. Mihovilovic „ Aryl Bromides and Aryl Chlorides for the Direct Arylation of Benzylic Amines Mediated by Ruthenium(II)“ *Eur. J. Org. Chem.* **2013**, in press.

ADMINISTRATION EXPERIENCE

-
- 09/2011-present **Teaching Assistant** – Vienna University of Technology
- Supervision support for master thesis of an undergraduate student.

WORK EXPERIENCE

-
- 02/2009–present Scientific Assistant at the Institute of Applied Synthetic Chemistry (Vienna University of Technology).
- 08/2012 Assistant at the “4th Young Investigator Workshop”, Vienna.
- 10/2007-07/2008 Scientific employee at the company 3M (Düsseldorf).

CONFERENCES & FELLOWSHIPS

-
- 2011 Summer School: Homogeneous Catalysis and Fine Chemicals, Antwerp, Belgium.
- 2010 Dalton Discussion 12: Catalytic C–H and C–X Bond Activation, Durham, UK.
- 2010 14th Blue Danube Symposium on Heterocyclic Chemistry, Podbanske, Slovakia.
- 2006 John-Loesch Fellowship